TESIS DE LA UNIVERSIDAD DE ZARAGOZA
2023
111

Juan Calvet Seral

Fighting antimicrobial resistance in mycobacteria: development of an antivirulence screening platform and a genetic methodology to confirm drug resistance phenotypes

Director/es
Martín Montañés, Carlos
Gonzalo Asensio, Jesús Ángel

ISSN 2254-7606

Prensas de la Universidad
Universidad Zaragoza

ISSN 2254-7606

Universidad Zaragoza
1542

Tesis Doctoral

FIGHTING ANTIMICROBIAL RESISTANCE IN MYCOBACTERIA: DEVELOPMENT OF AN ANTIVIRULENCE SCREENING PLATFORM AND A GENETIC METHODOLOGY TO CONFIRM DRUG RESISTANCE PHENOTYPES

Autor

Juan Calvet Seral

Director/es

Martín Montañés, Carlos
Gonzalo Asensio, Jesús Ángel

UNIVERSIDAD DE ZARAGOZA
Escuela de Doctorado

Programa de Doctorado en Bioquímica y Biología Molecular

2023

FACULTAD DE MEDICINA

Departamento de Microbiología, Pediatría, Radiología y Salud Pública de la Universidad de Zaragoza.

Fighting antimicrobial resistance in mycobacteria: development of an antivirulence screening platform and a genetic methodology to confirm drug resistance phenotypes.

Memoria para optar al grado de Doctor presentada por:

Juan Calvet Seral

Graduado en Biotecnología

Directores:

Jesús A. Gonzalo Asensio

Carlos Martín Montañés

Dr. **JESÚS ÁNGEL GONZALO ASENSIO**, Profesor Titular del Departamento de Microbiología, Pediatría, Radiología y Salud Pública de la Universidad de Zaragoza.

Dr. **CARLOS MARTÍN MONTAÑÉS**, Catedrático de Microbiología del Departamento de Microbiología, Pediatría, Radiología y Salud Pública de la Universidad de Zaragoza.

Co-directores de la Tesis Doctoral presentada por **JUAN CALVET SERAL** bajo el título:

Fighting antimicrobial resistance in mycobacteria: development of an antivirulence screening platform and a genetic methodology to confirm drug resistance phenotypes.

(Luchando contra la resistencia a antibióticos en micobacterias: desarrollo de una plataforma de cribado de moléculas antivirulencia y de una metodología genética para confirmar fenotipos de resistencia a drogas)

EXPONEN:

Que dicha Tesis Doctoral ha sido realizada bajo su dirección y reúne los requisitos necesarios para optar al grado de Doctor.

Por lo anterior, emiten el presente **INFORME FAVORABLE**.

Zaragoza, 13 de enero de 2023

Fdo.: Jesús A. Gonzalo Asensio

Fdo: Carlos Martín Montañés

Esta tesis doctoral ha sido elaborada en el Departamento de Microbiología, Pediatría, Radiología y Salud Pública de la Facultad de Medicina de la Universidad de Zaragoza, dentro del Programa de Doctorado en Bioquímica y Biología Molecular.

Juan Calvet ha sido beneficiario de una ayuda para la contratación de personal investigador predoctoral en formación concedida por el Departamento de Investigación e Innovación de la Diputación General de Aragón para el periodo 2017-2021, financiadas por el Programa Operativo FSE 2014-2020.

El trabajo experimental ha sido financiado por los siguientes proyectos de investigación:

- "Ingeniería de Genomas Multiplex e Iterativa (MIGE) en *Mycobacterium*. Aplicación al desarrollo de herramientas para la búsqueda de nuevos antibióticos" financiado por el Ministerio de Economía y Competitividad (BFU2015-72190-EXP).
- "Development of anti-virulence therapies and deciphering host-pathogen adaptation on the basis of evolutionary genetics of the *Mycobacterium tuberculosis* complex (adapTBvir)" financiado por el Ministerio de Ciencia e Innovación (PID2019-104690RB-I00).
- "TB antivirulence therapeutics: small molecule inhibitors targeting *M. tuberculosis* replication as a novel alternative to classic antibiotics" financiado por la Unión Europea (Openlab TC-262).

Durante su etapa predoctoral, Juan Calvet ha realizado dos estancias de investigación en el centro de I+D de GlaxoSmithKline Tres Cantos (España) de 3 meses y medio y 4 meses que han sido financiadas, respectivamente, por el Programa Ibercaja-CAI de Estancias de Investigación (referencia CM 2/21) y por el programa de Subvenciones de Fomento de la Movilidad de Personal Investigador en Formación, Convocatoria 2022 del Gobierno de Aragón (referencia MVB_01_22).

Parte del trabajo realizado ha sido realizado en las instalaciones del Servicio de análisis microbiológico del Servicio General de Apoyo a la Investigación-SAI de la Universidad de Zaragoza, así como en las instalaciones de Proteómica de los Servicios Científico Técnicos del CIBA (IACS-Universidad de Zaragoza) (las instalaciones de proteómica son miembro de ProteoRed, PRB2-ISCIII, apoyado por la subvención PT13/0001).

INDEX

INDEX OF FIGURES

INDEX OF TABLES

INDEX OF ACRONYMS

ADC	:	Albumin-dextrose-catalase
AES	:	Allelic exchange substrate
Amp	:	Ampicillin
AMs	:	Arabinomannans
ATZ	:	Acetazolamide
BC	:	Barcoding/barcode
BCG	:	Bacillus calmette-guérin
BSL	:	Biosafety level
CA	:	Carbonic anhydrase
CDC	:	Centers for disease control and prevention
CF	:	Culture filtrate fraction
CFP-10	:	Culture filtrate protein of 10 kda
CFUs	:	Colony forming units
CL	:	Culture lysate fraction
Cm	:	Chloramphenicol
DAT	:	Diacyltrehalose
DMSO	:	Dimethyl sulfoxide
DNA	:	Desoxiribonucleic acid
dsAES	:	Double strand allelic exchange substrate
EMA	:	European medicines agency
ESAT-6	:	6-kda early secretory antigenic target
ESX	:	ESAT-6 secretion system
ETZ	:	Ethoxzolaide
FDA	:	Food and Drug Administration
FRET	:	Foster resonance energy transfer
FRT	:	FLP recognition target
FU	:	Fluorescentceunits
GFP	:	Green fluorescent protein
hCA	:	Human carbonic anhydrases
HGT	:	Horizontal gene transfer
Hr	:	Isoniazid resistant
HTS		High throughput screening
IL	:	Interleukin
Km	:	Kanamycin
LAMs	:	Lipoarabinomannans
LB	:	Luria-bertani
LMs	:	Lipomannans
LTBI	:	Latent tuberculosis infection
MABC	:	Mycobacterium abscessus complex
MDR	:	Multi drug resistant
MES	:	2-(N-morpholino)ethanesulfonic acid
MIC	:	Minimal inhibitory concentration

MOPS	:	3-(N-morpholino)propanesulfonic acid
MRM	:	Multiple-reaction monitoring
MRM/MS	:	Multiple-Reaction Monitoring coupled to Mass Spectrometry
MS	:	Mass spectrometer
MTBC	:	*Mycobacterium tuberculosis* complex
mtbCA	:	Carbonic anhydrases of M. Tuberculosis
MTT	:	3-(4,5-dimethylthiazol-2-yl)-2,5-diphenyltetrazolium bromide
ncRNA	:	Non-coding ribonucleic acid
NTM	:	Non tuberculous mycobacteria
OD600	:	Optical density at 600 nm
PAMPs	:	Pathogen-associated molecular patterns
PAT	:	Polyacyltrehalose
PCR	:	Polymerase chain reaction
PDIM	:	Phthiocerol dimycocerosate
PGL	:	Phenolic glycolipid
PIMs	:	Phosphatidylinositol mannosides
PNAs	:	Peptide nucleic acids
Pre-XDR	:	Pre-extensive drug resistant
RD	:	Region of difference
REMA	:	Resazurin microtiter assay
RFU	:	Relative fluorescence units
RNA	:	Ribonucleic acid
RR	:	Rifampicin resistant
S/B	:	Signal to background
SL	:	Sulfolipid
SMphoPR	:	*M. smegmatis phoPR* genes
SNPs	:	Single nucleotide polymorphisms
SRM	:	Selected-reaction monitoring
ssAES	:	Single strand allelic exchange substrate
TAT	:	Twin arginine traslocation
TB	:	Tuberculosis disease
TBphoPR	:	*M. tuberculosis phoPR* genes
TDM	:	Trehalose dimycolate
TDR	:	Totally drug resistant
tdTomato	:	Tandem dymeric Tomato protein
TFD	:	Transcription factor decoys
TLRs	:	Toll like receptors
TMM	:	Trehalose monomycolate
TNF	:	Tumor necrosis factor
WGS	:	Whole genome sequencing
WHO	:	World health organization
XDR	:	Extensively drug resistant

SUMMARY

Tuberculosis disease (TB) caused 10.6 million new cases and 1.6 million deaths in 2021 according to the data from the World Health Organization (WHO). Its main causative agent is a single infectious microorganism called *Mycobacterium tuberculosis*. Although there is a preventive vaccine, BCG, and there are antibiotics available for the treatment of TB, the variable protection conferred by BCG against pulmonary TB and the emergence and spread of drug-resistant *M. tuberculosis* strains all around the world make TB nowadays the first cause of death due to bacterial infection.

Antimicrobial resistance is one of the top 10 global public health threats declared by the WHO, and it especially worries in the case of TB. The inappropriate use of antibiotics available for decades has led to the rise of multi-drug resistant and extensively drug resistant strains of *M. tuberculosis*, in which the therapeutic options are dramatically reduced. To overcome TB problematic there are different strategies being developed globally: improve prevention of the disease with new vaccine candidates with better protective efficacies than BCG, and development of new drugs to treat TB infected patients.

The discovery of new antibiotics active against sensitive and resistant forms of TB in the last decade has increased the clinical pipeline, and 17 new chemical classes of antibiotics are currently in Phase I and II clinical trials. However, there is still an urgent need of developing new antibiotics, but also new innovative strategies to fight TB, like host directed, phage or antivirulence based therapies.

In this thesis we have developed a platform for screening and characterization of new drugs with inhibitory activity against the PhoPR system of *M. tuberculosis*. The PhoPR system is a two component system which regulates a variety of virulence phenotypes of *M. tuberculosis*, and consequently, inhibitors of this system could be a potential antivirulence strategy against TB. The screening platform has been stablished constructing a panel of different PhoPR *M. tuberculosis* reporter strains. PhoPR reporter strains contain an integrative plasmid in which the green fluorescent protein is under control of a well characterized promoter regulated by the PhoPR system. In order to have a wider view of PhoPR inhibition, we constructed a panel of PhoPR reporter strains using different PhoPR regulated promoters (*mcr7* and *pks2*) that were introduced into different strains comprising the most widespread lineages of *M. tuberculosis* (L2 and L4). The secondary assays developed to characterize potential PhoPR inhibitors consist of a transcriptomic evaluation of the PhoPR regulon (*mcr7*, *pks2*, *pks3*, *espA*, *espC* and *espD*

genes), and a proteomic evaluation of the secretion of different virulence effectors (ESAT-6, CFP-10, EspA and EspC). The reporter strains and the secondary assays have been validated using isogenic Δ*phoPR* mutants and a PhoPR inhibitory molecule already described in the literature, named ethoxzolamide (ETZ).

We have also explored the possibility of using a non-pathogenic mycobacterium, *Mycobacterium smegmatis*, as *M. tuberculosis* surrogate for the discovery of PhoPR inhibitors. To do so, we have engineered a *M. smegmatis* strain to replace its endogenous PhoPR system by the heterologous system from *M. tuberculosis*. We have also constructed a Δ*phoPR* mutant as control of inactive PhoPR system in *M. smegmatis*. Reporter strains constructed in the different *M. smegmatis* strains have demonstrated preliminary but promising results of the reporter plasmids in *M. smegmatis* strains carrying the PhoPR system from *M. tuberculosis*.

Aside from *M. tuberculosis*, there are other non-tuberculous mycobacteria (NTM) in which antimicrobial resistance is worrying. Among them, *Mycobacterium abscessus* stands out because of its natural and easy development of acquired drug resistance. The growing use of Whole Genome Sequencing in the last years has allowed the identification of multiple potential single nucleotide polymorphisms (SNPs) conferring drug resistance phenotypes which need to be experimentally confirmed.

In this Thesis we have also developed a targeted chromosomal barcoding strategy to establish direct genotype-phenotype associations between SNPs and antibiotic resistance phenotypes in *M. abscessus.* To do so, we have used the recombineering technology to confirm the genotype-phenotype relationship of an *atpE* D29A mutation and bedaquiline resistance. The recombineering technology allowed us to introduce the *atpE* D29A mutation into its specific loci in the *M. abscessus* chromosome with the use of a single strand allelic exchange substrate (ssAES) and to subsequently recover bedaquiline resistant clones. The use of ssAES with additional silent barcode mutations surrounding the *atpE* D29A mutation allowed to easily confirm the specific integration of the mutation of interest into the *M. abscessus* chromosome using PCR based techniques. This barcoding strategy has been successfully used in two different *M. abscessus* genetic backgrounds, the clinical isolate *M. abscessus* SL541 and the laboratory reference strain ATCC19977. Additionally, we have used the barcoding strategy to confirm the association of a second bedaquiline resistance mutation, the *atpE* A64P, demonstrating the broad applicability of this methodology.

RESUMEN

La tuberculosis (TB) causó 10,6 millones de nuevos casos y 1,6 millones de muertes en 2021 según datos de la Organización Mundial de la Salud (OMS). Su principal agente causal es un único microorganismo infeccioso denominado *Mycobacterium tuberculosis*. Si bien existe una vacuna preventiva, la BCG, y hay antibióticos disponibles para el tratamiento de la TB, la protección variable que confiere la BCG contra la TB pulmonar y la aparición y propagación de cepas resistentes a antibióticos de *M. tuberculosis* en todo el mundo hacen que la TB sea hoy en día la primera causa de muerte por una infección bacteriana.

La resistencia a los antimicrobianos es una de las 10 principales amenazas mundiales para la salud pública declaradas por la OMS, y preocupa especialmente en el caso de la TB. El uso inapropiado de los antibióticos disponibles durante décadas ha llevado al surgimiento de cepas de *M. tuberculosis* multirresistentes (MDR) y extremadamente resistentes a los medicamentos (XDR), en las que las opciones terapéuticas se reducen drásticamente. Para afrontar la problemática de la TB, se están desarrollando diferentes estrategias a nivel mundial: mejorar la prevención de la enfermedad con nuevas vacunas candidatas con mejores eficacias protectoras que la BCG y el desarrollo de nuevos medicamentos para tratar a los pacientes infectados con TB.

El descubrimiento de nuevos antibióticos activos contra las formas sensibles y resistentes de la TB en la última década ha aumentado la cartera clínica, y 17 nuevas clases químicas de antibióticos se encuentran actualmente en ensayos clínicos de Fase I y II. Sin embargo, todavía existe una necesidad urgente de desarrollar nuevos antibióticos, pero también nuevas estrategias innovadoras para luchar contra la TB, como terapias dirigidas al huésped, basadas en fagos o en terapias antivirulencia.

En esta tesis hemos desarrollado una plataforma de cribado y caracterización para el descubrimiento de nuevos fármacos con actividad inhibitoria contra el sistema PhoPR de *M. tuberculosis*. El sistema PhoPR es un sistema de dos componentes que regula una gran variedad de fenotipos de virulencia de *M. tuberculosis* y, en consecuencia, los inhibidores de este sistema podrían ser una estrategia antivirulencia con potencial contra la TB. La plataforma de cribado se ha establecido construyendo un panel de diferentes cepas indicadoras (reporteras) del sistema PhoPR *M. tuberculosis*. Estas cepas reporteras contienen un plásmido integrado en el que la proteína fluorescente verde está bajo el control de un promotor bien caracterizado regulado por el sistema PhoPR. Para poder tener una visión más amplia de la inhibición del sistema PhoPR, hemos construido un panel de cepas reporteras del sistema PhoPR utilizando diferentes

promotores regulados por el sistema PhoPR (*mcr7* y *pks2*) y que han sido introducidos en diferentes cepas de los linajes más extendidos de *M. tuberculosis*. Los ensayos secundarios desarrollados para caracterizar los posibles inhibidores del sistema PhoPR consisten en una evaluación transcriptómica de diferentes genes del regulón PhoPR (los genes *mcr7*, *pks2*, *pks3*, *espA*, *espC* y *espD*), y una evaluación proteómica de la secreción de diferentes efectores de virulencia (ESAT-6, CFP-10, EspA y EspC). Las cepas indicadoras y los ensayos secundarios se han validado utilizando mutantes isogénicos ∆*phoPR* y una molécula inhibidora del sistema PhoPR ya descrita en la literatura, llamada etoxzolamida (ETZ).

También hemos explorado la posibilidad de utilizar una micobacteria no patógena, *Mycobacterium smegmatis*, como sustituta de *M. tuberculosis* para el descubrimiento de inhibidores del sistema PhoPR. Para hacerlo, hemos diseñado una cepa de *M. smegmatis* con su sistema PhoPR endógeno reemplazado por sistema heterólogo de *M. tuberculosis*. También hemos construido un mutante ∆*phoPR* como control del sistema PhoPR inactivo en *M. smegmatis*. Las cepas reporteras de *M. smegmatis* portadoras del sistema PhoPR de *M. tuberculosis* han mostrado resultados preliminares pero prometedores.

Aparte de *M. tuberculosis*, existen otras micobacterias no tuberculosas (NTM) en las que preocupa la problemática de la resistencia antimicrobiana. Entre ellos, *Mycobacterium abscessus* destaca por su natural y fácil desarrollo de resistencia adquirida a antibióticos. La mayor accesibilidad en los últimos años a la secuenciación de genomas completos permite actualmente la identificación de múltiples polimorfismos de nucleótido único (SNP) potenciales que confieran fenotipos de resistencia a fármacos que deben confirmarse.

En esta tesis, también hemos desarrollado una estrategia de "código de barras cromosómico" específica para establecer asociaciones directas de genotipo-fenotipo entre los SNP y los fenotipos de resistencia a los antibióticos en *M. abscessus*. Para ello, hemos utilizado la tecnología de recombinación para confirmar la relación genotipo-fenotipo de la mutación *atpE* D29A y la resistencia a bedaquilina. La tecnología de recombinación nos ha permitido introducir la mutación *atpE* D29A en la región específica del cromosoma de *M. abscessus* con el uso de un sustrato de intercambio alélico monocatenario (ssAES) y posteriormente recuperar clones resistentes a la bedaquilina. El uso de ssAES con mutaciones silenciosas adicionales como código de barras que rodea la mutación *atpE* D29A ha permitido confirmar fácilmente la integración específica de la mutación de interés en el cromosoma de *M. abscessus* mediate técnicas basadas

en PCR. Esta estrategia de “código de barras” ha sido utilizada con éxito en dos fondos genéticos diferentes de *M. abscessus,* el aislado clínico *M. abscessus* SL541 y la cepa referencia de laboratorio ATCC19977. Además, hemos utilizado la estrategia de “código de barras” para confirmar la asociación de una segunda mutación de resistencia a bedaquilina, la mutación *atpE* A64P, demostrando la amplia aplicabilidad de esta metodología.

INTRODUCTION

History of tuberculosis

According to the World Health Organization (WHO), in 2019 tuberculosis disease (TB) caused 10 million new cases. Even though deaths decreased almost a 40.8% since 2000, 1.4 millions of people died because of this disease (WHO, 2020a). However, the impact of the SARS-CoV-2/COVID-19 pandemic has led to a step back in the decreasing progression of new TB cases and deaths, raising to 10.6 million new cases and 1.6 deaths in 2021 (WHO, 2022a). TB incidence is especially relevant in unindustrialized countries of Africa and South-East Asia (***Figure 1A***). Historically, TB has caused a great number of deaths, becoming the most devastating infectious disease worldwide (***Figure 1B***) (Paulson, 2013).

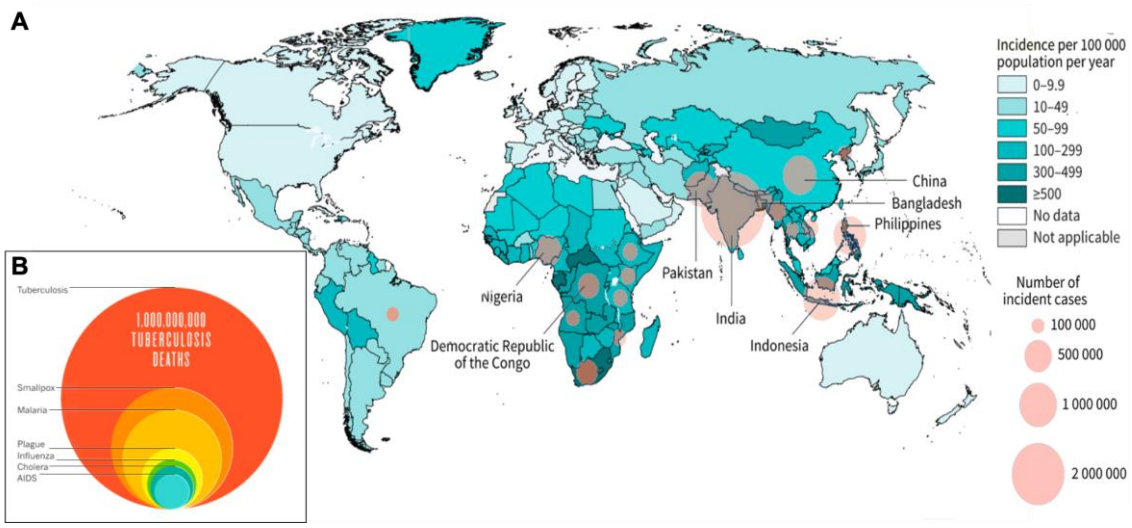

Figure 1: **Global incidence and historical deaths caused by TB** (**A**) Global distribution of TB incidence and new cases in 2021, adapted from (WHO, 2022a). (**B**) Deaths caused by TB in the last 200 years are higher than the ones caused by smallpox, malaria, plague, influenza, cholera, and AIDS, adapted from (Paulson, 2013).

It is thought that TB is one of the oldest human pathogen-caused diseases and that an early progenitor of its causative agent infected early hominids in East Africa around 3 million years ago. Since then, it has coevolved with humans until the present phylogeographical distribution of the *Mycobacterium tuberculosis* COMPLEX (MTBC) (Gutierrez et al., 2005)

Egyptian hieroglyphs from the Old Kingdom date (4th or 5th Dynasty, 2900 B.C.) already represented figures with deformities in the back, indicatives of the Pott's disease (tuberculosis spondylitis), a form of TB that affect the spine (Cave, 1939). DNA sequencing of a fragment recovered from a 5400-year-old Predynastic Egyptian skeleton with similar spinal deformities was consistent with an original *Mycobacterium* infection (Crubézy et al., 1998).

In classical Greece, TB was well known, and it was called "*phthisis*", φθίση, to define the languish TB patient's body due to the pulmonary disease. Hippocrates (460-370 B.C.) wrote in *Book I, of the Epidemics* "Consumption was the most considerable of the diseases which then prevailed, and the only one which proved fatal to many persons" (Daniel, 2006). In the Middle Ages and Modern Era, TB had also a high incidence. In the 17th century an outbreak of TB that lasted 200 years was known as the "Great White Plague" or "White Death" because of the characteristic paleness of the patients. Sylvilus de la Boë described in 1679 the characteristics lesions in the lungs as "tubercles" (from *tuberculum*, which mean protuberance). Until the term "tuberculosis" was coined 155 years later by Johann Lukas Schönlein, the disorder was mainly referred as "consumption" (Herzog, 1998).

The research in TB, in the strict sense, started in the 19th century. In 1840, Jakob Henle advanced three postulates for proving the infectiousness of a disease: (1) the causative agent must be found in every case of the disease; (2) it must not occur in another disease; and (3) its application must always provoke the same disease The first scientific who proved the transmissibility of TB was Philipp Klencke, in 1843, injecting material from a tubercle into rabbits, dying these animals of generalized TB. However, Klencke still considered the disease as a tumor (Herzog, 1998).

In 1865, Jean Antoine Villemin, a French military surgeon, postulated for the first time that the disease is caused by a specific microorganism. He demonstrated that TB from humans or cattle could be transmitted to rabbits or guinea pigs and that injecting blood or sputum extracted from tuberculous rabbits could transmit the disease to other laboratory animals, so TB had to be an infectious disease (Herzog, 1998).

Even though Theodor Klebs in 1877 was the first scientific who kept the causative agent of TB alive in artificial cultures and transferred it into laboratory animals, it was Robert Koch (1843-1910), Henle's student, the first one who described the specific microbe that caused the disease. He was able to prove that the slender rods he visualized by microscopy in tuberculous tissue (which he named *Mycobacterium tuberculosis*) led to the development of TB into laboratory animals after isolation in pure cultures. As a

consequence, R. Koch fulfilled the postulates of his teacher, Henle, which he presented to the scientific world on 24th March 1882 in his lecture "*Die Aetiologie der tuberculose"* (Herzog, 1998) and they are today the basis of the modern microbiology. Because of his whole work in TB, in 1905 Robert Koch became the fifth Nobel Prize laureate in Medicine.

Around 1850, sanatoriums became places to specifically treat TB. As Hermann Brehmer proposed in his doctoral dissertation *"Tuberculosis is a curable disease*", continuous fresh air, a rich diet, carefully supervised exercise, and rest had successful results; based in his healing from TB after travelling to the Himalayan Mountains, and his ideas concerning to the etiology of TB. Sanatoria were to dominate the treatment of TB for the next century after he opened the first sanatorium in Görbersdorf in 1862 (Barberis et al., 2017; Daniel, 2011).

Koch also tried to develop a treatment for TB producing a glycerin extract of dead tubercle bacilli, which he called tuberculin, through the last decades of 19th century. Although it proved to be a failure as treatment, it became a useful tool as diagnostic measure to distinguish infected from non-infected population (Sakula, 1979); Nowadays, intradermal inoculation of tuberculin is the basis of the Mantoux test, which is still one of the most used diagnostic tools for TB exposure (Gualano et al., 2019).

Following Louis Pasteur principles for attenuating the virulence of living microbes, Albert Calmette and Camille Guérin obtained in 1920 an attenuated strain from cattle-TB causing bacteria after 230 that they named Bacillus Calmette-Guérin (BCG) (Calmette, 1931; Pezzella, 2019). This strain demonstrated protection against TB when administered in laboratory animals and, since its first administration in 1921, it is the current and unique available vaccine against TB. The obtention of BCG had a huge impact, reducing TB incidence and saving countless lives (Daniel, 2011; Herzog, 1998).

The arrival of the antibiotic "Golden Age" also changed the TB landscape dramatically. The first antibiotic against *M. tuberculosis* , streptomycin, was discovered by Albert Schatz and Selman Waksman from *Streptomyces griseus*, which was used for first time to successfully treat a young woman with TB in 1944. During next years, new anti-tuberculous drugs were discovered: *p*-aminosalicylic acid (1949), isoniazid (1952), pyrazinamide (1954), cycloserine (1955), ethambutol (1962) and rifampicin (1963) (Herzog, 1998). Nowadays, the most used treatment for TB is still based in a combination of four of these antibiotics, rifampicin, isoniazid, ethambutol, and pyrazinamide, which are administered for the first two months together in an intensive phase of treatment. The following four months consist of a continuation phase in which rifampicin, and isoniazid are administered (Nahid et al., 2016; WHO, 2022b).

Even though BCG and antibiotics contributed to reduce TB incidence and mortality rates, different challenges have avoided the eradication of the disease. TB could not be successfully prevented due to the variable protection conferred by BCG against pulmonary TB. In addition, the emergence of drug resistant strains around the world; the wrong assumption of industrialized countries that TB disease was close to eradication, with a linked drop of TB control programs; and the worldwide emergence of HIV/AIDS epidemic since 1980's, increasing the immune susceptibility of the infected population, allowed TB re-emergence. Consequently, the WHO declared TB as a global health emergency in April of 1993 (WHO, 1993, 1994)

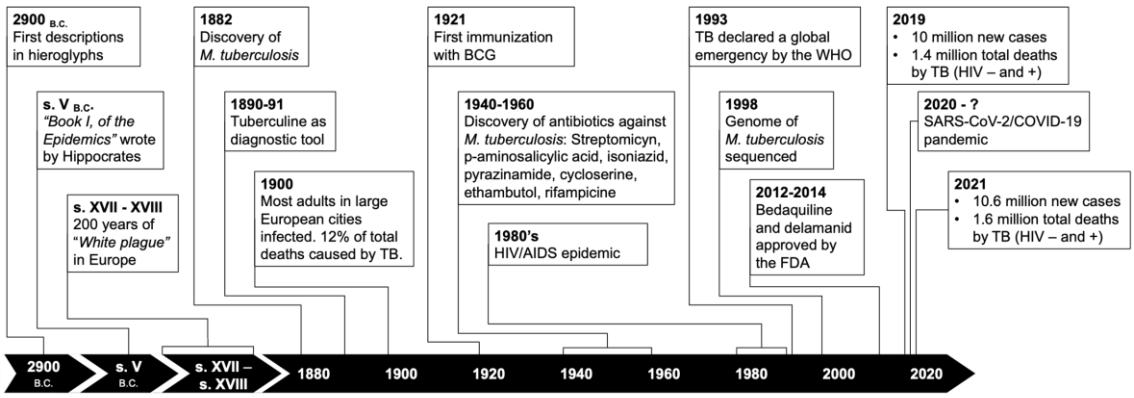

Figure 2: **Timeline of some relevant events in TB History**.

Biology of *M. tuberculosis*

Mycobacterium tuberculosis belongs to the *Mycobacterium* genus, included in the family *Mycobacteriaceae*, suborder *Corynebacterineae*, order *Actinomycetales* and phylum Actinobacteria (Stackebrandt et al., 1997). It has recently been proposed to divide the *Mycobacterium* genus into five different genera, differentiating the different clades in four new genera called *Mycobacteroides* ("*Abscessus – Chelonae*" clade), *Mycolicibacter* ("*Terrae*" clade), *Mycolicibacterium* ("*Fortuitum – Vaccae*" clade) and *Mycolicibacillus* ("*Triviale*" clade), plus the *Mycobacterium* genus ("*Tuberculosis – Simiae*" clade) (***Figure 3***) (Gupta et al., 2018). However, the medical community rapidly opposed to this dissection. They consider it did not add any advantage to clinicians and patient care, but increase errors in medical practice (Tortoli et al., 2019). So, the *Mycobacterium* genus is still the most accepted term, and bacteria belonging to the genus are commonly known as mycobacteria.

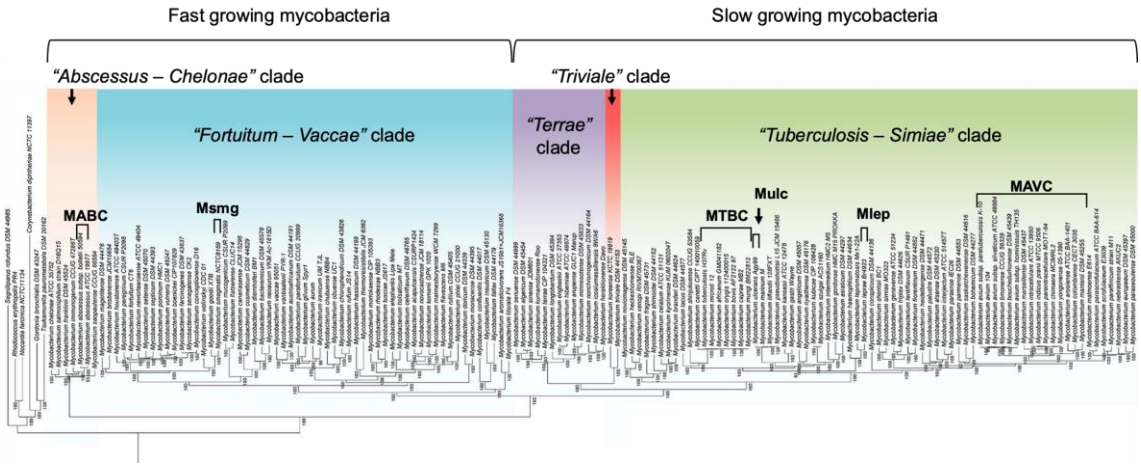

Figure 3: **Phylogenetic tree of 150 species from the *Mycobacterium* genus.** The *M. abscessus* complex (MABC), *M. smegmatis* (Msmg), the *M. tuberculosis* complex (MTBC), *M. ulcerans* (Mulc), *M. leprae* (MLep) and the *M. avium* complex (MAVC) are highlighted. Modified from (Gupta et al., 2018).

Mycobacterial species can be found widely distributed either in the environment or infecting different hosts, as they can be nonpathogenic, opportunistic, or strict pathogens. They are usually classified as fast or slow-growth species depending on their ability to develop colonies in less or more than 7 days, respectively. Slow growing mycobacteria include major human pathogen species such as species from the *M. tuberculosis* complex (MTBC) (Riojas et al., 2018), *M. ulcerans* or *M. leprae,* which cause TB, Buruli ulcer and leprosy, respectively. Fast growing species are usually opportunistic or nonpathogenic. However, the improvement of the diagnostic methods has allowed to detect different clinical outbreaks in the last decades of fast-growing mycobacteria, with special relevance of infections caused from species of the *M. abscessus* complex (MABC) (To et al., 2020).

As mycobacteria belong to the phylum Actinobacteria, they belong to the Gram-positive bacteria group. They are acid-fast, aerobe, non-motile and non-spore forming bacilli of 2-5 µm of length and 0.2-0.5 µm of width. However, they display notable differences with other Gram-positive bacteria, such as the high percentage of cytosine and guanine of their genome (over 60%), and they appear as neutral or like "ghosts" in Gram staining due to their cell wall envelope characteristics. Despite being structurally similar to Gram-positive cell walls, the mycobacterial envelope has mainly lipids, instead of polysaccharides. The uncommon lipids of the cell wall make mycobacteria retain the dye carbol-fuchsin after washing with an alcoholic solution in acid medium and they keep stained in red in contrast to the rest of bacteria that are decolorized in the Ziehl-Neelsen staining.

Life cycle and pathogenesis of *M. tuberculosis*

M. tuberculosis has evolved through thousands of years with humans as its unique reservoir. It's an obligate intracellular pathogen adapted to survive inside alveolar macrophages in the lungs. In addition, *M. tuberculosis* can colonize other tissues and cause disseminated (or extra-pulmonary) TB forms. Extrapulmonary infections are less common and pose a higher risk than pulmonary TB, but have no-impact in its transmission, as *M. tuberculosis* mainly spreads from human to human by aerosol droplets containing bacteria from infected individuals with active pulmonary disease. (Chandra et al., 2022; Kirschner et al., 2010; Silva Miranda et al., 2012).

When *M. tuberculosis* bacilli reach the lungs, they are recognized by the alveolar macrophages. Once phagocytosed, *M. tuberculosis* is able to block phagosome acidification and the fusion with the lysosomes by different mechanisms. After that, *M. tuberculosis* can disrupt the phagosome membrane allowing bacteria to reach the macrophage cytosol. There, *M tuberculosis* bypasses cell mechanisms of anti-bacterial defense and proper immune recognition to survive intracellularly (Queval et al., 2017; Simeone et al., 2015).

The progression of the infection will depend on the host's immune system. In 90% of cases, the host's immune system controls the progression of the infection to active disease, but bacteria persist in a latent state, known as latent TB infection (LTBI), contained in a microenvironment called granuloma. Granulomas are aggregates of different types of cells, primarily immune cells, including macrophages containing the bacilli, highly differentiated cells including multinucleated giant cells, epithelioid cells, and foam cells, surrounded by other cell types as neutrophils, dendritic cells, B and T cell, natural killer (NK) cells, fibroblast and cells that secrete extracellular matrix components (Chandra et al., 2022; Davis & Ramakrishnan, 2009; Silva Miranda et al., 2012). To contain the infection in the granuloma and prevent dissemination is important that the host develops an effective adaptative immune response (Chandra et al., 2022). Historically, it has been thought that granulomas benefit the host containing the bacilli from dissemination to the rest of the lung, however, it has been recently proposed that the granuloma structure can also benefit bacteria, providing a permissive environment and "protection" from specialized immune cells by limiting their traffic to the core, in which bacteria are contained (S. B. Cohen et al., 2022). In the LTBI, individuals do not have symptoms of the disease.

When containment in the granuloma fails, infection progresses to active TB. The granuloma necrotizes and breaks, and bacteria are able to spread through the lung

(pulmonary TB) or disseminate to other parts of the body. Individuals with pulmonary TB usually develop a productive cough and spread the bacilli to other individuals and transmit the disease. The latest models estimate that around one quarter of the global population (1.7 billion people) has LTBI and so, there is a high chance that 10% of these individuals will develop active TB during their lifetime (Chakaya et al., 2021; K. A. Cohen et al., 2019). This risk increases when the host's immune system gets compromised or is altered, due to malnutrition or co-infection with HIV, impairing the function of CD4+ cells. It has also been described that there are different progressions of infected individuals depending on their age. Individuals under 5 years old have an immature immune system and they are at high risk of developing disseminated forms of TB (extrapulmonary forms, including miliary TB or meningitis). Individuals from 5 to 15 years old are relatively resistant to TB. Risk increases in adolescents, and even more in older adults, but in these ages, pulmonary TB is the most frequent form of the disease (Donald et al., 2010; Harries & Dye, 2006).

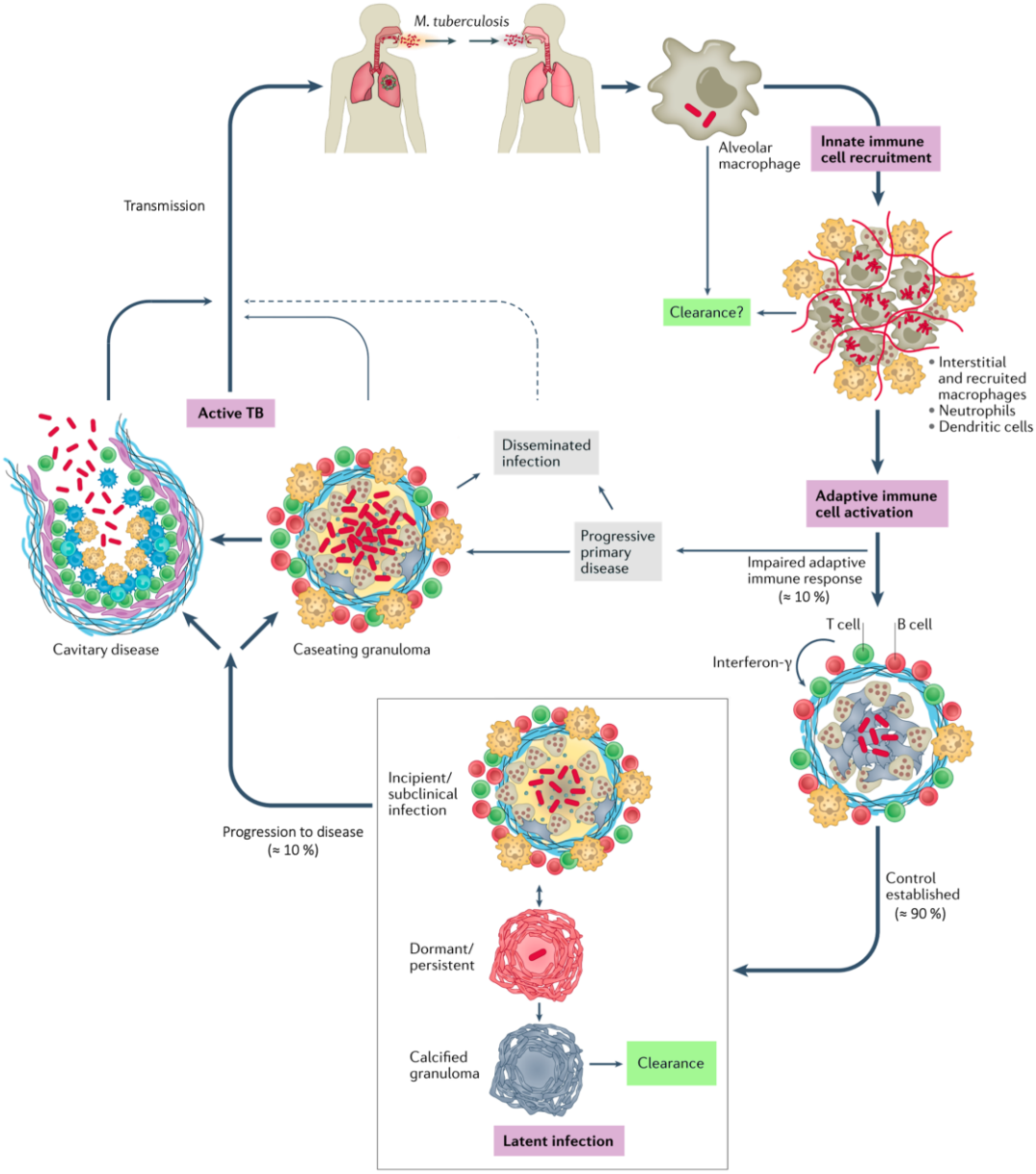

Figure 4: **Life cycle of *M. tuberculosis* infection**. Modified from (Chandra et al., 2022).

Virulence mechanisms of *M. tuberculosis*

The ability of a pathogen to cause disease is known as virulence. *M. tuberculosis* has multiple virulence factors that drive different molecular mechanisms to cause infection. Due to the strict intracellular lifestyle of *M. tuberculosis*, it has evolved to survive through the infection process, and a large portion of its genome encodes for virulence effectors o for enzymes involved in their synthesis. These effectors are from different biochemical nature, lipids, glycans, proteins, nucleic acids, or metabolites. All of them act in tune to favor infection at different stages, modulating different phases of the immune response

(Rahlwes Kathryn et al., 2022). Virulence factors can be essential structures of the bacteria, like the cell envelope or the chromosome, and/or been released to perform their action. The main *M. tuberculosis* virulence factors can be classified as components of the mycobacterial cell envelope and secreted effectors.

M. tuberculosis cell envelope and its role in virulence

The mycobacterial envelope has a particular molecular composition and organization. Its structure is key in the biology of mycobacteria and their intrinsic resistance to multiple antibiotics. It has a key importance in the host-pathogen interactions and so, it has an important impact in *M. tuberculosis* virulence through the infection process. From inside to outside, the organization of the different layers of the envelope consists as follows: a bacterial plasma membrane, periplasm space, a cell wall, the mycomembrane and the capsule (***Figure 5***). The composition of each layer in *M. tuberculosis* is:

- The plasma membrane is similar to other bacterial membranes, with phospholipids composed of hydrophilic head groups and fatty acids. There are also different glycolipids primarily orientated to the periplasmic space, like phosphatidylinositol mannosides (PIMs), lipomannans (LMs) and lipoarabinomannans (LAMs), which can be extended and reach different layers of the envelope (Dulberger et al., 2020) (***Figure 5***).
- The cell wall is composed of peptidoglycan and arabinogalactan. The peptidoglycan consists of N-acetylglucosamine and N-acetyl/glycolylmuramic acid molecules cross-linked with short peptides. The arabinogalactan is a heteropolysaccharide composed of arabinose and galactose monosaccharides linked to muramic acid by covalent phosphodiester bonds. The arabinogalactan is covalently attached to peptidoglycan by rhamnose- N-acetylglucosamine disaccharide links (Dulberger et al., 2020) (***Figure 5***).
- The mycomembrane is composed of lipids, glycolipids, and secreted proteins. Mycolic acids are long fatty acids (C60-C90) α-branched and β-hydroxylated which are covalently linked to terminal pentaarabinofuranosyl units of the arabinogalactan by ester bonds in the inner leaflet of the mycomembrane. Mycolic acids are sometimes considered as part of the cell wall due to their covalent linkage, covering the matrix formed by the peptidoglycan and the arabinogalactan. Mycolic acids can also be free or linked to trehalose sugar, making trehalose monomycolate (TMM) and trehalose dimycolate (TDM) in the outer leaflet, where there are also other free specific lipids and glycolipids like the trehalose ester families that include sulfolipid (SL), diacyltrehalose (DAT) and polyacyltrehalose (PAT), and phthiocerol dimycocerosate (PDIM) and closely

related phenolic glycolipid (PGL), which are not linked by covalent bonds to the mycolic acids (Dulberger et al., 2020; Jackson, 2014) (***Figure 5***).

- The outer layer of the *M. tuberculosis* envelope is the capsule. It is mainly composed of polysaccharides like α-D-glucans, arabinomannans (AMs) and mannans, but there are also proteins and minor amounts of lipids. The capsule is weakly attached to the rest of the envelope, and it can be easily detached from the bacteria by detergents, which are commonly used in laboratory media to grow mycobacterial cultures, or by shaking. Despite being the outer layer and possibly having a big importance in the infection process, the capsule has been less well characterized than the rest of the components of the mycobacterial envelope and more studies are needed to increase our understanding of the capsule (Kalscheuer et al., 2019) (***Figure 5***).

Different components of the *M. tuberculosis* envelope described above are involved in the TB infectious process.

- PDIM is thought to act masking pathogen-associated molecular patterns (PAMPs), impeding recognition *M. tuberculosis* PAMPs by the different receptors of host immune cells, like Toll like receptors (TLRs). PDIM also induce membrane rupture and phagosome escape and bacterial survival in concert with the ESX-1 system (Augenstreich et al., 2017), as mentioned below. It has been also suggested to take part in the modulation of cell death. *M. tuberculosis* Δ*fadD26* (Camacho et al., 2001; Cox et al., 1999) mutants lack PDIM and are attenuated in different infection models and produce more proinflammatory cytokines than their parental strains (Augenstreich & Briken, 2020; Infante et al., 2005; Rahlwes Kathryn et al., 2022) (***Figure 5***).
- PGL contribute to inhibition of phagosome maturation and inhibition of secretion of pro-inflammatory cytokines through antagonistic interaction with TLR2, interfering with T-cell receptor signaling (Arbués et al., 2016). PGL production has been linked with “hypervirulent” phenotype of Beijing strains from the MTBC Lineage 2 and is absent in L4 MTBC strains due to a frameshift mutation in *pks15/1* gene (Constant et al., 2002) (***Figure 5***).
- SL has been demonstrated to have a role in the inhibition of phagolysosome maturation and to have an antagonistic effect through TLR2 binding, resulting in the inhibition of innate immune responses (Blanc et al., 2017); but mutants lacking SL do not have impaired virulence (Passemar et al., 2014). However, SL

activate nociceptive receptors in the axons of neurons, triggering the cough reflex, essential for transmission of the bacteria (Ruhl et al., 2020) (***Figure 5***).

- DAT and PAT, even though they do not have direct effect in *M. tuberculosis* virulence, they stimulate entry of bacilli into macrophages and epithelial cells and have a role inhibiting phagosome maturation. DAT and PAT also can also inhibit T cell proliferation, preventing a more robust anti-TB adaptative immune response (Augenstreich & Briken, 2020; Rahlwes Kathryn et al., 2022) (***Figure 5***).
- TDM is also known as cording factor and mediates formation of long bacterial "cords" or filaments. TDM and TMM are recognized by macrophages and dendritic cells and induce production and release of different pro- and anti-inflammatory cytokines and chemokines attracting monocytes and neutrophils to infected cells and inducing granuloma formation and maintenance. The detection of mycolic acids induces recruitment of permissive macrophages (Augenstreich & Briken, 2020; Echeverria-Valencia et al., 2018; Rahlwes Kathryn et al., 2022).
- PIMs, LMs and LAMs induce phagocytosis by immune system cells of the host and are recognized by different ligands, like TLR2, to which PIMs and LMs act as agonists, and LAMs as antagonists of its action, modulating production of proinflammatory cytokines. They also induce phagocytosis in macrophages, dendritic cells and neutrophils and LAM inhibit maturation and acidification of the phagosome, inducing bacterial survival (Augenstreich & Briken, 2020; Echeverria-Valencia et al., 2018; Rahlwes Kathryn et al., 2022). (***Figure 5***)
- Mannans and AMs have similar implications like their LMs and LAMs derivates. α-D-glucan induces production of IL-10 and induces phagocytosis, and *M. tuberculosis* mutants deficient in α-D-glucan are highly attenuated in a mice infection model (Rahlwes Kathryn et al., 2022) (***Figure 5***).

It's important to remark that the composition of the mycobacterial envelope is heterogeneous and dynamic and *M. tuberculosis* can control the composition of the envelope depending on the stage of the infection, favoring pro- or anti-inflammatory immune response. Additionally, its components can also be transferred or translocated to host cell membranes by emission of membrane vehicles, by shedding of the capsular layer into the phagosome lumen, or by close physical contact between bacteria and host membranes. Together, this allows modulation of the lipid composition of different membranes of host cell, like plasma, phagosome, or even mitochondrial membrane (Augenstreich & Briken, 2020; Echeverria-Valencia et al., 2018; Rahlwes Kathryn et al., 2022).

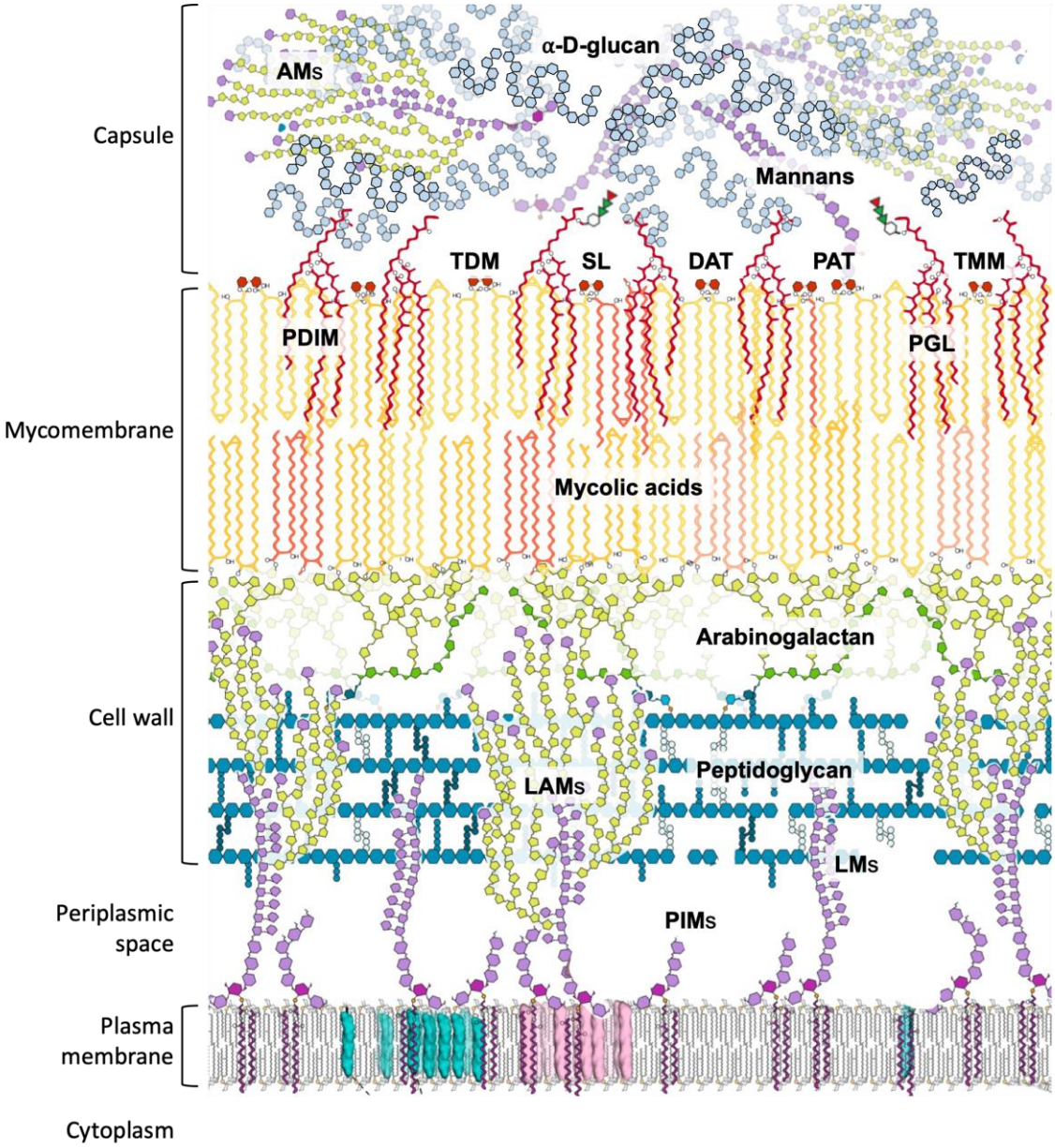

Figure 5: **Scheme of the structure of the envelope of *M. tuberculosis***. Phosphatidylinositol mannosides (PIMs), lipomannan (LM), lipoarabinomannan (LAM), peptidoglycan, arabinogalactan, mycolic acids, trehalose monomycolate (TMM), trehalose dimycolate (TDM), sulfolipid (SL), diacyltrehalose (DAT), polyacyltrehalose (PAT), phthiocerol dimycocerosate (PDIM), phenolic glycolipid (PGL), mannans, arabinomannan (AMs) and α-D-glucan are indicated. Modified from (Dulberger et al., 2020).

Protein virulence effectors of *M. tuberculosis*

M. tuberculosis has multiple proteins from different families that act as virulence factors, which can act as effectors with direct activity to cause the infection, or regulatory systems that control the biosynthesis of virulence effectors, whatever their biochemical natures are. Protein virulence effectors are frequently secreted or displayed in bacterial surface to play their role in virulence, and consequently, protein secretion systems have a key role in virulence. Mycobacteria possess three types of secretion pathways, the general secretion (SecA1) system, which also has a specialized pathway, SecA2; the twin arginine translocation (TAT) system; and five specialized type VII secretion systems, known as 6-kDa early secretory antigenic target (ESAT-6) secretion systems (ESX) (Digiuseppe Champion & Cox, 2007; Gröschel et al., 2016; Miller et al., 2017). Among their substrates we can find:

- Lipoproteins are mainly SecA1/2 substrates that display a N-terminal lipobox through which they are attached to bacterial cell envelope lipids in the different layers, acting on the cell envelope homeostasis, molecular transportation, and nutrient uptake (Becker & Sander, 2016; Echeverria-Valencia et al., 2018; Miller et al., 2017).
- Fibronectin binding proteins, or antigen 85 complex (Ag85), are TAT substrates, which are characterized by a N-terminal signal with a double arginine motif. Ag85 is composed of three proteins, Ag85A, Ag85B and Ag85C. Ag85 proteins allow binding to mucosal surfaces, can prevent phagosome maturation, and induce production of pro-inflammatory cytokines in Th1 cells. They also catalyze the biosynthesis of TDM and attachment of mycolic acids to the arabinogalactan (Karbalaei Zadeh Babaki et al., 2017; Wiker & Harboe, 1992).
- PE and PPE proteins are two large families of proteins which contain in their N-terminal proline-glutamate (P-E) or proline-proline-glutamate (P-P-E) sequences. These proteins are found in mycobacteria, but they are especially abundant in slow-growing pathogenic species, representing around 7-10 % of *M. tuberculosis* genome. They are mainly secreted through the ESX-3 and ESX-5 secretion systems (Ates, 2020; Delogu et al., 2017).
- ESAT-6 is co-secreted with the culture filtrate protein of 10 kDa (CFP-10) through the ESX-1 system of *M. tuberculosis*. For its proper secretion, ESAT-6 also needs the presence EspA, EspC and EspD proteins (Chen et al., 2012; Gröschel et al., 2016). ESAT-6, as it is probably the main virulence effector of *M. tuberculosis*. When secreted, ESAT-6 is involved in membrane permeabilization of the phagosome in coordination with PDIM and induce pore formations that can lead

to its collapse, allowing bacteria to reach the cytosol (Augenstreich et al., 2017; van der Wel et al., 2007). Additionally, it can bind antagonistically with TLR2 receptors, inhibiting production of pro-inflammatory cytokines and it can interfere with antigen presentation through MHCI to cytolytic T cells (Augenstreich & Briken, 2020; Chandra et al., 2022; Echeverria-Valencia et al., 2018; Rahlwes Kathryn et al., 2022). *M. tuberculosis* mutants that do not produce ESAT-6 are highly attenuated, like BCG vaccines mentioned below, in which the loss of ESAT-6 production due to their RD1 deletion is the main reason of their attenuation (Pym et al., 2002).

Mycobacteria, and bacteria in general, also possess regulatory systems that control the activation of the different pathways to promote bacterial survival, like two-component systems, essential for sensing extracellular stresses and vital to mycobacteria in the host-pathogen interaction (Parish, 2014; Stock et al., 2000). One of the most relevant two-component systems in *M. tuberculosis* virulence is the PhoPR system. *M. tuberculosis* Δ*phoP* or Δ*phoPR* mutants are highly attenuated (Gonzalo-Asensio et al., 2014; E. Pérez et al., 2001), and, as mentioned below, *phoP* mutation, with the additional mutation of *fadD26*, are the genetical basis of the MTBVAC vaccine candidate (Arbues et al., 2013).

Prevention of tuberculosis: vaccines

The centenary BCG (1921-2021) is the only and current vaccine licensed to be used against TB. In the beginning of the 20th century, Albert Calmette (1863-1933) and Camille Guérin (1872-1961) obtained the bacilli Calmette-Guérin (BCG) after 230 passages of a strain of *M. bovis*, an animal adapted strain of the MTBC which cause TB in cattle. They demonstrated that vaccination with BCG in laboratory animals protected against TB disease (Daniel, 2006; Herzog, 1998; Pezzella, 2019). The first time it was administered in humans, in 1921, BCG was delivered orally to a newborn whose mother had died of TB a few hours after birth. In addition, the child was under the care of a grandmother also suffering TB. As the child did not develop serious side effects, confirming BCG attenuation, and neither any sign of TB, this first anecdotal success was the beginning of a vaccination campaign in which, by 1924, more than 660 infants had been vaccinated with no ill reports, and by 1928 more than 100.000 children had been vaccinated with BCG, reducing mortality rates from 25% to less than 2% in vaccinated newborns with respect to unvaccinated individuals (Abdallah & Behr, 2017; Calmette, 1931). Since then, BCG vaccine has been used all around the world to prevent TB. Nowadays, BCG is still administered by intradermic route, and it is one of the most used vaccines in the history/world (Lange et al., 2022).

BCG has been studied in depth to understand its molecular and genetic characteristics behind its attenuation. The main cause is the loss of the region of difference 1 (RD1) in BCG bacilli which, when was deleted also in *M. tuberculosis* or *M. bovis,* led to attenuation of the bacteria infecting immunocompromised or immunocompetent mice . In addition, complementation with RD1 of BCG increased virulence of the bacilli, but it was not fully restored, indicating that other mutations, deletions, or insertions accumulated in the genome, might be contributing to the attenuation of BCG (Hsu et al., 2003; Lewis et al., 2003; Pym et al., 2002).

RD1 encodes some components of the ESX-1 secretion system of the MTBC. ESX-1 is the most characterized type-VII protein secretion system of the five that are encoded in MTBC genomes (Abdallah et al., 2007; Ates & Brosch, 2017). The RD1 of BCG comprises around 9.5 kilobases (kb), and 9 genes. Of these, the most important genes are *esxA* and *esxB*, which encode ESAT-6 and CFP-10, respectively.

BCG protects against the most severe forms of TB, disseminated TB, in children. However, protection in adults against pulmonary disease, which allows the bacteria to infect new individuals, is variable (Fine, 1995). Various reasons have been proposed to explain this variability, like pre-exposure with environmental mycobacteria, lack of central T cell memory production by BCG immunization, the loss of immunodominant antigens or the use of the different BCG substrains, which emerged through continuous subcultivation before master batches could be established by lyophilization or cryopreservation techniques (Fine, 1995; Martin et al., 2018; Orme, 2010). With this scenario, to cut off dissemination of TB, we need new vaccines able to overcome this lack, or variable, protection against pulmonary TB.

Current vaccines against tuberculosis in clinical trials

Different strategies are currently being developed to increase the protection efficacy of BCG. The new strategies require to improve BCG protection, which mean to be as safe as BCG and confer better protection in newborns or be safe and effective in adolescents and adults (Walker et al., 2010; WHO, 2018). By October 2022 there are sixteen new vaccine candidates against TB in different clinical trial stages that can be classified into whole cell vaccines, with live attenuated or inactivated mycobacteria; and subunits vaccines, which contain one or several immunodominant antigens of *M. tuberculosis*, classically administered as recombinant proteins with adjuvants or in viral vectors. However, with the recent development of mRNA technology due to COVID-19 pandemic, the interest in the development of new vaccine candidates against TB based in this technology has increased and at the end of September 2022, the first two mRNA vaccine

candidates against TB entered in phase I clinical trials, which might be classified in the group of subunits vaccines as they encode a pool of antigens against MTB, which are unpublished (***Figure 6***) (Andersen & Kaufmann, 2014; Andersen & Scriba, 2019; Frick, 2022; Kaufmann, 2021; WHO, 2022a).

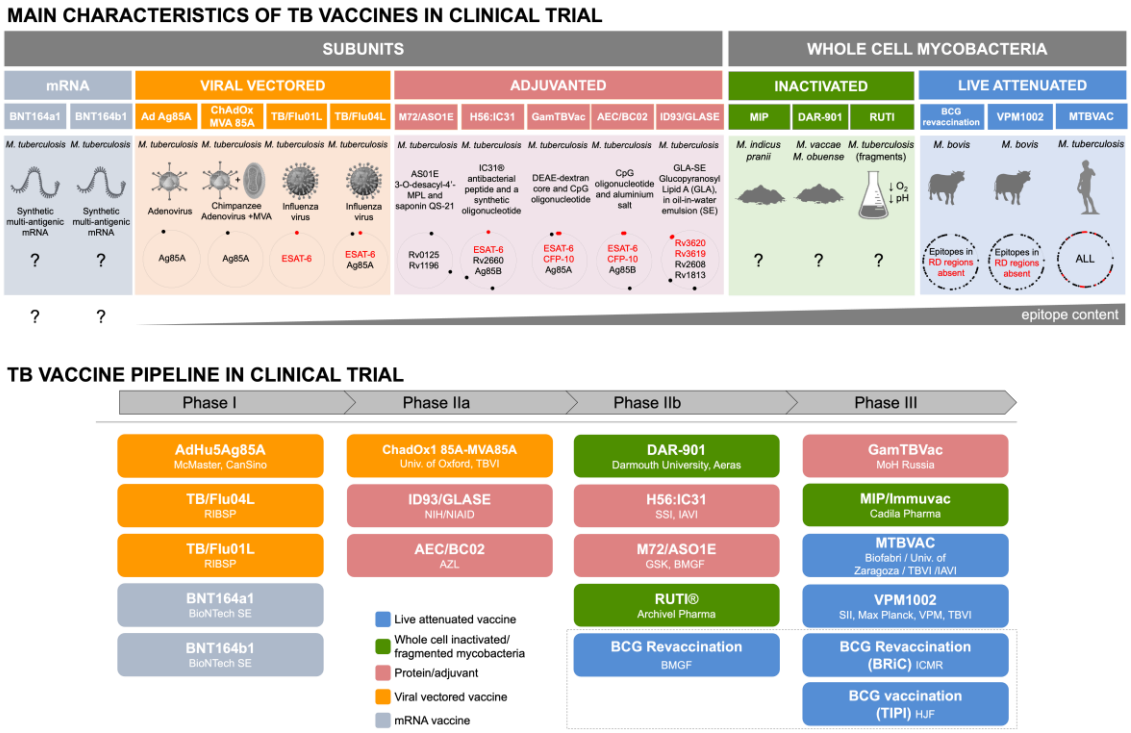

Figure 6: **New TB vaccines in clinical trials**. Main characteristics of new TB vaccine candidates in clinical trials (top) and its clinical stage phase of development (bottom) in comparison with BCG vaccine. Updated from (Martin et al., 2018) with (WHO, 2022a) data.

One of the most advanced vaccine candidates is the live attenuated vaccine candidate MTBVAC, the first and only vaccine candidate in clinical trials based on a human infecting strain of MTB, the MT103 strain, attenuated by genetic manipulation in the laboratory (Arbues et al., 2013). MTBVAC is based on two independent gene deletions, both contributing to the attenuation of the bacteria. These two genes, *phoP* and *fadD26*, are virulence factors of MTB and are irreversibly inactivated. MTBVAC was developed in the University of Zaragoza, in the Mycobacterial Genetics Group, in collaboration with the Pasteur Institute and the industrial partner Biofabri, which is the responsible of the industrial and clinical development of the vaccine candidate. MTBVAC has successfully demonstrated safety and protection in different preclinical animal models and phase I clinical trials have shown that it is safe in adults and newborns (Spertini et al., 2015;

Tameris et al., 2019). Results from Phase IIa clinical trials in adults and newborns are currently being analyzed and phase III is currently ongoing (NCT04975178), and it is going to enroll 6960 newborns to measure its effectiveness in comparison to BCG (Martín et al., 2021).

Treatment of *M. tuberculosis* infections

TB is a disease with high mortality rates without adequate treatment. The historical records of the disease have revealed that, in the absence of antibiotic treatment, the mortality rate of active pulmonary TB disease is between 20% in smear negative individuals to 70% in smear positive individuals (Tiemersma et al., 2011). Introduction of antibiotics has allowed to develop effective therapies that increased survival of TB patients over 85% (WHO, 2022a).

After initial monotherapies with the different antibiotics discovered through the antibiotic "Golden Age", a clinical study in 1950 demonstrated that combination of streptomycin and *p*-aminosalicylic acid was more effective and reduced emergence of drug resistance compared to the use of the single drugs, leading to the study of new combinations with antibiotics available and which each one discovered to be active against TB (Iseman, 2002; Ma et al., 2010). Nowadays, the latest "WHO guidelines for TB treatment" still recommend the four-drug oral regimen that was stablished in the 1980s, consisting of 2 months of rifampicin, isoniazid, ethambutol, and pyrazinamide, followed by a continuation phase of 4 months of rifampicin and isoniazid for patients with drug-susceptible TB. However, it has been also included new first-line regimens, like reduction of the standard treatment in patients between 3 months and 16 years old to 2 months of rifampicin, isoniazid, and pyrazinamide with optional ethambutol, followed by a continuation phase of 2 months of rifampicin and isoniazid; or 4 months of rifapentine, isoniazid, pyrazinamide, and moxifloxacin for patients older than 12 years (WHO, 2022a, 2022b).

However, the emergence of drug resistance reduces success rates of the treatments, which is aggravated by the fact that anti-tuberculous treatments, which are long and comprise and average of ten pills per day in the intensive phases, are poorly tolerated by a considerable proportion of the patients (Dartois & Rubin, 2022; Luetkemeyer et al., 2011; Ma et al., 2010; Tiberi et al., 2018). Uncomplete treatments increase the possibilities of apparition of drug resistance in *M. tuberculosis* strains.

Mechanisms of drug resistance in *M. tuberculosis*

Bacteria have different natural and acquired drug resistant mechanisms: limitation of drug permeability or uptake; expulsion of the drug by efflux mechanisms; modification of the drug target; or inactivation of the drug (Uddin et al., 2021). Additionally, transcription factors can modulate bacterial response to antibiotic stresses.

M. tuberculosis is intrinsically resistant to many antibiotics due to several factors. The special structure of the mycobacterial cell envelope, its thickness and hydrophobicity, makes an excellent permeability barrier (Xu et al., 2017); and the different efflux pumps genes encoded in its genome, like *p55* gene that encodes P55 efflux pump, which extrudes tetracyclines and aminoglycosides outside the bacteria (Silva et al., 2001); limiting intracellular concentration and reducing antibiotic efficacy (de Rossi et al., 2002). *M. tuberculosis* also encodes different genes for modifying enzymes, like *erm37,* which encodes a 23S rRNA methyltransferase, modifying the target of different macrolides (Madsen et al., 2005); or *blaC,* which encodes for a β-lactamase, which inactivate β-lactams (Flores et al., 2005); making *M. tuberculosis* resistant to different antibiotics. Additionally, *M. tuberculosis* encodes different regulatory proteins, like *whiB7*, that enables intrinsic responsive resistance to different antibiotics, inducing expression of genes involved in the processes mentioned above or overexpressing the drug target (J.-H. Lee et al., 2020).

M. tuberculosis can also acquire resistance trough accumulation of mutations in its genome that affect the processes mentioned above, like mutations affecting to RNA polymerase *rpoB* modifying its structure cause rifampicin resistance; or resistance to isoniazid is related with *katG* mutations, needed to transform the prodrug in the active drug, or in *inhA* promoter, increasing InhA protein expression (Khawbung et al., 2021).

Drug resistance in *M. tuberculosis*

Emergence and spread of drug or antimicrobial resistance is one of the top 10 global public health threats declared by the WHO (*Antimicrobial Resistance*, 2021). Almost half of the global cases of drug resistant TB are estimated to be present in three countries, India, Pakistan, and the Russian Federation (***Figure 7A***). Data from the WHO estimates that in 2021 at least 3.6% of new cases and 18% of relapses from patients with previous antibiotic treatment were drug resistant TB, computing a total of 450 000 drug resistant cases. That implies an increase of incidence of 3.1% from 2020, in which probably one of the main reasons has been the impact of SARS-CoV-2/COVID-19 pandemic (***Figure 7B***) (WHO, 2022a).

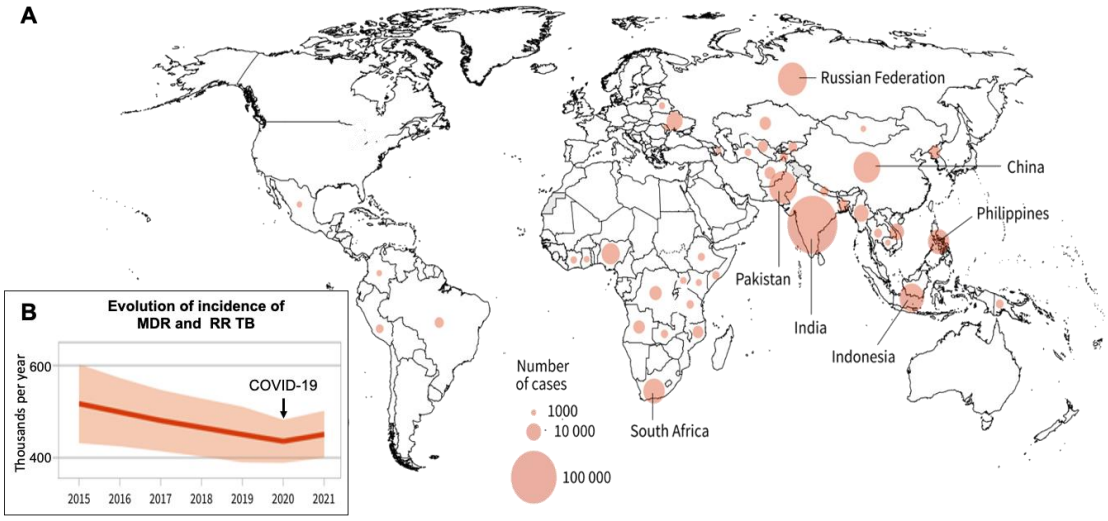

Figure 7: **Global incidence and evolution of MDR-TB.** (**A**) Global distribution of multi drug (MDR) and rifampicin resistance (RR) TB cases reported in 2021. (**B**) Annual evolution of MDR and RR TB estimated incidence. Adapted from (WHO, 2022a).

WHO guidelines to classify *M. tuberculosis* resistant strains have been recently updated, including, and redefining some terms accordingly to current recommended drug regimens, differentiating now into the following groups (WHO, 2020b):

- Isoniazid resistant (Hr) TB: caused by *M. tuberculosis* strains resistant to isoniazid.
- Rifampicin resistant (RR) TB: caused by *M. tuberculosis* strains resistant to rifampicin.
- Multi drug resistant (MDR) TB: caused by *M. tuberculosis* strains resistant to, at least, isoniazid and rifampicin.
- Pre-extensive drug resistant (Pre-XDR) TB: caused by MDR or RR *M. tuberculosis* strains that are also resistant to at least one fluoroquinolone (levofloxacin or moxifloxacin).
- Extensive drug resistant (XDR) TB: caused by Pre-XDR *M. tuberculosis* strains that are also resistant to at least one of bedaquiline or linezolid.

Additionally, the term “totally drug resistant” (TDR) TB was proposed in 2009 to define strains “virtually untreatable", resistant to all first line (isoniazid, rifampicin, ethambutol, pyrazinamide, streptomycin,) and second-line drugs available at that time (ethionamide, *p*-aminosalicylic acid, cycloserine, ofloxacin, amikacin, ciprofloxacin, capreomycin,

kanamycin) (Akbar Velayati et al., 2013). With current WHO guidelines, TDR strains now would be classified as MDR.

Patients infected with drug resistant *M. tuberculosis* strains cannot be treated with standard regimens, and their treatment needs to be supported by counselling to apply a standardized treatment for drug resistant strains or design it accordingly to the drug susceptibility tests and the clinical history of the patients. To this cause, the Guideline Development Group of the WHO classified the different second line drugs available to treat MDR TB into three groups of recommended use based on relative benefits (effectiveness) and harms (safety) (***Table 1***) (WHO, 2020c):

- Group A: drugs considered highly effective and strongly recommended for inclusion in all regimens unless contraindicated.
- Group B: recommended as agents of second choice.
- Group C: all other drugs.

Table 1: **Anti-tuberculous drugs classification.** Classification by recommended use of the second line drugs for TB by the Guideline development Group of the WHO (WHO, 2020c). Recently approved pretomanid drug is not listed in this table, probably because of the absence of commercial drug susceptibility test, which are under development.

Group A	**Group B**	**Group C**
Levofloxacin *or* Moxifloxacin	Clofacimine	Ethambutol
Bedaquiline	Cycloserine *or* Treizidone	Delamanid
Linezolid		Pyrazinamide
		Imipenem-cilastatin *or* Meropenem
		Amikacin (*or* streptomycin)
		Ethionamide *or* Prothionamide
		P-aminosalicylic acid

Even though the global concern about TB, drug resistance, and the urgent need of new effective antibiotics, no new drugs were approved for TB treatment from 1970s to 2010s. Between 2012 and 2014, the Food and Drug Administration (FDA) and the European Medicines Agency (EMA) approved two new chemical compounds, bedaquiline (Mahajan, 2013) and delamanid (Ryan & Lo, 2014) for its use against MDR TB. In 2019 the FDA approved de first regimen against XDR TB in which pretomanid is included, the triple combination of bedaquiline, pretomanid and linezolid (BPaL) (FDA, 2019;

Samoilova et al., 2022). In the last WHO report there are listed different clinical trials testing new regimen combinations of the available and repurposed drugs; 17 new antibiotics that have entered in Phase I and Phase II clinical trials and a total of 7 drugs in Phase II clinical trials that are intended to be used as Host Directed Therapies (***Table 2***) (WHO, 2022a), to enhance the efficacy of antibiotic treatment, improving the outcomes of the patients. This highlights the urgent need of new antibiotics, but also of new innovative therapies, to be developed to fight against TB. The use of mycobacteriophages, specific viruses that can recognize and kill mycobacteria; or the use of antivirulence molecules, drugs that can sabotage virulence mechanisms of the pathogen; are some of the innovative strategies proposed to combat drug resistance (Dickey et al., 2017).

Chapter 1 of this manuscript will deal with the development of a screening and characterization platform for the discovery of new drugs against TB with potential antivirulence activity.

Table 2: **Clinical stage of the new antibiotics and host directed drugs** (pale yellow highlight)

Phase I	Phase II
Macozinone	BTZ-043
BVL-GSK098	GSK-3036656
GSK-286 (GSK 2556286)	OPC-167832
TBAJ-587	SPR720 (Fobrepodacin)
TBAJ-876	Telacebec-(Q203)
TBI-166	TBA-7371
TBI-223	SQ109
	Sutezolid
	Sudapyridine (WX-081)
	Delpazolid
	Pravastatin
	Imatinib
	Metformin
	Everolimus
	Auranofin
	Vitamin D3
	CC-11050

Incidence of Nontuberculous mycobacteria infections

The number of pulmonary infections caused by nontuberculous mycobacteria (NTM) are increasing worldwide in the last decades (Ratnatunga et al., 2020; Stout et al., 2016). Pulmonary infection is the most common clinical manifestation of NTM infections, termed as pulmonary NTM disease, and can be presented in three forms: fibro-cavitary disease, nodular bronchiectasis disease, and hypersensitivity pneumonitis (Griffith et al., 2012). In 1987, the US centers for disease control and prevention (CDC) estimated the NTM disease rate of 1.8/100.000 (Kendall & Winthrop, 2013). Data from North American studies between 2006 and 2012 suggested a disease rate of 5 to 10 per 100,000 (Prevots & Marras, 2015). In Queensland, Australia, the increase of incidence has been well documented through the last decades, and projections show that the number of cases due to NTM infections can multiply from 2 to 4 times in the next 20 years (***Figure 8***).

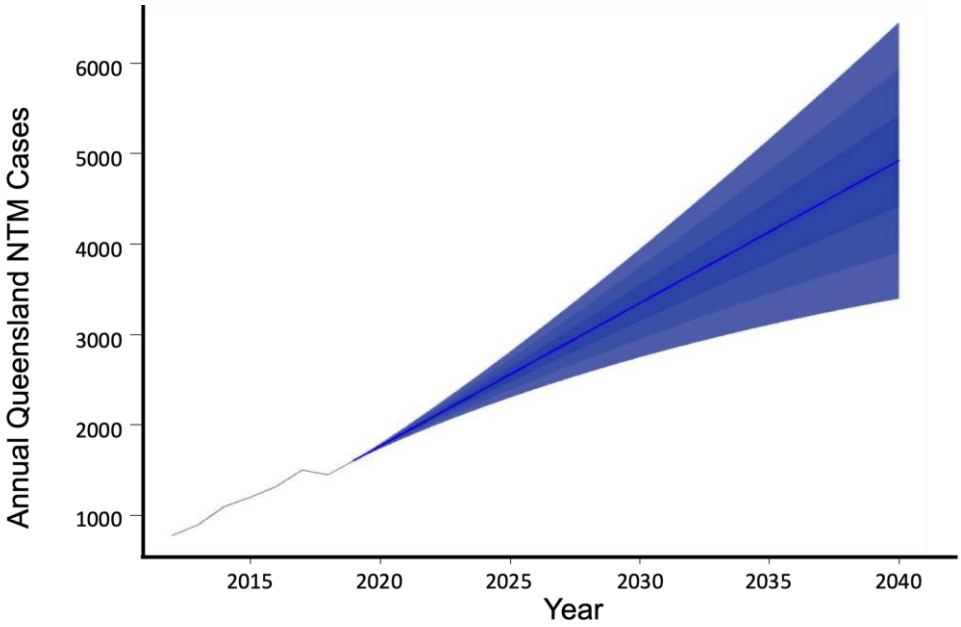

Figure 8: **Evolution and prediction of NTM incidence**. Number of NTM cases in Queensland, Australia, reported from 2012 to 2019, and predicted for the period from 2020 to 2040. Adapted from (Ratnatunga et al., 2020).

The historical incidence of NTM pulmonary disease is unknown as they cause similar clinical manifestations and lesions as *M. tuberculosis* infections. When isolating the first clinical strains there was a false belief that they were unusual *M. tuberculosis* strains (Falkinham, 1996). In areas with high incidence of TB, pulmonary NTM disease can be wrongly diagnosticated as TB or MDR-TB. One example is the case of a referral center

in Brazil in which 79 % of patient with pulmonary NTM infection were empirically treated up to six months for TB before the correct diagnostic because TB is generally diagnosed based on smear microscopy rather than culture (Prevots & Marras, 2015). The majority of NTM pulmonary infections have been primarily notified in industrialized countries (***Figure 9***) probably due to the absence of compulsory reporting in most countries and the limited access to proper diagnostic tools in all countries (Boehme et al., 2021; Mougari et al., 2016). However, the improvement of microbiologic and molecular diagnostic has allowed to identify the causative NTM species that cause pulmonary disease.

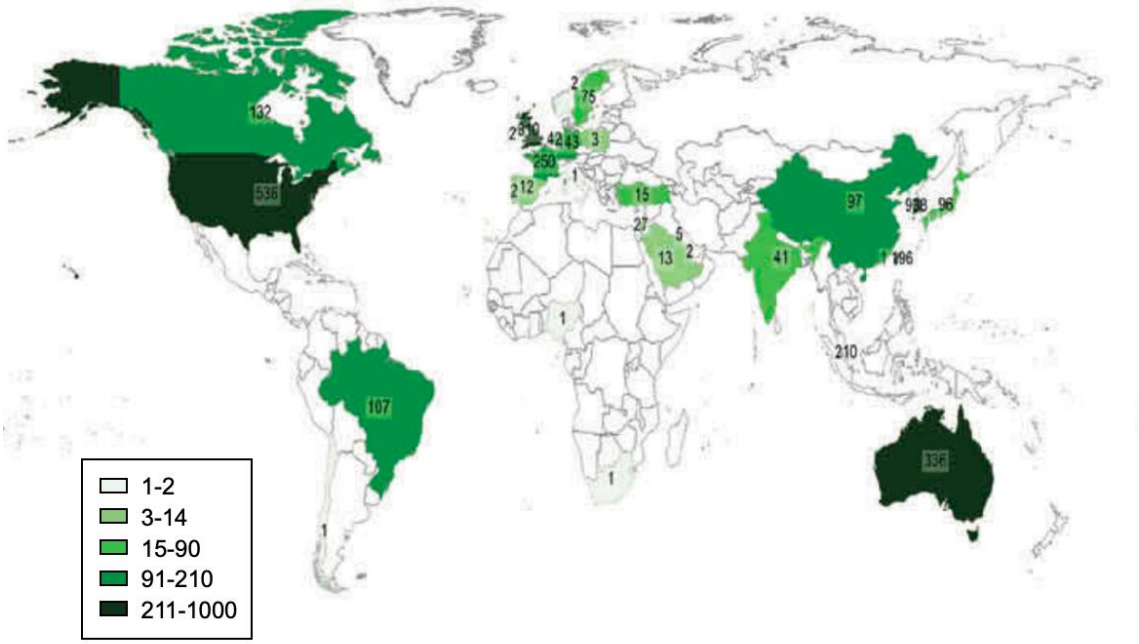

Figure 9: **Global distribution of pulmonary *M. abscessus* clinical isolates notified in PubMed from 1992 to 2015.** Adapted from (Mougari et al., 2016).

The term “nontuberculous mycobacteria” includes all those *Mycobacterium spp.* that do not belong to the MTBC and *M. leprae*. It comprises a wide variety of species, including slow growing mycobacteria like *M. ulcerans* and the *M. avium* complex, or rapid growing mycobacteria like *M. smegmatis* or the *M. abscessus* complex (***Figure 3***). NTM are usually environmental species, which are saprophytes or non-pathogenic to humans and animals (Gupta et al., 2018).

Although, alterations in the immunological predisposition of the host and the exposition with NTM environmental niches (soil and water) can allow certain species to cause very

serious diseases, including lung infections (Johansen et al., 2020). Among them, the most common organisms that cause pulmonary NTM disease are the slow-growing mycobacteria from the *Mycobacterium avium* complex, and the fast-growing mycobacteria from the *Mycobacterium abscessus* complex (MABC), considering them as emergent pathogens (Lim et al., 2018; Ratnatunga et al., 2020; Tan et al., 2018).

The concern of *M. abscessus*

The MABC is currently divided in three different subspecies, *M. abscessus* subsp. *abscessus* (*M. abscessus*), *M. abscessus* subsp. *abscessus massiliense (M. massiliense*) and *M. abscessus* subsp. *abscessus bolletii*. (*M. bolletii*) in which *M. abscessus* is the most common pathogen (Koh et al., 2014), especially in patients with chronic lung diseases, such as cystic fibrosis or chronic obstructive disease (Floto et al., 2016; Griffith et al., 2012). The intrinsic resistance of the *M. abscessus* complex make treatment similar to that of MDR TB with few therapeutic options available (Griffith & Daley, 2022; Nessar et al., 2012). Official guidelines for MABC pulmonary disease cannot state an optimal regimen of drugs and duration for MABC pulmonary infections. Treatment recommendations are based in the presence (typically *M. abscessus*) or absence (typically *M. massiliense*) of different resistant mechanisms to macrolides (Daley et al., 2020). Antimicrobial success rates depend on the antibiotic susceptibility of infecting strains. For example, treatment of *M. massiliense* is around 90% effective in sputum conversion, while treatment of *M. abscessus* is below 50% of sputum conversion (Griffith & Daley, 2022). This highlights the importance of identification and confirmation of the drug resistance mechanisms in clinical isolates and design of drug treatment regimens.

Chapter 2 of this manuscript will deal with the development of a methodology to stablish a genotype-phenotype relationship of drug resistance in *M. abscessus* and, therefore, a more extensive introduction will be provided in the corresponding in that section.

CHAPTER 1

INTRODUCTION

Two component systems in *M. tuberculosis*

Bacteria are ubiquitous, and they need to adapt through their lifetime to different changes in their environment in order to survive or proliferate in response to external signals or stresses. These adaptative phenotypic responses require molecular mechanisms to regulate the expression levels of different genes. Among them, we can find two-component systems, which are key to respond to changes in bacterial environment. Two-component systems are composed of a sensor protein and a response regulator. The stimuli or stresses are detected by dimers of the sensor protein, which are usually membrane associated proteins. They are histidine kinase proteins composed of a receiver domain in which lies the specificity of the signal detection and a transmitter domain with kinase activity. The sensor domain is in the extracellular side whereas the transmitter domain is in the cytosolic side of the membrane, bonded by a transmembrane domain. When the sensor proteins receive the appropriate signal, they autophosphorylate in a histidine residue and interact with the response regulators. The response regulators are cytoplasmatic proteins with a response regulator domain and a DNA binding domain, and act as transcription factors depending on their phosphorylation state on an aspartate residue (Jung et al., 2012; Parish, 2014; Stock et al., 2000).

In the case of *M. tuberculosis*, as a strict intracellular pathogen, it needs to adapt to the adverse conditions found in the intraphagosomal environment. *M. tuberculosis* genome encodes twelve two-component systems, eleven of them encoded as operons. Additionally, it has encoded an orphan sensor protein and four orphan response regulators. This relative low number of two-component systems present in *M. tuberculosis* genome might reflect its strict adaptation to the intracellular environment through its evolution (Bretl et al., 2011; Cole et al., 1998; Cook et al., 2009; Haydel & Clark-Curtiss, 2004; Parish, 2014). The role of each two-component system in *M. tuberculosis* is not known, neither all the roles of those that have been characterized. However, it is known that several of them are involved in the control of dormancy/persistence state (DosRST) and virulence (PhoPR, SenX3/RegX3, PrrAB and MprAB) of the bacteria (Bretl et al., 2011; Parish, 2014).

The PhoPR system in *M. tuberculosis*

One of the most characterized two-component systems in *M. tuberculosis* is the PhoPR system, which is one of the central research lines of our laboratory. The PhoPR system

consist of PhoP and PhoR proteins, which act as response regulator and sensor protein respectively, encoded by the genes Rv0757 (*phoP*) and Rv0758 (*phoR*), which are transcribed in a single operon. The impact of the PhoPR system in *M. tuberculosis* virulence phenotypes has been characterized in depth. The overexpression of *phoP* gene (Gonzalo-Asensio et al., 2014; Samper & Martín, 2007; Soto et al., 2004), and presumably *phoR* gene, in a rare *M. bovis* clinical strain due to the insertion of an *IS*6110 led to an unusual outbreak in the 1990s with high transmission by aerosols and has been demonstrated that increased the virulence of this strain. On the other hand, deletion mutants of *phoP* or *phoPR* genes in *M. tuberculosis* strains from different lineages showed attenuation in different *ex vivo* and animal infection models (Gonzalo-Asensio et al., 2006, 2014; Gonzalo-Asensio, Mostowy, et al., 2008; Gonzalo-Asensio, Soto, et al., 2008; E. Pérez et al., 2001). Indeed, one of the key differences between the laboratory strain *M. tuberculosis* H37Rv (virulent) and its close related H37Ra (avirulent) is a cytosine to thymine mutation in the 219th codon of the *phoP* gene. That SNP leads to a serine to leucine mutation in the PhoP protein which makes it unable to bind to the DNA and control virulence associated PhoPR phenotypes of *M. tuberculosis.* Complementation with the H37Rv *phoP* allele partially restores virulence phenotypes in H37Ra (Frigui et al., 2008; Gonzalo-Asensio, Soto, et al., 2008; J. S. Lee et al., 2008). The in-depth molecular characterization of the PhoPR system revealed that this system is involved in different processes linked to the virulence of *M. tuberculosis*. Even its not clear the exact stimuli sensed by PhoR protein, PhoR phosphorylates PhoP, and it changes its conformation, allowing its dimerization and controlling the expression of different genes (Sinha et al., 2008). It controls approximately 2-4% of the open reading frames of *M. tuberculosis* genome, involving the following phenotypic characteristics:

- The PhoPR system controls the expression of *pks2* and *pks3* genes, encoding for polyketide synthetase proteins involved in the biosynthesis of acylthrealose-derived lipids. Consequently, *M. tuberculosis* strains defective in the PhoPR system do not synthetize SL, and DAT and PAT (Gonzalo-Asensio et al., 2006; Walters et al., 2006) (***Figure 10***).
- *M. tuberculosis* strains defective in the PhoPR system do not secrete ESAT-6. The PhoPR system regulates ESAT-6 secretion in a complex manner. PhoP binds directly to the promoter of the *espACD* operon, which controls the secretion of ESAT-6 through the ESX-1 machinery. Additionally, PhoP controls the expression of *espR* and *whiB6*, two transcription factors that also activate the transcription of the *espACD* operon. In H37Rv and H37Ra strains, the *whiB6* promoter has a single nucleotide polymorphism that leads to the down regulation

of *whiB6* gene by the PhoPR system. This has been proved to reduce secretion of ESAT-6 in H37Rv in comparison with clinical *M. tuberculosis* strains (Broset et al., 2015) (***Figure 10***).

- *M. tuberculosis* strains with a defective PhoPR system increase secretion of several antigenic proteins through the TAT system. RNA-seq and ChIP-seq analysis revealed that the most upregulated region by the PhoPR system belongs to the non-coding RNA (ncRNA) *mcr7*. This ncRNA has been demonstrated to bind to the ribosome binding site of the *tatC* mRNA, downregulating its translation. *tatC* encodes the protein of the TAT system involved in the recognition of the N-terminal signal sequence of TAT substrates, a twin arginine motif (RR). Expression of *mcr7* reduces the secretion of TAT substrates, like the immunodominant antigens belonging to the Antigen 85 Complex, Ag85A and Ag85C. In the absence of an active PhoPR system, *mcr7* expression is absent and, therefore, there is no inhibition of the translation of *tatC* mRNA and the consequent increased secretion of TAT substrates (Solans et al., 2014) (***Figure 10***).

Recent studies applying metabolomics to study the impact of PhoPR inactivation in *M. tuberculosis* have led to discover new phenotypes controlled by this two-component system:

- PhoPR system-defective *M. tuberculosis* strains increase production and secretion of the c-di-AMP second messenger. The role of this cyclic (di)nucleotide in *M. tuberculosis* virulence and immunity is being explored. Overproduction of c-di-AMP in CDC1551 strain by *disA* overexpression led to higher attenuation in mice than the parental strain (Dey et al., 2015). Consequently, overproduction of c-di-AMP in *M. tuberculosis* strains because of an inactive PhoPR system may contribute to their attenuation (I. Pérez et al., 2022) (***Figure 10***).
- *M. tuberculosis* defective in the PhoPR system produce, or accumulate, more PIMs, reducing the number of anchored lipids such us LAMs and LM in the mycobacterial cell envelope, what might contribute to the attenuation of these bacteria (Díaz et al., 2019) (***Figure 10***).

Considering the experimentally demonstrated virulence phenotypes when genetically inactivating the PhoPR system in *M. tuberculosis* (***Figure 10***), this two-component system represents a promising target to develop an antivirulence therapy.

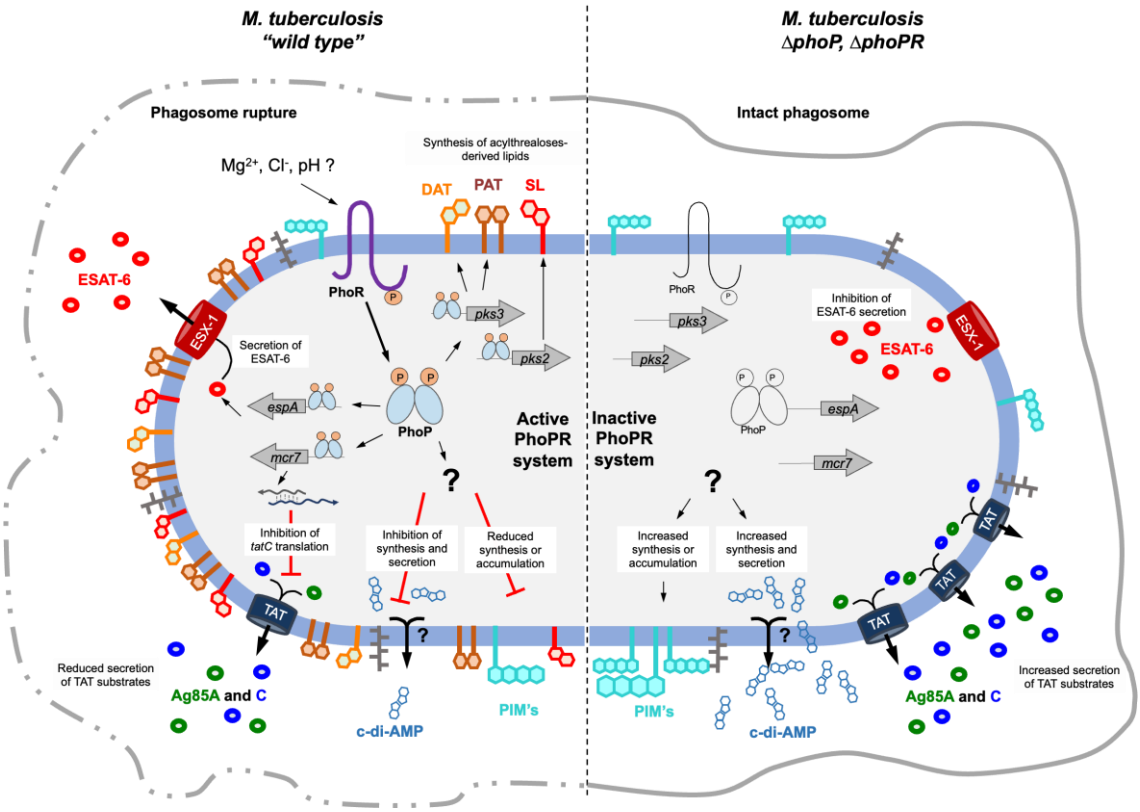

Figure 10: **Schematic representation of the impact of the PhoPR system in *M. tuberculosis* phenotypes.** An active PhoPR system (left) induces synthesis of acylthrealoses-derived lipids, SLs and DATs and PATs, and secretion of ESAT-6 protein; and inhibits secretion of TAT major antigens substrates; synthesis and secretion of second messenger c-di-AMP and accumulation of PIMs. All these allow *M. tuberculosis* to break macrophage's phagosomes to reach the cytosol. Inactivation of the PhoPR system (right) reverses these phenotypes, impeding phagosome scape.

Antivirulence therapies

The emergence and spread of antimicrobial resistance in bacterial pathogens are in the top 10 global public health threats declared by the World Health Organization (*Antimicrobial Resistance*, 2021). To fight against them, there are different strategies that the scientific community is following, including "classical" approaches like antimicrobial therapies against new and old targets, and "innovative" approaches like phage therapy or antivirulence approaches (***Figure 11A***) (Theuretzbacher et al., 2020).

Among the different innovative strategies, we have focused our interest in the antivirulence approach. Antivirulence strategies are based the inactivation of virulence factors of the pathogen. The inhibition of virulence factors does not directly kill or inhibit replication of the bacteria, but sabotage the pathogen to develop infection and cause disease. To develop an antivirulence strategy, we need a deep understanding of how

the pathogen cause the disease in the host and how their virulence factors are involved in the host-pathogen interactions (Dickey et al., 2017; Totsika, 2016). In the last years, the interest in antivirulence approaches has increased in the scientific community (***Figure 11B***).

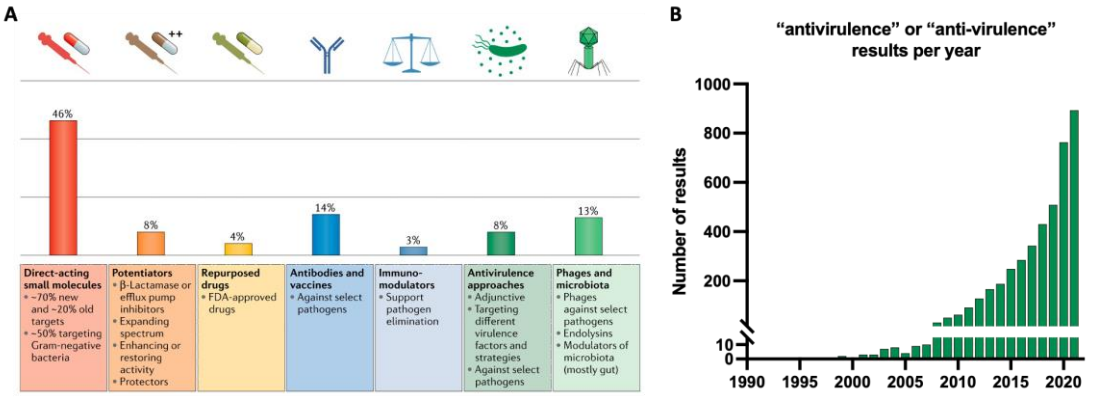

Figure 11: **Interest in novel strategies to combat drug resistance**. **(A)** Overview of the preclinical pipeline against bacterial pathogens. Adapted from reference (Theuretzbacher et al., 2020). **(B)** Number of results per year of "antivirulence" or "anti-virulence" terms in PubMed.

Antivirulence strategies should improve some aspects when comparing with "classical" antimicrobials, such as less off-target effects in the host microbiota or less selective pressure than antimicrobials. However, they would probably be also less effective than antimicrobials and could be not effective in all forms and times of the disease caused by the same pathogen or in the different strains (Dickey et al., 2017). Their potential use alone or in combination with other antimicrobials is being tested in different pathogens like *Pseudomonas aeruginosa* (Rezzoagli et al., 2020; Starkey et al., 2014), *Acinetobacter baumannii* (Bondareva et al., 2022; Lin et al., 2012), *Staphylococcus aureus* (Gao et al., 2022; J. Zhang et al., 2014) or *Enterobacteriaceae* (Thabit et al., 2022).

The development of antivirulence treatments for *M. tuberculosis* infections has also attracted interest. Blocking certain mycobacterial cell wall proteins (such as lipoarabinomannan, α-crystallin, or heparin-binding haemagglutinin) with human or mouse monoclonal antibodies can improve the outcomes of mice by preventing the mycobacteria from attaching, entering, and surviving inside cells. (Balu et al., 2011; Hamasur et al., 2004; Pethe et al., 2001). Comparison of activities in *M. tuberculosis in*

vitro growth inhibition assays and in an anticytolytic screening in infected fibroblasts led to the discovery of two compounds which had no effect in bacterial *in vitro* survival but protected fibroblast of being killed by *M. tuberculosis*. Characterization of these two compounds revealed that they have inhibitory activity against ESX-1 substrates like ESAT-6 (Rybniker et al., 2014). These two compounds have different mechanism of action, as one acts through the inhibition of the MprAB two component system and the second one appears to be an unspecific blockader of protein secretion systems in mycobacteria.

Due to the key role of the PhoPR system in *M. tuberculosis* virulence, the interest in developing drugs able to inhibit its activity has raised in the last years. Different groups have developed different platforms to screen potential PhoPR inhibitors based on *in vitro* target or whole cell phenotypic approaches. The platform developed by Johnson and colleges was used to test around 220,000 compounds in a high throughput screening (HTS) and led to the identification of Ethoxzolamide (ETZ) (***Figure 12A***) as inhibitor of *M. tuberculosis* PhoPR system (Johnson et al., 2015). ETZ is a benzothiazole-2-sulfonamide with carbonic anhydrase (CA) inhibitory activity which has been used as treatment of glaucoma, duodenal ulcers, and epilepsy (Kumar et al., 2021). ETZ inhibitory effect has been described not only for human carbonic anhydrases (hCA), but also for carbonic anhydrases of *M. tuberculosis* (mtbCA) (***Figure 12B***) (Carta et al., 2009). A deep characterization of the inhibitory effect of ETZ in *M. tuberculosis* strains led to the confirmation of the PhoPR inhibitory activity by confirming the absence of production of SL, reduced secretion of ESAT-6 and overlap of transcription profiles of bacteria in the presence of ETZ and PhoPR mutants. Additionally, ETZ treatment was shown to reduce bacterial replication of *M. tuberculosis* in macrophage and mice infection models (Johnson et al., 2015).

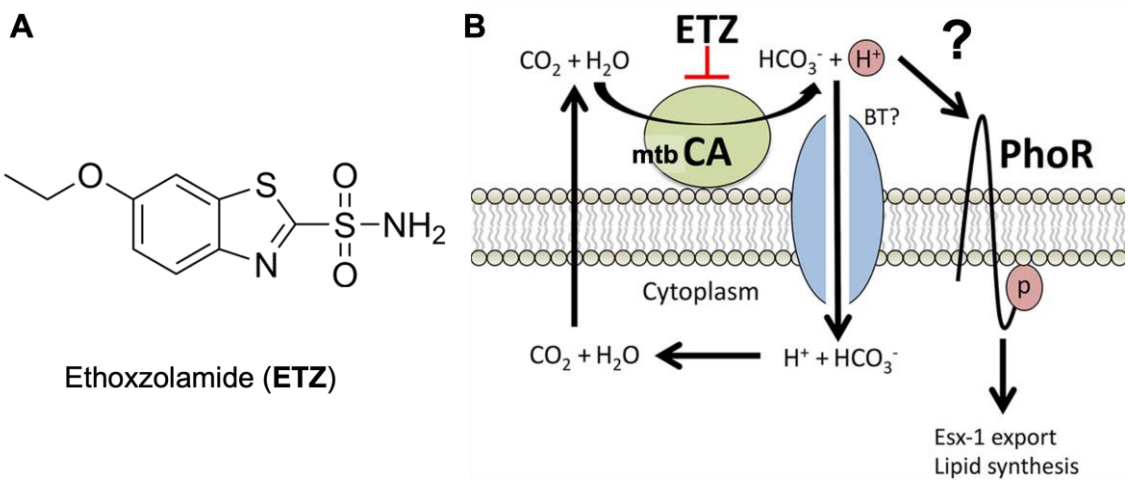

Figure 12: **ETZ and its hypothesized mechanism of action** (**A**) Structure of ethoxzolamide (ETZ). (**B**) Proposed mechanism of action of ETZ, adapted from (Johnson et al., 2015).

In order to set up our own PhoPR screening platform, we propose to use ETZ as control compound to set up the screening platform and the secondary assays to characterize potential PhoPR inhibitors, based on the different assays used in the Mycobacterial Genetics Group to characterize the PhoPR system through the last decades.

In a previous PhD project accomplished in the Mycobacterial Genetics Group, different PhoPR reporter strains were constructed to attempt to determine the signals modulating its expression (Arnal, 2016). These reporter strains were constructed using the integrative pFPV27 plasmid as backbone (Barker et al., 1998), in which different PhoPR regulated promoters were cloned controlling the expression of the GFP mut2 gene (Kremer et al., 1995). Of the different strains constructed in the *M. tuberculosis* H37Rv genetic background, those carrying the *pks2* promoter controlling the GFP reporter gene, showed the best correlation with PhoPR activity. Accordingly, we decided to explore the potential of this strain to be used for the discovery of PhoPR inhibitors.

OBJECTIVES

The general objective of this Chapter is to develop a proof-of-concept for screening potential PhoPR inhibitors. With the aim to develop a High Throughput Screening platform to identify and characterize molecules with potential antivirulence activity against *M. tuberculosis*.

To achieve this objective, the following sub-objectives has been established:

- Validation of ETZ as control compound with inhibitory activity in *M. tuberculosis* PhoPR system and verification of existing *M. tuberculosis* reporter strains.
- Construction and characterization of new *M. tuberculosis* reporter strains with enhanced GFP fluorescence under the control of two different PhoPR regulated promoters, *mcr7* and *pks2*, using different genetic backgrounds of the MTBC.
- Set up of secondary assays to characterize PhoPR inhibitors to evaluate the downregulation of the PhoPR core regulon genes and the inhibition of the secretion of the main virulence effector controlled by the PhoPR system.
- Transfer the PhoPR system of *M. tuberculosis* to a non-pathogenic mycobacterium, *M. smegmatis,* to be used it as a safer surrogate for the screening of potential antivirulence compounds.

MATERIALS AND METHODS

Basic microbiology procedures

Manipulation of *Escherichia coli* and mycobacterial strains was performed in a biosafety level 1 laboratory (BSL1), in a biosafety level 2 laboratory (BSL2) or biosafety level 3 laboratory (BSL3), with facilities notification A/ES/10/I-05, A/ES/06/I-02 and A/ES/04/I-05 respectively.

Plasmids used and constructed are listed in ***Table 3***. Bacterial strains used and obtained in this work are listed in ***Table 4***.

E. coli strains and culture conditions

E. coli strains were grown at 37°C in Luria-Bertani (LB) broth or LB agar supplemented with ampicillin (Amp; 100 µg/mL), Kanamycin (Km; 20 µg/mL) or Chloramphenicol (Cm; 12.5 µg/mL), when necessary.

E. coli DH10B containing a BAC library of the H37Rv chromosome cloned in pBeloBAC11 (Brosch et al., 1998) was grown at 30°C when contained the thermosensitive pKD46 plasmid, and 0.15% arabinose was used for induction of recombineering genes encoded in pKD46 plasmid.

Mycobacterial strains and culture conditions

Mycobacterial strains were grown at 37°C in 7H9 medium (Difco). 7H9 was supplemented with 0.05% Tween 80, 0.2% glycerol, and 10% (v/v) albumin-dextrose-catalase (ADC, Middlebrook) (7H9Tw-ADC); 0.05% Tween 80, 0.2% glycerol, and 0.2% dextrose, 0.085% NaCl and 0.0003% beef catalase (7H9Tw-Dex); or tyloxapol 0.025%, glycerol 0.2% and ADC 10% (7H9Tyl-ADC). When needed, MES (2-(N-morpholino)ethanesulfonic acid) or MOPS (3-(N-morpholino)propanesulfonic acid) buffer was used at 100 mM to maintain 7H9 broth at pH 5.5 or 7, respectively. For the induction of the recombineering system 0.2% (w/v) acetamide was used to supplement 7H9Tw-ADC.

For growth in solid medium, 7H10 was used supplemented with 0.5% glycerol and 10% ADC. When required, Km or Hygromycing B (Hyg) was used at concentration 20 µg/mL

Long term storage

For long term storage a final concentration of 15% of glycerol was added to bacterial cultures in late logarithmic phase. Aliquots of 1 mL were stored at -80°C.

Table 3: **Plasmids used in chapter 1**.

Plasmid name	Replicative Origin	Antibiotic resistance	Characteristics/Modifications	Reference
pFPV27 *pks2*::GFP	*E. coli* + Integrative in mycobacteria	Km	derived from pFPV27 int with *pks2* promoter controlling the expression of GFPmut2 gene	(Arnal, 2016)
pMV361 *pks2*::eGFP	*E. coli* + Integrative in mycobacteria	Km	derived from pMV361 *pks2*::eGFP-*ssrA* without the *ssrA* tail	This work
pMV361 *mcr7*::eGFP	*E. coli* + Integrative in mycobacteria	Km	derived from pMV361 *mcr7*::eGFP-*ssrA* without the *ssrA* tail	This work
pMV361 *pks2*::eGFP *smyc*::tdTomato	*E. coli* + Integrative in mycobacteria	Km	derived from pMV361 *pks2*::eGFP with tdTomato gene constitutively expressed	This work
pMV361 *mcr7*::eGFP *smyc*::tdTomato	*E. coli* + Integrative in mycobacteria	Km	derived from pMV361 *mcr7*::eGFP with tdTomato gene constitutively expressed	This work
pKD46	*E. coli* (thermosensitive)	Amp	*λ*-Red recombineering system inducible by arabinose	(Datsenko & Wanner, 2000)
pJV53H	*E. coli* + Mycobacteria	Hyg	Che9c gp60-61 recombineering system inducible by acetamide	(van Kessel & Hatfull, 2007)
pKD4	*E. coli*	Km	contains the Km resistance cassette flanked by FRT recombination sites	(Datsenko & Wanner, 2000)
pBeloBAC418	*E. coli*	Cm	Contain phoPR genes from H37Rv	(Brosch et al., 1998)
pBeloBAC418 phoPR-Km	*E. coli*	Cm + Km	Contain phoPR genes from H37Rv followed by FRT-Km cassette	This work
pRES-FLP-Mtb	*E. coli* + Mycobacteria	Hyg	contain the Flp recombinase with codon usage optimized to Mtb to remove Km cassette flanked by FLP recognition target sites	(Song & Niederweis, 2007)

Table 4: **Mycobacterial strains used in the chapter 1.**

Mycobacterium tuberculosis strains				
Strain name	**Plasmid**	**Antibiotic resistance**	**Characteristics**	**Reference**
H37Rv	-	-		(Cole et al., 1998)
H37Rv Δ*phoPR*	-	Hyg	H37Rv with *phoPR* genes disrupted by Hyg resistance cassette	(Gonzalo-Asensio et al., 2014)
H37Rv Δ*phoPR* pWM222	pWM222	Hyg, Km	H37Rv Δ*phoPR* complemented with *phoPR* genes from H37Rv	(Gonzalo-Asensio et al., 2014)
GC1237	-	-		(Caminero et al., 2001)
GC1237 Δ*phoPR*	-	Hyg	GC1237 with *phoPR* genes disrupted by Hyg resistance cassette	(Gonzalo-Asensio et al., 2014)
GC1237 Δ*phoPR* pWM222	pWM222	Hyg, Km	GC1237 Δ*phoPR* complemented with *phoPR* genes from H37Rv	(Gonzalo-Asensio et al., 2014)
CDC1551	-	-		(Fleischmann et al., 2002)
H37Rv pFPV27	pFPV27 *pks2*::GFP	Km		(Arnal, 2016)
H37Rv pMV361 *pks2*::eGFP	pMV361 *pks2*::eGFP	Km		This work
H37Rv pMV361 *mcr7*::eGFP	pMV361 *mcr7*::eGFP	Km		This work
H37Rv pMV361 *pks2*::eGFP *smyc*::tdTomato	pMV361 *pks2*::eGFP *smyc*::tdTomato	Km		This work

H37Rv pMV361 *mcr7*::eGFP *smyc*::tdTomato	pMV361 *mcr7*::eGFP *smyc*::tdTomato	Km	This work
H37Rv Δ*phoPR* pFPV27	pFPV27 *pks2*::GFP	Km, Hyg	(Arnal, 2016)
H37Rv Δ*phoPR* pMV361 *pks2*::eGFP	pMV361 *pks2*::eGFP	Km, Hyg	This work
H37Rv Δ*phoPR* pMV361 *mcr7*::eGFP	pMV361 *mcr7*::eGFP	Km, Hyg	This work
H37Rv ΔphoPR pMV361 *pks2*::eGFP *smyc*::tdTomato	pMV361 *pks2*::eGFP *smyc*::tdTomato	Km, Hyg	This work
H37Rv Δ*phoPR* pMV361 *mcr7*::eGFP *smyc*::tdTomato	pMV361 *mcr7*::eGFP *smyc*::tdTomato	Km, Hyg	This work
GC1237 pFPV27	pFPV27 *pks2*::GFP	Km	This work
GC1237 pMV361 *pks2*::eGFP	pMV361 *pks2*::eGFP	Km	This work
GC1237 pMV361 *mcr7*::eGFP	pMV361 *mcr7*::eGFP	Km	This work
GC1237 pMV361 *pks2*::eGFP *smyc*::tdTomato	pMV361 *pks2*::eGFP *smyc*::tdTomato	Km	This work
GC1237 pMV361 *mcr7*::eGFP *smyc*::tdTomato	pMV361 *mcr7*::eGFP *smyc*::tdTomato	Km	This work
GC1237 Δ*phoPR* pFPV27	pFPV27 *pks2*::GFP	Km, Hyg	This work
GC1237 Δ*phoPR* pMV361 *pks2*::eGFP	pMV361 *pks2*::eGFP	Km, Hyg	This work
GC1237 Δ*phoPR* pMV361 *mcr7*::eGFP	pMV361 *mcr7*::eGFP	Km, Hyg	This work
GC1237 Δ*phoPR* pMV361 *pks2*::eGFP *smyc*::tdTomato	pMV361 *pks2*::eGFP *smyc*::tdTomato	Km, Hyg	This work
GC1237 ΔphoPR pMV361 *mcr7*::eGFP *smyc*::tdTomato	pMV361 *mcr7*::eGFP *smyc*::tdTomato	Km, Hyg	This work

CDC1551 pFPV27	pFPV27 *pks2*::GFP	Km		This work
CDC1551 pMV361 *pks2*::eGFP	pMV361 *pks2*::eGFP	Km		This work
CDC1551 pMV361 *mcr7*::eGFP	pMV361 *mcr7*::eGFP	Km		This work
CDC1551 pMV361 *mcr7*::eGFP *smyc*::tdTomato	pMV361 *mcr7*::eGFP *smyc*::tdTomato	Km		This work

Mycobacterium smegmatis strains

Strain name	**Plasmid**	**Antibiotic resistance**	**Characteristics**	**Reference**
mc^2 155	-	-		
mc^2 155 pJV53H	pJV53H	Hyg	mc^2 155 strain with the mycobacterial recombineering system	(van Kessel & Hatfull, 2007)
mc^2 155 ΔSM*phoPR*	-	-	mc^2 155 with endogenous *phoPR* genes disrupted	This work
mc^2 155 ΔSM*phoPR*::TB*phoPR*	-	-	mc^2 155 with *phoPR* genes from H37Rv replacing its endogenous *phoPR* genes	This work
mc^2 155 pFPV27	pFPV27 *pks2*::GFP	Km		This work
mc^2 155 pMV361 *pks2*::eGFP	pMV361 *pks2*::eGFP	Km		This work
mc^2 155 pMV361 *mcr7*::eGFP	pMV361 *mcr7*::eGFP	Km		This work
mc^2 155 pMV361 *pks2*::eGFP *smyc*::tdTomato	pMV361 *pks2*::eGFP *smyc*::tdTomato	Km		This work
mc^2 155 pMV361 *mcr7*::eGFP *smyc*::tdTomato	pMV361 *mcr7*::eGFP *smyc*::tdTomato	Km		This work
mc^2 155 ΔSM*phoPR* pFPV27	pFPV27 *pks2*::GFP	Km		This work

mc^2 155 ΔSM*phoPR* pMV361 *pks2*::eGFP	pMV361 *pks2*::eGFP	Km	This work
mc^2 155 ΔSM*phoPR* pMV361 *mcr7*::eGFP	pMV361 *mcr7*::eGFP	Km	This work
mc^2 155 ΔSM*phoPR* pMV361 *pks2*::eGFP *smyc*::tdTomato	pMV361 *pks2*::eGFP *smyc*::tdTomato	Km	This work
mc^2 155 ΔSM*phoPR* pMV361 *mcr7*::eGFP *smyc*::tdTomato	pMV361 *mcr7*::eGFP *smyc*::tdTomato	Km	This work
mc^2 155 ΔSM*phoPR*::TB*phoPR* pFPV27	pFPV27 *pks2*::GFP	Km	This work
mc^2 155 ΔSM*phoPR*::TB*phoPR* pMV361 *pks2*::eGFP	pMV361 *pks2*::eGFP	Km	This work
mc^2 155 ΔSM*phoPR*::TB*phoPR* pMV361 *mcr7*::eGFP	pMV361 *mcr7*::eGFP	Km	This work
mc^2 155 ΔSM*phoPR*::TB*phoPR* pMV361 *pks2*::eGFP *smyc*::tdTomato	pMV361 *pks2*::eGFP *smyc*::tdTomato	Km	This work
mc^2 155 ΔSM*phoPR*::TB*phoPR* pMV361 *mcr7*::eGFP *smyc*::tdTomato	pMV361 *mcr7*::eGFP *smyc*::tdTomato	Km	This work

Nucleic acid and genetic engineering techniques

DNA extraction

Miniprep from *E. coli*

Bacteria were resuspended in 500 µL of TE. Samples were incubated at room temperature after addition of 100 µL of Solution I (50 mM Glucose, 10 mM EDTA, 25 mM Tris/HCl pH 8 and 4 mg/mL of lysozyme). Subsequently, 200 µL of fresh Solution II (0.2 M sodium hydroxide, NaOH and 1% of sodium dodecyl sulfate, SDS) were added and tubes were inverted several times to favor the lysis of the bacteria. After 5 min of incubation on ice, 150 µL of ice-cold Solution III (3 M potassium acetate, KAc, 11.5% v/v acetic acid glacial) were added and incubated on ice during 5 min after vortex the mixture.

The aqueous phase (upper) was mixed with 500 µL of chloroform:isoamyl alcohol 24:1 (v/v) by inversion. After centrifugation (12000 rpm for 5 min), the upper phase was added to a fresh tube containing 0.1 volumes of 3 M KAc and 2 volumes of absolute ethanol and incubated at -20°C for 30 min. Plasmid DNA was pelleted by centrifugation (12000 rpm for 30 min at 4°C) and washed with 70% ethanol. Hereafter, pellet was dried in a vacuum drier and dissolved in 50 µL of double-distilled water. To remove co-purified RNA, samples were incubated at 37°C for 15 min with 1 µL of RNase A (1 mg/mL).

Plasmid extraction was also performed using High Pure Plasmid Purification Kit (Roche) following manufacturer's instructions.

Fast DNA extraction from mycobacteria for PCR

This method releases plasmidic and genomic DNA from mycobacteria, usually in enough quantity to detect the presence of target genes by PCR.

1 mL of liquid culture was centrifuged (12,000 rpm for 5 min) and pellet resuspended in 400 µl TE, or a colony was dispersed in 400 µl TE. The bacterial suspensions were inactivated by heating at 90°C for 30 min. After centrifugation (12,000 rpm for 10 min), 350 µl of supernatant were transferred to a fresh tube and mixed with 350 µl of chloroform:isoamyl alcohol 24:1 by vortexing for 10-20 s. After centrifugation (12,000 rpm for 5 min) the aqueous phase was transferred to a fresh tube. Typically, 1 µl of this DNA solution was used in a standard PCR reaction.

Alternatively, bacterial pellet or dispersed colony was boiled 15 min in 20-50 µL of sterilized water and centrifuged at maximal speed. 1 µL of the supernatant was used in standard PCR reactions.

Extraction of genomic DNA from mycobacteria

Mycobacteria were resuspended in 400 µL of TE (100 mM Tris/HCl, 10 mM ethylenediaminetetraacetic acid, EDTA, pH = 8) and heated at 85°C during 20 min. Samples were incubated at 37°C overnight after addition of 0.5 mg of lysozyme. Subsequently, 0.05 mg of proteinase K and 72.5 µL of 10% SDS were added and incubated at 65 °C for 10 min. 100 µL of CTAB (Cetyltrimetylammonium bromide)/sodium chloride, NaCl. 10% CTAB in 0.7 M of NaCl, pre-warmed at 65°C was added to the samples and incubated at 65°C for 10 min. The aqueous phase was collected after adding 750 µL of chloroform:isoamyl alcohol 24:1 (v/v), vortex for 10 seg and centrifuged for 5 min at 12000 rpm. Genomic DNA was precipitated by adding 0.6 volumes of isopropanol and an incubated of 30 min at -20°C. Precipitated nucleic acids were collected by centrifugation (5 min at 12000 rpm) and washed with 70% ethanol by tube inversion. Nucleic acids were collected again by centrifugation (12000 rpm for 5 min). Pellets were dissolved in 50 µL of double-distilled water after the complete evaporation of the ethanol. DNA was quantified by Abs260/Abs280 readings using a ND-1000 spectrophotometer (NanoDrop).

PCR

PCR amplifications were performed in a final volume of 10 µL or 50 µL with 0.38 and 1.87 U of Mytaq DNA polymerase respectively (Bioline), 25 µM of each primer (***Table 5***) and MyTaq Reaction Buffer 5x. PCR program consisted of an initial step of 1 min at 95 °C, followed by 30 cycles (95°C 15 s, 58°C 15 seg and 72°C 1 min/kb) and a final step of 7 min at 72°C. For colony PCR, initial step was 95°C for 10 min. PCR amplification products were analyzed in 0.8-2% agarose gel electrophoresis. For molecular weight comparison, DNA Molecular Weight 100 bp. When needed, PCR products were purified by High Pure PCR product purification Kit (Roche) or ExoSAP-IT® PCR Product Cleanup (Affymetrix) for use them as allelic exchange substrates (AES) or for Sanger Sequencing, respectively.

Design and construction of PhoPR reporter plasmids

The new PhoPR reporter plasmids were constructed using GenScrip Gene Synthesis services. We have used the pMV361 plasmid as backbone (Stover et al., 1991), which carries the *E. coli* pBR332 replication origin suitable for plasmid expansion, the Km resistance cassette as selection marker in *E. coli* and mycobacteria, the mycobacteriophage L5 *attP* site and integrase for a stable integration in mycobacterial chromosome, and the *hps60* promoter followed by the *rrnB* transcription terminator for gene expression in mycobacteria. The first fragment designed contained the *pks2* promoter controlling the reporter gene, composed by the eGFP gene optimized in *M.*

tuberculosis codon usage (Andersson & Sharp, 1996) This fragment was designed to be cloned between *Aat*II and *Hind*III sites of pMV361, replacing the *hsp60* promoter, leading to the pMV361 *pks2*::eGFP. An *Eco*RI site was added between *pks2* promoter and the reporter gene to allow easy promoter (cutting in *Aat*II and *Eco*RI sites) or reporter gene (cutting in *Eco*RI and *Hind*III sites) replacements. Synthesis of the *mcr7* promoter flanked by *Aat*II and *Eco*RI sites allowed to replace *pks2* promoter, leading to the pMV361 *mcr7*::eGFP. Finally, the tdTomato gene was synthetized under control of the synthetic *smyc* constitutive promoter (Carroll et al., 2010). As this fragment was designed to be cloned between *Hind*III and *Cla*I sites, which are placed in the 3' UTR of eGFP gene, and before the *rrnB* transcription terminator, a second *rrnB* sequence was introduced upstream of the *smyc* promoter to maintain the transcription terminator for the eGFP gene. The introduction of this fragment led to pMV361 *pks2*::eGFP *smyc*::tdTomato and pMV361 *mcr7*::eGFP *smyc*::tdTomato plasmids.

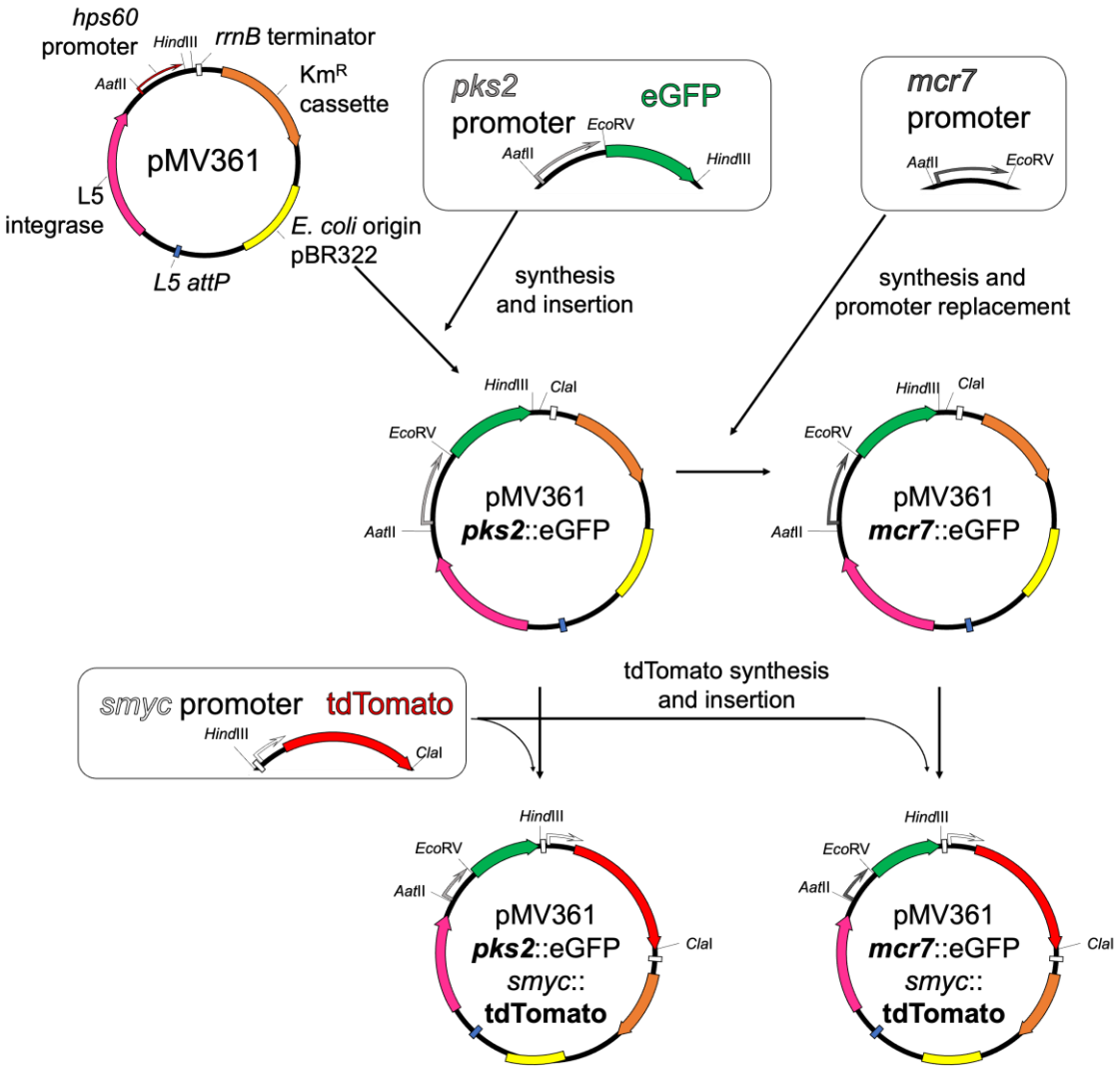

Figure 13: **Workflow designed for the construction of the different PhoPR reporter plasmids.** Synthesis and cloning processes have been performed in GenScript Biotech Corp.

RNA techniques

RNA extraction

Mycobacterial cultures were grown in 7H9Tw-ADC at 37°C to mid-logarithmic phase (OD_{600} = 0.4-0.5). Cells from 10 mL of culture were harvested (4,000 rpm for 5 min at 37°C). To minimize RNA degradation, cells were resuspended in 1 mL of RNA protect reactive (Qiagen). Cellular suspensions were incubated for 5 min at RT and were centrifuged (14,000 rpm for 5 min at RT). Pellets were resuspended in 400 µl of lysis buffer (0.5% SDS, 20 mM NaAc, 0.1 mM EDTA) and 1 mL of acid-phenol:chloroform (5:1, pH 4.5) was added. Bacterial suspensions were transferred to tubes containing

glass beads (Lysing Matrix B, MP Biomedicals) and were lysed by mechanical traction (Fast-prep instrument) in two cycles (45 seg at speed 6.5 m/s) cooling the samples on ice for 5 min between the pulses. Samples were centrifuged (12,000 rpm for 5 min at 4°C). The upper phase (aqueous) was recovered and transferred to a fresh tube that contained pre-chilled chloroform:isoamyl alcohol 24:1. Tubes were inverted carefully before centrifugation (14,000 rpm for 5 min at 4°C). The upper (aqueous) phase was then transferred to a fresh tube containing 90 µl of 0.3 M NaAc (pH 5.5) and 900 µl of isopropanol and samples were incubated overnight at -20°C. Precipitated nucleic acids were collected by centrifugation (12,000 rpm for 1 hour at 4°C). The pellets were rinsed with 70% ethanol and air dried before being re-dissolved in RNase-free water. DNA was removed from RNA samples using Turbo DNA free (Ambion) by incubation at 37°C for 1 hour. Then RNA was purified with acid-phenol:chloroform (5:1, pH 4.5) and the same steps to precipitate, collect and dry were repeated to dissolve RNA in RNase-free water. The concentration of the extracted RNA was estimated from the Abs260/Abs280 readings using a ND-1000 spectrophotometer. DNA contamination was ruled out by lack of amplification products after 35 cycles of PCR. RNA integrity was assessed by agarose gel electrophoresis. RNA samples were stored at -80°C.

RNA extraction was also performed using RNeasy® Mini Kit (Quiagen)

cDNA synthesis

Reverse transcription was performed using 500 ng of RNA, 2 µL of PrimeScriptTM RT Master Mix (Takara) and RNase Free dH2O (Takara) until a total volume of 10 µL per reaction. cDNA was obtained after 15 min at 37°C and 15 seg at 85°C for enzyme inactivation

qRT-PCR

For qRT-PCR reaction, TB Green Premix Ex TaqTM (Tli Rnase H Plus) (Takara) was used. Gene-specific primers at final concentration of 0.25 µM and cDNA obtained as described above diluted one tenth were used. The reaction was performed in the StepOne Plus Real Time PCR System (Applied Biosystems). Meting curves were performed for each pair of primers (***Table 5***) to verify that they produce a single specific product. PCR amplification program used was 95°C for 10 min; 40 cycles of 95°C for 15 s, 60°C for 1 min).

Table 5: **Oligonucleotides used in chapter 1.**

Name	Sequence 5' → 3'	Use
***pks2*-Fw**	CATGGATCCTCAGAACGACATTGG GTTTCGCGTC	confirmation pFPV27 *pks2*::GFP
***pks2*-Rv**	CCTGGTACCCTGACGCCGCCGAC CCCAAG	confirmation pFPV27 *pks2*::GFP
pMV361-A	CAGGAGCATTGCCGTTCC	confirmation pMV361 derived plasmids
eGFPrv	CGTCGCCGTCCAGCTCGACCAG	confirmation pMV361 derived plasmids
RT GFP Rv	TCCAGCAGGACCATGTGATC	confirmation pMV361 derived plasmids
5' UTR SM*phoP*-P1	CGTGCAGGAATACTCCAACAGATA GCGACAGCATTGGGTAGTGTAGG CTGGAGCTGCTTC	AES amplification for knocking out *M. smegmatis phoPR* genes
5' SM*phoR*-P2	GTGTGGTGGGCGCGCGCCGCGG GGCCTGCGCCCAACTCCTCATATG AATATCCTCCTTAGT	AES amplification for knocking out and replacing *M. smegmatis phoPR* genes
3' UTR TBphoR-P1	GCGGTCGACGTTGGCAAAGCCGA AATCACTGAGGCTGCGGGTGTAG GCTGGAGCTGCTTC	AES amplification for knocking in Km resistance cassette in pBeloBAC11 Rv148
3' Rv0759c-P2	GCTGGAAGTGCCCCACCTACACAT CCACGTGTTTCCCACCATATGAAT ATCCTCCTTAGT	AES amplification for knocking in Km resistance cassette in pBeloBAC11 Rv148
5'UTR SM*phoP*-5'TB*phoP*	CGTGCAGGAATACTCCAACAGATA GCGACAGCATTGGGTAATGCGGAA AGGGGTTGATC	AES amplification for replacing *M. smegmatis phoPR* genes
5' UTR SM*phoP*	CGGTCACGGTGCGCTGTAC	confirmation of *M. smegmatis phoPR* mutants
5' SM*phoR* rv	CAGGGCCCGCACCGAC	confirmation of *M. smegmatis phoPR* mutants
Assemb_2-Rv	CATAAAACCGCCCAGTCTAGCTAT CGC	confirmation of *M. smegmatis phoPR* mutants
Assemb_3-Fw	TCGCCTTCTATCGCCTTCTTGACG	confirmation of *M. smegmatis phoPR* mutants
***phoR*-DOWN-500-fw**	TCTTGGCCTGCGCTTCGTCC	confirmation of *M. smegmatis phoPR* mutants

***phoR*-DOWN-500-rv**	ACCTACCGGGTGAATAAGGCCGG	confirmation of *M. smegmatis phoPR* mutants
P1-inv	GAAGCAGCTCCAGCCTACAC	confirmation of *M. smegmatis phoPR* mutants
P2-inv	ACTAAGGAGGATATTCATATG	confirmation of *M. smegmatis phoPR* mutants
RTpks3 Fw	GACGCTCGCTGAATCACAAA	qRT-PCR
RTpks3 Rv	TCGCCGTGTGTCAGTCCTAC	qRT-PCR
RT*pks2* Fw	GCATCGGTGAAGACCAACTTC	qRT-PCR
RT*pks2* Rv	GATTACGTGGAACCACACCATGT	qRT-PCR
RT *mcr7* Fw	ACGCCGCGAGGACATG	qRT-PCR
RT *mcr7* Rv	AGGGAGCTGCTTGGACAGAA	qRT-PCR
RT espA Fw	GGCACCCTCGGAGAAGTGT	qRT-PCR
RT espA Rv	AGCTCTTTCAGGCCGTTGAG	qRT-PCR
RT espC Fw	TGTACTTGACTGCCCACAATGC	qRT-PCR
RT espC Rv	TCGACACCGGCCGTATG	qRT-PCR
RT espD Fw	CAACAGGTCGATGCAGATGAA	qRT-PCR
RT espD Rv	TCGCCCACGGTCTTACGTA	qRT-PCR
RT sigA Fw	CCGATGACGACGAGGAGATC	qRT-PCR
RT sigA Rv	CGGAGGCCTTGTCCTTTTC	qRT-PCR
RTphoPfw	GCCTCAAGTTCCAGGGCTTT	qRT-PCR
RTphoPrv	CCGGGCCCGATCCA	qRT-PCR and confirmation of M. smegmatis phoPR mutants

Preparation of electrocompetent bacteria

Mycobacteria

50-200 mL of bacterial cultures were grown until OD_{600} 0.6-0.8 (for *M. tuberculosis* strains 20 mL of 2 M glycine were added and incubated overnight at 37°C). After two washes with water-0.05% Tween-80 and one with 10% glycerol-0.05% Tween-80, bacteria were resuspended in 2 mL of 10% glycerol-0.05% Tween-80. Aliquots of 100 µL were transformed with 500 ng of plasmidic DNA in 0.2 cm cuvettes (Bio-Rad) with a single pulse in a GenePulser XcellTM (Bio-Rad) (2500 V, 25 µF, 1000 Ω). Bacteria were recovered in 1 mL of 7H9Tw-ADC and incubated at 37 °C overnight to allow the expression antibiotic resistance. Serial dilutions were plated onto 7H10-ADC containing the required antibiotic for selection.

E. coli

50 mL of bacterial culture were grown until OD_{600} 0.4-0.6. When the optimal OD was reached, bacteria cultures were incubated on ice for 30 min. After two washes with chilled water and one with chilled 10% glycerol, bacteria were resuspended in 500 µL of 10% glycerol. Electroporation of 250 ng of plasmid was performed in 50 µL of aliquoted competent cells in a 0.2 cm cuvette (Bio-Rad) with a single pulse in a GenePulser XcellTM (Bio-Rad) (2500 V, 25 µF, 200 Ω). Cells were recovered in 1 mL of LB and incubated at 30°C for 1 h to allow the expression of the resistance to the antibiotic and then serial dilutions were plated onto LB containing desired antibiotic. Colonies were isolated after incubation at 37°C overnight.

Recombineering

BAC recombineering in *M. smegmatis*

For electroporation of pKD46 plasmid with the *λ*-Red system to *E. coli* pBeloBAC418, the procedure described in the previous section, but transformant colonies were isolated at 30°C due to the thermosensitive replication origin pKD46 plasmid. Confirmed colonies with both plasmids were grown in 50 mL of bacterial culture until OD_{600} = 0.4-0.6 at 30°C in presence of Amp and Cm. The *λ*-Red system was induced with 0.15% arabinose w/v at OD_{600} = 0.1. When the optimal OD_{600} was reached, bacteria were processed as explained in previous section. Electroporation of 500 ng of AES (purified PCR amplification product) was performed in 100 µL of aliquoted competent cells in a 0.2 cm cuvette (Bio-Rad) with a single pulse in a GenePulser XcellTM (Bio-Rad) (2500 V, 25 µF, 200 Ω). Cells were recovered in 1 mL of LB and incubated at 37°C for 1 h to allow the expression of the resistance to the antibiotic and then serial dilutions were plated onto LB containing Km. Recombinant colonies were confirmed by PCR and recombinant pBeloBAC418 plasmids were used as templates for AES

50-100 mL of *M. smegmatis* strains containing pJV53H plasmid were grown until OD_{600} 0.4- 0.5. Acetamide was added to a final concentration of 0.2% (w/v) and incubated at 37 °C for 3-4 hours. Bacteria were resuspended in 0 mL of 10% glycerol-0.05% Tween 80 after four washes with 10% glycerol-0.05%. Aliquots of 100 µL were transformed with 500 ng of AES (purified PCR amplification product from) in 0.2 cm cuvettes (Bio-Rad) with a single pulse in a GenePulser XcellTM (Bio-Rad) (2500 V, 25 µF, 1000 Ω). Bacteria were recovered in 1 mL of 7H9Tw-ADC, incubated overnight at 37°C and plated onto 7H10-ADC with Km.

Protein techniques

Whole cell and culture filtrate protein extraction

Mycobacteria were grown in 7H9Tw-ADC. Bacteria were pelleted and washed twice with PBS to remove albumin and resuspended in PBS. Bacteria were transferred to 7H9Tw-Dex to avoid interference of albumin in the secreted fraction. 50 mL of bacterial cultures were grown until late log-phase (OD_{600} = 0.8). Bacteria were pelleted by centrifugation.

To obtain the Culture Filtrate fraction (CF), the supernatant fractions were filtered through a 0.22 µm-pore-size low protein binding and 10% (v/v) of trichloroacetic acid (TCA) was added and incubated on ice for 2 h to favor protein precipitation. Hereafter, samples were centrifuged (1 h at 4000 rpm at 4°C) and pellets were washed with acetone. Supernatants were discarded after centrifugation (4000 rpm for 10 min) and pellets were air dried and dissolved in 250 µL of Tris 150 mM pH 8.8.

For extraction of cellular proteins, bacterial pellets were resuspended in 1 mL of PBS containing 1% Triton X-100 and transferred to tubes containing glass beads (MP Biomedicals) to obtain the Culture Lysate fraction (CL). Mycobacterial suspensions were disrupted by Fast-Prep (6.5 m/s, 45 s) twice and samples were incubated on ice for 5 min between the cycles. Supernatants containing the CL were collected after centrifugation (12000 rpm for 5 min at 4°C). For SRM experiments, CL were precipitated with TCA and dissolved in Tris 150 mM pH = 8.8 as described above for CF.

Samples were quantified using the QuantiPro BCA assay (Sigma Aldrich) and stored at -20°C.

Gel electrophoresis

Samples were heated at 100°C for 10 min in presence of LaemmLi sample buffer (150 mM Tris/HCl pH = 7.4, 3% SDS, 0.3 mM sodium molybdate, 30 mM sodium pyrophosphate, 30 mM sodium floride, NaF, 30% glycerol, 30% mercaptoethanol and 0.06% bromophenol blue). Equivalent quantities of proteins were separated in 12-17% polyacrylamide gels containing 0.1% SDS in running buffer (25 mM Tris, 192 mM glycine, 3.4 mM SDS) at constant amperage of 30 mA per gel.

PageRuler Plus Prestained Protein Ladder (Thermo Scientific) was used as molecular weight marker (kDa).

Western blot analysis

Proteins were transferred to a PDFV membrane (preactivated with methanol) in transfer buffer (48 mM Tris/HCl pH = 8.3, 39 mM glycine, 0.037% SDS, 20% methanol) for 1 h at

20 V with a semi-dry electrophoretic transfer cell (Trans-Blot® Semi-Dry Transfer cell, Bio- Rad).

Membranes were blocked with 5% (w/v) of skimmed milk in TBS-T buffer (25 mM Tris pH = 7.5, 150 mM NaCl, 0.05% Tween 20) for 30 min and incubated overnight with primary antibodies. Subsequently membranes were washed with TBS-T buffer three times before incubation with human serum adsorbed secondary antibodies conjugated with peroxidase for 1 h. Signals were detected using chemiluminescent substrate (Western BrightTM Quantum, Advansta).

Immunodetection was carried out using PhoP-antiserum (1:5000) with the incubation with secondary antibody anti-rabbit IgG human serum adsorbed conjugate (1:5000) (KPL) to detect PhoP. Incubation with monoclonal antibody antibody anti- GroEL2 (Hsp65) (1:2500) (Invitrogen) followed by incubation with anti-mouse IgG human serum adsorbed conjugate (1:5000) (KPL) were used to detect GroEL2.

Multiple-Reaction Monitoring coupled to Mass Spectrometry (MRM/MS)

Selected-Reaction Monitoring (SRM) is a very sensitive and specific technique, and it was used to detect and quantify Multiple (MRM) proteins ESAT-6, CFP-10, EspA and EspC from CF. For in-solution digestion, 20 µg of protein was mixed with 10 µL of denaturing buffer (6 M urea, 100 mM Tris-HCl pH 7.8). After 30 min at RT, cysteines were reduced adding 1 µL of DTT 200 mM for 30 min at 37°C and alkylated with 6 µL of iodoacetamide 200 mM for 30 min in the dark. Unreacted iodoacetamide was consumed by adding 6 µL of the reducing agent (DTT 200 mM) for 30 min at room temperature. Samples were diluted with 75 µL of ammonium bicarbonate 50 mM to a final concentration of less than 1 M urea. Protein digestion was carried out with trypsin (Trypsin Gold, Promega) at a 1:20 ratio (enzyme/protein) for 18 h at 37°C. The reaction was stopped by adding concentrated formic acid (Sigma). Samples were dried in a vacuum concentrator and reconstituted with 80 µL of 2% acetonitrile and 0.1% formic acid. Peptide concentration of resultant samples was measured by Qubit Assay Protein kit in a Qubit 3.0 fluorimeter (ThermoFisher).

Protein identification was performed on a triple quadrupole/linear ion trap mass spectrometer (MS) QTRAP 6500+ (SCIEX, Foster City, CA, USA) coupled to nano/micro-HPLC (Eksigent LC 425, SCIEX). Sample preconcentration and desalting of tryptic digests were performed on a C18 column (Luna 0.3 mm id, 20 mm, 5 mm particle size, Phenomenex, CA, USA) at 10 µL/min flow for 3 min. Then, 1 µg of tryptic peptides was injected and then separated using a C18 column (Luna 0.3 mm id, 150 mm, 3 mm particle size, Phenomenex, CA, USA) at a flow rate of 5 µL/min at 40°C, with a linear

gradient from 5 to 35% acetonitrile in 0.1% formic acid for 30 min. The mass spectrometer was interconnected with an electrospray injector (Turbo V) using a hybrid electrode of 25 µm inner diameter and was operated in positive ion mode. Mass spectrometer source parameters were as follows: capillary voltage 5,000 V, decluttering potential (DP) 85 V, gas curtain with ion source gas (nitrogen) 25 psi, and collision gas (nitrogen) 15 psi, and source temperature 150°C.

Analyses were performed using an information-dependent acquisition (IDA) method with the following steps: single enhanced mass spectra (EMS, 400-1,400 m/z), from which the most intense peaks were subjected to an enhanced product ion (EPI [MS/MS]) scan. Peptide identity was confirmed using an MRM-initiated detection and sequencing (MIDAS) algorithm using Mascot (v.2.3, Matrix Science, UK) and Swiss-Prot. Quantification was performed using Skyline (MacCoss Lab Software, Seattle, WA, versión 21.2.0.568), selecting proteolytic peptides from desired protein sequences, prioritizing reported peptides in SRMAtlas (https://srmatlas.org/). Selected peptides were 7-25 aa long and at least 3 transitions of each peptide were selected.

The identified and quantified peptides were as follows: for ESAT-6, LAAAWGGSGSEAYQGVQQK, WDATATELNNALQNLAR, TISEAGQAMASTEGNVTGMFA; for CFP-10, TQIDQVESTAGSLQGQWR, GAAGTAAQAAVVR, TDAATLAQEAGNFER, FQEAANK and QELDEISTNIR; for EspA, NHVNFFQELADLDR, APVEADAGGGQK and YSEGAAAGTEDAER; and for EspC, IYSEADEAWR. As equivalent results were obtained for the different peptides, results from ESAT-6 peptides LAAAWGGSGSEAYQGVQQK, TISEAGQAMASTEGNVTGMFA; CFP-10 peptides TQIDQVESTAGSLQGQWR, TDAATLAQEAGNFER, FQEAANK and QELDEISTNIR; and EspA peptides, NHVNFFQELADLDR and YSEGAAAGTEDAER are not presented to clarify results.

In silico protein analysis

PhoP and PhoR protein sequences from *M. tuberculosis* and *M. smegmatis* have been compared using Blastp (https://blast.ncbi.nlm.nih.gov/Blast.cgi) and MUSCLE algorithm (https://www.ebi.ac.uk/Tools/msa/muscle/), protein domains were predicted with InterPro (https://www.ebi.ac.uk/interpro/), and structure prediction was performed by Alphafold software (Jumper et al., 2021). Structure visualization and superposition was performed using PyMol software (Schrödinger & DeLano, 2020).

Phenotypic characterization

PhoPR-inhibition assay

Mycobacterial strains were grown to mid-late exponential phase (OD_{600} = 0.6-0.8) in 7H9Tyl-ADC in static conditions. Inoculums of 0.4 were prepared adjusting OD_{600} with 7H9Tyl-ADC. When pH control was needed, bacteria was pelleted and resuspended in 7H9Tyl-ADC with 100 mM of MES or MOPS buffer and adjusted to OD_{600} = 0.4. Serial two-fold microdilutions of the different compounds were prepared in 100 µL of the 7H9Tyl-ADC (with MES or MOPS 100 mM if needed) in 96-well polypropylene flat bottom plates and 100 µL of inoculums were added to each well. Initial OD_{600} of the culture in the plates was 0.2. Plates were incubated at 37°C up to 8 days. OD_{600} and fluorescence was measured in a Biotek Synergy HT system. Filters used: GFP (Ex: 485/20, Em: 516/20) and tdTomato (Ex: 540/35, Em: 590/20). Analysis of the results were performed using Graphpad Prism software version 9.0.1 for macOS.

RESULTS

Setup of a PhoPR screening platform

Validation of *M. tuberculosis* reporter strains and confirmation of ETZ as a control PhoPR inhibitor

As mentioned above, an antivirulence strategy should not kill, or inhibit the *in vitro* growth of the bacteria, but it should target virulence factors required for the development of the disease. The use of *M. tuberculosis* PhoPR reporter strains, with the GFP gene under the control of a PhoPR regulated promoter, have the potential to distinguish the activity of the compounds tested, as growth inhibition could be tracked by measuring the optical density at 600 nm (OD_{600}), and the PhoPR inhibition could be tracked by measuring the fluorescence units of GFP (FU GFP). Molecules with bactericidal or bacteriostatic effect would show inhibition in FU GFP and OD_{600}, while specific PhoPR inhibitors would show inhibition in FU GFP, but not in OD_{600}. We reasoned that the H37Rv pFPV27 *pks2*::GFP strains, which carry the GFP mut2 gene under the control of the *pks2* promoter, strongly regulated by the PhoPR system, would be suitable to confirm the specific activity of ETZ over the PhoPR system.

The specific PhoPR inhibitory activity of ETZ was confirmed using the H37Rv pFPV27 *pks2*::GFP strain and its Δ*phoPR* mutant. ETZ was tested in two-fold serial dilutions with 500 µM of maximal concentration. It has been described that acidic pH induces the PhoPR system (Abramovitch et al., 2011), and that ETZ is also active at acidic pH (Johnson et al., 2015). Thus, we confirmed the inhibitory activity of ETZ in both acid (buffered with MES pH 5-5.5) and neutral (buffered with MOPS pH 6.5-7) pH media. After 6 days of incubation, we measured the FU GFP and OD_{600}. We observed that ETZ is active in both 7H9Tyl-ADC MES and 7H9Tyl-ADC MOPS, inhibiting GFP production at higher concentrations in the H37Rv pFPV27 pks::GFP strain (***Figure 14A and B***) with no significant effect in bacterial growth at the concentrations tested (***Figure 14C and D***). As expected, we do not observe GFP inhibition in the H37Rv Δ*phoPR* pFPV27 pks::GFP strain, due to the absence of a functional PhoPR system susceptible of been inhibited by ETZ, just producing a basal GFP fluorescence (***Figure 14 A and B***). Both strains grew better with MOPS buffer, than with MES buffer (***Figure 14 C and D***).

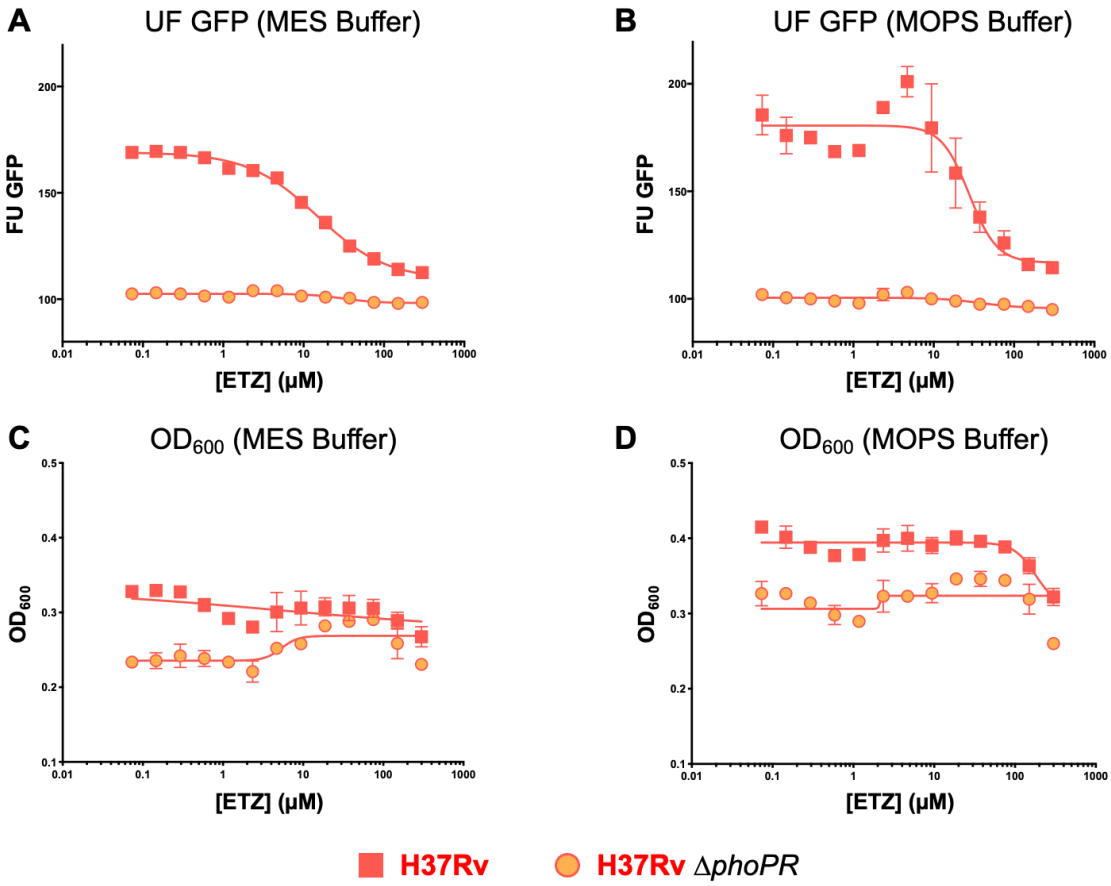

Figure 14: **Dose response effect of ETZ in H37Rv pFPV27 *pks2*::GFP reporter strains.** Effect of different doses of ETZ in GFP fluorescence in H37Rv (red squares) and H37Rv Δ*phoPR* (orange circles) carrying the pFPV27 *pks2*::GFP plasmid in acid (**A**) and neutral (**B**) pH, and in growth in acid (**C**) and neutral (**D**) pH. FU GFP IC50 values from H37Rv in MES and MOPS buffer of presented graphs are 14.8 and 30.6 µM, respectively.

Construction and validation of reporter strains in different genetic background

After confirming the ETZ inhibitory activity of the PhoPR system in the *M. tuberculosis* H37Rv genetic background with the pFPV27 *pks2*::GFP plasmid, we decided to construct new reporter strains in different genetic backgrounds covering the most widespread lineages of *M. tuberculosis*. This would allow us to test if ETZ, and future potential PhoPR inhibitors, are active in representative strains of the MTBC or whether they are lineage or strain specific. The H37Rv strain is a laboratory adapted strain from the Lineage 4 of the MTBC. We selected two different genetic backgrounds to construct the new reporter strains: CDC1551, a different strain belonging to the MTBC L4, and

GC1237, a clinical isolate from the Beijing family of the MTBC L2, and its related Δ*phoPR* mutant. After electroporation with the pFPV27 *pks2*::GFP plasmid, the presence of the plasmid in the Km resistant colonies recovered was confirmed by PCR. The new strains were tested with ETZ both acid and neutral pH, as described above.

After incubation with different doses of ETZ, the inhibitory profiles observed in the new reporter strains were similar to those observed in the H37Rv background: the fluorescence of CDC1551 pFPV27 *pks2*::GFP and GC1237 pFPV27 *pks2*::GFP strains, with a functional PhoPR system, decreased at higher concentrations of ETZ, with no detectable effect in bacterial growth at the concentrations tested. In addition, GC1237 Δ*phoPR* pFPV27 *pks2*::GFP strain was not sensitive for ETZ, being the absence of GFP inhibition due to the absence of a functional PhoPR system (***Figure 15A and B***). All the strains grew better in 7H9Tyl-ADC with MOPS buffer (***Figure 15D***), than with MES buffer (***Figure 15C***).

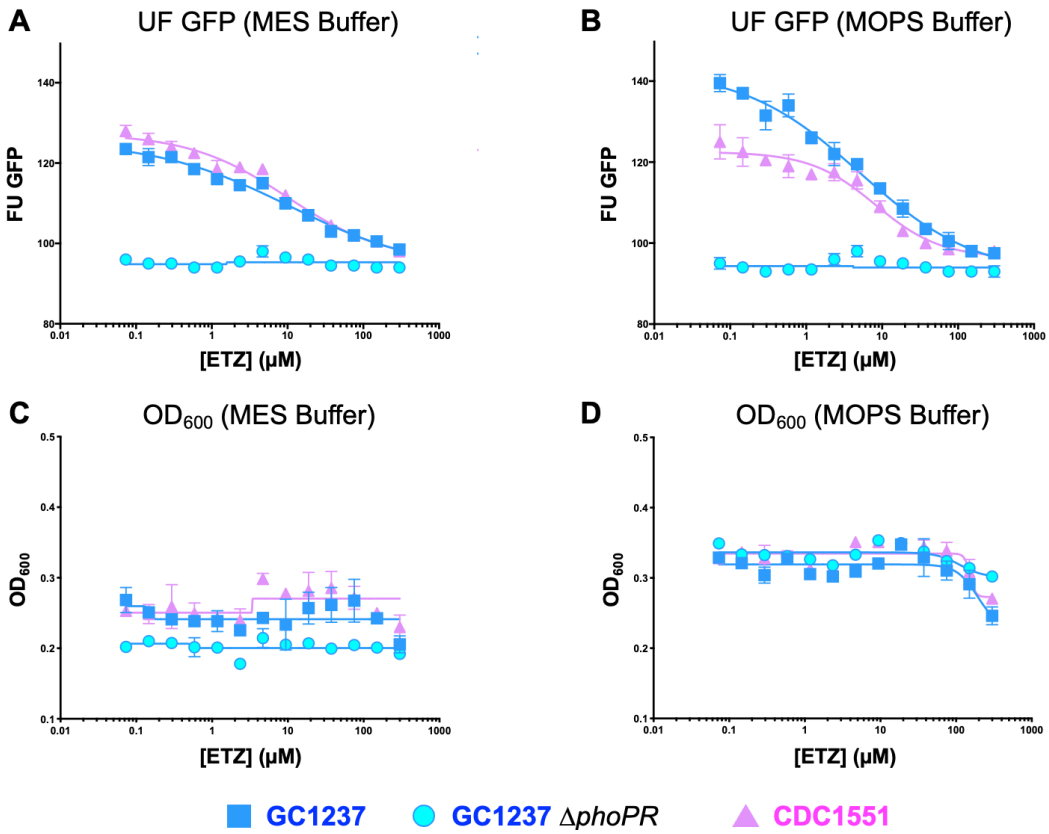

Figure 15: **Dose response effect of ETZ in GC1237 and CDC pFPV27 *pks2*::GFP reporter strains.** Effect of different doses of ETZ in GFP fluorescence in GC1237 (blue squares), GC1237 ΔphoPR (light blue circles) and CDC1551 (pink triangles) carrying the pFPV27 *pks2*::GFP plasmid in acid (**A**) and neutral (**B**) pH, and in growth in acid (**C**) and neutral (**D**) pH. FU GFP IC50 values in MES and MOPS buffer of presented graphs are: GC1237, 10.6 and 5.1 μM; CDC1551, 10.1 and 8.2 μM, respectively.

Construction and validation of new reporter plasmids

Transcriptional studies with microarrays from different groups allowed the identification of *pks2* promoter as one of the most strongly regulated promoters by the PhoPR system (Gonzalo-Asensio, Mostowy, et al., 2008; Walters et al., 2006). Recent techniques like RNA-seq and ChIP-seq in presence of the PhoP protein confirmed the strong regulation and binding of PhoP to *pks2* promoter (Solans et al., 2014). However, these techniques also allowed to identify that *mcr7* promoter is the strongest regulated promoter by the PhoPR system. The use of reporter strains with a second promoter would help to confirm the inhibitory activity of future PhoPR inhibitors, as it could allow to distinguish between compounds with a "promoter-specific" activity or "general" PhoPR inhibition.

We designed different new plasmids, carrying the *pks2* or the *mcr7* promoter, for the construction of new *M. tuberculosis* reporter strains. We decided to use the pMV361 plasmid as backbone for the design and construction of the new plasmids. The first two plasmids contained the eGFP gene optimized for *M. tuberculosis* codon usage (Andersson & Sharp, 1996) under the control of the *pks2* or the *mcr7* promoter, leading to the pMV361 *pks2*::eGFP and pMV361 *mcr7*::eGFP plasmids. These plasmids are expected to produce increased GFP fluorescence in PhoPR active bacteria, with the use of the eGFP gene optimized for *M. tuberculosis* codon usage instead of the GFP mut2 that is encoded in the pFPV27 plasmid (Barker et al., 1998). These two plasmids were electroporated to *M. tuberculosis* H37Rv, H37Rv Δ*phoPR*, GC1237, GC1237 Δ*phoPR* and CDC1551 strains.

Even though pH has been described as an important inductor of the PhoPR system, GFP inhibition results obtained in presence of MES and MOPS buffers were similar, but showed worst growth rates in MES buffer (***Figure 14*** and ***Figure 15***). Because to differentiate between PhoPR inhibitors and antimicrobials, an optimal growth of the bacteria is needed, we decided to compare the GFP production and growth of the *M. tuberculosis* reporter strains in the tree genetic backgrounds (H37Rv, GC1237 and CDC1551) in acid and neutral pH to test which condition was more optimal to perform future experiments. As it has been already mentioned, both H37Rv and CDC1551 belong to the lineage 4 of the MTBC and GC1237 belongs to lineage 2. H37Rv has a SNP in *phoR* gene that leads to a P172 polymorphism in PhoR protein, which is the only difference among the PhoPR systems of the three strains (***Figure 16A***). The different reporter strains carrying either the original pFPV27 *pks2*::GFP (***Figure 16B***) or the new pMV361 *mcr7*::eGFP plasmid (***Figure 16D***) produced similar levels of GFP fluorescence when grown in MES or MOPS containing media, but with worst growth rates in presence of MES buffer that in MOPS (***Figure 16C***). After these observations, we decided to

perform hereafter the experiments in standard 7H9Tyl-ADC, which has a pH of 6.6, without addition of MES or MOPS buffers, unless otherwise indicated.

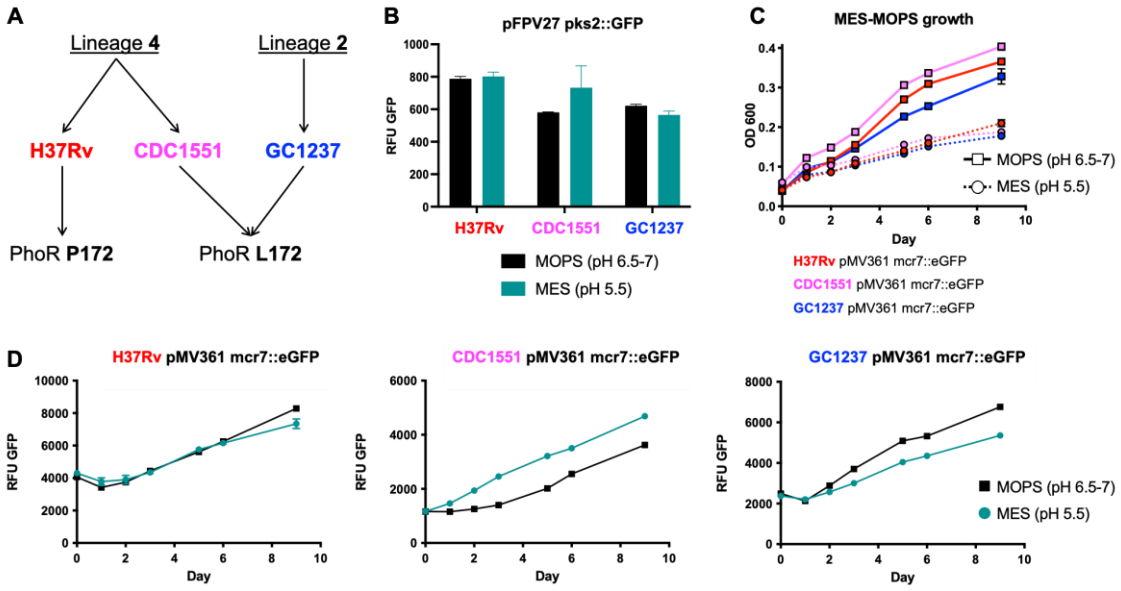

Figure 16: **Comparison of MES and MOPS buffer in *M. tuberculosis* PhoPR reporter strains.** (**A**) Scheme of lineage belonging and PhoR polymorphisms of H37Rv, CDC1551 and GC1237. (**B**) Relative expression of GFP fluorescence of H37Rv, CDC1551 and GC1237 carrying pFPV27 *pks2*::GFP plasmid in MOPS (black) and MES (teal) containing media at day 8. (**C**) Evolution of growth of H37Rv, CDC1551 and GC1237 carrying pMV361 *mcr7*::eGFP plasmid in MOPS (solid lines) and MES (dotted lines) mediums through 9 days. (**D**) Evolution relative expression of GFP fluorescence of H37Rv, CDC1551 and GC1237 carrying pMV361 *mcr7*::eGFP plasmid in MOPS (black lines) and MES (teal lines) mediums through 9 days.

Next, we tested the new reporter strains in the presence of ETZ in dose-response experiments. All of them shared similar behavior to their related pFPV27 *pks2*::GFP strains: H37Rv, GC1237 and CDC1551 carrying either pMV361 *pks2*::eGFP or pMV361 *mcr7*::eGFP plasmid reduced GFP expression at higher ETZ concentrations, whereas H37Rv Δ*phoPR* and GC1237 Δ*phoPR* derived strains just produced a background signal of GFP that does not change in presence of ETZ (***Figure 17A, B, and C***). Interestingly, strains carrying pMV361 *mcr7*::eGFP plasmid produced higher GFP fluorescence intensity than those carrying pMV361 *pks2*::eGFP in the three different genetic backgrounds. As expected, *M. tuberculosis* strains containing the pMV361 *pks2*::eGFP

produced enhanced FU GFP than those carrying the pFPV27 *pks2*::GFP plasmid. The difference in GFP intensities is not because of different bacterial growth as all the strains grew to the same range (***Figure 17D, E, and F***). This reinforces the idea that *mcr7* promoter is the most regulated promoter by the PhoPR system.

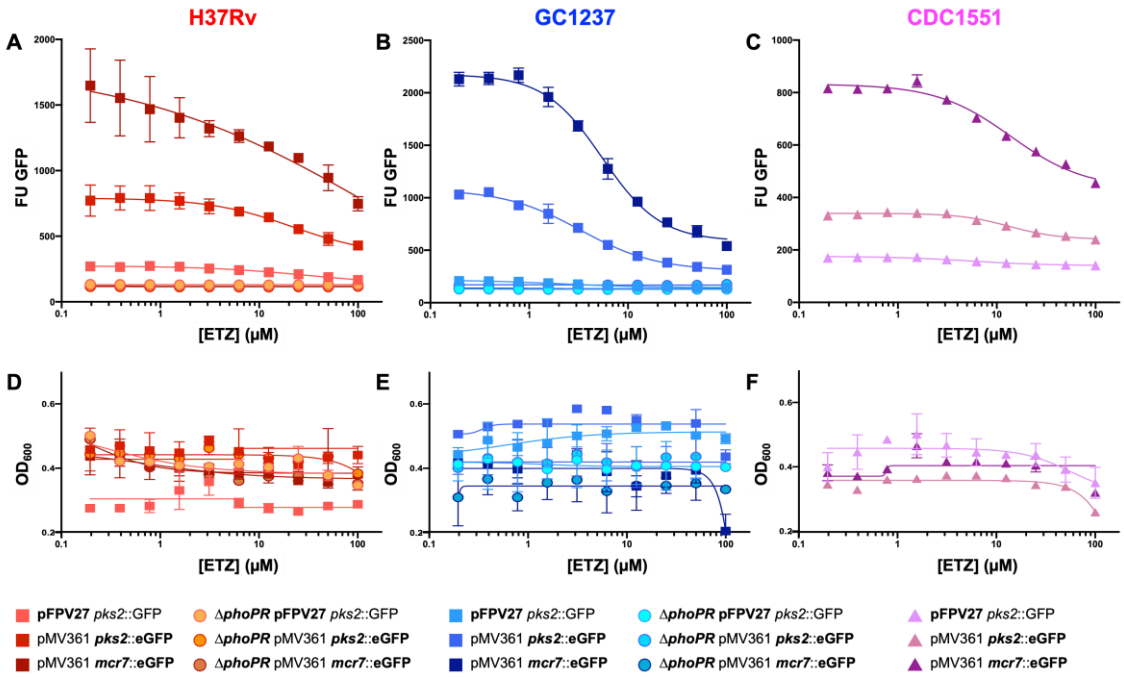

Figure 17: **Dose response effect of ETZ in the new *M. tuberculosis* PhoPR reporter strains.** Effect of different doses of ETZ in GFP fluorescence of the different *M. tuberculosis* PhoPR reporter strains with H37Rv (**A**), GC1237 (**B**) and CDC1551 (**C**) genetic background. Effect of ETZ in growth of the different PhoPR reporter strains with H37Rv (**D**), GC1237 (**E**) and CDC1551 (**F**) genetic background. FU GFP IC50 values in presented graphs are: H37Rv pFPV27*pks2*::GFP, pMV361 *pks2*::eGFP and pMV361 *mcr7*::eGFP, 32.6, 21.8 and 164.9 μM; GC1237 pFPV27*pks2*::GFP, pMV361 *pks2*::eGFP and pMV361 *mcr7*::eGFP, 2.2, 3.3 and 5.5 μM; CDC1551 pFPV27*pks2*::GFP, pMV361 *pks2*::eGFP and pMV361 *mcr7*::eGFP, 5.5, 13.5 and 13.9 μM; respectively.

Once demonstrated that the new constructed plasmids worked properly for the generation of *M. tuberculosis* PhoPR reporter strains, we designed variants of pMV361 *pks2*::eGFP and pMV361 *mcr7*::eGFP plasmids, in which we added a second reporter gene, encoding for the tdTomato protein with red fluorescence, controlled by the strong constitutive *smyc* promoter, whose regulation is independent of the PhoPR system (Carroll et al., 2010). This led to the construction of pMV361 *pks2*::eGFP *smyc*::tdTomato and pMV361 *mcr7*::eGFP *smyc*::tdTomato plasmids, which were transformed into *M.*

tuberculosis H37Rv, H37Rv Δ*phoPR*, GC1237, GC1237 Δ*phoPR* and CDC1551 strains. These double reporter strains produced similar levels of GFP fluorescence than their related plasmids without the tdTomato protein, with the additional production of red fluorescence. As we could observe, in H37Rv (***Figure 18A***), GC1237 (***Figure 18C***) and CDC1551 (***Figure 18E***) strains, GFP fluorescence from cultures in exponential growth increased from strains carrying the pFPV27 *pks2*::GFP plasmid to strains carrying the pMV361 *pks2*::eGFP, with or without the *smyc*::tdTomato sequence. The derived strains carrying the *mcr7* promoter produced the higher GFP fluorescence, but only strains carrying the tdTomato derived plasmids produced red fluorescence (data for CDC1551 pMV361 *pks2*::eGFP *smyc*::tdTomato is not shown because no colonies were obtained for this strain (***Figure 18E***)). However, H37Rv Δ*phoPR* (***Figure 18B***) and GC1237 Δ*phoPR* (***Figure 18D***) produced a basal GFP fluorescence with the five different plasmids, but tdTomato derived strains maintained the production of red fluorescence.

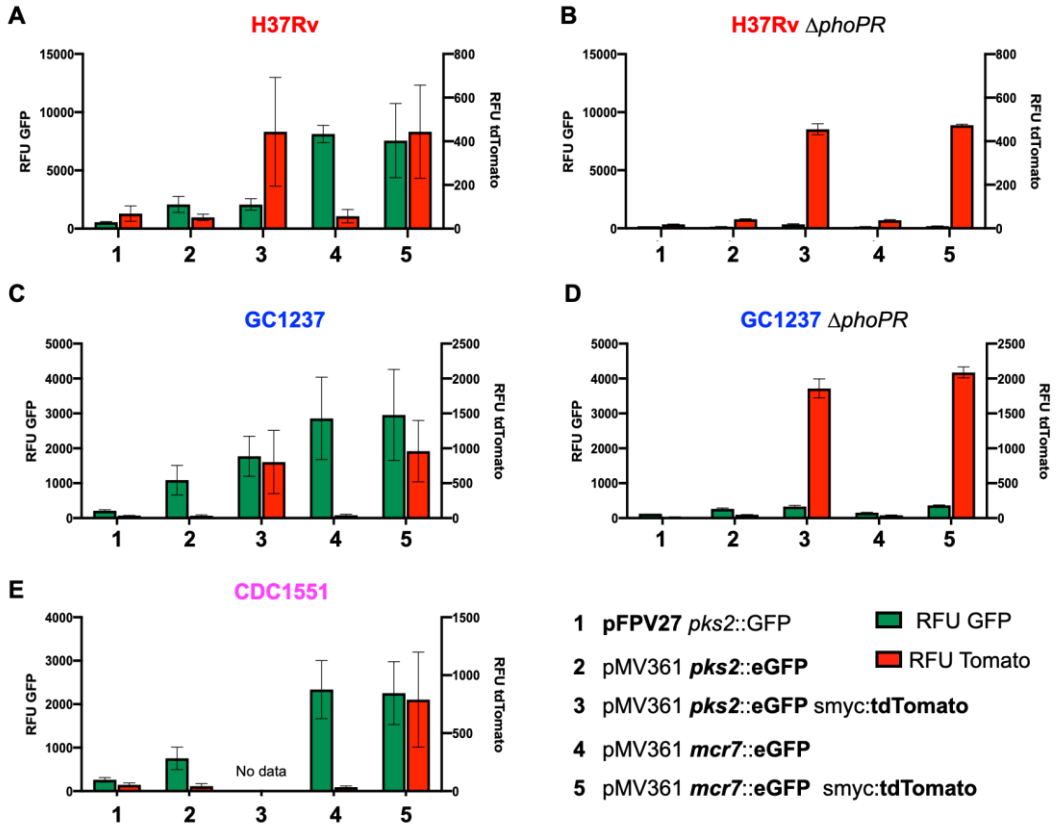

Figure 18: **Fluorescence comparison of the complete *M. tuberculosis* PhoPR reporter strain panel.** Comparison of relative fluorescence units (RFU) of GFP (green, left axis) and tdTomato (red, right axis) of the different PhoPR reporter strains obtained with the different plasmids in H37Rv (**A**), H37Rv Δ*phoPR* (**B**), GC1237 (**C**), GC1237 Δ*phoPR* (**D**) and CDC1551 (**E**).

Comparison of the Signal-Background and Z-factor parameters of the different *M. tuberculosis* PhoPR reporter strains.

In order to compare the potential of each strain to be used for a HTS we decided to calculate a signal to background ratio (S/B) and a Z-factor of each strain for the different parameters we can measure of each strain: FU GFP and OD_{600}. The S/B is a comparison of the means of positive and negative controls of the assay indicating and indicates the dynamic range of the assay (***Eq. 1***) and the Z-factor is a statistical parameter which compares means and standard deviations (SD) of positive and negative controls indicating the robustness of the assay (***Eq. 2***) (Zhang et al., 1999).

Eq. 1: $S/B = \frac{\text{mean}_{\text{control+}}}{\text{mean}_{\text{control-}}}$

Eq. 2: $Z = 1 - \frac{3*(SD_{\text{control+}} + SD_{\text{control-}})}{|\text{mean}_{\text{control+}} - \text{mean}_{\text{control-}}|}$

Future high-throughput screening assays will require positive and negative controls for growth and fluorescence production to distinguish between PhoPR inhibitors (which inhibit FU GFP but not OD_{600} and FU tdTomato), potential antibiotics (which inhibit FU GFP, OD_{600}, and FU tdTomato), and inactive compounds (which do not inhibit FU GFP, OD_{600}, and FU tdTomato). We used rifampicin at 1 µM concentration (4-8 times the minimal inhibitory concentration) as negative control of growth and fluorescence production; and the same volume of DMSO as positive control of growth and fluorescence production. S/B and Z-factor of inhibition of FU GFP and OD_{600} were calculated for all the reporter strains carrying an active PhoPR system.

After 6 days of growth in 96-well plates, we could observe that almost all strains showed a robust Z-factor > 0.5 (green wells in ***Table 6***) in both FU GFP and OD_{600}. Only FU GFP from CDC1551 pFPV27 *pks2*::GFP, pMV361 *pks2*::eGFP and pMV361 *mcr7*::eGFP *smyc*::tdTomato had Z-factor values < 0.5 (red and yellow wells in ***Table 6*** red and yellow squares in ***Figure 19***). At day 6, all the strains carrying the tdTomato variant plasmids produced very low FU tdTomato (***Figure 19***), resulting in even lower fluorescence intensities in presence of DMSO than in rifampicin 1 µM (***Figure 19*** grey squares) which is translated in values of S/B < 1 (grey wells in ***Table 6***) and Z-factor < 0.5.

Table 6: **Z-factor and S/B results of the whole panel of *M. tuberculosis* PhoPR reporter strains after 6 days of incubation.** Each positive and negative controls were tested in 8 wells (one column). Green wells indicate Z-factor > 0.5 (excellent assay), yellow 0.5 > Z-factor > 0 and red Z-factor ≤ 0. Grey wells indicate S/B < 1 (lower signal in the positive control than in negative control). Z-factor and S/B parameters of the FU tdTomato from the strains carrying the pFPV27 *pks2*:GFP, pMV361 *pks2*::eGFP or pMV361*mcr7*::eGFP plasmid are not calculated as they do not produce the tdTomato protein.

		H37RV		GC1237		CDC1551	
		Z-Factor	S/B	Z-Factor	S/B	Z-Factor	S/B
pFPV27 *pks2*:GFP	FU GFP:	0.875	1.992	0.837	1.573	-0.097	1.121
	OD_{600}:	0.537	1.851	0.644	2.057	0.597	1.702
pMV361 *pks2*::eGFP	FU GFP:	0.701	1.825	0.590	3.679	0.467	1.697
	OD_{600}:	0.561	1.423	0.701	2.158	0.677	1.975
pMV361 *mcr7*::eGFP	FU GFP:	0.902	3.940	0.884	3.915	0.681	2.478
	OD_{600}:	0.643	1.759	0.759	1.941	0.654	1.883
pMV361 *pks2*::eGFP *smyc*:tdTmt	FU GFP:	0.703	2.484	0.623	2.695		
	OD_{600}:	0.616	1.773	0.747	1.976		
	FU tdTomato:	-0.025	0.823	-7.637	0.974		
pMV361 *mcr7*::eGFP *smyc*:tdTmt	FUGFP:	0.889	2.767	0.874	4.131	0.404	2.696
	OD_{600}:	0.633	1.678	0.651	2.105	0.705	1.991
	FU tdTomato:	0.482	0.756	0.069	1.271	-2.150	1.169

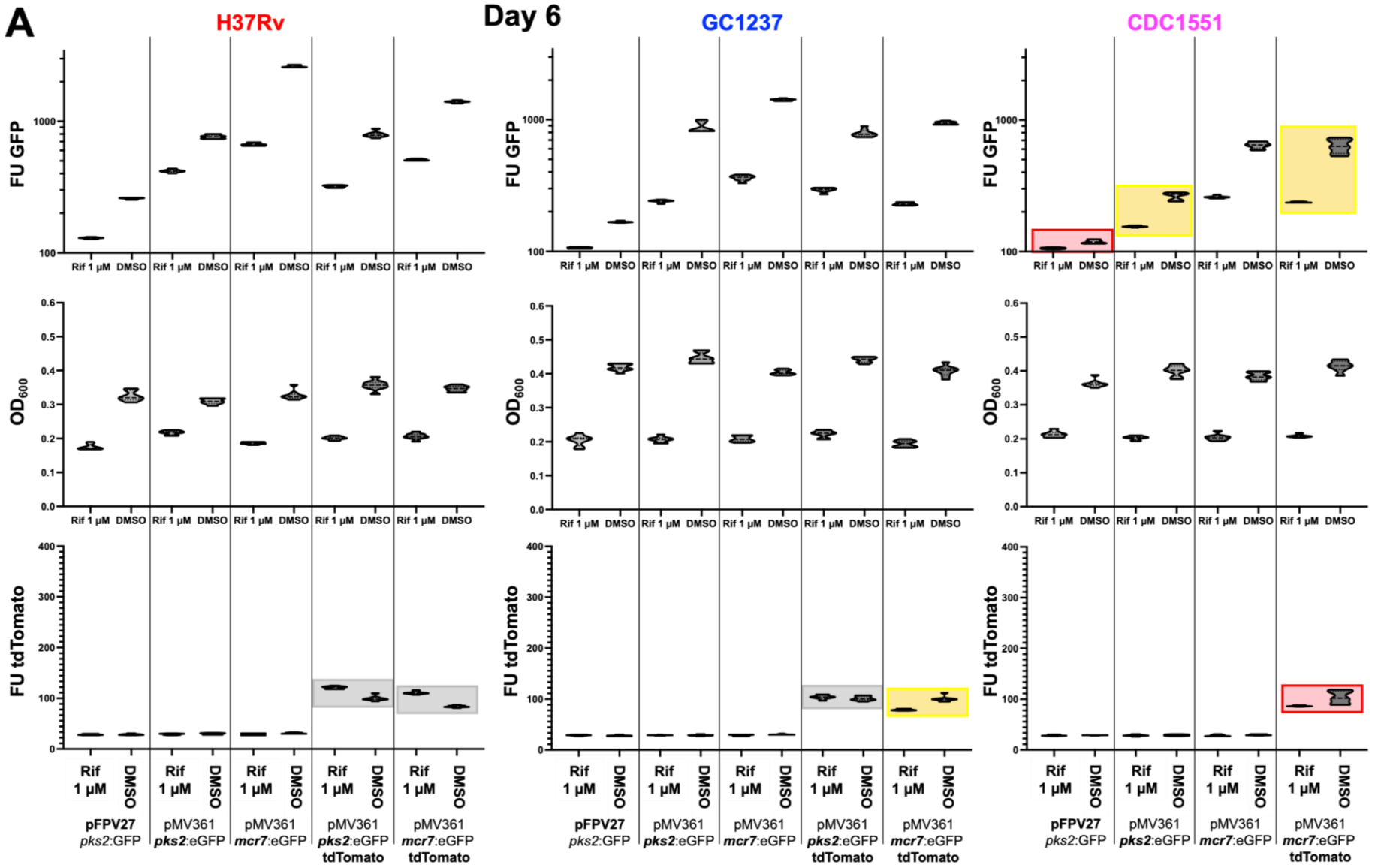
A
Day 6
H37Rv
GC1237
CDC1551
FU GFP
OD600
FU tdTomato
Rif 1 µM
DMSO
pFPV27 pks2:GFP
pMV361 pks2:eGFP
pMV361 mcr7:eGFP
pMV361 pks2:eGFP tdTomato
pMV361 mcr7:eGFP tdTomato

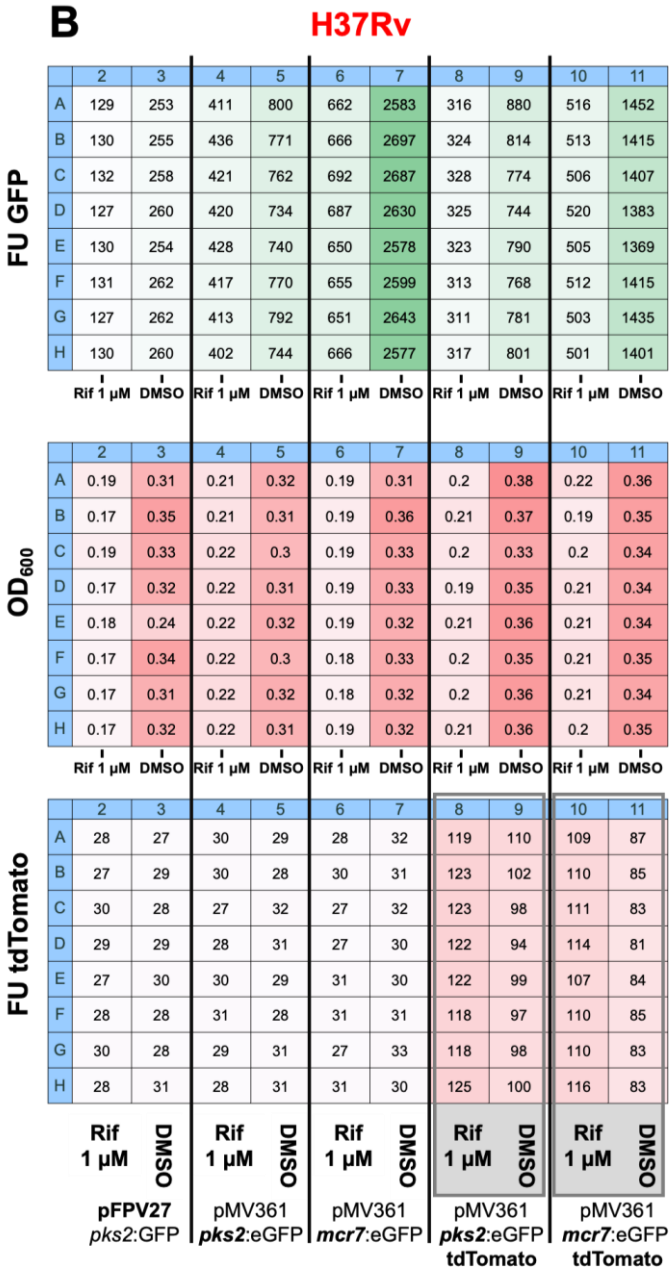

Figure 19: **Fluorescence and growth values of the whole panel of *M. tuberculosis* PhoPR reporter strains after 6 days of incubation.** (**A**) FU GFP (up, logarithmic scale), OD_{600} (middle) and FU tdTomato (down) values obtained at day 6 with rifampicin 1 µM (left) and DMSO (right) to calculate S/B and Z-factor parameters with all the reporter strains carrying an active PhoPR system. (**B**) Example of the numeric values from H37Rv reporter strains and heat map of the FU GFP (up), OD_{600} (middle) and FU tdTomato (down) at day 6 with rifampicin 1 µM (left) and DMSO (right) used to calculate S/B and Z-factor, and plot the graph **A**. Yellow squares indicate 0.5 > Z-factor > 0 and red Z-factor ≤ 0. Grey squares indicate S/B < 1. FU tdTomato values from the strains carrying the pFPV27 *pks2*:GFP, pMV361 *pks2*::eGFP or pMV361*mcr7*::eGFP plasmid do not change in presence or absence of rifampicin they do not produce the tdTomato protein and the fluorescence detected belongs to the background from the medium and the bacteria.

To test whether Z-factor and S/B parameters change when increasing incubation times, we also measured FU GFP, OD_{600} and FU tdTomato after 8 days of growth. As we could observe, after 8 days of incubation at 37°C in 96-well plates, all positive controls (with DMSO) produced higher signals of FU GFP, OD_{600} and FU tdTomato (S/B values > 1, ***Table 7***) and all the strains increased their S/B in FU GFP, OD_{600} and FU tdTomato, increasing the dynamic range of the assay (except for H37Rv pFPV27 *pks2*::GFP, which remained constant). More important is that after 8 days, the Z-factors that at day 6 were < 0.5 raised over 0.5, indicating an improvement of the assay, with the exception of the FU tdTomato from CDC1551 pMV361 *mcr7*::eGFP *smyc*::tdTomato, whose Z-factor remained < 0 due to the high variability of the FU tdTomato obtained in DMSO wells (***Table 7*** and ***Figure 20*** red square).

These results show that all the reporter strains developed in this study have a potential uses in HTS assays, as they exhibit robust differences in OD_{600} and fluorescence measures to distinguish growth and PhoPR inhibiting molecules. The robustness of the study can be improved changing incubations times (from 6 to 8 days), or the signal measured (OD_{600} or FU tdTomato). Accordingly, these assays should be performed before starting a HTS campaign to choose the best *M. tuberculosis* reporter strain and the conditions of the assay.

Table 7: **Z-factor and S/B results of the whole panel of *M. tuberculosis* PhoPR reporter strains after 8 days of incubation.** Each positive and negative controls were tested in 8 wells (one column). Green wells indicate Z-factor > 0.5 (excellent assay), yellow 0.5 > Z-factor > 0 and red Z-factor ≤ 0. Grey wells indicate S/B < 1.

		H37RV		GC1237		CDC1551	
		Z-Factor	S/B	Z-Factor	S/B	Z-Factor	S/B
pFPV27 *pks2*:GFP	FU GFP:	0.859	1.928	0.829	1.856	0.542	1.278
	OD_{600}:	0.620	2.019	0.578	2.926	0.672	2.060
pMV361 *pks2*::eGFP	FU GFP:	0.782	2.232	0.688	5.071	0.586	2.549
	OD_{600}:	0.579	1.564	0.694	2.860	0.545	2.397
pMV361 *mcr7*::eGFP	FU GFP:	0.914	4.964	0.893	5.804	0.749	3.862
	OD_{600}:	0.569	1.914	0.867	2.591	0.664	2.133
pMV361 *pks2*::eGFP *smyc*:tdTmt	FU GFP:	0.759	3.620	0.746	4.782		
	OD_{600}:	0.533	1.968	0.772	2.562		
	FU tdTomato:	0.703	2.599	0.561	2.834		
pMV361 *mcr7*::eGFP *smyc*:tdTmt	FUGFP:	0.878	4.319	0.856	5.861	0.541	4.314
	OD_{600}:	0.533	1.968	0.648	2.572	0.645	2.328
	FU tdTomato:	0.703	2.599	0.774	3.860	-0.242	2.381

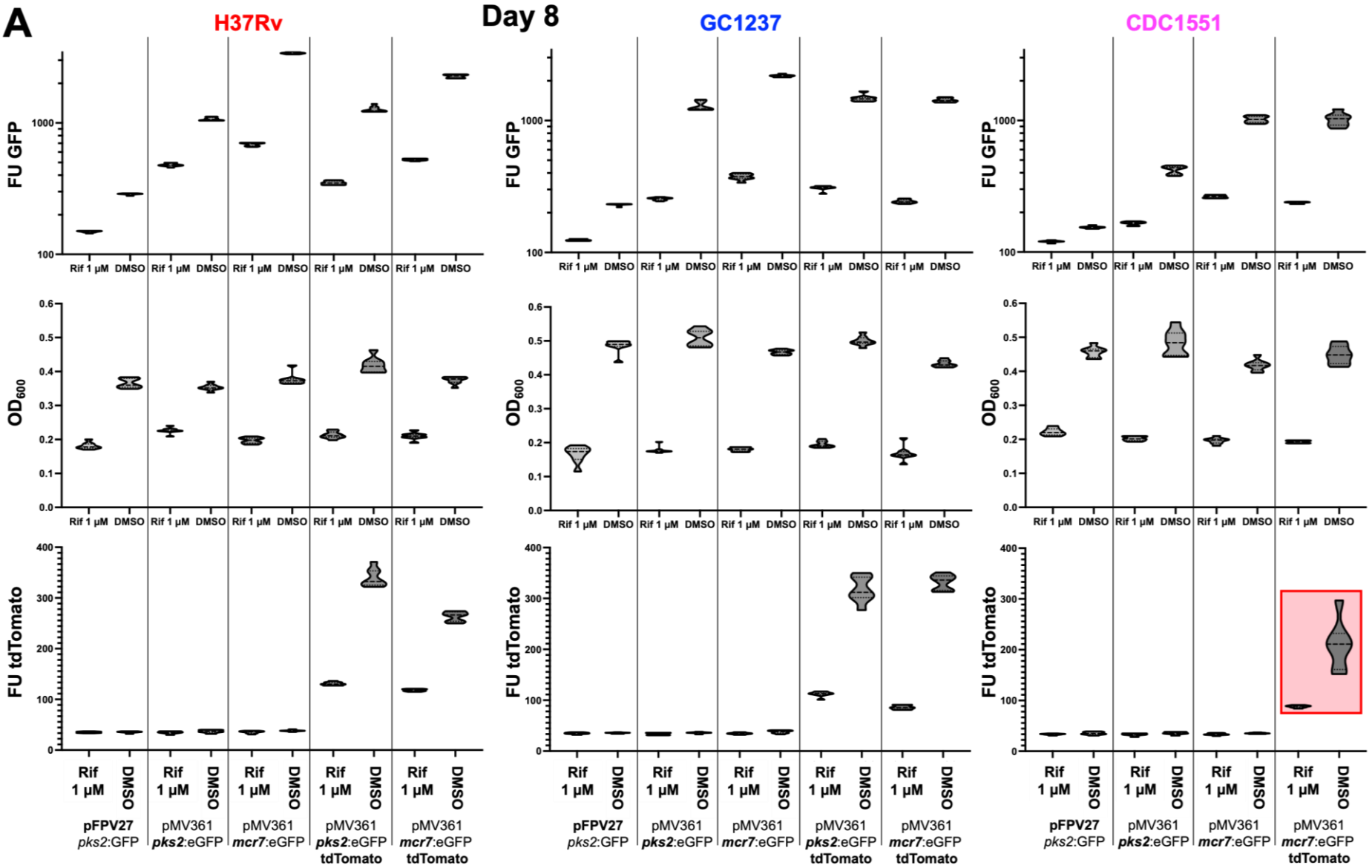
A
Day 8
H37Rv
GC1237
CDC1551
FU GFP
OD600
FU tdTomato
Rif 1 µM
DMSO
pFPV27 pks2:GFP
pMV361 pks2:eGFP
pMV361 mcr7:eGFP
pMV361 pks2:eGFP tdTomato
pMV361 mcr7:eGFP tdTomato

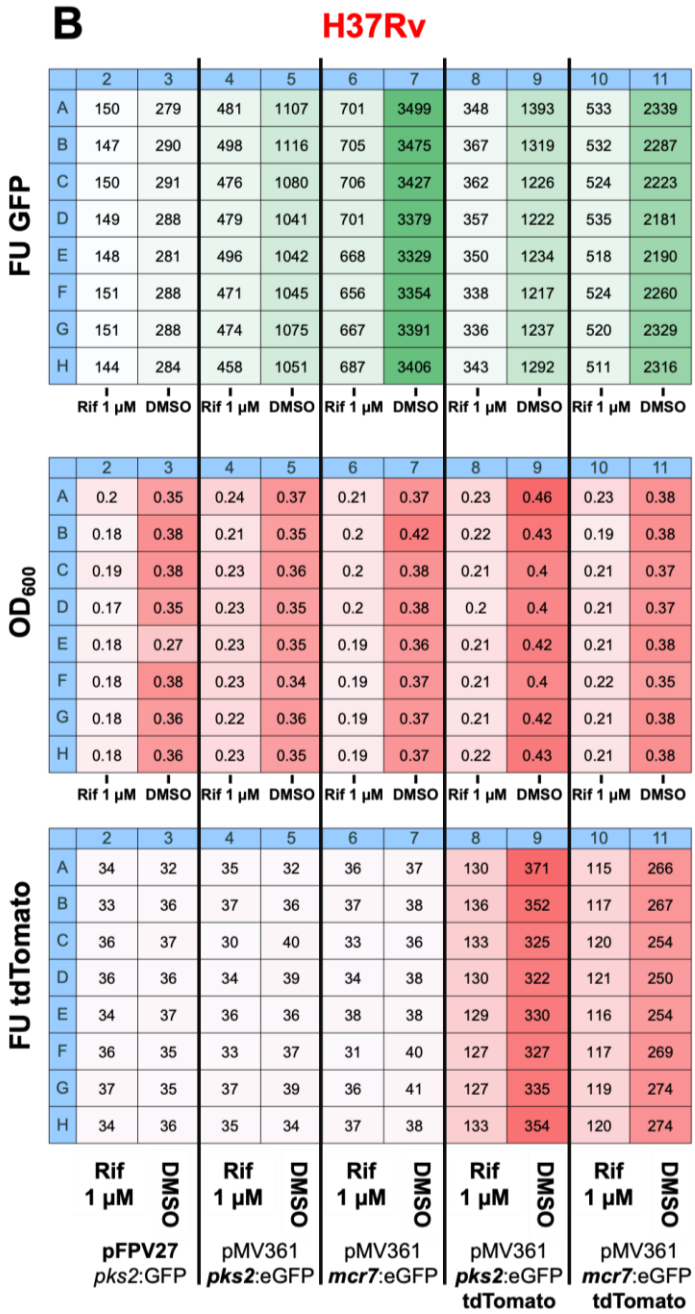

Figure 20: **Fluorescence and growth values of the whole panel of *M. tuberculosis* PhoPR reporter strains after 8 days of incubation.** (**A**) FU GFP (up, logarithmic scale), OD_{600} (middle) and FU tdTomato (down) values obtained at day 6 with rifampicin 1 µM (left) and DMSO (right) to calculate S/B and Z-factor parameters with all the reporter strains carrying an active PhoPR system. The red square indicates a Z-factor ≤ 0. (**B**) Example of the numeric values from H37Rv reporter strains and heat map of the FU GFP (up), OD_{600} (middle) and FU tdTomato (down) at day 6 with rifampicin 1 µM (left) and DMSO (right) used to calculate S/B and Z-factor, and plot the graph **A**. FU tdTomato values from the strains carrying the pFPV27 *pks2*:GFP, pMV361 *pks2*::eGFP or pMV361*mcr7*::eGFP plasmid do not change in presence or absence of rifampicin they do not produce the tdTomato protein and the fluorescence detected belongs to the background from the medium and the bacteria.

Secondary assays to confirm PhoPR inhibition.

To confirm the mode of action of potential PhoPR inhibitors it is important to conduct further characterization. Reliable secondary assays can be used to confirm the specificity and potency of PhoPR inhibitor candidates, as the PhoPR inhibition in reporter strain experiments is only indirectly measured through a reduction in GFP fluorescence. It is crucial to confirm the mechanism of action of PhoPR inhibitors in order to better understand their potential as therapeutic agents. Using ETZ as control molecule, here we propose to perform a transcriptional characterization of the PhoPR inhibitor to confirm their impact in the PhoPR regulon, and to evaluate the secretion of different ESX-1 dependent proteins.

Transcriptional characterization of the PhoPR regulon

After confirming the inhibitory activity of ETZ *in vitro* in different *M. tuberculosis* reporter strains with an active PhoPR system, we decided to continue with a transcriptional characterization of the inhibitory activity of ETZ. We tested the effect of an inhibitory concentration of ETZ in two different genetic backgrounds, the H37Rv form the MTBC L4, and the GC1237 from the MTBC L2, with their related Δ*phoPR* mutants and complemented Δ*phoPR::phoPR-TB* mutants, which recover the active PhoPR system by the introduction of the integrative plasmid pWM222 (Gonzalo-Asensio et al., 2014). *M. tuberculosis* strains were inoculated in rich medium with an initial OD_{600} of 0.2 in presence of 60 µM of ETZ or an equivalent volume of DMSO. Total RNA was isolated from the different samples in exponential phase of growth and qRT-PCR was performed to evaluate the expression of different genes of the PhoPR regulon: *mcr7* (ncRNA which blockades translation of *tatC* mRNA), *pks2*, *pks3* (polyketide synthases involved in SL, and DAT and PAT biosynthesis, respectively), and *espA*, *espC* and *espD* genes (required for ESAT-6 secretion), using *sigA* gene (RNA polymerase sigma factor) expression as endogenous control of normalization. ETZ was able to downregulate the expression of all the genes tested from the PhoPR regulon in parental strains from both L2 (***Figure 21A***) and L4 (***Figure 21B***) genetic backgrounds, with no effect in gene expression of Δ*phoPR* mutants. Complemented Δ*phoPR::phoPR-TB* mutants recovered the expression of the different genes of the PhoPR regulon, but addition of ETZ also resulted in decreased expression of these genes.

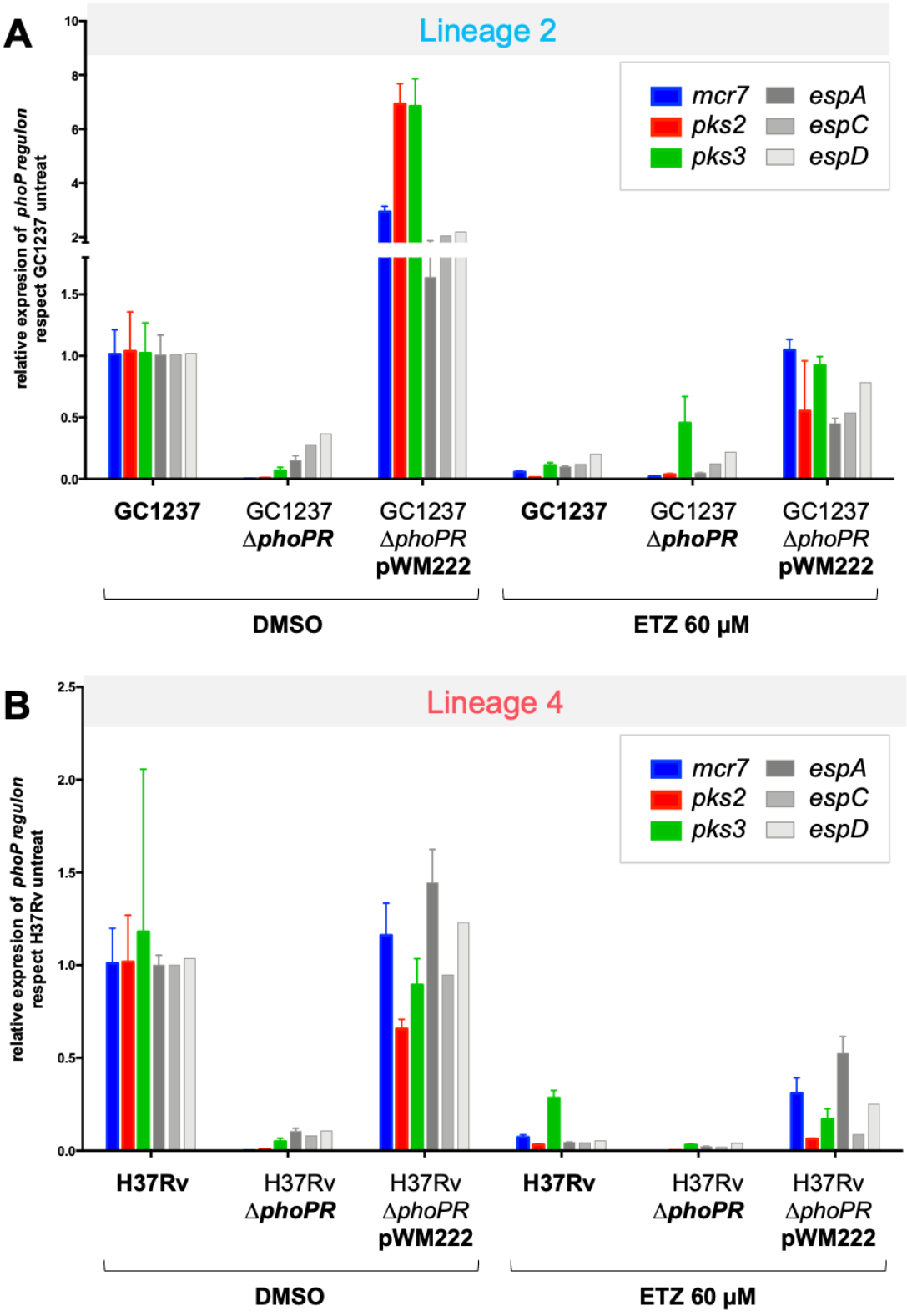

Figure 21: **Effect of ETZ in the PhoPR regulon of H37Rv and GC1237 strains.** Quantification of different gene expression by qRT-PCR of different genes from the PhoPR regulon in strains from L2-GC1237 (**A**) and L4-H37Rv (**B**) genetic backgrounds with their native PhoPR systems, their related Δ*phoPR* mutants and pWM222 complemented strains in absence or presence of ETZ 60 µM.

We also sought to observe the effect of different doses ETZ in the regulation of the PhoPR regulon. In order to be able to follow PhoPR inhibition trough time, we incubated the H37Rv pFPV27 *pks2*::GFP strain with different concentrations of ETZ and we used its Δ*phoPR* mutant as control. Total RNA was extracted and subjected to qRT-PCR as described above. We firstly noticed that relative fluorescence units of GFP (RFU GFP) of the samples recorded right before cell processing and normalized between untreated and Δ*phoPR* controls almost perfectly match with the *pks2* expression values measured by qRT-PCR (***Figure 22***), indicating the reliability of our reporter strain.

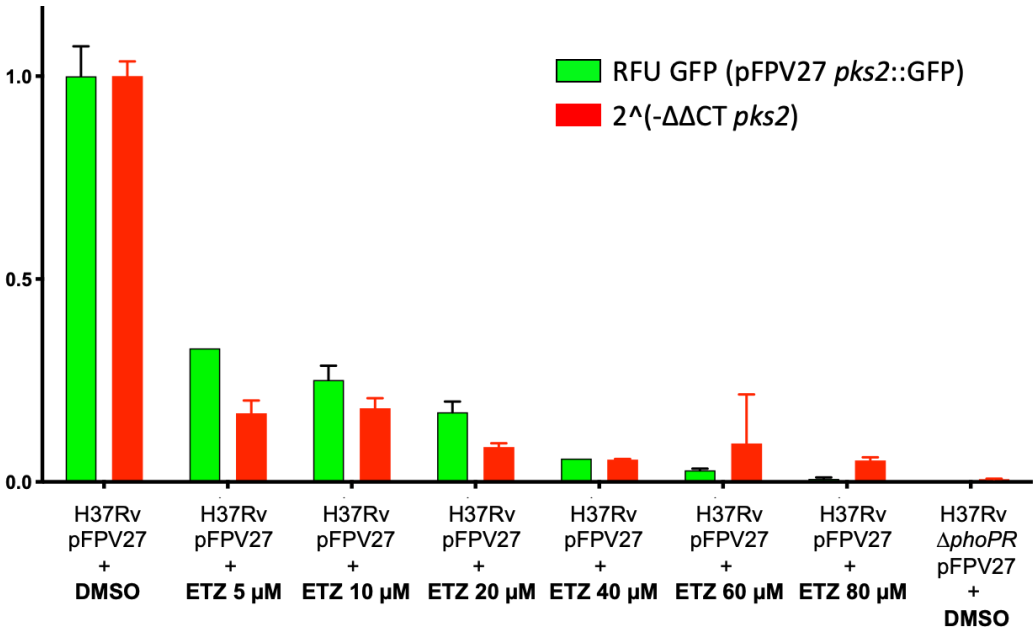

Figure 22: **Correlation of fluorescence and transcriptional inhibition**. Comparison of normalized RFU and relative expression of *pks2* gene measured by qRT-PCR of H37Rv pFPV27 *pks2*::GFP at different ETZ concentrations and H37Rv Δ*phoPR* pFPV27 *pks2*::GFP.

Incubation of H37Rv pFPV27 *pks2*::GFP strain with different doses of ETZ also allowed the observation of two different profiles in the six genes quantified by qRT-PCR. As we can observe, *mcr7*, *pks2* and *pks3* were downregulated with the smallest concentration tested, ETZ 5 µM, whereas *espA*, *espC* and *espD* genes have a dose-response profile, being more downregulated with increasing ETZ concentration (***Figure 23***). The shared phenotype of *espA*, *espC* and *espD* genes is somewhat expected as the three genes are regulated by the same promoter in a single operon. These differences in the regulation might be due to the direct regulation of PhoP in *mcr7*, *pks2* and *pks3*, but a more complex regulation of the *espACD* operon, which is directly and indirectly regulated by PhoP, WhiB6 and EspR proteins (Broset et al., 2015).

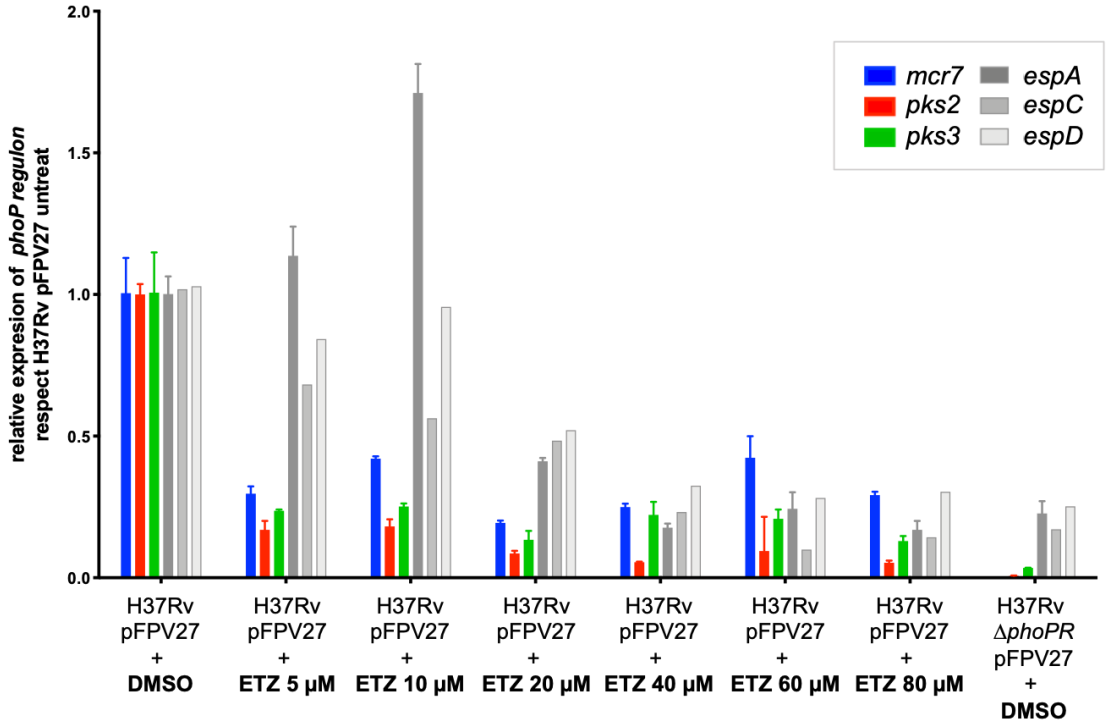

Figure 23: **Effect of different doses of ETZ in the PhoPR regulon of H37Rv.** Quantification of different gene expression by qRT-PCR of different genes from the PhoPR regulon in H37Rv pFPV27 *pks2*::GFP at different ETZ concentrations and H37Rv Δ*phoPR* pFPV27 *pks2*::GFP.

Secretion of ESX-1 dependent proteins

One of the main phenotypes controlled by the PhoPR system is the ESX-1 dependent secretion of ESAT-6, one of the key virulent factors of *M. tuberculosis*. In Δ*phoPR* mutants, ESAT-6 is expressed but not secreted due to the downregulation of the *espACD* operon. This phenotype is one of the most important characteristics of the attenuated Δ*phoPR* mutants. We evaluated the effect of ETZ in the secretion of ESX-1 dependent proteins. Culture filtrates from *M. tuberculosis* GC1237, GC1237 Δ*phoPR*, GC1237 Δ*phoPR* pWM222 and GC1237 treated with ETZ 60 µM were analyzed by targeted MRM-MS. Different specific peptides were analyzed and quantified from ESAT-6, CFP-10, EspA and EspC proteins. As we can observe ESAT-6 is detected in the secreted fraction of GC1237 and complemented strain, but not in the Δ*phoPR* mutant. Addition of ETZ 60 µM to GC1237 resulted in the absence of ESAT-6 in supernatant as in the Δ*phoPR* strain (***Figure 24A and B***). Similar effect is observed in secretion of other ESX-1 dependent proteins as CFP-10 (***Figure 24C and D***), EspA (***Figure 24E and F***) and EspD (***Figure 24G and H***). Although ESAT-6 is co-secreted with CFP-10, an absence of total secretion of CFP-10 is not expected as it has been reported that the vaccine

candidate MTBVAC, which carries a Δ*phoP* mutation, is able to secrete CFP-10 independently of ESAT-6 (Aguilo et al., 2017).

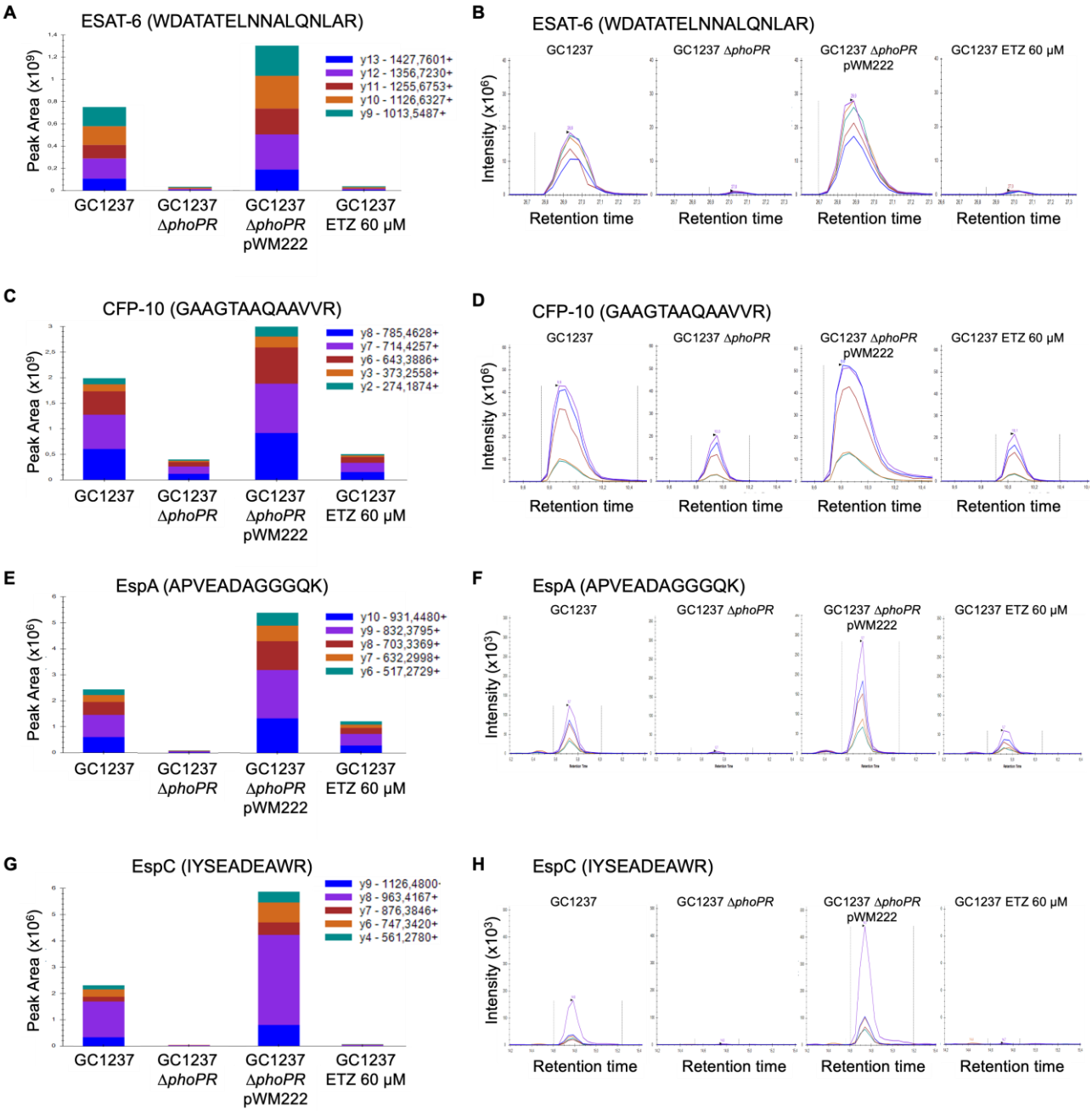

Figure 24: **Effect of ETZ in the inhibition of secretion of ESX-1 substrates in GC1237.** Quantification of protein levels in the secreted fraction of GC1237, GC1237 Δ*phoPR*, GC1237 Δ*phoPR* pWM222 and GC1237 in presence of ETZ 60 µM. Peak areas and intensities detected from peptides of ESAT-6 (**A** and **B**), CPF-10 (**C** and **D**), EspA (**E** and **F**) and EspC (**G** and **H**) are represented respectively.

PhoP expression is independent of ETZ treatment.

We hypothesize that the inhibition of the PhoPR system could be achieved by two main mechanisms: (1) preventing the synthesis of the PhoPR system by knocking-down the transcription of the *phoPR* operon or blockading the translation of *phoPR* mRNA; or (2) inactivating the activity of PhoP, PhoR, both, or possible accessory proteins that contribute to the proper functioning of the PhoPR system.

We evaluated the effect of ETZ 60 µM in the expression of the PhoP gene and protein. Measuring the expression of the *phoP* cDNA from GC1237 samples revealed that addition of ETZ treatment does not substantially affect the expression of *phoP* (***Figure 25A***). When protein was extracted from whole cell lysates of GC1237 samples we can observe that ETZ does not affect expression of PhoP protein in samples of GC1237 wild type and GC1237 Δ*phoPR* pWM222 complemented strains, being undetectable in GC1237 Δ*phoPR* samples (***Figure 25B***). These results suggest that ETZ does not act preventing *phoP* gene or PhoP protein expression, but ETZ acts, somehow, inhibiting the activity of the PhoPR system.

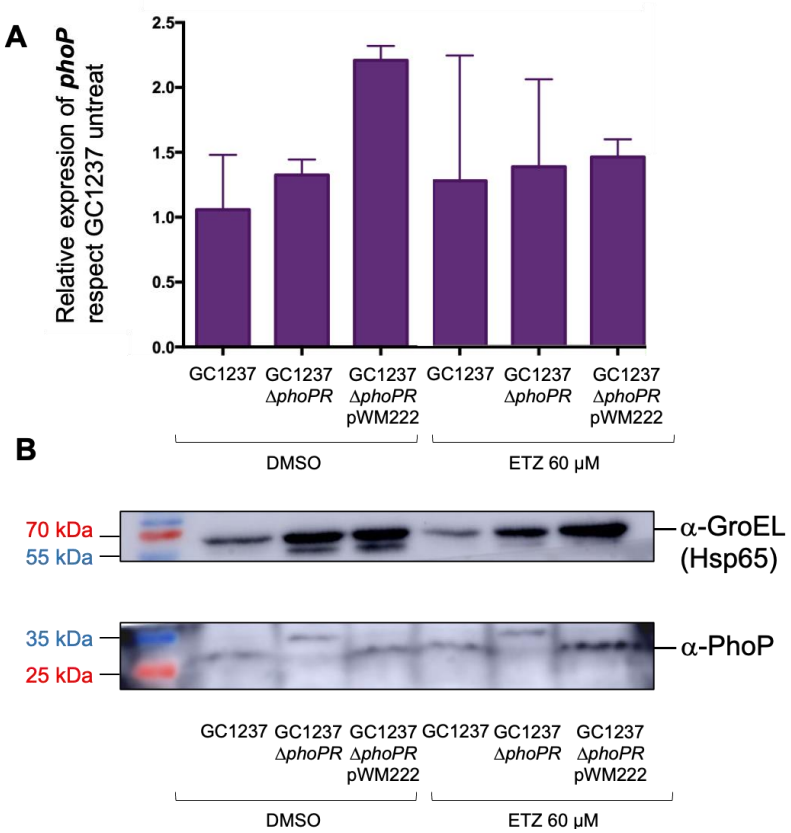

Figure 25: **Effect of ETZ in PhoP gene and protein expression in GC1237 strains.** Quantification of *phoP* gene expression by qRT-PCR in GC1237, GC1237 Δ*phoPR* and GC1237 Δ*phoPR* strains in presence or absence of ETZ 60 µM (**A**). Western blot analysis of whole cell protein lysates from GC1237, GC1237 Δ*phoPR* and GC1237 Δ*phoPR* strains in presence or absence of ETZ 60 µM (**B**).

Comparative effects of therapeutic carbonic anhydrase inhibitors on the PhoPR inhibition

It has been hypothesized that the inhibitory activity of ETZ in the PhoPR system acts through the inhibition of the CAs form *M. tuberculosis* (mtbCAs) (Johnson et al., 2015). Other molecules have been also identified as mtbCA inhibitors. Acetazolamide (ATZ) is another CA inhibitor that is currently in use in the clinic for of epilepsy, altitude sickness, idiopathic intracranial hypertension, and heart failure (Kumar et al., 2021). It has been probed that ATZ has inhibitory activity in purified mtbCAs proteins with higher potency than ETZ (***Table 8***).

Table 8: **Inhibition of hCA II and mtbCA 1, 2 and 3 by ATZ and ETZ.** Adapted from (Carta et al., 2009).

Inhibitor	hCA II (μM)	mtbCA 1 (μM)	mtbCA 3 (μM)	mtbCA 2 (μM)
ATZ	0.012	0.481	0.104	0.009
ETZ	0.008	1.03	0.594	0.027

We decided to test the inhibitory activity of ATZ in the PhoPR system using the H37Rv pFPV27 *pks2*::GFP strain in acid and neutral pH. ATZ has no effect inhibiting the GFP production *in vitro* neither with acid (***Figure 26A***) or neutral pH (***Figure 26B***). Like ETZ, ATZ has no effect in bacterial growth at the concentration tested (***Figure 26C and D***). Therefore, we hypothesize that ETZ PhoPR inhibition is independent of its mtbCA inhibitory activity.

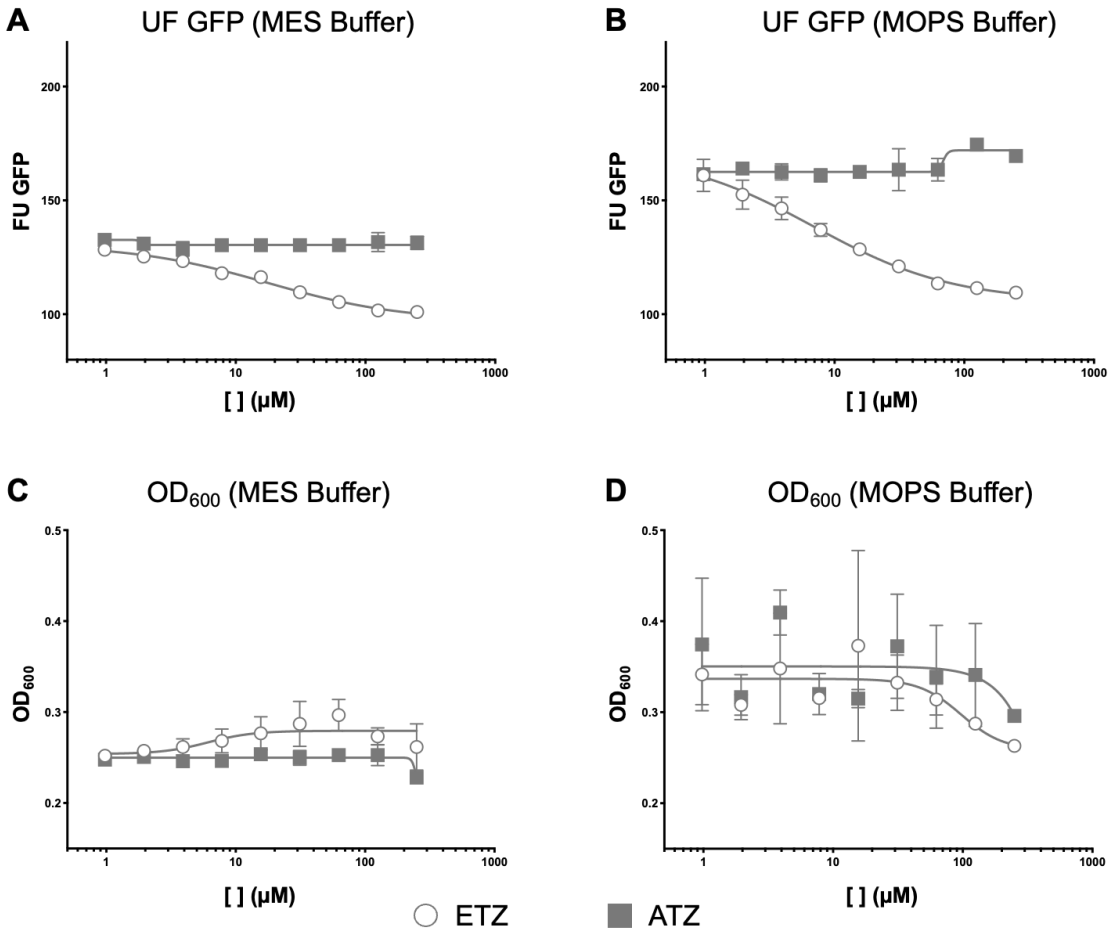

Figure 26: **Comparative effect of different CAs inhibitors in H37Rv pFPV27 *pks2::*GFP.** Effect of different doses of ETZ (circles) and ATZ (grey squares) in H37Rv pFPV27 *pks2*::GFP in GFP fluorescence in acid (**A**) and neutral (**B**) pH, and in growth in acid (**C**) and neutral (**D**) pH. FUGFP IC50 values for ETZ inhibition in MES and MOPS buffers in presented graphs were 17.6 and 6.9 µM, respectively.

Engineering *M. smegmatis* as a surrogate of *M. tuberculosis* PhoPR reporter strain.

Comparative of PhoPR proteins from *M. tuberculosis* and *M. smegmatis*.

M. tuberculosis strains are pathogenic bacteria that require Biosafety Level 3 laboratories, special infrastructures that require specific licenses for their construction and formation of trained personnel. In addition, *M. tuberculosis* strains are slow growing bacteria, with typical doubling times of 24 h, what makes the experiments long lasting in comparison with other species.

M. smegmatis is an environmental non-pathogenic *Mycobacterium* which has been used as safe laboratory model for mycobacterial genetics and drug resistance studies as it can be handled in Biosafety Level 1 laboratories. In addition, typical doubling times of *M. smegmatis* are about 3 hours, making it a relatively fast-growing mycobacteria, in comparison with *M. tuberculosis*.

The PhoPR two components system of *M. smegmatis* is highly similar to *M. tuberculosis*. PhoP protein sequences share a 92.7% identity. A deeper observation reveals that identities in the Response regulatory domain and the OmpR/PhoP-type (DNA binding) domain rise to 94.8% and 95.9% respectively, and mutations have been accumulated outside these two domains (***Figure 27A***).

PhoR protein sequences are more distant than those of PhoP proteins, sharing a 71% of protein identity. A deeper look reveals that the two transmembrane domains share an 80% and 75% of identity (that rise to 80% when correcting the specific L172P mutation/allele of the H37Rv *M. tuberculosis* background (Schreuder et al., 2015), as L172 is the predominant allele in *M. tuberculosis* strains), the extracellular sensor domains share a 49.6% identity, the HAMP domains share a 84.9% of identity, and the Histidine kinase domains share a 79.6% identity, comprising the dimerization DHp domains and the ATP catalytic and binding domains, with 85,4% and 78,9% identities respectively. Mutations in PhoR have been accumulated in N and C-terminal regions and in the extracellular sensor domain (***Figure 27B***).

Structures of PhoP and PhoR proteins from *M. tuberculosis* and *M. smegmatis* have been modelled/predicted by Alphafold software. Superposition of *M. smegmatis* PhoP predicted structure with PDB 5ed4 (He et al., 2016), in which *M. tuberculosis* PhoP protein structure was solved in complex with DNA, almost perfectly match, maintaining structure and domains (***Figure 27C***). We can observe that position of residues as Asp 71 (Asp 63 in *M. smegmatis* PhoP), the phosphorylation site of PhoP, or Ser 219 (Ser

211 in *M. smegmatis* PhoP), important residue in DNA recognition by PhoP, completely overlap in both structures (***Figure 27C***). Superposition of PhoR modelled structures from *M*. *tuberculosis* and *M. smegmatis* reveal the conserved structure of PhoR and its domains (***Figure 27D***). We can observe that the phosphorylation site of PhoR, His 259 (His 258 in *M. smegmatis* PhoR) in the DHp domain, or the Leu 172 from H37 background and the Pro 171 from *M. smegmatis*, which is the main allele in the *M. tuberculosis* isolates (Broset et al., 2015), almost perfectly overlap in both models. However, the Gly 71 residue (Gly 70 in *M. smegmatis* PhoR), even the secondary structure of the sensor domain is highly conserved, is located in a disordered region of the domain and predictions are different (***Figure 27D***).

The similarities and differences observed between the PhoPR systems of *M. tuberculosis* and *M. smegmatis* might indicate that both systems share similar mechanisms of action, as the PhoP domains and HAMP and Histidine kinase domains from PhoR are highly conserved, but the two component systems may respond to different stimuli as higher differences are observed in the sensor protein, PhoR, especially in the extracellular sensor domain. To develop a safer organism, like *M. smegmatis*, to test potential inhibitors of the PhoPR system, we need to express the heterologous PhoPR system to which we want to screen the potential inhibitors. Introducing the *M. tuberculosis* PhoPR system directly into a *M. smegmatis* strain might appear an interesting approach, however, simultaneous expression of two different PhoPR systems at the same time in the same organism might lead to cross activation or repression of both systems, leading to confusing results. In order to avoid this phenotype, we decided to replace the endogenous PhoPR system from *M. smegmatis* by its homologous system from *M. tuberculosis*. In addition, we also decided to construct a knock-out mutant of the PhoPR system in *M. smegmatis* as control strain with an inactive PhoPR system.

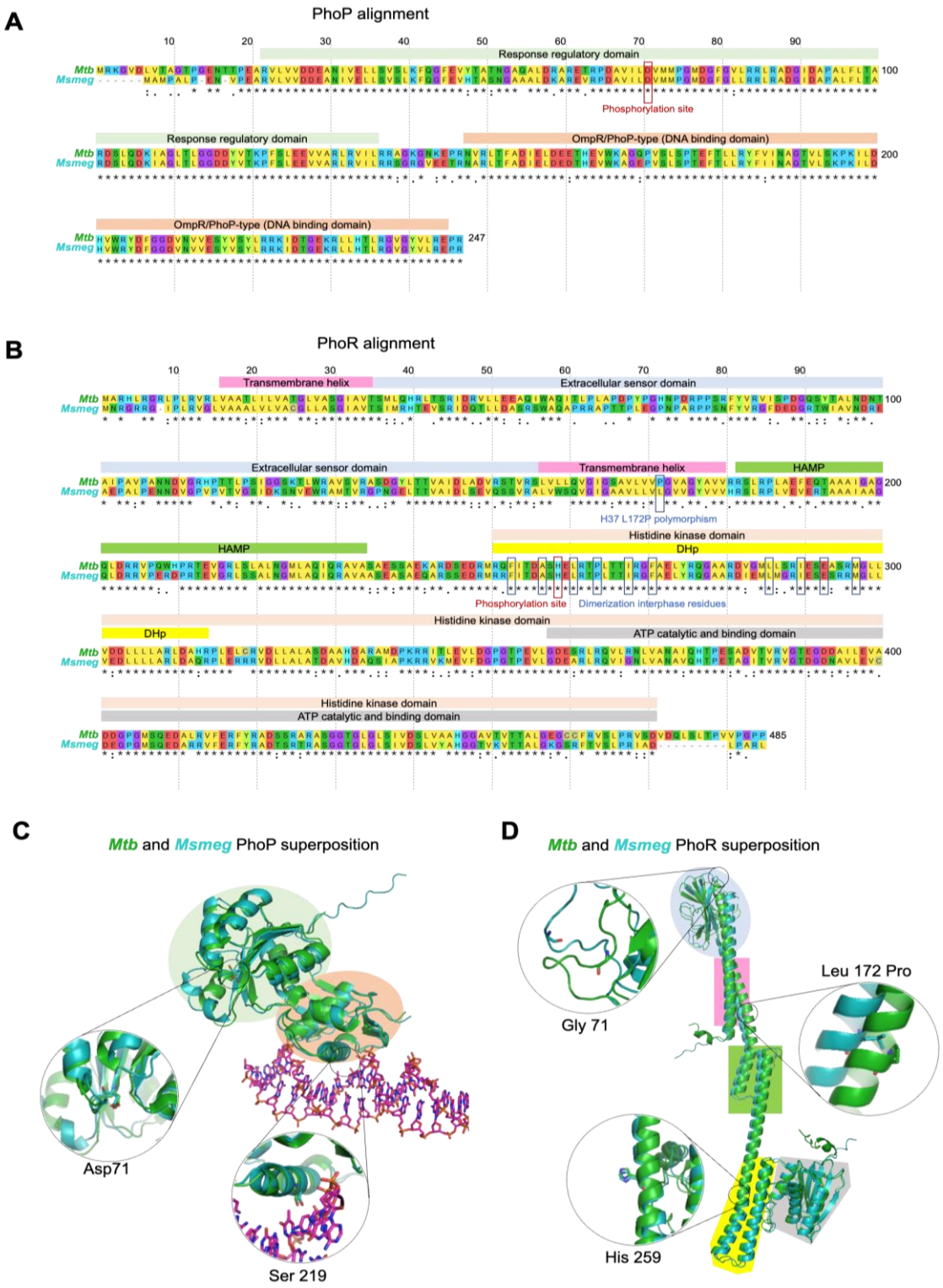

Figure 27: **Comparative of PhoP and PhoR proteins from *M. smegmatis* and *M. tuberculosis*.** Alignment of PhoP (**A**) and PhoR (**B**) protein sequences from *M. tuberculosis* (upper sequence) and *M. smegmatis* (lower sequence) with MUSCLE algorithm in MEGA (Tamura et al., 2021). Alignment of *M. tuberculosis* PhoP's structure (green) and bonded DNA (pink) from PDB 5ed4 and *M. smegmatis* PhoP modeled structure with Alphafold (cyan) (**C**). Alignment of PhoR protein structures from *M. tuberculosis* (green) and *M. smegmatis* (cyan) modeled with Alphafold (**D**). Relevant aminoacids for PhoP and PhoR activity are highlighted.

Construction of *M. smegmatis* carrying a *phoPR* allele from *M. tuberculosis.*

Inactivation of *M. smegmatis phoPR* (SM*phoPR*) genes was achieved by recombineering using a double strand AES (dsAES) amplified by PCR from pKD4 plasmid using long oligonucleotides (60-mers). The 3' sequence of these oligonucleotides aligned to P1 or P2 sites, allowing amplification of Km resistance cassette flanked by FLP recognition target (FRT) sites, and their 5' sequence introduced identity arms for recombination in SMphoPR genes (***Figure 28A***). Then, the dsAES was electroporated to recombineering induced *M. smegmatis* mc^2155 pJV53H. Km resistant colonies were isolated and correct inactivation of SM*phoPR* genes in mc^2155 chromosome was confirmed by PCR (***Figure 28B***), obtaining the *M. smegmatis* mc^2155 ΔSM*phoPR*::Km strain. To obtain the unmarked strain, pJV53H plasmid was cured culturing bacteria in absence of Hyg. When pJV53H loss was obtained, bacteria were electroporated with pRES-FLP-Mtb plasmid and Hyg resistant colonies were isolated. Km resistant cassette elimination was confirmed phenotypically by absence of growth of colony replicates in Km and by PCR (***Figure 28C***), obtaining the *M. smegmatis* mc^2155 ΔSM*phoPR* strain.

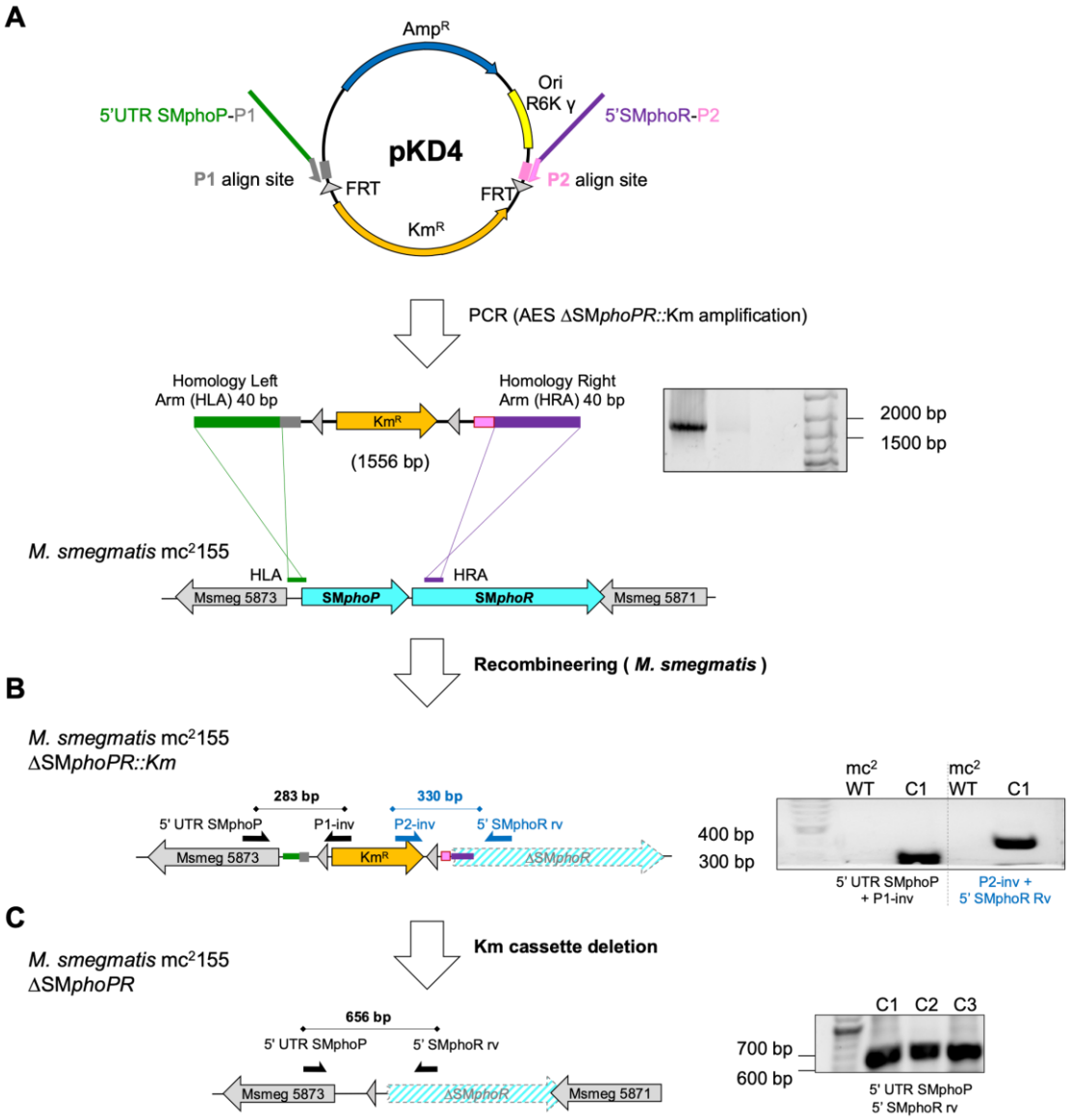

Figure 28: **Graphical representation of the construction of the *M. smegmatis* mc²155 ΔSM*phoPR* strain.** An AES containing the Km resistant cassette flanked by FRT sites was amplified by PCR from pKD4 plasmid (**A**). The AES was electroporated to *M. smegmatis* mc²155 with the recombineering system induced, knocking out their native SM*phoPR* genes, obtaining the *M. smegmatis* mc²155 ΔSM*phoPR*::Km strain (**B**). Km cassette was removed electroporating the pRES-FLP-Mtb plasmid obtaining the *M. smegmatis* mc²155 ΔSM*phoPR* strain (**C**).

Substitution of SM*phoPR* genes by *M. tuberculosis phoPR* (TB*phoPR*) was achieved using a BAC recombineering strategy (Aguilo et al., 2017). *E. coli* containing TB*phoPR* sequence in pBeloBAC11 Rv148 (Brosch et al., 1998) (***Figure 29A***) and the pKD46 plasmid with the γ, β and exo recombineering proteins from the *E. coli* λ phage (Datsenko & Wanner, 2000) induced with arabinose was electroporated with an dsAES amplified by PCR. This dsAES was amplified from pKD4 with long oligonucleotides, as described above, but with homology sequences that match in the TB*phoR* 3' UTR sequence (***Figure 29B***). *E. coli* Km resistant colonies containing the pBeloBAC11 Rv148 (TB*phoPR*::Km) were confirmed by PCR (***Figure 29C***). This mutated pBeloBAC11 was purified and used as template to amplify by PCR the dsAES containing the TB*phoPR*::Km sequence with long oligonucleotides which introduce identity arms to the SM*phoP* 5'UTR and 5' of SM*phoR*, allowing the replacement of endogenous SM*phoPR* sequence by TB*phoPR* (***Figure 29D***). This dsAES was electroporated to *M. smegmatis* mc^2155 pJV53H strain after induction of the recombineering, resulting in recovery of Km resistant colonies, which correct *phoPR* substitution was confirmed by PCR, obtaining the *M. smegmatis* mc^2155 ΔSM*phoPR::*TB*phoPR*::Km (***Figure 29E***). To obtain the unmarked strain, pJV53H plasmid was cured as described above and resulting bacteria were electroporated with pRES-FLP-Mtb plasmid. Km resistant cassette curation was confirmed phenotypically by absence of growth of colony replicates in Km and by PCR in Hyg resistant colonies (***Figure 29F***), obtaining the *M. smegmatis* mc^2155 ΔSM*phoPR::*TB*phoPR* strain.

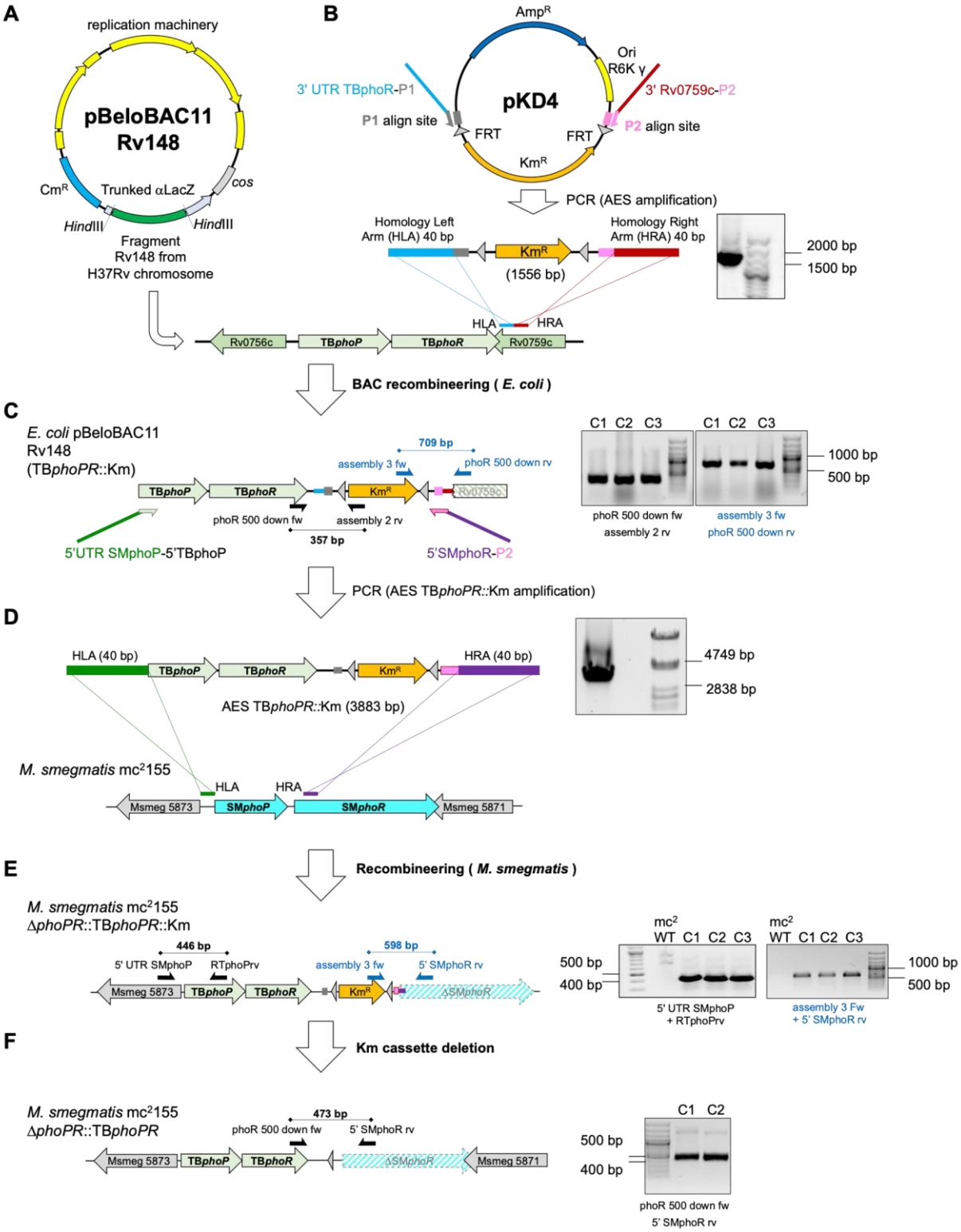

Figure 29: **Graphical representation of the construction of the *M. smegmatis* mc²155 ΔSM*phoPR*::TB*phoPR* strain**. The PhoPR system of *M. tuberculosis* H37Rv (TB*phoPR*) is encoded in pBeloBAC11 Rv148 from Brosch et al. 1998, in *E. coli* (**A**). A first AES containing the Km resistant cassette flanked by FRT sites was amplified by PCR from pKD4 plasmid (**B**). This AES was electroporated to *E. coli* containing pBeloBAC11 Rv148 and the λ Red recombineering system induced, knocking in the Km resistant cassette in the 3' UTR of the TB*phoPR* genes (**C**). A

second AES was amplified by PCR from pBeloBAC11 Rv148 TB*phoPR*::Km containing the TB*phoPR* genes and the Km resistant cassette (**D**). This second AES was electroporated to *M. smegmatis* mc^{2}155 with the recombineering system induced, replacing SM*phoPR* genes for the TB*phoPR*::Km sequence, obtaining the *M. smegmatis* mc^{2}155 ΔSM*phoPR*:: TB*phoPR*::Km strain (**E**). Km cassette was removed electroporating the pRES-FLP-Mtb plasmid obtaining the *M. smegmatis* mc^{2}155 ΔSM*phoPR*:: TB*phoPR* strain (**F**).

Construction and characterization of *M. smegmatis* PhoPR reporter strains

In order to construct reporter strains derived from *M. smegmatis* mc^{2}155, mc^{2}155 ΔSM*phoPR* and mc^{2}155 ΔSM*phoPR*::TB*phoPR* strains and to compare the specificity of their PhoPR activity, pMV361 *pks2*::eGFP, pMV361 *mcr7*::eGFP plasmids, their *smyc*::tdTomato variants (***Figure 30A***) and pFPV27 *pks2*::GFP plasmids (***Figure 30B***) were electroporated to the different strains and Km resistant colonies were confirmed by PCR.

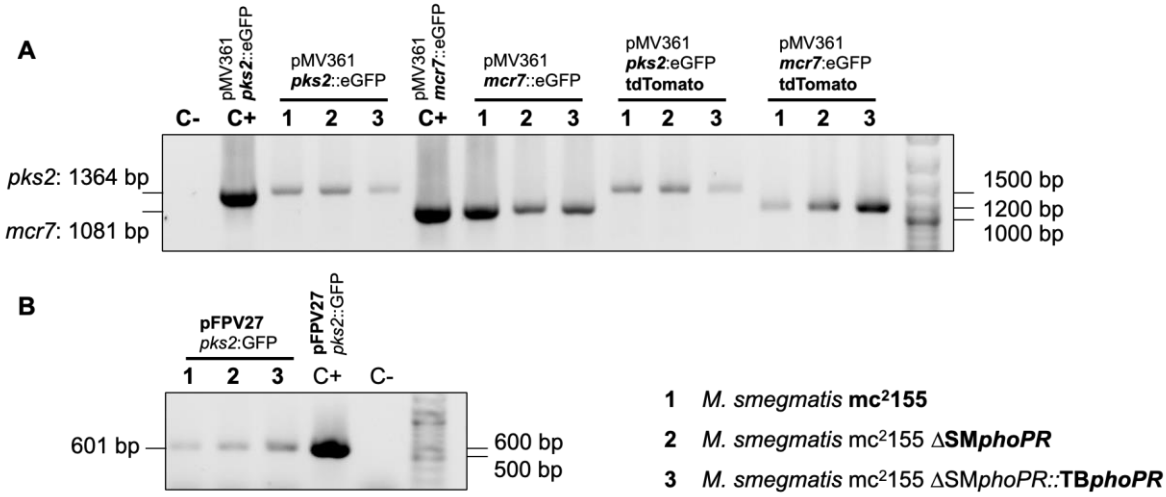

Figure 30: **PCR confirmation of *M. smegmatis* reporter strains.** *M. smegmatis* mc^{2}155, mc^{2}155 ΔSM*phoPR* and mc^{2}155 ΔSM*phoPR*::TB*phoPR* containing pMV361 *pks2*::eGFP, pMV361 *mcr7*::eGFP, pMV361 *pks2*::eGFP *smyc*::tdTomato, pMV361 *mcr7*::eGFP *smyc*::tdTomato (**A**) or pFPV27 *pks2*::GFP (**B**) were confirmed by PCR.

The fluorescence of these new reporter strains was compared when grown in rich medium at different pH, in 7H9Tyl-ADC MES (pH 5.5) and 7H9Tyl-ADC MOPS (pH 6.5-7). After 6 days of growth, we can observe differences in GFP fluorescence between *M. smegmatis* mc^{2}155 and mc^{2}155 ΔSM*phoPR*::TB*phoPR* derived strains. When strains

were grown in MOPS buffer, we observed that mc²155 derived strains produce a slightly higher GFP fluorescence than mc²155 ΔSM*phoPR*, whereas mc²155 ΔSM*phoPR*::TB*phoPR* derived strains produced high levels of GFP fluorescence (black columns in ***Figure 31A, B, C, E and F***). However, when the same strains were grown in presence of MES buffer, GFP fluorescence of mc²155 derived strains increase and in mc²155 ΔSM*phoPR*::TB*phoPR* derived strains is slightly reduced (teal columns in ***Figure 31A, B, C, E and F***). All strains carrying the tdTomato derived plasmids produced similar levels of red fluorescence in both MES and MOPS media (***Figure 31D and G***).

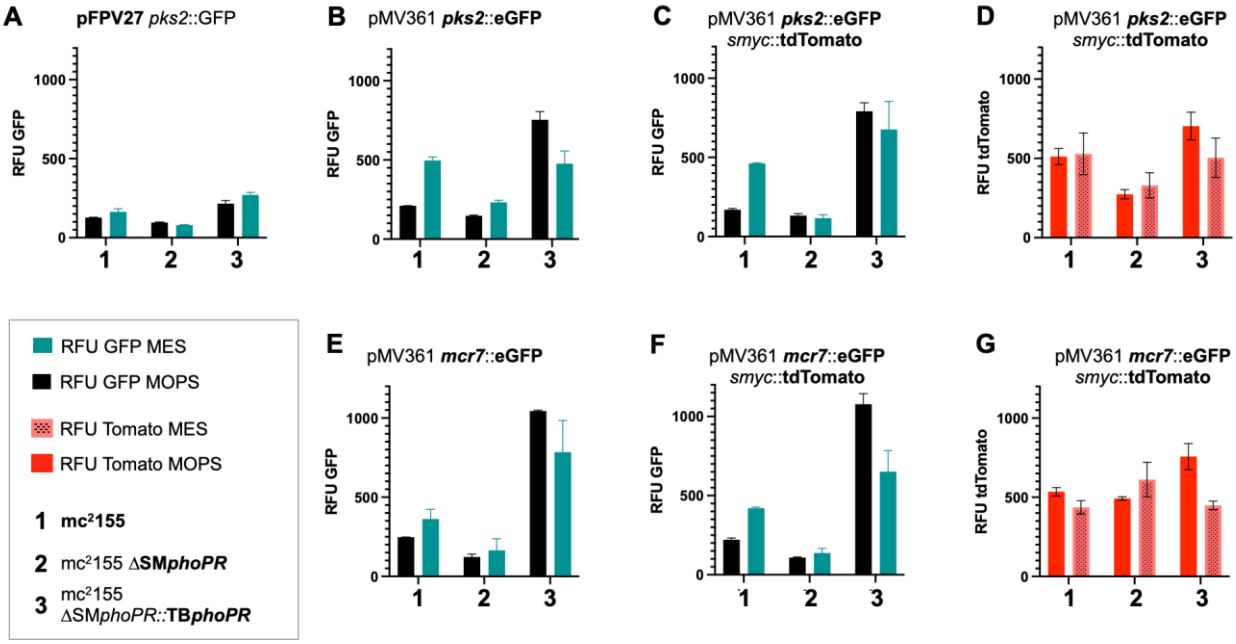

Figure 31: **Fluorescence comparison of the *M. smegmatis* PhoPR reporter strain in presence MES and MOPS buffers.** Comparison of relative fluorescence units (RFU) of GFP and tdTomato of the different PhoPR reporter strains obtained from *M. smegmatis* mc²155, mc²155 ΔSM*phoPR* and mc²155 ΔSM*phoPR*::TB*phoPR* strains in MES and MOPS medium with pFPV27 *pks2*::GFP (**A**), pMV361 *pks2*::eGFP (**B**, GFP), pMV361 *pks2*::eGFP *smyc*::tdTomato (**C**, GFP; **D**, tdTomato), pMV361 *mcr7*::eGFP (**E**, GFP) and pMV361 *mcr7*::eGFP *smyc*::tdTomato (**F**, GFP; **G**, tdTomato) plasmids.

Following the growth and GFP fluorescence in liquid media of *M. smegmatis* mc²155, mc²155 ΔSM*phoPR* and mc²155 ΔSM*phoPR*::TB*phoPR* strains carrying pMV361 *pks2*::eGFP or pMV361 *mcr7*::eGFP plasmid for ten days led to the following observations. Similarly to *M. tuberculosis* strains, acid conditions slow down growth of *M. smegmatis* reporter strains (***Figure 32A and E***). MES buffer induces fluorescence in both mc²155 *pks2* and *mcr7* reporter strains from the first day (***Figure 32B and F***), but

in MOPS buffer the fluorescence is very similar to mc²155 ΔSM*phoPR* reporter strains (***Figure 32C and G***), suggesting that mc²155 reporter strains are only active in presence of MES buffer. On the contrary, mc²155 ΔSM*phoPR*::TB*phoPR pks2* and *mcr7* reporter strains produced similar levels of fluorescence in presence of MES and MOPS buffer (***Figure 32D and H***), suggesting that the reporter systems from mc²155 ΔSM*phoPR*::TB*phoPR* strains are active in both conditions, and maybe with higher activity in MOPS buffer.

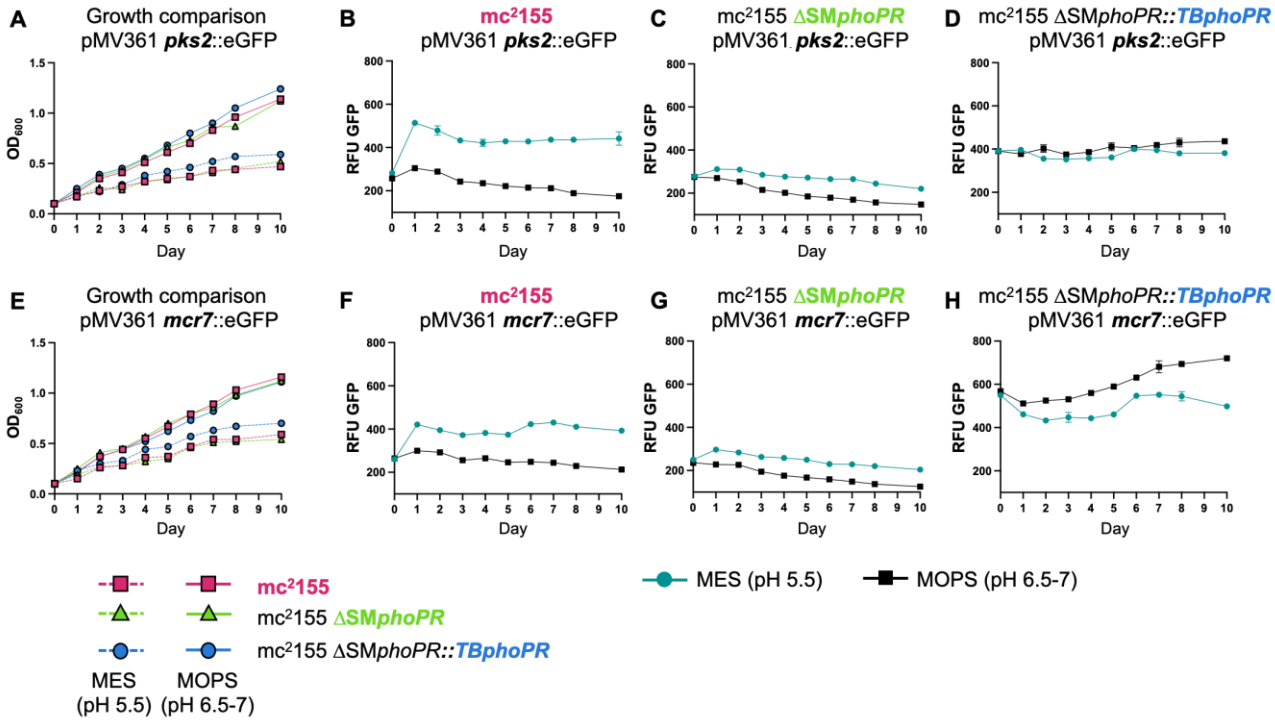

Figure 32: **Evolution of fluorescence and growth of *M. smegmatis* PhoPR reporter strains.** (**A**) Evolution of growth of *M. smegmatis* mc²155, mc²155 ΔSM*phoPR* and mc²155 ΔSM*phoPR*::TB*phoPR* strains carrying pMV361 *pks2*::eGFP plasmid in MOPS (solid lines) and MES (dotted lines) mediums through 10 days. Evolution relative expression of GFP fluorescence of (**B**) *M. smegmatis* mc²155, (**C**) mc²155 ΔSM*phoPR* and (**D**) mc²155 ΔSM*phoPR*::TB*phoPR* strains carrying pMV361 *pks2*::eGFP plasmid in MOPS (black lines) and MES (teal lines) mediums through 10 days. (**E**) Evolution of growth of *M. smegmatis* mc²155, mc²155 ΔSM*phoPR* and mc²155 ΔSM*phoPR*::TB*phoPR* strains carrying pMV361 *mcr7*::eGFP plasmid in MOPS (solid lines) and MES (dotted lines) mediums through 10 days. Evolution relative expression of GFP fluorescence of (**F**) *M. smegmatis* mc²155, (**G**) mc²155 ΔSM*phoPR* and (**H**) mc²155 ΔSM*phoPR*::TB*phoPR* strains carrying pMV361 *mcr7*::eGFP plasmid in MOPS (black lines) and MES (teal lines) mediums through 10 days.

Because both mc²155 and mc²155 ΔSM*phoPR*::TB*phoPR* reporter strains have activity in MES buffer, we tested whether ETZ was active to inhibit GFP production in the different reporter strains. Dose response experiments were performed using ETZ at 1000 µM of highest concentration and serial two-thirds dilutions in 96-well plates and they were measured at day 8. We can observe that ETZ was not active inhibiting GFP production in mc²155, showing similar production of GFP intensities at the different concentrations tested with the different plasmids (***Figure 33A***), while high concentrations of ETZ were able to reduce fluorescence levels in mc²155 ΔSM*phoPR*::TB*phoPR* reporter strains (***Figure 33C***) with the expected absence of GFP fluorescence production in mc²155 ΔSM*phoPR* strains (***Figure 33B***). All the strains had a similar growth rate at the different doses of ETZ tested (***Figure 33D, E and F***). However, due to the low consistency of the experiments and reproducibility of the results obtained with dose response experiments in the different *M. smegmatis* reporter strains, and the absence of secondary assays to confirm the inhibition of the PhoPR system in *M. smegmatis* (either carrying its endogenous PhoPR system or the recombinant system from *M. tuberculosis*), no confident conclusions could be drawn from these results. Further work is needed to standardize dose response experiments in *M. smegmatis* PhoPR reporter strains to obtain reliable results.

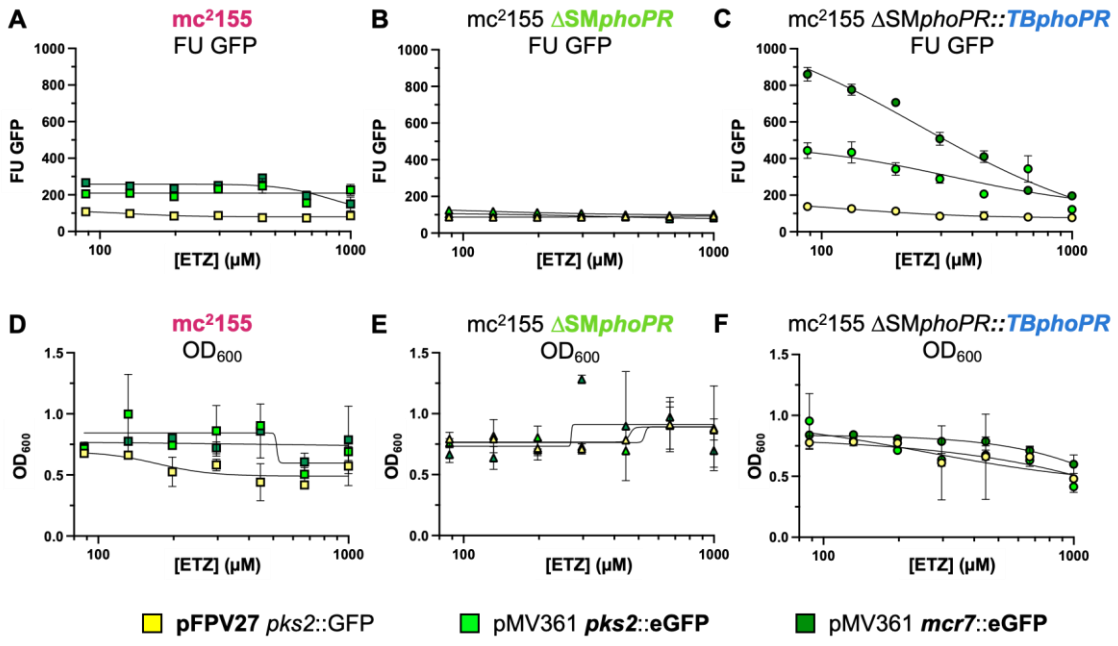

Figure 33: **Dose response effect of ETZ in *M. smegmatis* PhoPR reporter strains.** Effect of different doses of ETZ in fluorescence and growth of *M. smegmatis* mc²155 (**A** and **D**), mc²155 ΔSM*phoPR* (**B** and **E**) and mc²155 ΔSM*phoPR*::TB*phoPR* (**C** and **F**) carrying the pFPV27 *pks2*::GFP (yellow), pMV361 *pks2*::eGFP (light green) or pMV361 *mcr7*::eGFP (dark green) plasmid.

DISCUSSION

The importance of the PhoPR system in *M. tuberculosis* virulence has been in depth demonstrated in multiple studies (Gonzalo-Asensio et al., 2006, 2014; Gonzalo-Asensio, Mostowy, et al., 2008; E. Pérez et al., 2001; Soto et al., 2004; Walters et al., 2006). As the PhoPR system has no substantial impact on *M. tuberculosis in vitro* growth, drugs targeting this system would not act as "classical" antimicrobial strategies directly killing bacteria, but would reduce their virulence, hindering survival during infection. The interest in the discovery of PhoPR inhibitors has grown in the last years, as its inhibition arises as a promising antivirulence therapy which could act in synergy with classical antimicrobial treatments. Accordingly, different laboratories have constructed platforms to search potential PhoPR inhibitors.

A recent platform developed a *M. bovis* BCG strains in which the *luxABCDE* operon is under control of the *phoP* promoter (Zhu et al., 2022). This first platform allowed detection of drugs which silence *phoP* expression (***Figure 34A***). As it is going to be discussed below, *M. bovis* BCG, although being attenuated and safer that *M. tuberculosis* strains, lacks a functional PhoPR system due to a mutation in PhoR.

Another platform that utilizes reporter strains for PhoPR inhibitors screening used the CDC1551 strain with a replicative plasmid containing the GFP gene under control of the *aprA* (acid and phagosome regulated) promoter (which is the same promoter of the non-coding RNA *mcr7*) (Johnson et al., 2015). This platform was used in the identification of ETZ as PhoPR inhibitor, our control molecule. In comparison with the previous platform, this second one allows detection of drugs that downregulate *phoP* or *phoR* genes expression, but also drugs with inhibitory activity in the PhoPR system itself or in any stage of the regulatory network upstream the promoter used (***Figure 34B***).

A different platform developed an *in vitro* target assay, in which purified PhoP-DNA complexes are challenged with the different compounds. The potential inhibitory activity of the PhoP-DNA interaction is measured by Foster resonance energy transfer (FRET) between fluorescent labels in PhoP and the DNA molecules (Wang et al., 2016). This platform allows detection of compounds acting in the PhoP-DNA interactions (***Figure 34C***).

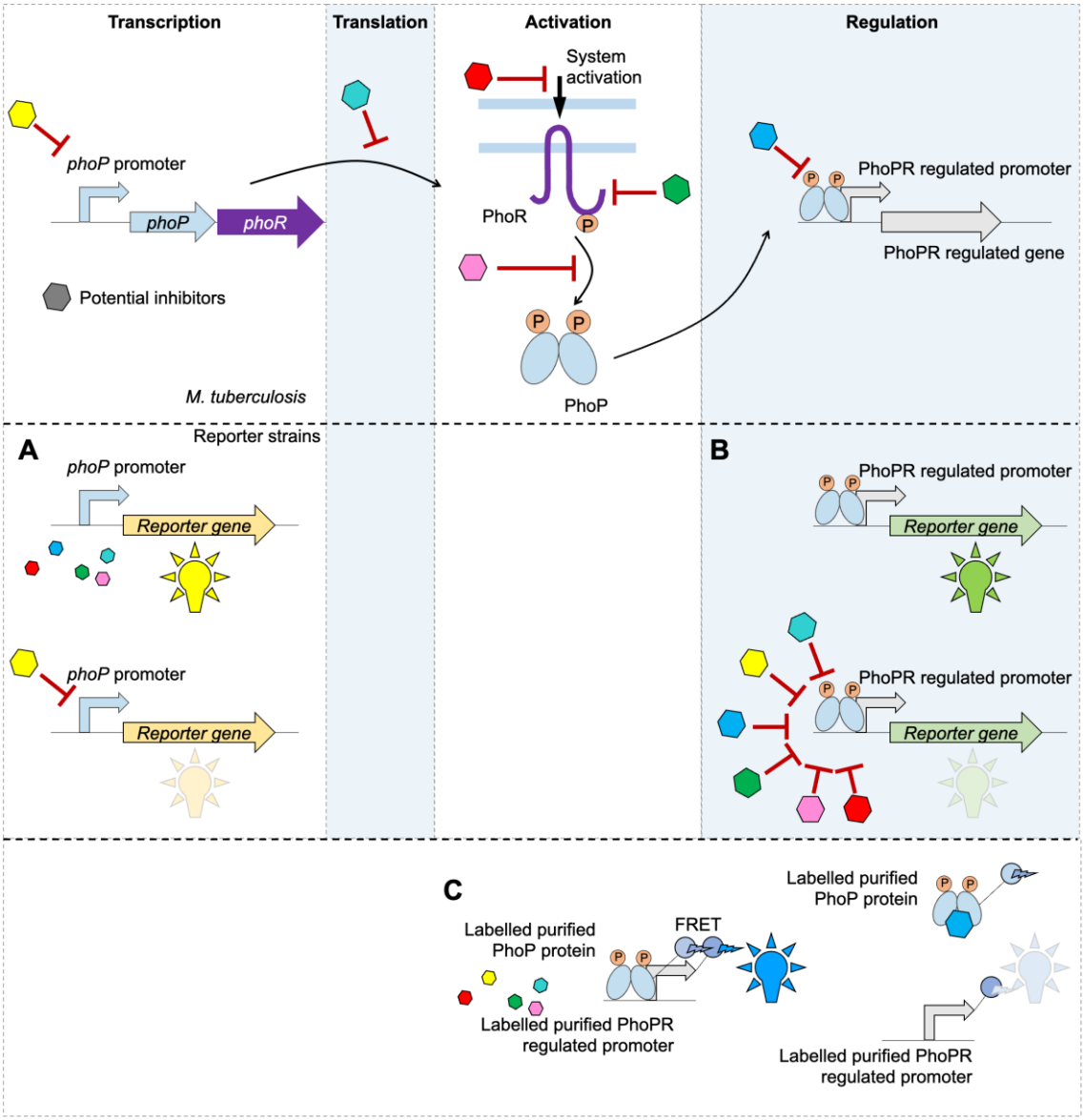

Figure 34: **Scheme of potential targets of PhoPR inhibitors throughout the transcription to regulation cascade.** As it is represented, reporter strains carrying the reporter gene controlled by the *phoP* promoter (**A**) just could sense the activity of inhibitors that act controlling the transcription levels of *phoP* gene. Reporter strains carrying a promoter from the PhoP-core regulon (**B**) could sense the inhibitory activity of compounds acting at any stage of the whole transcription to regulation cascade. (**C**) Screening systems based in purified PhoP protein and its DNA binding sequences (PhoPR regulated promoters) labelled to detect PhoP-DNA interaction by FRET are only sensible to inhibitors of the PhoP-DNA interactions.

In this chapter we have constructed and validated a wide repertoire of mycobacterial reporter strains in order to be used for screening inhibitory molecules of the PhoPR system of *M. tuberculosis*, and a variety of secondary assays to confirm and characterize their inhibitory activity using the ETZ as control compound. Our platform is composed by

M. tuberculosis strains belonging to two of the most widespread lineages of the MTBC, the lineage 2 (GC1237) and lineage 4 (H37Rv and CDC1551) (***Figure 17***). Furthermore, we have constructed PhoPR reporter strains using two different promoters from unrelated genes of the PhoPR core regulon (***Figure 34B***), *pks2* and *mcr7*, in order to be able to have a wider view of the PhoPR inhibition. Additionally, our reporter plasmids are integrative, allowing for stability inside bacteria without the need for selective pressure. Accordingly, we can avoid the use of antibiotic selection in future HTS assays, eliminating the risk of interference with the molecules being tested. Integrative plasmids also allow stability for their use in different infection models, from *ex vivo* macrophage infection to *in vivo* infections, in which the second red tdTomato fluorescence from double reporter plasmids might be especially useful to track viable infecting bacteria, and the green GFP fluorescence to track the PhoPR activity.

All our PhoPR reporter strains are designed to reduce their GFP fluorescence when the activity of the PhoPR system decreases, as the GFP gene is controlled by strong promoters of PhoP activated genes, like *mcr7* and *pks2*. However, it is important to confirm that any decrease in fluorescence is not due to an inhibition of bacterial viability through a secondary readout, such as measuring the optical density, to ensure that there is no growth inhibition The alternative use of a promoter strongly repressed by the PhoPR system, like the promoter from *pe8* gene (Johnson et al., 2015; Solans et al., 2014), could lead to an increase of fluorescence in the absence of PhoPR activity, thus avoiding confusion with phenotypes of molecules with bactericidal or bacteriostatic activity. In this contexts, construction of *M. tuberculosis* PhoPR strains carrying the *pe8* promoter is currently on going.

By validating the inhibitory activity of ETZ, we have demonstrated that ETZ is active not only in strains from lineage 4 but also in lineage 2 strains (***Figure 15*** and ***Figure 17***). As ETZ is a CA inhibitor which demonstrated activity in the inhibition of mtbCAs (Carta et al., 2009) it has been proposed that, by an unknown mechanism, there is a link between mtbCAs and PhoPR regulation, being the inhibition of the first ones the cause of PhoPR inhibition (***Figure 12B***) (Johnson et al., 2015). However, when we tested a second CA inhibitor, ATZ, which has been proved active *in vitro* inhibiting mtbCAs (Carta et al., 2009), we did not observe inhibitory activity in our reporter strains (***Figure 26***). In line with our observations, it has been recently published that knocking-out or knocking-down mtbCA genes, *canA*, *canB* and *canC*, does not alter the expression of *aprA* gene (Shelby J et al., 2022), suggesting a regulation of the PhoPR system independent of mtbCAs. To confirm these speculations, it would be necessary to verify *in* vivo the inhibitory activity of ATZ in mtbCAs, as it has been done with ETZ (Johnson et al., 2015). Thereby, the

precise mechanism of action of ETZ inhibiting the PhoPR system, by direct action, or through accessory proteins-modules, remains to be answered.

A relationship between acid pH and PhoPR activation has been observed in CDC1551 reporter strains (Abramovitch et al., 2011; Baker et al., 2014; Schreuder et al., 2015). It has been hypothesized that the specific PhoR P172 polymorphism of H37Rv genetic backgrounds makes it unable to sense acid pH because it already starts from an active state of the system, while CDC1551 could respond to acid pH with higher PhoPR activation in acid media due to the absence of the PhoR P172 polymorphism (Schreuder et al., 2015). Our results agree with these observations as we detect higher relative expression levels of GFP under both *mcr7* and *pks2* promoters at acidic pH in CDC1551 strains but not in H37Rv related strains (***Figure 16B*** and ***D***). However, our GC1237 reporter strains, which carry the same PhoR allele than CDC1551, do not produce higher fluorescence at acid pH (***Figure 16D***). Furthermore, isogenic mutants of H37Rv carrying PhoR L172 allele also lack PhoPR acid activation (Schreuder et al., 2015). These observations suggest that the relationship between the PhoPR system and pH sensing is complex and depends on the genetic background of *M. tuberculosis* strains. They also highlight the need of testing potential PhoPR inhibitors in different genetic backgrounds, as indirect PhoPR inhibition might be different through lineages or in PhoPR variants.

In a screening for PhoPR inhibitors with *M. tuberculosis* reporter strains we need to distinguish among compounds which act inhibiting the expression of the reporter gene and compounds which are inhibiting bacterial replication. To do so, is important have a proper bacterial growth and a correct expression of the reporter system. All our *M. tuberculosis* reporter strains grew better in MOPS buffer but only CDC1551 strains reported higher relative fluorescence MES buffer (***Figure 16***). As our laboratory reference strain of *M. tuberculosis* is H37Rv, we opt to stablish future HTSs for PhoPR inhibitors without acidic conditions.

It is important to establish reliable secondary assays to confirm the specificity and potency of PhoPR inhibitor candidates, as in experiments with reporter strains, the PhoPR inhibition is measured indirectly, by reduction of GFP fluorescence. This reduction of fluorescence could be achieved due to an unspecific effect of the molecule out of the PhoPR system, for example, quenching or degrading the GFP protein. We have set up a varied repertoire of secondary assays to characterize PhoPR inhibitors that we have validated using different *M. tuberculosis* lineages and their Δ*phoPR* and complemented strains and ETZ as control compound. Exploring the effect on the transcription of different genes of the PhoPR core regulon can provide us a wide

overview of the activity of the compound (***Figure 21*** and ***Figure 23***), and evaluation of the inhibition of ESAT-6 can suggest that the compound is reducing the virulence of the bacteria (***Figure 24***). However, it would be necessary to stablish different models of infection to confirm the inhibition of *M. tuberculosis* virulence.

We have transferred the PhoPR system from pathogenic *M. tuberculosis* into a surrogate non-pathogenic mycobacterium, *M. smegmatis*, in order to explore the possibility of developing a safer platform to test potential PhoPR inhibitors. PhoP and PhoR structures from both species are highly conserved (***Figure 27***), especially in the transcription factor PhoP, with a 92.7% of protein identity. The main differences are located in the sensor protein, PhoR, especially in the extracellular sensor domain, which could be the reason of different fluorescence profiles observed among reporter strains, with better fluorescence records in mc^{2}155 ΔSM*phoPR*::TB*phoPR* reporter strains (***Figure 31*** and ***Figure 32***), which also seems to be sensitive to inhibition by ETZ (***Figure 33***). However, it is still unknown the relevance of the endogenous PhoPR system in *M. smegmatis* and the impact of its inactivation or substitution by *M. tuberculosis* PhoPR system beyond the fluorescence records obtained in this study. It would be necessary to compare *M. smegmatis* mc^{2}155, mc^{2}155 ΔSM*phoPR* and mc^{2}155 ΔSM*phoPR*::TB*phoPR* strains transcription profiles by RNA-seq in different conditions to understand the function of the PhoPR system in *M. smegmatis* chromosome regulation. Additionally, further phenotypic characterization like drug sensitive profiles or cell-wall permeability could provide interesting information about the new strains constructed. With those results, we could develop secondary assays to confirm the possible PhoPR inhibition observed with *M. smegmatis* reporter strains. The characterization of these mutants is being used as a starting point for a future thesis project in which it is expected to study the role of the PhoPR system in different mycobacterial species.

The use of *M. smegmatis* as surrogate of *M. tuberculosis* for drug testing is not new. However, the differences in cell-wall permeability and the higher amount of efflux pumps in *M. smegmatis* usually are translated in higher resistance for the non-pathogenic mycobacterium (Altaf et al., 2010). This could be the reason of interfere in the low reproducibility of our results when testing ETZ in with our reporter strains. Other common strains used as safer model organisms for testing drugs against *M. tuberculosis* are the avirulent strain H37Ra and *M. bovis* BCG vaccine. However, for developing a PhoPR screening platform, both strains might not be the more suitable strains. The avirulent phenotype of H37Ra is mainly due to a S219L mutation in PhoP, which makes it unable to bind to the DNA. *M. bovis* BCG, even though its avirulent phenotype is due to the loss of the RD1 region (in which is encoded the main virulence factor of *M. tuberculosis*,

ESAT-6), also possesses the G71P mutation in PhoR protein. This mutation has been demonstrated to inactivate the PhoPR system of *M. africanum* and animal adapted clades/strains (Gonzalo-Asensio et al., 2014). Consequently, the use of our reporter plasmids in H37Ra or BCG, with the reporter gene under control of a PhoPR strongly regulated promoter, strains would not be useful as in both strains the PhoPR system is inactive. Following a replacement strategy in the PhoPR system as the one we used in *M. smegmatis* would restore virulence to the H37Ra strain (Frigui et al., 2008; Gonzalo-Asensio, Soto, et al., 2008; J. S. Lee et al., 2008). However, it would be interesting to explore the use of attenuated *M. tuberculosis* strains with an active PhoPR system, like *M. tuberculosis* ΔRD1 mutants (Lewis et al., 2003), or auxotrophic strains (Jain et al., 2014), once demonstrated its security to be used in biosafety level 2 laboratories and no interference between genes inactivated and the PhoPR regulation.

The antivirulence approach that we want to develop is based on the inhibition of PhoPR system activity using small molecules. Nevertheless, it would be also interesting to explore the use other approaches involving nucleic acids that may also work inhibiting its activity. It would be interesting to study the potential application of transcription factor decoys (TFDs) as inhibitors of the PhoPR system. TFDs are DNA structures which mimic the binding sites of transcription factors, recruiting them outside the chromosome and impeding their action in genetic regulation (Marín-Menéndez et al., 2017). Other strategy is related to silence *phoPR* genes, that could be achieved using antisense siRNAs or ncRNAs against *phoP* and/or *phoR* mRNAs, inducing their degradation or blockading the ribosome binding to avoid mRNA translation (Alshaer et al., 2021). However, nucleic acid approaches might be difficult to apply due to the mycobacterial cellular envelope which make them difficult to be transformed, even with the use of nanoparticles as carriers, and this may be the reason there are no public studies about them in *Mycobacterium spp.* A last similar approach could be the use of peptide nucleic acids (PNAs), a synthetic scaffold that mimics DNA in which the deoxyribose phosphate backbone is replaced by a pseudo peptide backbone, maintaining the nitrogenous bases (Hyrup & Nielsen, 1996). These PNAs can be designed to bind as antisense of mRNAs, avoiding translation, or directly bind to DNA, forming different dsDNA-PNA complexes that can blockade transcription of the desired genes, as in our case, could be *phoP* and *phoR* genes. This strategy has been used once in mycobacteria when researchers used PNAs as anti-*inhA,* resulting in inhibition of growth in *M. smegmatis* and morphology changes (Kulyté et al., 2005). The *M. tuberculosis* reporter strains developed in this Thesis should be suitable to test any of these approaches to test their efficacy.

Antivirulence based in PhoPR inhibition must be tested for possible interferences with current anti-tuberculous therapies. Comparison of *in vitro* antibiotic susceptibilities of H37Rv and H37Ra revealed that both strains have similar susceptibilities to anti-tuberculous drugs, with higher susceptibility in H37Ra to some antibiotics (Heinrichs et al., 2018). As the PhoPR system controls the expression of different components of the mycobacterial cell envelope, it can affect to the permeability to different molecules. But the similar drug susceptibilities observed between H37Rv and H37Ra venture that PhoPR inhibition would not lead to changes in *in vitro* resistance against current anti-tuberculous drugs. However, we have to remember that H37Ra also possesses additional polymorphisms in comparison with H37Rv, like loss of production of PDIM (J. S. Lee et al., 2008). To ensure that PhoPR inhibition do not affect drug susceptibility, it would be necessary to compare H37Rv and other strains with their isogenic Δ*phoPR* mutants. Recent studies that evaluated the use of β-lactams amoxicillin and meropenem in combination with β-lactamase inhibitor clavulanate isolated resistant mutants with SNP in *phoP* gene (Olivença et al., 2022), and some mutations are predicted to be important in PhoP dimerization (He et al., 2016). This possible higher resistance against β-lactams inactivating the PhoPR system is not unexpected as BlaC protein is secreted through the TAT system, and inhibition of the PhoPR system, through downregulation of the *mcr7* ncRNA, leads to increased secretion of TAT substrates, including BlaC, increasing β-lactamase activity (Solans et al., 2014). β-lactams are not currently used in anti-TB regimes due to the natural resistance of *M. tuberculosis* strains due to the presence of BlaC. However, it is highly possible that those *phoP* mutants described in (Olivença et al., 2022) would be attenuated and with an impaired ability to cause infection. Anyway, it should be tested that potential PhoPR inhibitors do not induce resistance to the antibiotics used in TB treatment regimens, or alternatively act with them synergistically.

A robust antivirulence therapy based in the inhibition of the PhoPR system would tune infecting mycobacteria to behave like Δ*phoPR* mutants, and hence, similar to the vaccine candidate against TB, MTBVAC. This way, the antivirulence therapy could have the potential to attenuate bacteria, but even induce proper immune recognition that could lead to protection against ongoing or future infections or relapses. Meanwhile the current vaccination route in humans is intradermal, preclinical data of pulmonary vaccination with BCG have shown better protective efficacy against *M. tuberculosis* infection than intradermal vaccination in animal models (Aguilo et al., 2014; Mata et al., 2021), arousing interest of testing this route of administration with other vaccine candidates. Although no challenge studies have been reported of pulmonary vaccination with MTBVAC, immune

signatures of pulmonary vaccination in rhesus macaques suggest enhanced protective immune response with MTBVAC than with BCG, both improved with the pulmonary route (Dijkman et al., 2021). Antivirulence PhoPR based drugs could tune infecting *M. tuberculosis* bacteria in the lung, resembling to pulmonary vaccination with MTBVAC. Moreover, it has been tested that different MTBVAC constructions in different human infecting lineages of the MTBC also confer protection against *M. tuberculosis* (I. Pérez et al., 2020) suggesting that, if effective in different lineages, a PhoPR inhibition based therapy could arise immune protection independently of the linage of the infecting strain. However, we have to consider that MTBVAC, in addition to the Δ*phoP* mutation, also carries the Δ*fadD26* mutation, impeding the biosynthesis of PDIM, which together synergistically attenuate the TB bacilli (Arbues et al., 2013). Thus, a PhoPR inhibition therapy would reduce the virulence of *M. tuberculosis*, but not as much as observed in MTBVAC.

Finally, exploring the potential use of antivirulence therapies in latent forms of TB has a great potential to control eventual disease progression in this population. Recent studies estimate that close to one quarter of the global population is infected with LTBI, amounting to 1.4-1.7 billion people (Ding et al., 2022; Houben & Dodd, 2016). A PhoPR inhibition-based therapy effective in LTBI models, which could improve recognition of the bacteria by the immune system, and even conferring some protection, might have a significant impact on the battle to end TB.

CHAPTER 2

INTRODUCTION

Treatment of *M. abscessus* infections

Success rates of *M. abscessus* treatment are very low. Only 25-42% of treated patients achieve sputum conversion and, furthermore, healed patients still have high chances of relapse (Griffith & Daley, 2022). Similar to MDR-TB, *M. abscessus* lung diseases are difficult to treat due to limited therapeutic options and its intrinsic and easy development of drug resistance (Nessar et al., 2012). For years, the only available oral drugs for *M. abscessus* were macrolides, making essential the additional use of injectable antimicrobials (Floto et al., 2016). In addition *M. abscessus* can develop an inducible macrolide resistance conferred by the ribosomal methyltransferase gene *erm(41)* or acquired resistance due to mutations in 23S rRNA gene *rrl* (Shallom et al., 2015). Therefore, there is a need to study new strategies to combat *M. abscessus* infections, especially for macrolide resistant strains. The study of repurposed antimicrobials used in different mycobacterial infections like clofazimine (Choi et al., 2017), used to treat *M. leprae* and MDR-TB; or linezolid (Inoue et al., 2018; Winthrop et al., 2015), used for MDR-TB is expanding the repertoire available oral drugs. Recently, different national and international Health institutions have stablished an updated guideline for the treatment of different NTM, in which there are some recommendations for the treatment of *M. abscessus* pulmonary infections. These recommendations include an initial intensive phase with parenteral and oral drugs, and a continuation phase, with oral or inhaled drugs. The duration of each phase and election of the number of drugs used mainly depends on *M. abscessus* resistance to macrolides, but the final election of the drugs used depends on the susceptibility to the rest of the drugs. Treatments comprise from 2 to 5 drugs in the intensive phase, and last at least 5 moths, but they can be extended (Daley et al., 2020). These long-term and multidrug treatments are usually poorly tolerated by patients due to the apparition of side effects and drug related toxicity against the different drugs used (Koh et al., 2014; Lyu et al., 2011; Victoria et al., 2021). Parenteral drugs available are an aminoglycoside (amikacin, which can be also administered inhaled in the continuation phase), β-lactams (cefoxitin or imipenem) and a glycylcycline (tigecycline); and oral drugs available are macrolides (azithromycin or clarithromycin), an iminophenazine (clofazimine) and an oxazolidinone (linezolid) (Daley et al., 2020). A last oral drug has been recently included in the recommended treatment regimens as last option, bedaquiline (Andries et al., 2005; Griffith & Daley, 2022), the

first drug approved by the Food and Drug Administration in 40 years for treatment of MDR TB.

Bedaquiline is a diarylquinoline that inhibits the mycobacterial ATP synthase by targeting the subunit C of the F0/V0 complex, preventing rotor ring from acting as ion shuttle (Preiss et al., 2015). Sequencing of spontaneous resistant mutants obtained in the laboratory reveals that mutations in the coding gene of the ATPase subunit C, the *atpE* gene, are responsible of acquired resistant against bedaquiline in different mycobacterial species (Segala et al., 2012) (***Figure 35***).

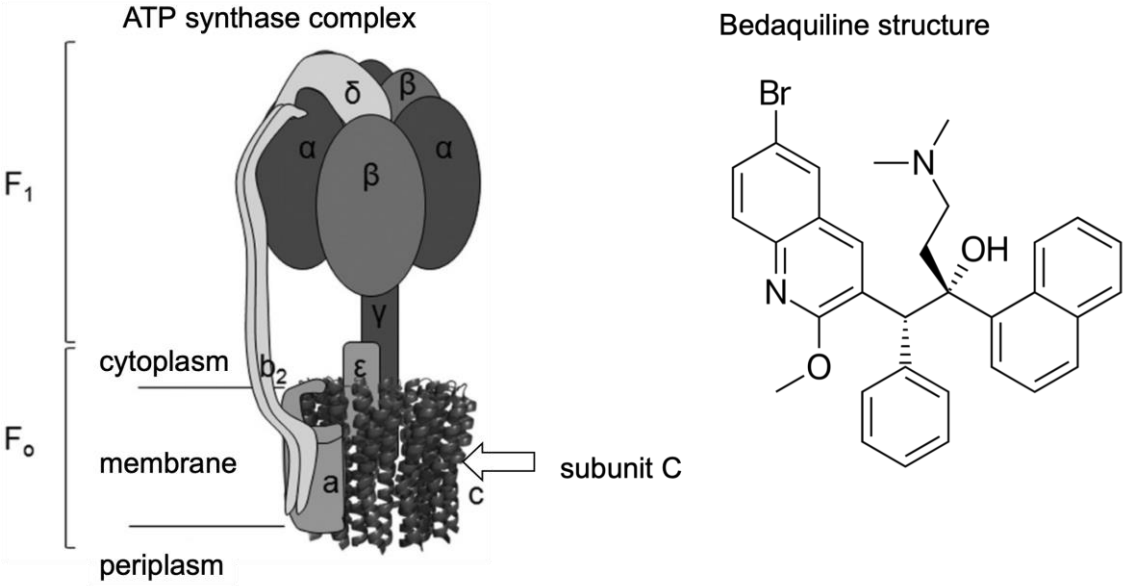

Figure 35: **Structure of the ATP synthase complex with the arrangement of the different subunits and the bedaquiline molecule.** The *atpE* gene encodes de subunit C. Several subunits C form the C-ring in the transmembrane F0 complex. Bedaquiline interacts with the C-ring, preventing rotation. Adapted from (Segala et al., 2012).

Emergence and spread of antimicrobial resistance are one of the top 10 global public health threats declared by the WHO (*Antimicrobial Resistance*, 2021). As new mutations are identified each day more and more easily in drug-resistant isolates thanks to lowering costs and the implementation of Whole Genome Sequencing (WGS) technology, characterization of these new mutations is needed to be done to understand its impact in bacterial biology. This would allow confirmation of the genetic-phenotype association of new mutations and discard other mechanisms like drug tolerance, based in phenotypic tolerability of drug and not in genetic changes (Windels et al., 2020).

Genetic manipulation in *M. abscessus*

One strategy commonly followed to confirm the genetic-phenotypic association of a mutant resistant allele is the complementation and overexpression of the mutant allele in a sensitive strain with a plasmid. However, the resultant strain carries both mutant and sensitive alleles, which might lead to unconclusive results. For example, the F0/V0 complex is composed of several subunits C in which, if one of the subunits is susceptible of been blocked by bedaquiline, the whole rotor ring can be blocked. This case has been observed when trying to confirm two *atpE* mutations in *M. abscessus* (D29V and A64P) in which the expression of the mutant alleles of the *atpE* gene in the multicopy plasmid pMV261 did not increased the MIC values against bedaquiline of plasmid carrying strains. However, when selective pressure leaded to a spontaneous recombination replacing the sensitive allele and plasmid curation, leaving the mutant allele integrated in the *M. abscessus* chromosome, the resultant bacteria increased MIC 256 times (Dupont et al., 2017).

Thus, an optimal strategy to confirm genetic-phenotypic associations in antimicrobial resistance needs to perform genetic manipulations directly in the bacterial chromosome. However, if genetic tools for mycobacteria are limited (in comparison with more used microorganisms like *E. coli*), genetic manipulation of *M. abscessus* is even more restricted. For example, some genome mutagenesis systems that work in other species of mycobacteria, like thermosensitive ts-sacB system and mycobacteriophage system, do not work in *M. abscessus* (Medjahed & Reyrat, 2009). In the last years, suicide plasmids strategies based in counterselection with the *M. tuberculosis katG* gene or the *E. coli*'s *galK* gene have been used successfully to generate different *M. abscessus* mutants (Belardinelli et al., 2022; Gregoire et al., 2017; Rominski et al., 2017; Viljoen et al., 2018).

Recombineering system is one of the most used methods to perform genetic manipulations in the chromosome of mycobacteria. It was firstly described in *E. coli* in 2000 (Datsenko & Wanner, 2000) and later applied to *M. smegmatis* and *M. tuberculosis* (van Kessel & Hatfull, 2007) (***Figure 36A***). It consists in the transformation of an AES in a strain expressing the Gp60 and Gp61 proteins from the Che9c mycobacteriophage (van Kessel & Hatfull, 2007). Using a double strand AES (dsAES) (***Figure 36B***) with long homology arms (around 1000-1500 bp) flanking an antibiotic resistant cassette, recombineering works with an acceptable efficiency in *M. abscessus*. However, the percentage of double crossing-over mutants of *M. abscessus* are very low in comparison with other mycobacteria due to the natural ability of *M. abscessus* to re-circularize lineal dsDNA fragments (Dubée et al., 2014; Halloum et al., 2016; Medjahed & Reyrat, 2009).

Recombineering system also allows the use of short simple strand oligonucleotides as AES (ssAES) (***Figure 36C***) in mycobacteria (van Kessel & Hatfull, 2008), however, as far as we are concern, there are no reports of the use of ssAES in *M. abscessus* to perform chromosome mutations.

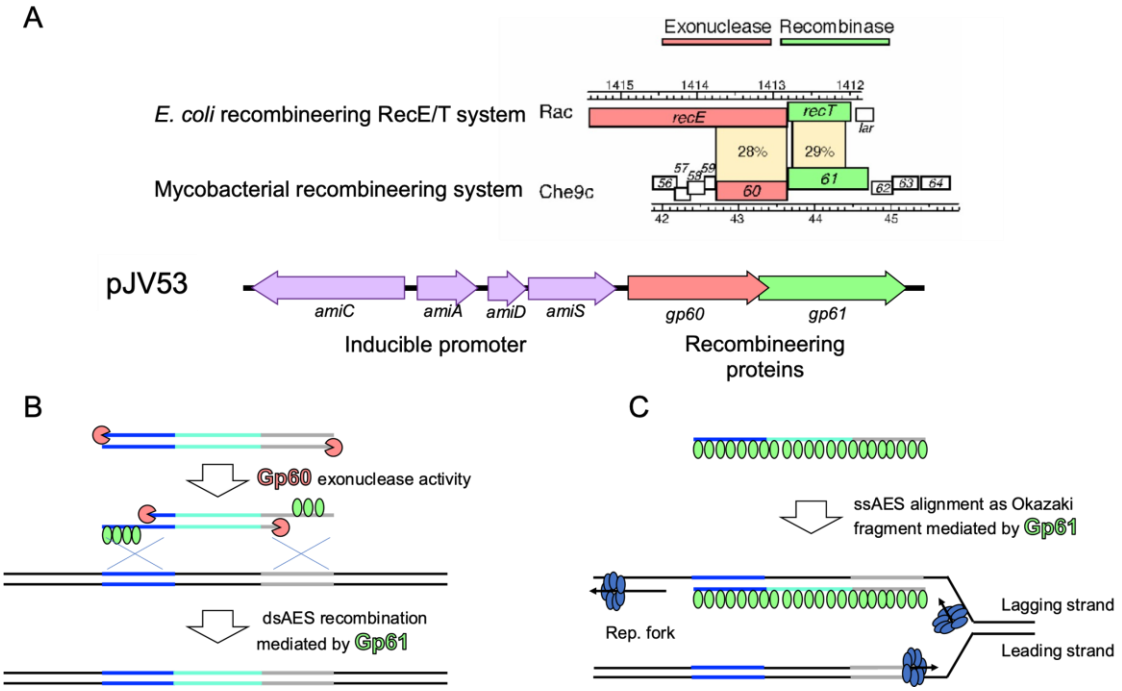

Figure 36: **Recombineering system of mycobacteria**. (**A**) Che9c Gp60 and Gp61 are RecE and RecT homologues respectively. Che9c *gp60* and *gp61* genes were cloned by van Kessel under an inducible promoter to construct the pJV53 plasmid (Adapted from (van Kessel & Hatfull, 2007)). Mechanisms of action proposed for recombineering for dsAES (**B**) and ssAES (**C**).

Identification of a bedaquiline resistant mutant in a clinical isolate of *M. abscessus*.

In The Cliniques Universitaires Saint-Luc, Belgium, a clinical isolate was isolated from a patient showing sputum sample from a patient with cystic fibrosis that was confirmed as *M. abscessus* by Maldi-ToF (Isolate 81327881541). This strain showed resistance to cefoxitin, imipenem, tobramycin, ciprofloxacin, moxifloxacin, trimethoprim, sulfamethoxazole and doxycycline using RAPMYCO2 sentititre test. Subsequently, bedaquiline spontaneous resistant mutants were isolated using the passage method and, genomes of Isolate 81327881541 and its spontaneous mutant (541BQR) were sequenced in the Unit of Human Bacterial Diseases, Sciensano Belgium. Comparison of their sequences revealed a non-synonymous polymorphism in the 29th codon of the *atpE*

gene, encoding the AtpC subunit of the ATP synthase, replacing the original aspartic (D) amino acid for alanine (A) (*atpE* D29A mutation).

In this chapter, we used the recombineering system to perform oligo-mediated mutagenesis on the genome of the *M. abscessus* clinical isolate 81327881541 and in the laboratory strain *M. abscessus* ATCC19977 to confirm the bedaquiline resistant phenotype of the *atpE* D29A sequenced mutation.

OBJECTIVES

The general objective of this Chapter is to develop a fast and reliable recombineering based technology to confirm genotype-phenotype relationship of single nucleotide polymorphisms associated to drug resistance in *M. abscessus*.

To achieve this objective, the following sub-objectives has been established:

- Construction and validation of a *M. abscessus* strain carrying a functional recombineering system for its use with single stranded oligonucleotides as allelic exchange substrates (ssAES).
- Design of ssAES carrying the bedaquiline resistance mutation *atpE* D29A with flanking silent mutations, to construct a genetic barcode able to be introduced into the *M. abscessus* chromosome.
- Use of the previous barcoding technology to confirm a second unrelated mutation conferring bedaquiline resistance in *M. abscessus* in the *atpE* gene.

MATERIALS AND METHODS

Basic microbiology procedures

Manipulation mycobacterial strains was performed in a biosafety level 2 laboratory (BSL2), with facilities notification A/ES/06/I-02.

Bacterial strains used and obtained in this work are listed in ***Table 9*** together with the plasmids used.

Mycobacterial strains and culture conditions

Mycobacterial strains were grown at 37°C in 7H9 broth (Difco). 7H9 was supplemented with 0.05% Tween 80, 0.2% glycerol, and 10% (v/v) albumin-dextrose-catalase (ADC, Middlebrook) (7H9Tw-ADC), or tyloxapol 0,025%, glycerol 0,2% and ADC 10% (7H9Tyl-ADC). For growth in solid medium, 7H10 was used supplemented with 0.5% glycerol and 10% ADC. When required, Km was used at concentration 50 µg/mL and bedaquiline was used at 3 µg/mL. For the induction of the recombineering system 0.2% (w/v) acetamide was used to supplement 7H9Tw-ADC.

Long term storage

For long term storage a final concentration of 15% of glycerol was added to bacterial cultures in late logarithmic phase. Aliquots of 1 mL were stored at -80°C.

Table 9: **Mycobacterial strains used in chapter 2**.

Strain	Description	Source
M. abscessus SL541	Clinical *M. abscessus* isolate 81327881541	From Cliniques Universitaires Saint-Luc
M. abscessus SL541BQR	Clinical *M. abscessus* isolate resistant to bedaquiline with D29A mutation in *atpE* protein.	Cliniques universitaires Saint-Luc.
M. abscessus SL541 pJV53	Clinical *M. abscessus* isolate 81327881541 containing the recombineering plasmid pJV53, with chec9 genes *gp60* and *gp61* under the control of the acetamidase promoter and Km resistance cassette (van Kessel & Hatfull, 2007)	This work
M. abscessus ATCC19977	*M. abscessus* reference strain from the American Type Culture Collection.	(Ripoll et al., 2009)
M. abscessus UZ pJV53	*M. abscessus* ATCC19977 reference strain containing the recombineering plasmid pJV53, with chec9 genes *gp60* and *gp61* under the control of the acetamidase promoter and Km resistance cassette (van Kessel & Hatfull, 2007)	This work

Nucleic acid and genetic engineering techniques

Preparation of electrocompetent Mycobacteria

Electrocompetent mycobacteria were prepared as described by Medjahed H. and Singh A. K. (Medjahed & Reyrat, 2009). 100 mL of bacterial culture was grown to an OD_{600} of 0.4-0.6. Bacterial pellets were washed several times in 10% glycerol-0.05% Tween-80 and finally resuspended in 1 mL of 10% glycerol. Aliquots of 100-200 µL were storage at -80°C for further use. The washing process was performed in cold conditions.

Aliquots of 100-200 µL electrocompetent cells were electroporated with 300-500 µg of pJV53 plasmid (van Kessel & Hatfull, 2007). 0.2 gap cuvettes (Bio-Rad) were used with a single pulse (2.5kV, 25µF, 1000Ω) in a GenePulser XcellTM (Bio-Rad). Cells were recovered with 5 mL of 7H9Tw-ADC and incubated overnight at 37°C, to express the antibiotic resistance genes. Serial 10-fold dilutions were plated in 7H10-ADC plates containing 50 µg/mL of Km. Recombinant colonies typically appeared in 8-10 days and tested by PCR.

Recombineering

Recombineering in *M. abscessus*

In the case of culturing bacteria with the recombineering system, protocol of preparation of electrocompetent *Mycobacteria* was used with some modifications: acetamide was added to a final concentration of 0.2% (W/V) approximately one doubling time of the strain used before preparing the competent cells (3-4 hours) to allow the correct expression of the recombineering system and cells aliquots were electroporated with 300-600 µg of the ssAES for recombineering (***Table 10***). Cells were recovered with 5 mL of 7H9Tw-ADC and incubated overnight at 37°C, to express the antibiotic resistance genes. Serial 10-fold dilutions were plated in 7H10-ADC plates containing 3 µg/mL of Bq. Recombinant colonies typically appeared in 8-10 days and tested by PCR.

Single strand Allelic Exchange Substrates design

ssAES were designed as 133-nt long single strand (ss) oligonucleotides (***Table 10***) which could align to *M. abscessus* genome as Okazaki fragments in the replicative fork (***Figure 36C***) and introduce different mutations in the *atpE* gene .

DNA extraction

Fast DNA extraction from Mycobacterium for PCR

This method releases plasmidic and genomic DNA from mycobacteria, usually in enough quantity to detect the presence of target genes by PCR. A bacterial colony was dispersed

in 20 µL of sterilized water and suspension was boiled 15 min and centrifuged at maximal speed. 1 µL of the supernatant was used in PCR reactions.

PCR

Allele-specific PCR/Barcode PCR

The genomic DNA from the different recombinant *M. abscessus* colonies was subjected to PCR amplification in a final volume of 10 µL with 0.38 U of Mytaq DNA polymerase (Bioline), 25 µM of each primer (***Table 10***) and MyTaq Reaction Buffer 5X. PCR program consisted of an initial step of heat denaturation at 95°C for 10 min followed by 30 cycles of 95°C for 15 s, the corresponding annealing temperature for 15 seg and 72°C for 30 s; and then a final extension at 72°C for 2 min. PCR products were visualized in 1% agarose gels containing ethidium bromide. For molecular weight comparison, GeneRuler 100 bp Plus DNA Ladder was used.

Allele-specific RT-PCR/Barcode RT-PCR

Recombinant *M. abscessus* colonies were subjected to Real Time PCR amplification TB Green Premix Ex TaqTM (Tli Rnase H Plus) (Takara) was used in a final volume of 10µL, using 20 µM of each primer (***Table 10***). 1 µL of fast extracted DNA was used for each reaction. The reaction was performed in the StepOne Plus Real Time PCR System (Applied Biosystems).PCR program consisted of an initial step of heat denaturation at 95°C for 10 min followed by 40 cycles of 95°C for 10 s, 62°C for 10 seg and 72°C for 50 s. PCR products were visualized. Amplification of the specific Barcode-mutation was compared with amplification of *16s* RNA gene, as positive control of amplification.

Table 10: **Oligonucleotides used in chapter 2.** Mismatching nucleotides of the ssAES for recombineering introducing SNPs are highlighted in **bold**.

Name	Sequence 5' → 3'	Use
ssAES *atpE* **WT**	gaacagccggccctgagcctcgggctgacgagccacac cggagatcagagcgttaccggcgataccgtcaccgata ccggcaccgatggcgcctccggccatgatcaacccacc accgatgagggcaccagca	AES for recombineering
ssAES *atpE* **D29A**	gaacagccggccctgagcctcgggctgacgagccacac cggagatcagagcgttaccggcgataccg**G**caccgata ccggcaccgatggcgcctccggccatgatcaacccacc accgatgagggcaccagca	AES for recombineering
ssAES **BC** *atpE* **D29A**	gaacagccggccctgagcctcgggctgacgagccacac cggagatcagagcgttacc**C**gc**A**at**C**ccg**G**c**C**cc**A**at**C** ccggcaccgatggcgcctccggccatgatcaacccacc accgatgagggcaccagca	AES for recombineering
ssAES **BC** *atpE* **A64P**	ttagctggcgccgggagtcgcgaagacgaacaacgcca tgaaggccaggttgatgaa**A**tacg**GC**gc**T**tc**C**acca**AC** ccgacggtgatgaagaacggggtgaacagccggccctg agcctcgggctgacgagcc	AES for recombineering
Seq Mabsc *atpE* Fw	gccctgttcgtcttcgtctgc	PCR amplification and Sanger sequencing
Seq Mabsc *atpE* Rv	tcctcaagaatgccgcgcc	PCR amplification, Sanger sequencing and "Barcoding" PCR and RT-PCR
BC *atpE* **D29A** Fw	gattggggccgggattgcg	"Barcoding" PCR and RT-PCR
BC *atpE* **A64P** Fw	gttggtggaagcgccgtat	"Barcoding" PCR and RT-PCR
16S-F	aggattagataccctggtagtcca	RT-PCR
16S-R	aggcccgggaacgtattcac	RT-PCR
gp60-fw	atccggctctacgccgac	PCR amplification
gp61-Rv	cggcaaatgactcttgcgt	PCR amplification

Phenotypic characterization

In vitro susceptibility assays, Minimal Inhibitory Concentration

Resazurin Microtiter Assay (REMA) in agar plates

Serial microdilutions were made to determine the Minimal Inhibitory Concentration (MIC) of bedaquiline in agar plates against the different *M. abscessus* strains. bedaquiline was added to melted 7H10-ADC agar in a two-fold dilution range from 4 to 0.25 µg/mL and dispensed in 24 well polypropylene flat bottom plates. 10^5 colony forming units (CFUs) were added to each well and plates were incubated for 4 days at 37°C. Then, 50 µL of 0.1 mg/mL filter-sterilized resazurin (Sigma-Aldrich) were added to each well. The color change from blue (indicative of no bacterial growth) to pink (indicative of bacterial growth)

was recorded after 24 hours. The MIC was defined as the lowest concentration of bedaquiline capable of inhibiting resazurin conversion.

MTT assay in broth

Serial microdilutions were made to determine the MIC of bedaquiline in broth against the different *M. abscessus* strains. bedaquiline was tested 7H9Tyl-ADC in a two-fold dilution range from 8 to 0.0078 µg/mL in 96 well polypropylene flat bottom plates with an initial concentration of 10^5 CFUs/mL, and plates were incubated for 4 days at 37 °C. Then, 30 µL of 2.5 mg/mL MTT [3-(4,5-dimethylthiazol-2-yl)-2,5-diphenyltetrazolium bromide] were added to each well. The color change from blue (indicative of no bacterial growth) to pink (indicative of bacterial growth) was recorded after 24 hours. The MIC was defined as the lowest concentration of bedaquiline capable of inhibiting MTT conversion.

RESULTS

Construction of *M. abscessus* recombineering strain

Establishing a direct genotype-phenotype association in the context of antimicrobial resistance should follow molecular Koch's postulates. Accordingly, the candidate gene (or mutation) responsible for drug resistance should be exclusively present in resistant, but not in susceptible bacteria. Then, introduction of the candidate gene (or mutation) into a susceptible bacterium would lead to development of drug resistance. However, introduction of a gene outside its original location might produce undesirable effects in the context of non-physiological expression of the mRNA or protein products. Further, introduction of genes using plasmids has two main disadvantages: on the one hand, this strategy usually leads to merodiploid bacteria carrying the wild type and mutated copies of the gene of interest. On the other hand, plasmidic expression of genes does not resemble nor the copy number, nor the expression levels of chromosomal genes. With this scenario, we reasoned that an optimal strategy to confirm the role of a suspected gene (or mutation) in drug resistance, would require the replacement of the wild type allele in the chromosome. This strategy has the additional advantage that chromosomal replacements would eventually lead to drug resistant bacteria which could be selected in antibiotic containing plates. To do so, we decided to apply the recombineering technique using ssAES, adapted in 2008 to its use in *M. smegmatis* and *M. tuberculosis* (van Kessel & Hatfull, 2007). Accordingly, we aimed to develop a genetic strategy to stablish and confirm a direct relationship between the genetic *atpE* mutation and the phenotypic resistance to bedaquiline in *M. abscessus* (***Figure 37***).

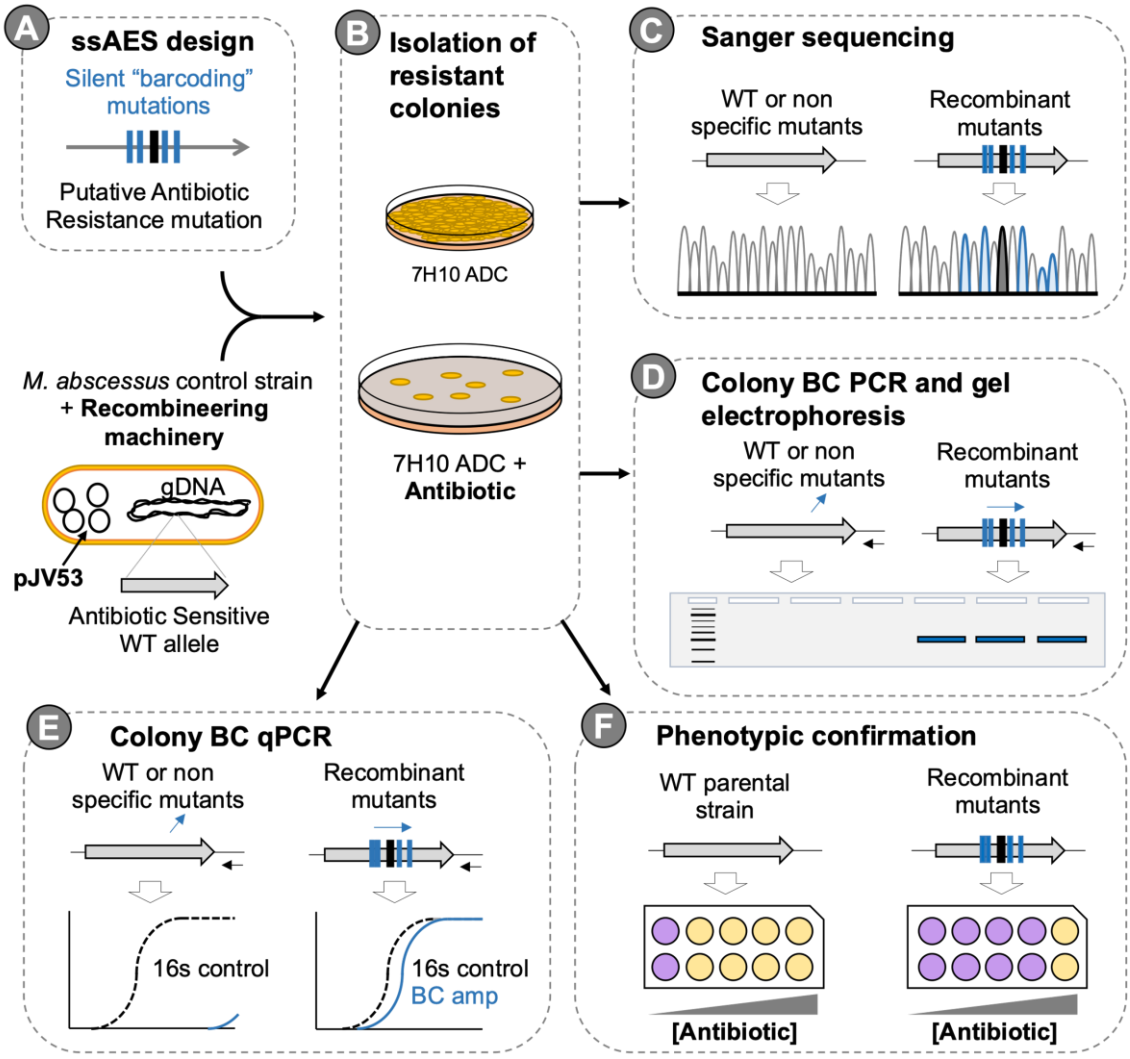

Figure 37: **Workflow scheme followed in the chapter 2.** Design of ssAES carrying silent "barcoding" (BC) mutations and the antibiotic resistance mutation (**A**) allow the selection of resistant colonies (**B**) after electroporation of *M. abscessus* carrying the recombineering machinery. Sanger sequencing (**C**) or Barcoding (BC)-PCR methods (**D** and **E**) can be used to confirm genotype of recombinant colonies recovered. Confirmation of the phenotype-genotype association of the mutation under study can be assessed by calculating the MIC to the antibiotic (**F**).

Recombineering plasmid pJV53 was transformed into electrocompetent *M. abscessus* SL541 and colonies were selected in 7H10-ADC agar plates containing Km 50 µg/mL after one week of incubation at 37°C. Recombinant colonies were confirmed by PCR with gp60-fw and gp61-Rv oligonucleotides (***Table 10***), which amplify *gp60* and *gp61* genes from the Che9c mycobacteriophage, the two essential proteins for recombineering in mycobacteria (***Figure 38***).

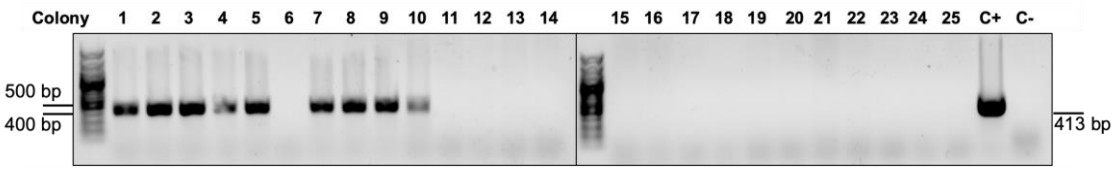

Figure 38: **PCR confirmation of *M. abscessus* SL541 carrying the pJV53 plasmid.** PCR of different *M. abscessus* Km resistant colonies after electroporation of the pJV53 plasmid. The presence of the plasmid was confirmed by the specific 413 bp amplification corresponding to the *gp60* and *gp61* genes from the Che9c mycobacteriophage. Purified pJV53 plasmid was used as positive control (C+) of the reaction and genomic DNA of *M. abscessus* as negative control (C-).

We confirmed that the presence of plasmid pJV53 does not confer increased resistance to *M. abscessus* ATCC19977 against bedaquiline as MIC in 7H10 of *M. abscessus* ATCC19977 with and without pJV53 plasmid was 0.5 µg/mL, whereas the MIC of bedaquiline in the clinical isolate *M. abscessus* SL541 was above 4 µg/mL (***Figure 39***), indicating that the *M. abscessus* SL541 pJV53 is suitable to obtain recombinant bedaquiline resistant strains.

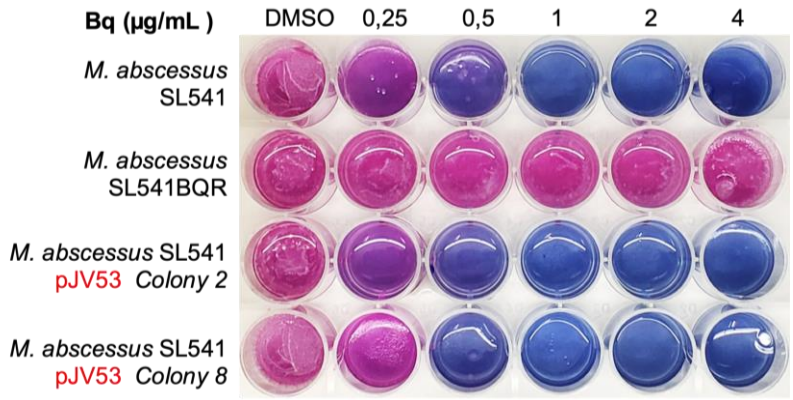

Figure 39: **REMA in 7H10-ADC to determine MIC of bedaquiline against different *M. abscessus* strains.** Wells with viable bacteria are shown in pink, whereas wells with absence of growth are shown in blue, after addition of resazurin.

Specific chromosomal replacements at the *atpE* D29 codon position results in bedaquiline resistance in *M. abscessus*

Once constructed the *M. abscessus* with the recombineering machinery, we induced the expression of the recombineering genes and introduced different AES containing the desired mutations by electroporation. Specifically, AES consisted of single stranded oligonucleotides carrying either the wild type codon (GAC coding for Asp) (ssAES *atpE* WT), or the mutated codon (GCC coding for Ala) (ssAES *atpE* D29A) in the central position of the 133 nt long ssDNA substrates. As some *atpE* D29A mutant might also arise by spontaneous mutation, we also included a ssAES containing the mutated GCC codon flanked by three silent mutations at each side (ssAES BC *atpE* D29A) (***Table 10***; ***Figure 40***). These silent modifications are aimed to act as a barcode to selectively detect the incorporation of the GCC mutation by recombineering, thus ruling out spontaneous mutations arisen during manipulation.

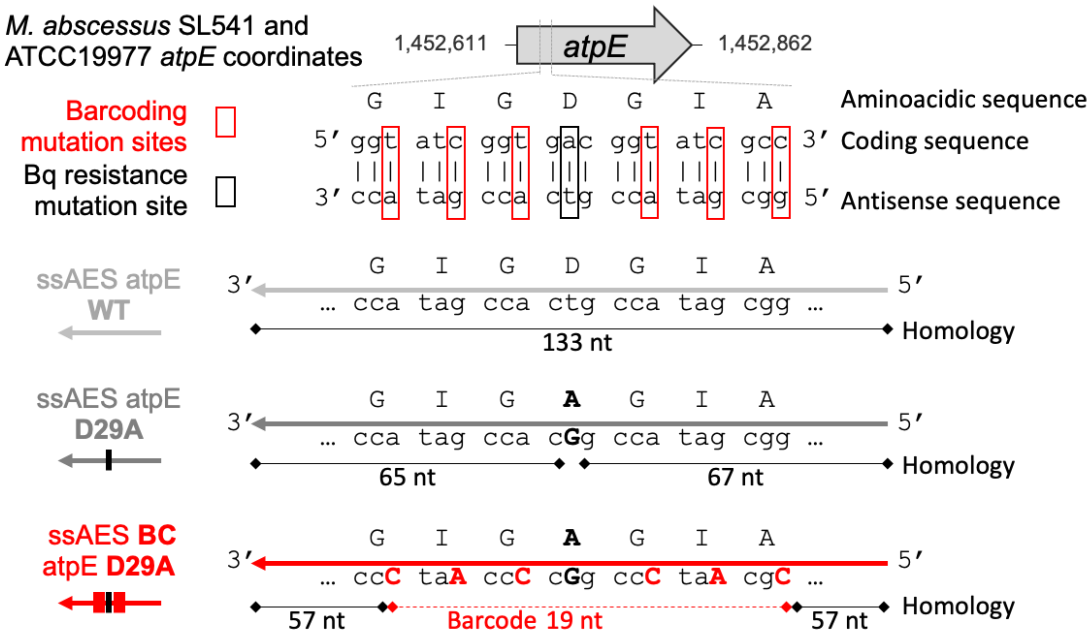

Figure 40: **Graphical representation of the three ssAESs used to mutate the 29th codon of the *atpE* gene** and their alignment in *M. abscessus* ATTC19977's genome.

Electroporated bacteria were plated in 7H10-ADC containing 3 µg/mL of Bq. Presence of resistant colonies was detectable after 7-10 days of incubation in samples electroporated with the AES containing the *atpE* D29A mutation, the "ssAES *atpE* D29A"

and the “ssAES BC *atpE* D29A”. To ensure that bedaquiline resistant bacteria arose from a similar number of transformants, we also plated bacteria without antibiotic, indicating equivalent number of CFUs in bacteria transformed with wild type and mutant alleles (***Figure 41***).

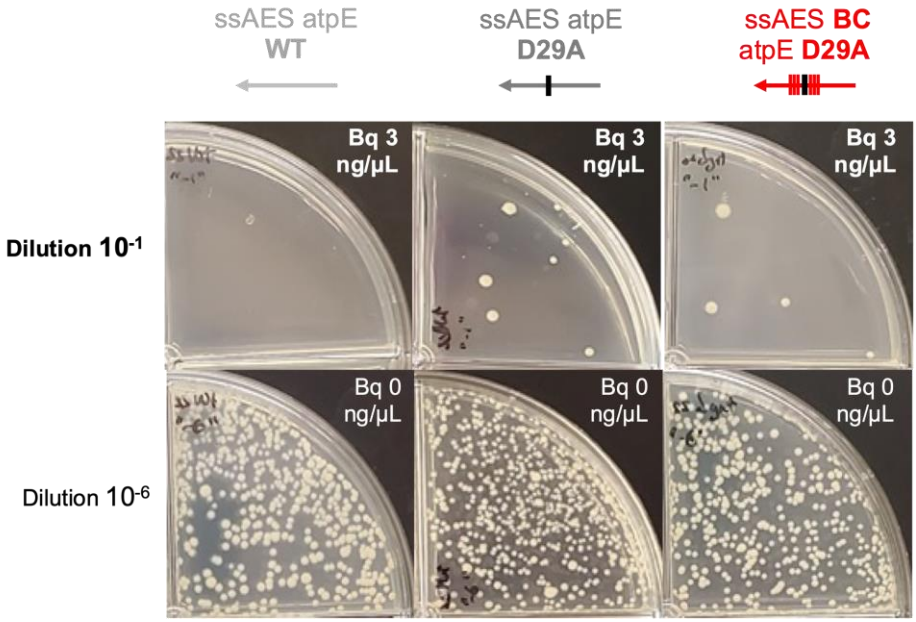

Figure 41: **Obtention of *M. abscessus* SL541 *atpE* D29A recombinants**. Electroporated bacteria with “ssAES *atpE* WT”, “ssAES *atpE* D29A” and “ssAES BC *atpE* D29A” were plated in presence (dilution 10^{-1}) or absence (dilution 10^{-6}) of bedaquiline 3 µg/mL.

These bedaquiline resistant colonies were further confirmed by their increased MIC to bedaquiline relative to the *M. abscessus* SL541 recombineering strain and the resistant clinical isolate in 7H9Tyl-ADC. All the recombinant colonies showed a MIC above 8 µg/mL, whereas the parental strain with the recombineering plasmid showed a MIC of 0.5 µg/mL of bedaquiline (***Figure 42***).

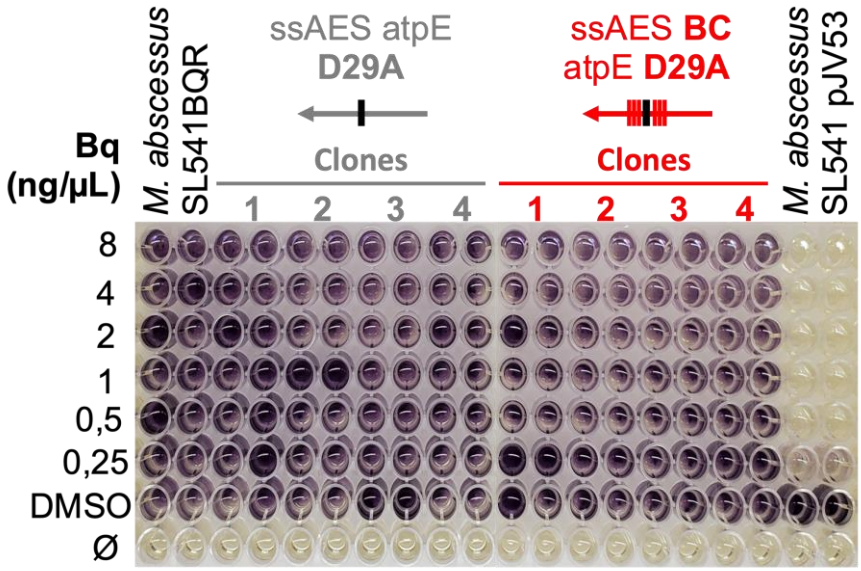

Figure 42: **Susceptibility to bedaquiline of *M. abscessus* SL541 *atpE* D29A recombinants**. MTT in 7H9Tyl-ADC to determine the MIC of different isolated recombinant colonies. Wells with viable bacteria are shown in dark purple, whereas wells with absence of growth are shown in yellow, after addition of MTT.

Sequencing of the *atpE* region of different isolated colonies clearly showed that all recombinants contained the GCC sequence at the 29th position relative to the wild type GAC codon. This indicates that this mutation is putatively responsible of the bedaquiline resistant phenotype in our recombinant colonies. Interestingly, all colonies transformed with the "ssAES BC *atpE* D29A" also contained the 29th codon flanked by the barcode silent mutation (***Figure 43***). This barcoding strategy allowed to unequivocally demonstrate that introduction of the GCC codon (D29A) by recombineering at the *atpE* chromosomal location is responsible for bedaquiline resistance in the transformants and that they have not arisen by spontaneous mutation.

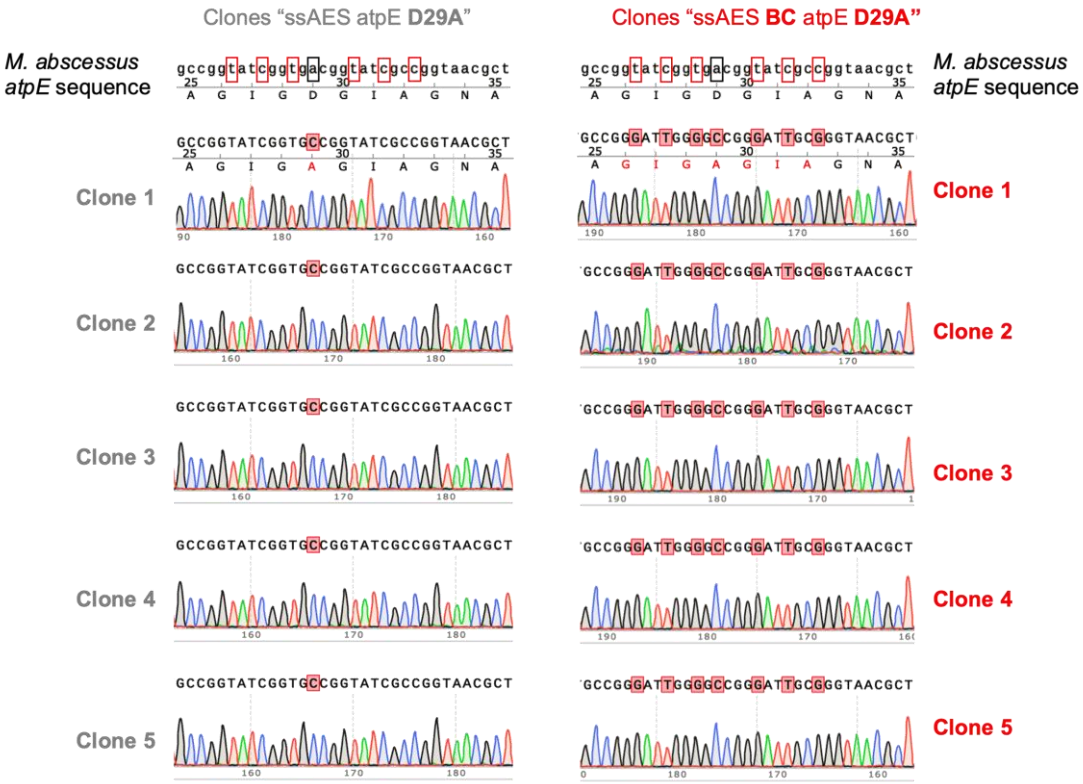

Figure 43: **Sequencing results of *M. abscessus atpE* D29A recombinants.** Sanger sequencing chromatograms of recombinant colonies of *M. abscessus* electroporated with "ssAES *atpE* D29A" (left) and "ssAES BC *atpE* D29A" (right).

Allele-specific PCR of bedaquiline resistant colonies allows the detection of chromosomal replacements at the *atpE* D29 codon position

Once demonstrated the utility of our genetic barcoding strategy to specifically detect the incorporation of the desired mutation by genomic sequencing, we prompted to optimize PCR-based methods to accelerate the whole process. To do so, we designed an allele-specific, that we have named barcode-PCR, using an oligonucleotide annealing to the barcode sequence, but not to the wild type sequence, and a second oligonucleotide outside the barcode location (***Figure 44***).

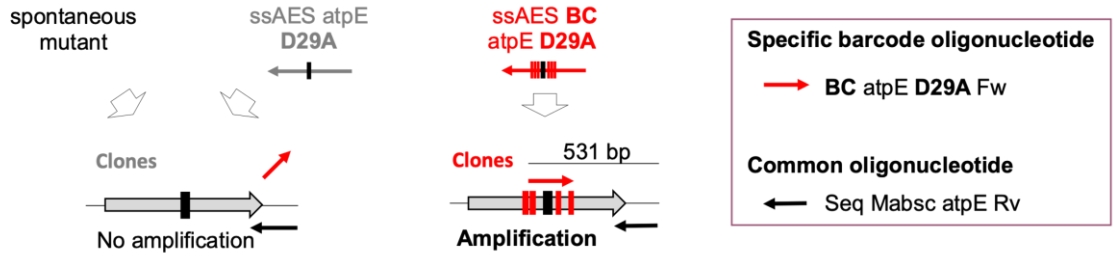

Figure 44: **Graphical representation of the barcode-PCR oligonucleotide design**.

After growth of new recombinant bedaquiline resistant transformants using "ssAES *atpE* D29A" and "ssAES BC *atpE* D29A", we tested the ability of the barcode-PCR to detect the genetic barcode associated to the D29A mutation. After a PCR reaction, using a small portion of the recombinant colonies as genetic material, we confirmed the presence of the specific 531 bp PCR band in 10/12 bedaquiline resistant colonies transformed with the "ssAES BC *atpE* D29A", but not in colonies transformed with the "ssAES *atpE* D29A", containing solely the GCC mutation in the central position (***Figure 45***). Overall, the whole process, from the transformation of the *M. abscessus* recombineering strain with the desired mutant ssAES, to the barcode-PCR verification of mutant colonies, requires less than two weeks.

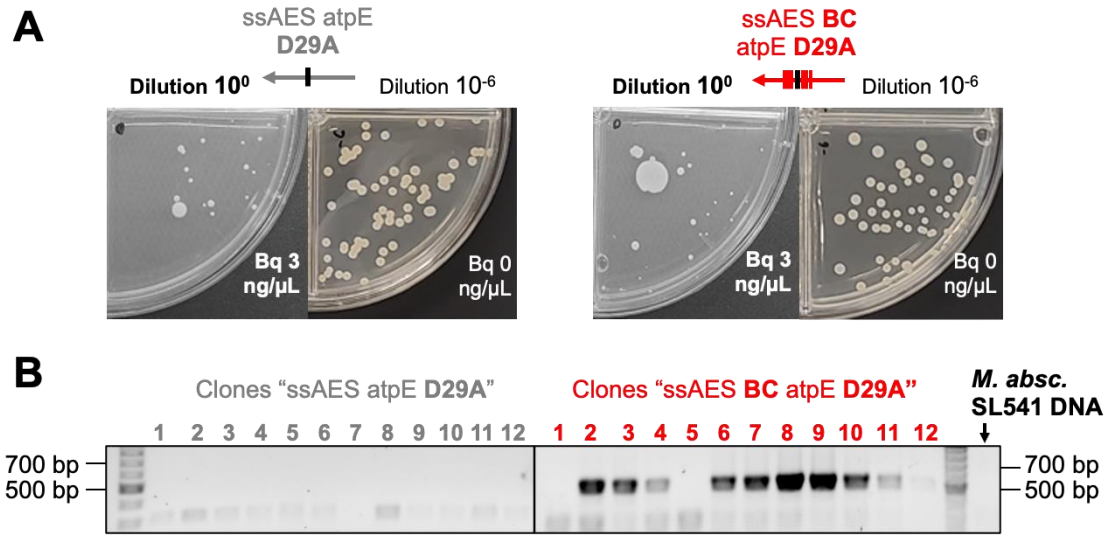

Figure 45: **Barcode-PCR with *M. abscessus* SL541 *atpE* D29A recombinants.** (**A**) Electroporated bacteria with "ssAES *atpE* **D29A**" and "ssAES **BC** *atpE* **D29A**" was plated in absence (dilution 10^{-6}) or presence (dilution 10^{0}) of bedaquiline 3 µg/mL. (**B**) Resistant colonies were subjected to barcode-PCR.

Alternatively, we used Real Time-PCR to detect barcode-PCR amplification without the need for agarose gel electrophoresis. Results showed amplification of the 16S rRNA control gene in colonies with either “ssAES *atpE* D29A” or “ssAES BC *atpE* D29A” (Ct≈25). However, using the D29A barcode-specific oligonucleotide, we were able to specifically detect amplification in “ssAES BC *atpE* D29A” transformants (Ct≈25), in contrast to the recombinant colonies transformed with the “ssAES *atpE* D29A” only containing the GCC mutation (Ct>31) (***Figure 46***). Using detection by Real Time PCR, the entire process lasted roughly 10 days.

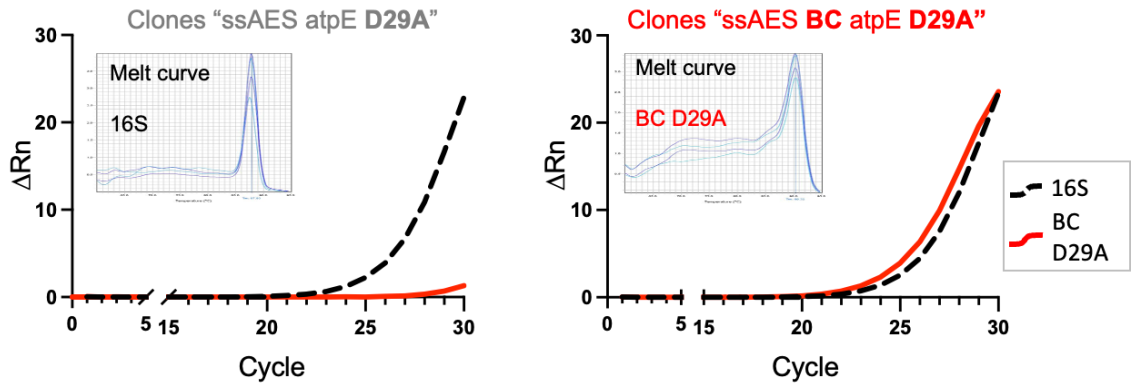

Figure 46: **Barcode-RT-PCR with *M. abscessus* SL541 *atpE* D29A recombinants.** ΔRn values of amplification of the 16S RNA gene (dashed grey) or the specific D29A barcode (continuous pink) in “ssAES *atpE* **D29A**” or “ssAES **BC** *atpE* **D29A**” *M. abscessus* transformants obtained by Barcode RT-PCR. Melting curves show the specificity of qRT-PCR amplifications.

In another attempt to demonstrate the robustness of our method, we aimed to reproduce the technique described in this section with a second different *M. abscessus* recombineering strain, the laboratory reference strain *M. abscessus* ATCC 19977. We successfully reproduced results obtained with either “ssAES *atpE* WT”, “ssAES *atpE* D29A” or “ssAES BC *atpE* D29A” (***Figure 47***).

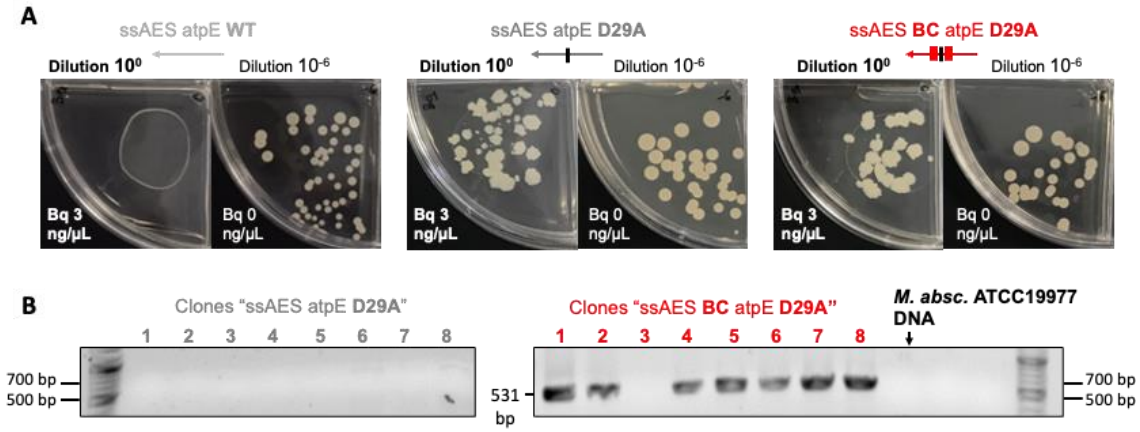

Figure 47: **Barcode-PCR with *M. abscessus* ATCC19977 *atpE* D29A recombinants.** (**A**) Electroporated *M. abscessus* UZ pJV53 with "ssAES *atpE* WT", "ssAES *atpE* D29A" and "ssAES BC *atpE* D29A" was plated in absence (dilution 10^{-6}) or presence (dilution 10^{0}) of bedaquiline 3 µg/mL. (**B**) Resistant colonies were subjected to Barcode-PCR.

Surprisingly, all *M. abscessus* ATCC 19977 bedaquiline resistant recombinants displayed a morphotype change from smooth to rough morphology, indicating absence or nearly absence of glycopeptidolipid in their cell envelope, this change was not observed in recombinants from *M. abscessus* SL541 strain (***Figure 48***). Altogether, our results demonstrate the robustness and reproducibility of our genetic replacement strategy, and lay foundations to apply these methods in independent laboratories.

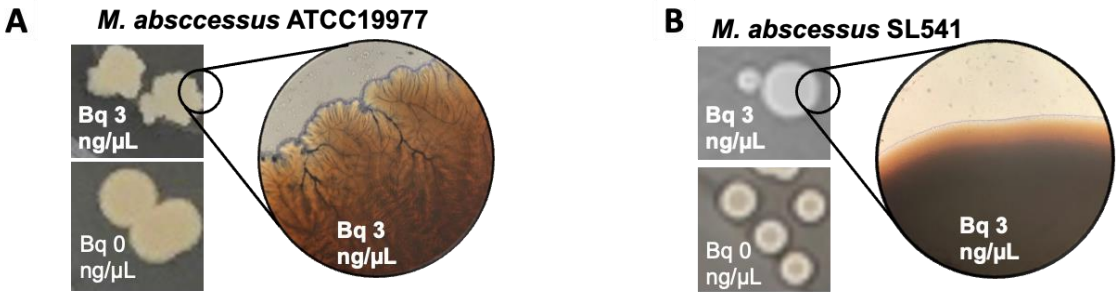

Figure 48: **Morphology comparison of *M. abscessus* ATCC19977 and SL541 recombinants.** (**A**) Morphology of recombinant colonies obtained in presence of bedaquiline 3 µg/mL from *M. abscessus* ATCC 19977 changed from smooth to rough. No change is observed in *M. abscessus* SL541 recombinants (**B**).

The barcoding genetic strategy was proven useful to detect D29A unrelated mutations in *M. abscessus*

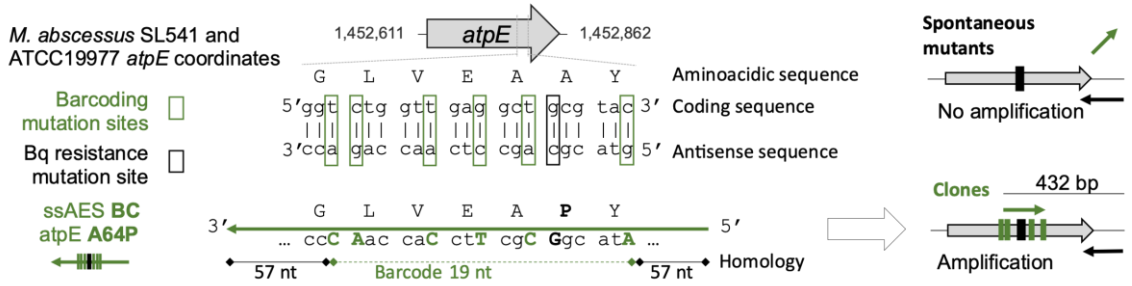

Figure 49: **Graphical representation of the "ssAES BC *atpE* A64P" used to mutate the 64th codon of the *atpE* gene** and its alignment in *M. abscessus* ATTC 19977 genome and barcode-PCR to detect recombinant colonies.

In order to use our genetic barcoding method as a general strategy to confirm antibiotic resistance mutations in *M. abscessus* we need to confirm that it also works in alternative polymorphisms. To do so, we selected an independent drug resistance mutation in *M. abscessus*. The A64P mutation in the *atpE* protein has been also described in *M. abscessus* (Dupont et al., 2017; Segala et al., 2012) and *M. tuberculosis* (Andries et al., 2005; Segala et al., 2012) as a polymorphism conferring bedaquiline resistance. Accordingly, we designed a new barcoding ssAES carrying the 64th Pro codon flanked by synonymous substitutions (ssAES BC *atpE* A64P) which should allow detection of recombinant colonies by barcode-PCR (***Table 10*** and ***Figure 49***).

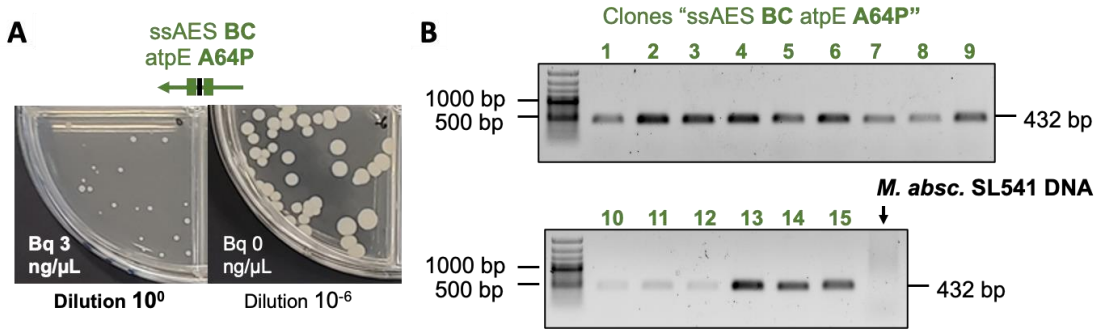

Figure 50: **Barcode-PCR with *M. abscessus* SL541 *atpE* A64P recombinants.** **(A)** Electroporated bacteria with "ssAES BC *atpE* A64P" were plated in absence (dilution $1/10^6$) or presence (dilution $1/10^0$) of bedaquiline 3 µg/mL. **(B)** Barcode-PCR of bedaquiline resistant colonies.

Transformation of our *M. abscessus* recombineering strain with "ssAES BC *atpE* A64P**"**, and culturing transformants in bedaquiline-containing plates, resulted in the growth of several drug resistant colonies (***Figure 50A***). Then, we used our barcode-PCR-based methods described above to confirm that specific incorporation of the barcode AES is responsible for the bedaquiline resistance of the transformants. By conventional, allele-specific PCR, we confirmed PCR amplification of the 432 bp specific band in all the assayed colonies (***Figure 50B***). We also confirmed specific Real Time PCR amplification of the barcoded *atpE* gene in recombinant (Ct≈18), but not in "wild type" SL541 (Ct>31) strains (***Figure 51***). Again, the verification process lasted from 10 to 14 days, depending on the use of Real Time-PCR or conventional PCR, respectively.

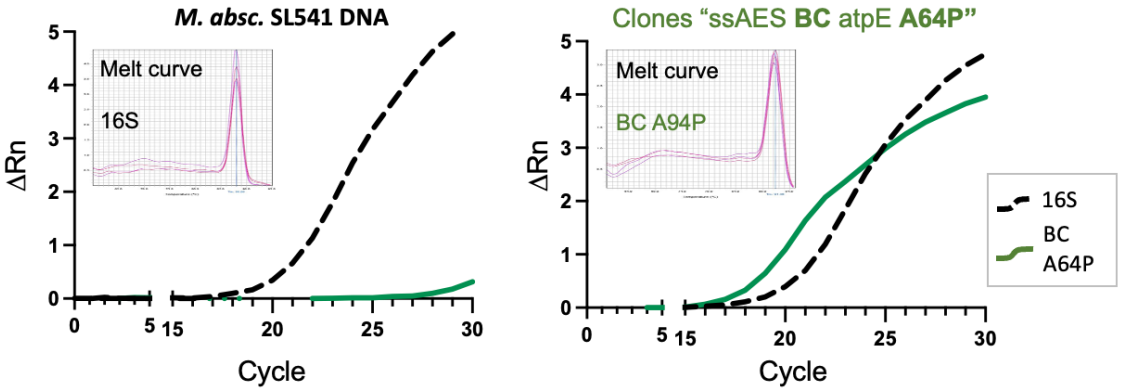

Figure 51: **Barcode-RT-PCR with *M. abscessus* SL541 *atpE* A64P recombinants**. ΔRn values of amplification of the 16S RNA gene (dashed grey) and the specific A64P barcode (continuous green) from *M. abscessus* "wild type" SL541 or "ssAES **BC** *atpE* **A64P**" transformants obtained by RT-PCR. Melting curves show the specificity of qRT-PCR amplifications.

The bedaquiline resistance of "ssAES BC *atpE* A64P" *M. abscessus* transformants was quantitatively confirmed by the MIC, which resulted >8 ng/μl, in contrast to the susceptible profile of the *M. abscessus* recombineering strain (***Figure 52***).

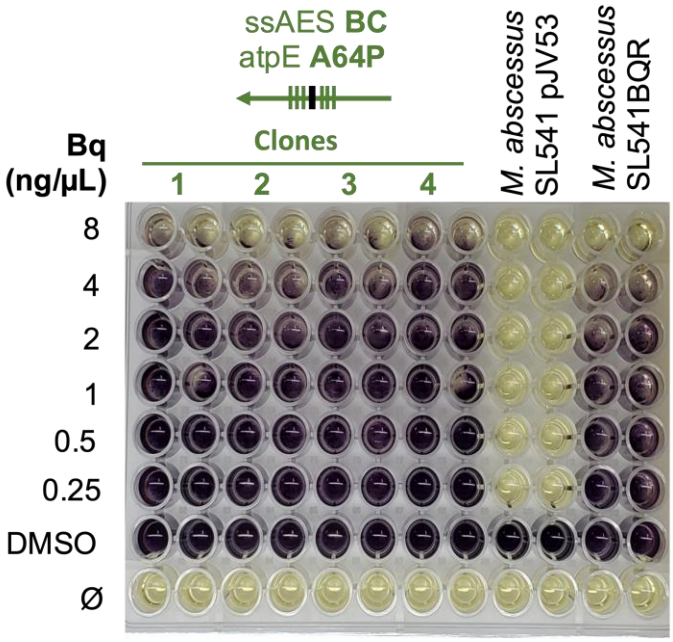

Figure 52: **Susceptibility to bedaquiline of *M. abscessus* SL541 *atpE* A64P recombinants.** MTT in 7H9Tyl-ADC to determine the MIC of different isolated recombinant colonies. Wells with viable bacteria are shown in dark purple, whereas wells with absence of growth are shown in yellow, after addition of MTT.

DISCUSSION

Antimicrobial resistance is a growing threat that endanger an effective treatment of infectious diseases and is indeed one of the health challenges for the 21st century (*Antimicrobial Resistance*, 2021). This is particularly important for mycobacterial infections since a limited repertoire of clinically approved drugs is available. Accordingly, mycobacterial infections usually require long term treatments with multiple drugs with the objective to reduce the chance of emergence of drug resistant strains (Quang & Jang, 2021; Victoria et al., 2021). However, an inadequate adherence to treatment, prescription of inadequate drugs, or failure in drug supply, lead to antibiotic resistant mycobacteria. Drug resistance has been extensively studied in *M. tuberculosis* in the last years, which has led to an extensive catalogue of genome polymorphisms in the *inhA*, *katG*, and *rpoB* genes associated to resistance against isoniazid and rifampicin, the first line anti-tuberculous drugs (K. A. Cohen et al., 2019; Khawbung et al., 2021). Other antibiotic resistance polymorphisms have been also discovered for the first line drugs pyrazinamide and ethambutol, and, also, to second line drugs, which include bedaquiline and delamanid, recently incorporated to the anti-TB regimes (Mahajan, 2013; Ryan & Lo, 2014).

In the era of WGS, these datasheets of antibiotic resistance polymorphisms are useful to delineate the possible drug resistance, or susceptibility profiles, by exploring genome data from clinical isolates. In this same context, PCR-based commercial systems to detect polymorphisms associated to drug resistance are widely available for *M. tuberculosis* (Cuong et al., 2021; de Faria et al., 2021; Theron et al., 2011). However, these genomic methods have previously required establishing a direct link between chromosomal polymorphisms and antimicrobial resistance, and this has been otherwise the result of long-term observation and characterization of clinical isolates.

Here, we propose a genetic method aiming to accelerate the validation of drug resistance mutations in *M. abscessus*, a bacterium which similarly to drug-resistant *M. tuberculosis*, possess few therapeutic options (Nessar et al., 2012; Quang & Jang, 2021; Victoria et al., 2021). We have focused here on bedaquiline resistance mutations, since the use of this drug against *M. abscessus* infections was introduced in 2015 (Philley et al., 2015) and, accordingly, it is expected that bedaquiline resistance mutations are yet emerging after the recent introduction of the treatment. In addition, since the bedaquiline target is ATP synthase, whose *atp* coding genes show a high level of conservation between different mycobacteria, it is expected that results obtained with *M. abscessus* might be translated to related members of the genus. Our method has been proven robust and

reliable since it has been successfully tested with two unrelated mutations and in two independent *M. abscessus* strains.

This strategy presents several advantages with respect to other genetic methods: First, the specific chromosomal replacement avoids the use of ectopic gene expression, either in episomal or chromosomal locations. Second, the use of an available recombineering strain, and the synthesis of specific oligonucleotides, avoid the use of time-consuming cloning procedures. Third, results can be obtained in a reasonable short time, mostly limited to the growth of drug resistant colonies, which usually takes more than a week. Fourth, our strategy is scalable and allows simultaneous testing of various drug resistance genotypes. These advantages might be useful to deconvolve sequencing data related to drug resistant isolates. It is key to remember that interrogation of genome data does not always result in a list of polymorphisms located in well-known genes associated to drug resistance. Accordingly, in these scenarios, each individual polymorphism should be genetically evaluated for its specific contribution to drug resistance (K. A. Cohen et al., 2019). Additionally, as this barcoding strategy allows easily identification of our mutants, it can be optimized to compare different isogenic mutants and track how mutant populations evolve upon exposure to an antibiotic pressure, resembling signature-tagged mutagenesis, a technique used to distinguish desirable mutations in pools of transposon mutants in *M. tuberculosis* (Lamrabet & Drancourt, 2012). Barcoding could be also useful to be applied in studies of horizontal gene transfer (HGT) in mycobacteria. Current studies in HGT rely on the use antibiotic resistance cassettes to detect DNA transmission between donor and recipient strains (Boritsch et al., 2016; Madacki et al., 2021). However, barcodes are codified in smaller portions of the chromosome and could be used to mark clinically relevant drug resistance mutations, like mutations in *inhA* or *katG* genes, or potential new resistance mutations like the ones studied in this chapter in the *atpE* gene.

It remains to be answered whether the method described here is useful to detect low-level drug resistance, since we rely on the growth of drug resistant transformants on plates containing the corresponding drug. In this same context, further work is needed to ascertain whether other drug resistant mutations, aside from bedaquiline, can be tested by our method. However, regarding this latter observation, we should remember that our barcoding method is suitable to establish genotype-phenotype relationships in those polymorphisms located within coding regions, because of the need to introduce silent mutations in the vicinity of the targeted polymorphisms. Accordingly, it is not always possible to introduce such silent mutation in non-coding regions, as the ribosomal RNA subunits, which are the targets of aminoglycosides and macrolides used in the treatment

of *M. abscessus* infections. These latter cases affecting non-coding RNA targets could be otherwise examined using non-barcoded oligonucleotides, and the subsequent verification of the gene sequence. Even though the non-barcoded method does not rule out the appearance of spontaneous mutations at the studied locus, a uniformity in the allele sequences from resistant colonies might be indicative of recombineering-derived drug resistant colonies.

Another aspect to consider is that silent mutations introduced in coding regions with this barcoding strategy could alter protein expression levels due to bacterial codon usage with the consequent change in bacterial fitness. It has been recently reported that *M. bovis* BCG is able to react to stress by tRNA reprograming and codon-biased translation. By this mechanism, BCG can drive the "over- or down-translation" mRNAs codon-biased from different families (Chan et al., 2018; Chionh et al., 2016). Taking this into account, barcoding mutations could interfere in bacterial fitness if barcoded strains are used in different experiments (like *ex vivo* and *in vivo* infection experiments). mRNA structure and hybridization with other RNA structures of the bacteria could also be affected by barcoding mutations. However, these possible problems could be minimized with a rational design of the mutations. We can try to maintain percentage of codon usage, for example, if different Ala codons are affected, switching them. On the other hand, *in silico* RNA analyzing servers are improving continuously and prediction of RNA structures and interactions could also be used to help in the design of our desired mutations.

Results described here could be theoretically applied to new candidate drugs which are currently in pre-licensing phases (WHO, 2022a). This would allow researchers to identify possible mechanisms of resistance prior to clinical evaluation of these forthcoming drugs, which might be useful to optimize diagnostic methods for the eventual drug resistant isolates. On the other side, since chromosomal replacements using recombineering have been described in different *Mycobacterium* species, including *M. tuberculosis, M. smegmatis, M. chelonae* (de Moura et al., 2014), *M. canettii* (our unpublished results), we propose that our method could be transferable to other mycobacteria. This opens attractive possibilities to study not only drug resistance polymorphisms, but also metabolic, physiological, or virulence traits in *Mycobacterium*. Overall, our barcoding strategy might help to accelerate the understanding the role of specific polymorphisms associated to drug resistance, with possible parallel application to understand mycobacterial biology.

CONCLUSIONS

Chapter 1:

- ETZ acts as control compound of PhoPR inhibition in *M. tuberculosis* and it has been used to characterize the different *M. tuberculosis* reporter strains and the secondary assays of this Thesis. Our results also suggest that its PhoPR inhibitory activity is independent of its inhibitory activity in *M. tuberculosis* carbonic anhydrases.
- A wide panel of *M. tuberculosis* PhoPR reporter strains has been constructed using plasmids carrying the GFP under the control of *pks2* and *mcr7* promoters. These reporter strains have been constructed and validated in three different *M. tuberculosis* strains from the two most widespread lineages of the MTBC.
- Two secondary assays have been established to confirm transcriptional downregulation of *mcr7*, *pks2*, *pks3, espA, espC* and *espD* genes, and the inhibition of secretion of ESAT-6, CFP-10, EspA and EspD proteins.
- A *M. smegmatis* reporter strain has been constructed with potential application as a surrogate of *M. tuberculosis* for the screening of PhoPR inhibitors.

Chapter 2:

- Two *M. abscessus* recombineering strains have been constructed for their use with single stranded DNA recombinogenic substrates (ssAES).
- The introduction of a genetic barcode into the *M. abscessus* chromosome using ssAES is useful for detecting the *atpE* D29A bedaquiline resistance mutation by PCR based methodologies.
- The genetic barcoding strategy was proven useful to confirm a second unrelated mutation in the *atpE* gene conferring bedaquiline resistance in *M. abscessus*.

CONCLUSIONES

Capítulo 1:

- La ETZ actúa como compuesto control de inhibición del sistema PhoPR en *M. tuberculosis* y ha sido usada para caracterizar as diferentes cepas reporteras y los ensayos secundarios de esta Tesis. Nuestros resultados también sugieren que su actividad inhibitoria del sistema PhoPR es independiente de su actividad inhibidora de las anhidrasas carbónicas de *M. tuberculosis.*
- Se ha construido un amplio panel de cepas de *M. tuberculosis* reporteras del sistema PhoPR usando plásmidos con la GFP bajo el control de los promotores *mcr7* y *pks2.* Estas cepas reporteras han sido introducidas y validadas en tres cepas diferentes de *M. tuberculosis* pertenecientes a los dos linajes del MTBC más extendidos.
- Se han establecido dos ensayos secundarios para confirmar la desregulación transcripcional de los genes *mcr7*, *pks2*, *pks3, espA, espC* y *espD*; y la inhibición de la secreción de las proteínas ESAT-6, CFP-10, EspA y EspD.
- Se ha construido una cepa reportera de *M. smegmatis* con potencial aplicación como sustituta para el cribado de inhibidores del sistema PhoPR de *M. tuberculosis*.

Capítulo 2:

- Se han construido dos cepas de *M. abscessus* con el sistema de “recombineering” para su uso con sustratos de recombinación de DNA de cadena simple (ssAES).
- La introducción de un código de barras genético en el cromosoma de *M. abscessus* mediante el uso de ssAES es útil para detectar la mutación de resistencia a bedaquilina *atpE* D29A mediante metodologías basadas en PCR.
- La estrategia de uso de un código de barras genético ha demostrado ser útil para confirmar una segunda mutación independiente en el gen *atpE* que confiere resistencia a bedaquilina en *M. abscessus*.

BIBLIOGRAPHY

Abdallah, A. M., & Behr, M. A. (2017). Evolution and strain variation in BCG. In *Advances in Experimental Medicine and Biology* (Vol. 1019, pp. 155–169). Adv Exp Med Biol. https://doi.org/10.1007/978-3-319-64371-7_8

Abdallah, A. M., Gey van Pittius, N. C., DiGiuseppe Champion, P. A., Cox, J., Luirink, J., Vandenbroucke-Grauls, C. M. J. E., Appelmelk, B. J., & Bitter, W. (2007). Type VII secretion - Mycobacteria show the way. *Nature Reviews Microbiology*, *5*(11), 883–891. https://doi.org/10.1038/nrmicro1773

Abramovitch, R. B., Rohde, K. H., Hsu, F. F., & Russell, D. G. (2011). aprABC: A Mycobacterium tuberculosis complex-specific locus that modulates pH-driven adaptation to the macrophage phagosome. *Molecular Microbiology*, *80*(3), 678–694. https://doi.org/10.1111/j.1365-2958.2011.07601.x

Aguilo, N., Gonzalo-Asensio, J., Alvarez-Arguedas, S., Marinova, D., Gomez, A. B., Uranga, S., Spallek, R., Singh, M., Audran, R., Spertini, F., & Martin, C. (2017). Reactogenicity to major tuberculosis antigens absent in BCG is linked to improved protection against Mycobacterium tuberculosis. *Nature Communications*, *8*(May), 16085. https://doi.org/10.1038/ncomms16085

Aguilo, N., Toledo, A. M., Lopez-Roman, E. M., Perez-Herran, E., Gormley, E., Rullas-Trincado, J., Angulo-Barturen, I., & Martin, C. (2014). Pulmonary Mycobacterium bovis BCG vaccination confers dose-dependent superior protection compared to that of subcutaneous vaccination. *Clinical and Vaccine Immunology*, *21*(4), 594–597. https://doi.org/10.1128/CVI.00700-13

Akbar Velayati, A., Farnia, P., & Reza Masjedi, M. (2013). The totally drug resistant tuberculosis (TDR-TB). *International Journal of Clinical and Experimental Medicine*, *6*(4), 307–309.

Alshaer, W., Zureigat, H., al Karaki, A., Al-Kadash, A., Gharaibeh, L., Hatmal, M. M., Aljabali, A. A. A., & Awidi, A. (2021). siRNA: Mechanism of action, challenges, and therapeutic approaches. *European Journal of Pharmacology*, *905*(May), 174178. https://doi.org/10.1016/j.ejphar.2021.174178

Altaf, M., Miller, C. H., Bellows, D. S., & O'Toole, R. (2010). Evaluation of the Mycobacterium smegmatis and BCG models for the discovery of Mycobacterium tuberculosis inhibitors. *Tuberculosis*, *90*(6), 333–337. https://doi.org/10.1016/j.tube.2010.09.002

Andersen, P., & Kaufmann, S. H. E. (2014). Novel vaccination strategies against tuberculosis. *Cold Spring Harbor Perspectives in Medicine*, *4*(6). https://doi.org/10.1101/cshperspect.a018523

Andersen, P., & Scriba, T. J. (2019). Moving tuberculosis vaccines from theory to practice. In *Nature Reviews Immunology* (Vol. 19, Issue 9, pp. 550–562). Nat Rev Immunol. https://doi.org/10.1038/s41577-019-0174-z

Andersson, S. G. E., & Sharp, P. M. (1996). Codon usage in the Mycobacterium tuberculosis complex. *Microbiology*, *142 (Pt 4*, 915–925. https://doi.org/10.1099/00221287-142-4-915

Andries, K., Verhasselt, P., Guillemont, J., Göhlmann, H. W. H. H., Neefs, J.-M. M., Winkler, H., van Gestel, J., Timmerman, P., Zhu, M., Lee, E. E., Williams, P., de Chaffoy, D., Huitric, E., Hoffner, S., Cambau, E., Truffot-Pernot, C., Lounis, N., & Jarlier, V. (2005). A Diarylquinoline Drug Active on the ATP Synthase of Mycobacterium tuberculosis. *Science*, *307*(5707), 223–227. https://doi.org/10.1126/science.1106753

Antimicrobial resistance. (2021). https://www.who.int/news-room/fact-sheets/detail/antimicrobial-resistance

Arbues, A., Aguilo, J. I., Gonzalo-Asensio, J., Marinova, D., Uranga, S., Puentes, E., Fernandez, C., Parra, A., Cardona, P. J., Vilaplana, C., Ausina, V., Williams, A., Clark, S., Malaga, W., Guilhot, C., Gicquel, B., & Martin, C. (2013). Construction, characterization and preclinical evaluation of MTBVAC, the first live-attenuated M. tuberculosis-based vaccine to enter clinical trials. *Vaccine*, *31*(42), 4867–4873. https://doi.org/10.1016/j.vaccine.2013.07.051

Arbués, A., Malaga, W., Constant, P., Guilhot, C., Prandi, J., & Astarie-Dequeker, C. (2016). Trisaccharides of Phenolic Glycolipids Confer Advantages to Pathogenic Mycobacteria through Manipulation of Host-Cell Pattern-Recognition Receptors. *ACS Chemical Biology*, *11*(10), 2865–2875. https://doi.org/10.1021/acschembio.6b00568

Arnal, C. (2016). *In deep study of new tuberculosis vaccine candidates based on phoP and fadD26 mutations*.

Ates, L. S. (2020). New insights into the mycobacterial PE and PPE proteins provide a framework for future research. *Molecular Microbiology*, *113*(1), 4–21. https://doi.org/10.1111/MMI.14409

Ates, L. S., & Brosch, R. (2017). Discovery of the type VII ESX-1 secretion needle? In *Molecular Microbiology* (Vol. 103, Issue 1, pp. 7–12). John Wiley & Sons, Ltd. https://doi.org/10.1111/mmi.13579

Augenstreich, J., Arbues, A., Simeone, R., Haanappel, E., Wegener, A., Sayes, F., le Chevalier, F., Chalut, C., Malaga, W., Guilhot, C., Brosch, R., & Astarie-Dequeker, C. (2017). ESX-1 and phthiocerol dimycocerosates of Mycobacterium tuberculosis act in concert to cause phagosomal rupture and host cell apoptosis. *Cellular Microbiology*, *19*(7), e12726. https://doi.org/10.1111/cmi.12726

Augenstreich, J., & Briken, V. (2020). Host Cell Targets of Released Lipid and Secreted Protein Effectors of Mycobacterium tuberculosis. *Frontiers in Cellular and Infection Microbiology*, *10*(October), 618. https://doi.org/10.3389/fcimb.2020.595029

Baker, J. J., Johnson, B. K., & Abramovitch, R. B. (2014). Slow growth of Mycobacterium tuberculosis at acidic pH is regulated by phoPR and host-associated carbon sources. *Molecular Microbiology*, *94*(1), 56–69. https://doi.org/10.1111/mmi.12688

Balu, S., Reljic, R., Lewis, M. J., Pleass, R. J., McIntosh, R., van Kooten, C., van Egmond, M., Challacombe, S., Woof, J. M., & Ivanyi, J. (2011). A Novel Human IgA Monoclonal Antibody Protects against Tuberculosis. *The Journal of Immunology*, *186*(5), 3113–3119. https://doi.org/10.4049/jimmunol.1003189

Barberis, I., Bragazzi, N. L., Galluzzo, L., & Martini, M. (2017). The history of tuberculosis: From the first historical records to the isolation of Koch's bacillus. *Journal of Preventive Medicine and Hygiene*, *58*(1), E9–E12. https://doi.org/10.15167/2421-4248/jpmh2017.58.1.728

Barker, L. P., Brooks, D. M., & Small, P. L. C. (1998). The identification of Mycobacterium marinum genes differentially expressed in macrophage phagosomes using promoter fusions to green fluorescent protein. *Molecular Microbiology*, *29*(5), 1167–1177. https://doi.org/10.1046/j.1365-2958.1998.00996.x

Becker, K., & Sander, P. (2016). Mycobacterium tuberculosis lipoproteins in virulence and immunity – fighting with a double-edged sword. In *FEBS Letters* (Vol. 590, Issue 21, pp. 3800–3819). John Wiley & Sons, Ltd. https://doi.org/10.1002/1873-3468.12273

Belardinelli, J. M., Verma, D., Li, W., Avanzi, C., Wiersma, C. J., Williams, J. T., Johnson, B. K., Zimmerman, M., Whittel, N., Angala, B., Wang, H., Jones, V., Dartois, V., Moura, V. C. N. de, Gonzalez-Juarrero, M., Pearce, C., Schenkel, A. R., Malcolm,

K. C., Nick, J. A., … Jackson, M. (2022). Therapeutic efficacy of antimalarial drugs targeting DosRS signaling in Mycobacterium abscessus. *Science Translational Medicine*, *14*(633), 3860. https://www.science.org/doi/abs/10.1126/scitranslmed.abj3860

Blanc, L., Gilleron, M., Prandi, J., Song, O.-R., Jang, M.-S., Gicquel, B., Drocourt, D., Neyrolles, O., Brodin, P., Tiraby, G., Vercellone, A., & Nigou, J. (2017). Mycobacterium tuberculosis inhibits human innate immune responses via the production of TLR2 antagonist glycolipids. *Proceedings of the National Academy of Sciences of the United States of America*, *114*(42), 11205–11210. https://doi.org/10.1073/pnas.1707840114

Boehme, C., Hannay, E., & Pai, M. (2021). Promoting diagnostics as a global good. *Nature Medicine*, *27*(3), 367–368. https://doi.org/10.1038/s41591-020-01215-3

Bondareva, N. E., Soloveva, A. v., Sheremet, A. B., Koroleva, E. A., Kapotina, L. N., Morgunova, E. Y., Luyksaar, S. I., Zayakin, E. S., & Zigangirova, N. A. (2022). Preventative treatment with Fluorothiazinon suppressed Acinetobacter baumannii-associated septicemia in mice. *The Journal of Antibiotics 2022 75:3*, *75*(3), 155–163. https://doi.org/10.1038/s41429-022-00504-y

Boritsch, E. C., Khanna, V., Pawlik, A., Honoré, N., Navas, V. H., Ma, L., Bouchier, C., Seemann, T., Supply, P., Stinear, T. P., & Brosch, R. (2016). Key experimental evidence of chromosomal DNA transfer among selected tuberculosiscausing mycobacteria. *Proceedings of the National Academy of Sciences of the United States of America*, *113*(35), 9876–9881. https://doi.org/10.1073/pnas.1604921113

Bretl, D. J., Demetriadou, C., & Zahrt, T. C. (2011). Adaptation to Environmental Stimuli within the Host: Two-Component Signal Transduction Systems of Mycobacterium tuberculosis. *Microbiology and Molecular Biology Reviews*, *75*(4), 566–582. https://doi.org/10.1128/MMBR.05004-11/ASSET/4980981C-1A22-4E29-922C-6CBCC2C5AE52/ASSETS/GRAPHIC/ZMR9990922810001.JPEG

Brosch, R., Gordon, S. v., Billault, A., Garnier, T., Eiglmeier, K., Soravito, C., Barrell, B. G., & Cole, S. T. (1998). Use of a Mycobacterium tuberculosis H37Rv bacterial artificial chromosome library for genome mapping, sequencing, and comparative genomics. *Infection and Immunity*, *66*(5), 2221–2229. https://doi.org/10.1128/iai.66.5.2221-2229.1998

Broset, E., Martín, C., & Gonzalo-Asensio, J. (2015). Evolutionary landscape of the mycobacterium tuberculosis complex from the viewpoint of phoPR: Implications for virulence regulation and application to vaccine development. *MBio*, *6*(5). https://doi.org/10.1128/mBio.01289-15

Calmette, A. (1931). Preventive Vaccination against Tuberculosis with BCG. *Journal of the Royal Society of Medicine*, *24*(11), 1481–1490. https://doi.org/10.1177/003591573102401109

Camacho, L. R., Constant, P., Raynaud, C., Lanéelle, M. A., Triccas, J. A., Gicquel, B., Daffé, M., & Guilhot, C. (2001). Analysis of the phthiocerol dimycocerosate locus of Mycobacterium tuberculosis. Evidence that this lipid is involved in the cell wall permeability barrier. *Journal of Biological Chemistry*, *276*(23), 19845–19854. https://doi.org/10.1074/jbc.M100662200

Caminero, J. A., Pena, M. J., Campos-Herrero, M. I., Rodríguez, J. C., García, I., Cabrera, P., Lafoz, C., Samper, S., Takiff, H., Afonso, O., Pavón, J. M., Torres, M. J., van Soolingen, D., Enarson, D. A., & Martin, C. (2001). Epidemiological evidence of the spread of a Mycobacterium tuberculosis strain of the Beijing genotype on Gran Canaria Island. *American Journal of Respiratory and Critical Care Medicine*, *164*(7), 1165–1170. https://doi.org/10.1164/AJRCCM.164.7.2101031

Carroll, P., Schreuder, L. J., Muwanguzi-Karugaba, J., Wiles, S., Robertson, B. D., Ripoll, J., Ward, T. H., Bancroft, G. J., Schaible, U. E., & Parish, T. (2010). Sensitive detection of gene expression in mycobacteria under replicating and non-replicating conditions using optimized far-red reporters. *PLoS ONE*, *5*(3). https://doi.org/10.1371/journal.pone.0009823

Carta, F., Maresca, A., Covarrubias, A. S., Mowbray, S. L., Jones, T. A., & Supuran, C. T. (2009). Carbonic anhydrase inhibitors. Characterization and inhibition studies of the most active β-carbonic anhydrase from Mycobacterium tuberculosis, Rv3588c. *Bioorganic and Medicinal Chemistry Letters*, *19*(23), 6649–6654. https://doi.org/10.1016/j.bmcl.2009.10.009

Cave, A. J. E. (1939). The evidence for the incidence of tuberculosis in ancient Egypt. *The British Journal of Tuberculosis*. https://doi.org/10.1016/s0366-0850(39)80016-3

Chakaya, J., Khan, M., Ntoumi, F., Aklillu, E., Fatima, R., Mwaba, P., Kapata, N., Mfinanga, S., Hasnain, S. E., Katoto, P. D. M. C., Bulabula, A. N. H., Sam-Agudu,

N. A., Nachega, J. B., Tiberi, S., McHugh, T. D., Abubakar, I., & Zumla, A. (2021). Global Tuberculosis Report 2020 – Reflections on the Global TB burden, treatment and prevention efforts. *International Journal of Infectious Diseases*, *113*, S7–S12. https://doi.org/10.1016/j.ijid.2021.02.107

Chan, C., Pham, P., Dedon, P. C., & Begley, T. J. (2018). Lifestyle modifications: Coordinating the tRNA epitranscriptome with codon bias to adapt translation during stress responses. *Genome Biology*, *19*(1), 1–11. https://doi.org/10.1186/S13059-018-1611-1/FIGURES/3

Chandra, P., Grigsby, S. J., & Philips, J. A. (2022). Immune evasion and provocation by Mycobacterium tuberculosis. *Nature Reviews Microbiology*, *20*(12), 750–766. https://doi.org/10.1038/s41579-022-00763-4

Chen, J. M., Boy-Röttger, S., Dhar, N., Sweeney, N., Buxton, R. S., Pojer, F., Rosenkrands, I., & Cole, S. T. (2012). EspD is critical for the virulence-mediating ESX-1 secretion system in Mycobacterium tuberculosis. *Journal of Bacteriology*, *194*(4), 884–893. https://doi.org/10.1128/JB.06417-11

Chionh, Y. H., McBee, M., Babu, I. R., Hia, F., Lin, W., Zhao, W., Cao, J., Dziergowska, A., Malkiewicz, A., Begley, T. J., Alonso, S., & Dedon, P. C. (2016). TRNA-mediated codon-biased translation in mycobacterial hypoxic persistence. *Nature Communications*, *7*(1), 1–12. https://doi.org/10.1038/ncomms13302

Choi, H., Kim, S. Y., Kim, D. H., Huh, H. J., Ki, C. S., Lee, N. Y., Lee, S. H., Shin, S., Shin, S. J., Daley, C. L., & Koh, W. J. (2017). Clinical characteristics and treatment outcomes of patients with acquired macrolide-resistant Mycobacterium abscessus lung disease. *Antimicrobial Agents and Chemotherapy*, *61*(10). https://doi.org/10.1128/AAC.01146-17

Cohen, K. A., Manson, A. L., Desjardins, C. A., Abeel, T., & Earl, A. M. (2019). Deciphering drug resistance in Mycobacterium tuberculosis using whole-genome sequencing: Progress, promise, and challenges. *Genome Medicine*, *11*(1), 1–18. https://doi.org/10.1186/s13073-019-0660-8

Cohen, S. B., Gern, B. H., & Urdahl, K. B. (2022). The Tuberculous Granuloma and Preexisting Immunity. *Annual Review of Immunology*, *40*(1), 589–614. https://doi.org/10.1146/annurev-immunol-093019-125148

Cole, S. T., Brosch, R., Parkhill, J., Garnier, T., Churcher, C., Harris, D., Gordon, S. v., Eiglmeier, K., Gas, S., Barry, C. E., Tekaia, F., Badcock, K., Basham, D., Brown,

D., Chillingworth, T., Connor, R., Davies, R., Devlin, K., Feltwell, T., … Bartell, B. G. (1998). Deciphering the biology of Mycobacterium tuberculosis from the complete genome sequence. *Nature*, *396*(6707), 190. https://doi.org/10.1038/24206

Constant, P., Perez, E., Malaga, W., Lanéelle, M. A., Saurel, O., Daffé, M., & Guilhot, C. (2002). Role of the pks15/1 gene in the biosynthesis of phenolglycolipids in the Mycobacterium tuberculosis complex. Evidence that all strains synthesize glycosylated p-hydroxybenzoic methyl esters and that strains devoid of phenolglycolipids harbor a frameshift . *The Journal of Biological Chemistry*, *277*(41), 38148–38158. https://doi.org/10.1074/JBC.M206538200

Cook, G. M., Berney, M., Gebhard, S., Heinemann, M., Cox, R. A., Danilchanka, O., & Niederweis, M. (2009). Physiology of Mycobacteria. *Advances in Microbial Physiology*, *55*(09). https://doi.org/10.1016/S0065-2911(09)05502-7

Cox, J. S., Chess, B., McNeil, M., & Jacobs, W. R. (1999). Complex lipid determines tissue-specific replication of Mycobacterium tuberculosis in mice. *Nature*, *402*(6757), 79–83. https://doi.org/10.1038/47042

Crubézy, E., Ludes, B., Poveda, J.-D., Clayton, J., Crouau-Roy, B., & Montagnon, D. (1998). Identification of Mycobacterium DNA in an Egyptian Pott's disease of 5400 years old. *Comptes Rendus de l'Académie Des Sciences - Series III - Sciences de La Vie*, *321*(11), 941–951. https://doi.org/10.1016/s0764-4469(99)80009-2

Cuong, N. K., Ngoc, N. B., Hoa, N. B., Dat, V. Q., & Nhung, N. V. (2021). GeneXpert on patients with human immunodeficiency virus and smear-negative pulmonary tuberculosis. *PloS One*, *16*(7). https://doi.org/10.1371/JOURNAL.PONE.0253961

Daley, C. L., Iaccarino, J. M., Lange, C., Cambau, E., Wallace, R. J., Andrejak, C., Böttger, E. C., Brozek, J., Griffith, D. E., Guglielmetti, L., Huitt, G. A., Knight, S. L., Leitman, P., Marras, T. K., Olivier, K. N., Santin, M., Stout, J. E., Tortoli, E., van Ingen, J., … Winthrop, K. L. (2020). Treatment of Nontuberculous Mycobacterial Pulmonary Disease: An Official ATS/ERS/ESCMID/IDSA Clinical Practice Guideline. *Clinical Infectious Diseases*, *71*(4), e1–e36. https://doi.org/10.1093/CID/CIAA241

Daniel, T. M. (2006). The history of tuberculosis. *Respiratory Medicine*, *100*(11), 1862–1870. https://doi.org/10.1016/j.rmed.2006.08.006

Daniel, T. M. (2011). Hermann Brehmer and the origins of tuberculosis sanatoria. *The International Journal of Tuberculosis and Lung Disease : The Official Journal of the International Union against Tuberculosis and Lung Disease*, *15*(2), 161–162.

Dartois, V. A., & Rubin, E. J. (2022). Anti-tuberculosis treatment strategies and drug development: challenges and priorities. *Nature Reviews Microbiology*, 1–17. https://doi.org/10.1038/s41579-022-00731-y

Datsenko, K. A., & Wanner, B. L. (2000). One-step inactivation of chromosomal genes in Escherichia coli K-12 using PCR products. *Proceedings of the National Academy of Sciences of the United States of America*, *97*(12), 6640–6645. https://doi.org/10.1073/pnas.120163297

Davis, J. M., & Ramakrishnan, L. (2009). The Role of the Granuloma in Expansion and Dissemination of Early Tuberculous Infection. *Cell*, *136*(1), 37–49. https://doi.org/10.1016/j.cell.2008.11.014

de Faria, M. G. B. F., de Paula Andrade, R. L., Camillo, A. J. G., de Souza Leite, K. F., Saita, N. M., Bollela, V. R., de Rezende, C. E. M., & Monroe, A. A. (2021). Effectiveness of GeneXpert® in the diagnosis of tuberculosis in people living with HIV/AIDS. *Revista de Saúde Pública*, *55*. https://doi.org/10.11606/S1518-8787.2021055003125

de Moura, V. C. N., Gibbs, S., & Jackson, M. (2014). Gene replacement in mycobacterium chelonae: Application to the construction of porin knock-out mutants. *PLoS ONE*, *9*(4). https://doi.org/10.1371/journal.pone.0094951

de Rossi, E., Arrigo, P., Bellinzoni, M., Silva, P. E. A., Martín, C., Aínsa, J. A., Guglierame, P., & Riccardi, G. (2002). The multidrug transporters belonging to major facilitator superfamily (MFS) in Mycobacterium tuberculosis. *Molecular Medicine*, *8*(11), 714–724. https://doi.org/10.1007/bf03402035

Delogu, G., Brennan, M. J., & Manganelli, R. (2017). PE and PPE Genes: A tale of conservation and diversity. In *Advances in Experimental Medicine and Biology* (Vol. 1019, pp. 191–207). Adv Exp Med Biol. https://doi.org/10.1007/978-3-319-64371-7_10

Dey, B., Dey, R. J., Cheung, L. S., Pokkali, S., Guo, H., Lee, J. H., & Bishai, W. R. (2015). A bacterial cyclic dinucleotide activates the cytosolic surveillance pathway and mediates innate resistance to tuberculosis. *Nature Medicine*, *21*(4), 401–408. https://doi.org/10.1038/nm.3813

Díaz, C., Pérez Del Palacio, J., Valero-Guillén, P. L., Mena García, P., Pérez, I., Vicente, F., Martín, C., Genilloud, O., Sánchez Pozo, A., & Gonzalo-Asensio, J. (2019). Comparative Metabolomics between Mycobacterium tuberculosis and the MTBVAC Vaccine Candidate. *ACS Infectious Diseases*, *5*(8), 1317–1326. https://doi.org/10.1021/acsinfecdis.9b00008

Dickey, S. W., Cheung, G. Y. C., & Otto, M. (2017). Different drugs for bad bugs: Antivirulence strategies in the age of antibiotic resistance. *Nature Reviews Drug Discovery*, *16*(7), 457–471. https://doi.org/10.1038/nrd.2017.23

Digiuseppe Champion, P. A., & Cox, J. S. (2007). Protein secretion systems in Mycobacteria. *Cellular Microbiology*, *9*(6), 1376–1384. https://doi.org/10.1111/J.1462-5822.2007.00943.X

Dijkman, K., Aguilo, N., Boot, C., Hofman, S. O., Sombroek, C. C., Vervenne, R. A. W., Kocken, C. H. M., Marinova, D., Thole, J., Rodríguez, E., Vierboom, M. P. M., Haanstra, K. G., Puentes, E., Martin, C., & Verreck, F. A. W. (2021). Pulmonary MTBVAC vaccination induces immune signatures previously correlated with prevention of tuberculosis infection. *Cell Reports Medicine*, *2*(1). https://doi.org/10.1016/j.xcrm.2020.100187

Ding, C., Hu, M., Guo, W., Hu, W., Li, X., Wang, S., Shangguan, Y., Zhang, Y., Yang, S., & Xu, K. (2022). Prevalence trends of latent tuberculosis infection at the global, regional, and country levels from 1990–2019. *International Journal of Infectious Diseases*, *122*, 46–62. https://doi.org/10.1016/J.IJID.2022.05.029

Donald, P. R., Marais, B. J., & Barry, C. E. (2010). Age and the epidemiology and pathogenesis of tuberculosis. *The Lancet*, *375*(9729), 1852–1854. https://doi.org/10.1016/S0140-6736(10)60580-6

Dubée, V., Bernut, A., Cortes, M., Lesne, T., Dorchene, D., Lefebvre, A. L., Hugonnet, J. E., Gutmann, L., Mainardi, J. L., Herrmann, J. L., Gaillard, J. L., Kremer, L., & Arthur, M. (2014). β-Lactamase inhibition by avibactam in Mycobacterium abscessus. *Journal of Antimicrobial Chemotherapy*, *70*(4), 1051–1058. https://doi.org/10.1093/jac/dku510

Dulberger, C. L., Rubin, E. J., & Boutte, C. C. (2020). The mycobacterial cell envelope — a moving target. *Nature Reviews Microbiology*, *18*(1), 47–59. https://doi.org/10.1038/s41579-019-0273-7

Dupont, C., Viljoen, A., Thomas, S., Roquet-Banères, F., Herrmann, J. L., Pethe, K., & Kremer, L. (2017). Bedaquiline inhibits the ATP synthase in mycobacterium abscessus and is effective in infected zebrafish. *Antimicrobial Agents and Chemotherapy*, *61*(11). https://doi.org/10.1128/AAC.01225-17

Echeverria-Valencia, G., Flores-Villalva, S., & Espitia, C. I. (2018). Virulence Factors and Pathogenicity of Mycobacterium. In *Mycobacterium - Research and Development*. IntechOpen. https://doi.org/10.5772/intechopen.72027

Falkinham, J. O. (1996). Epidemiology of infection by nontuberculous mycobacteria. *Clinical Microbiology Reviews*, *9*(2), 177–215. https://doi.org/10.1128/CMR.9.2.177

FDA. (2019). FDA approves new drug for treatment-resistant forms of tuberculosis that affects the lungs. *FDA Press Announcements*. https://doi.org/10.31525/cmr-1a2db41

Fine, P. E. M. (1995). Variation in protection by BCG: implications of and for heterologous immunity. *The Lancet*, *346*(8986), 1339–1345. https://doi.org/10.1016/S0140-6736(95)92348-9

Fleischmann, R. D., Alland, D., Eisen, J. A., Carpenter, L., White, O., Peterson, J., DeBoy, R., Dodson, R., Gwinn, M., Haft, D., Hickey, E., Kolonay, J. F., Nelson, W. C., Umayam, L. A., Ermolaeva, M., Salzberg, S. L., Delcher, A., Utterback, T., Weidman, J., … Fraser, C. M. (2002). Whole-genome comparison of Mycobacterium tuberculosis clinical and laboratory strains. *Journal of Bacteriology*, *184*(19), 5479–5490. https://doi.org/10.1128/JB.184.19.5479-5490.2002

Flores, A. R., Parsons, L. M., & Pavelka, M. S. (2005). Genetic analysis of the β-lactamases of Mycobacterium tuberculosis and Mycobacterium smegmatis and susceptibility to β-lactam antibiotics. *Microbiology*, *151*(2), 521–532. https://doi.org/10.1099/mic.0.27629-0

Floto, R. A., Olivier, K. N., Saiman, L., Daley, C. L., Herrmann, J. L., Nick, J. A., Noone, P. G., Bilton, D., Corris, P., Gibson, R. L., Hempstead, S. E., Koetz, K., Sabadosa, K. A., Sermet-Gaudelus, I., Smyth, A. R., van Ingen, J., Wallace, R. J., Winthrop, K. L., Marshall, B. C., & Haworth, C. S. (2016). US Cystic Fibrosis Foundation and European Cystic Fibrosis Society consensus recommendations for the management of non-tuberculous mycobacteria in individuals with cystic fibrosis. *Thorax*, *71*(Suppl 1), i1–i22. https://doi.org/10.1136/THORAXJNL-2015-207360

Frick, M. (2022). *Tuberculosis Vaccines: Persistent impatience*.

Frigui, W., Bottai, D., Majlessi, L., Monot, M., Josselin, E., Brodin, P., Garnier, T., Gicquel, B., Martin, C., Leclerc, C., Cole, S. T., & Brosch, R. (2008). Control of M. tuberculosis ESAT-6 secretion and specific T cell recognition by PhoP. *PLoS Pathogens*, *4*(2). https://doi.org/10.1371/journal.ppat.0040033

Gonzalo-Asensio, J., Maia, C., Ferrer, N. L., Barilone, N., Laval, F., Soto, C. Y., Winter, N., Daffe, M., Gicquel, B., Martín, C., & Jackson, M. (2006). The virulence-associated two-component PhoP-PhoR system controls the biosynthesis of polyketide-derived lipids in Mycobacterium tuberculosis. *Journal of Biological Chemistry*, *281*(3), 1313–1316. https://doi.org/10.1074/jbc.C500388200

Gonzalo-Asensio, J., Malaga, W., Pawlik, A., Astarie-Dequeker, C., Passemar, C., Moreau, F., Laval, F., Daffé, M., Martin, C., Brosch, R., & Guilhot, C. (2014). Evolutionary history of tuberculosis shaped by conserved mutations in the PhoPR virulence regulator. *Proceedings of the National Academy of Sciences of the United States of America*, *111*(31), 11491–11496. https://doi.org/10.1073/pnas.1406693111

Gonzalo-Asensio, J., Mostowy, S., Harders-Westerveen, J., Huygen, K., Hernández-Pando, R., Thole, J., Behr, M., Gicquel, B., & Martín, C. (2008). PhoP: A missing piece in the intricate puzzle of Mycobacterium tuberculosis virulence. *PLoS ONE*, *3*(10). https://doi.org/10.1371/journal.pone.0003496

Gonzalo-Asensio, J., Soto, C. Y., Arbués, A., Sancho, J., Menéndez, M. D. C., García, M. J., Gicquel, B., & Martín, C. (2008). The Mycobacterium tuberculosis phoPR operon is positively autoregulated in the virulent strain H37Rv. *Journal of Bacteriology*, *190*(21), 7068–7078. https://doi.org/10.1128/JB.00712-08

Gregoire, S. A., Byam, J., & Pavelka, M. S. (2017). GalK-based suicide vector mediated allelic exchange in mycobacterium abscessus. *Microbiology (United Kingdom)*, *163*(10), 1399–1408. https://doi.org/10.1099/mic.0.000528

Griffith, D. E., Aksamit, T., Brown-Elliott, B. A., Catanzaro, A., Daley, C., Gordin, F., Holland, S. M., Horsburgh, R., Huitt, G., Iademarco, M. F., Iseman, M., Olivier, K., Ruoss, S., von Reyn, C. F., Wallace, R. J., & Winthrop, K. (2012). An Official ATS/IDSA Statement: Diagnosis, Treatment, and Prevention of Nontuberculous Mycobacterial Diseases. *Https://Doi.Org/10.1164/Rccm.200604-571ST*, *175*(4), 367–416. https://doi.org/10.1164/RCCM.200604-571ST

Griffith, D. E., & Daley, C. L. (2022). Treatment of Mycobacterium abscessus Pulmonary Disease. In *Chest* (Vol. 161, Issue 1, pp. 64–75). Chest. https://doi.org/10.1016/j.chest.2021.07.035

Gröschel, M. I., Sayes, F., Simeone, R., Majlessi, L., & Brosch, R. (2016). ESX secretion systems: Mycobacterial evolution to counter host immunity. *Nature Reviews Microbiology*, *14*(11), 677–691. https://doi.org/10.1038/nrmicro.2016.131

Gualano, G., Mencarini, P., Lauria, F. N., Palmieri, F., Mfinanga, S., Mwaba, P., Chakaya, J., Zumla, A., & Ippolito, G. (2019). Tuberculin skin test - Outdated or still useful for Latent TB infection screening? *International Journal of Infectious Diseases*, *80*, S20–S22. https://doi.org/10.1016/j.ijid.2019.01.048

Gupta, R. S., Lo, B., & Son, J. (2018). Phylogenomics and Comparative Genomic Studies Robustly Support Division of the Genus Mycobacterium into an Emended Genus Mycobacterium and Four Novel Genera. *Frontiers in Microbiology*, *9*(FEB). https://doi.org/10.3389/FMICB.2018.00067

Gutierrez, M. C., Brisse, S., Brosch, R., Fabre, M., Omaïs, B., Marmiesse, M., Supply, P., & Vincent, V. (2005). Ancient origin and gene mosaicism of the progenitor of Mycobacterium tuberculosis. *PLoS Pathogens*, *1*(1), 0055–0061. https://doi.org/10.1371/journal.ppat.0010005

Halloum, I., Carrère-Kremer, S., Blaise, M., Viljoen, A., Bernut, A., le Moigne, V., Vilchèze, C., Guérardel, Y., Lutfalla, G., Herrmann, J. L., Jacobs, W. R., & Kremer, L. (2016). Deletion of a dehydratase important for intracellular growth and cording renders rough Mycobacterium abscessus avirulent. *Proceedings of the National Academy of Sciences of the United States of America*, *113*(29), E4228–E4237. https://doi.org/10.1073/PNAS.1605477113/SUPPL_FILE/PNAS.201605477SI.PDF

Hamasur, B., Haile, M., Pawlowski, A., Schröder, U., Källenius, G., & Svenson, S. B. (2004). A mycobacterial lipoarabinomannan specific monoclonal antibody and its F(ab′)2 fragment prolong survival of mice infected with Mycobacterium tuberculosis. *Clinical and Experimental Immunology*, *138*(1), 30–38. https://doi.org/10.1111/j.1365-2249.2004.02593.x

Harries, A. D., & Dye, C. (2006). Tuberculosis. *Annals of Tropical Medicine & Parasitology*, *100*(3), 245–249. https://doi.org/10.1179/136485906x91477

Haydel, S. E., & Clark-Curtiss, J. E. (2004). Global expression analysis of two-component system regulator genes during Mycobacterium tuberculosis growth in human macrophages. *FEMS Microbiology Letters*, *236*(2), 341–347. https://doi.org/10.1016/J.FEMSLE.2004.06.010

He, X., Wang, L., & Wang, S. (2016). Structural basis of DNA sequence recognition by the response regulator PhoP in Mycobacterium tuberculosis. *Scientific Reports*, *6*(December 2015), 1–11. https://doi.org/10.1038/srep24442

Heinrichs, M., May, R., Heider, F., Reimers, T., B. Sy, S., Peloquin, C., & Derendorf, H. (2018). Mycobacterium tuberculosis Strains H37ra and H37rv have equivalent minimum inhibitory concentrations to most antituberculosis drugs. *International Journal of Mycobacteriology*, *7*(2), 156. https://doi.org/10.4103/ijmy.ijmy_33_18

Herzog, H. (1998). History of tuberculosis. *Respiration*, *65*, 5–15. https://doi.org/10.1159/000029220

Houben, R. M. G. J., & Dodd, P. J. (2016). The Global Burden of Latent Tuberculosis Infection: A Re-estimation Using Mathematical Modelling. *PLOS Medicine*, *13*(10), e1002152. https://doi.org/10.1371/JOURNAL.PMED.1002152

Hsu, T., Hingley-Wilson, S. M., Chen, B., Chen, M., Dai, A. Z., Morin, P. M., Marks, C. B., Padiyar, J., Goulding, C., Gingery, M., Eisenberg, D., Russell, R. G., Derrick, S. C., Collins, F. M., Morris, S. L., King, C. H., & Jacobs, W. R. (2003). The primary mechanism of attenuation of bacillus Calmette-Guerin is a loss of secreted lytic function required for invasion of lung interstitial tissue. *Proceedings of the National Academy of Sciences of the United States of America*, *100*(21), 12420–12425. https://doi.org/10.1073/PNAS.1635213100

Hyrup, B., & Nielsen, P. E. (1996). Peptide nucleic acids (PNA): Synthesis, properties and potential applications. *Bioorganic and Medicinal Chemistry*, *4*(1), 5–23. https://doi.org/10.1016/0968-0896(95)00171-9

Infante, E., Aguilar, L. D., Gicquel, B., & Pando, R. H. (2005). Immunogenicity and protective efficacy of the Mycobacterium tuberculosis fadD26 mutant. *Clinical and Experimental Immunology*, *141*(1), 21–28. https://doi.org/10.1111/j.1365-2249.2005.02832.x

Inoue, T., Tsunoda, A., Nishimoto, E., Nishida, K., Komatsubara, Y., Onoe, R., Saji, J., & Mineshita, M. (2018). Successful use of linezolid for refractory Mycobacterium

abcessus infection: A case report. *Respiratory Medicine Case Reports*, *23*, 43. https://doi.org/10.1016/J.RMCR.2017.11.007

Iseman, M. D. (2002). Tuberculosis therapy: Past, present and future. *European Respiratory Journal, Supplement*, *20*(36). https://doi.org/10.1183/09031936.02.00309102

Jackson, M. (2014). The mycobacterial cell envelope-lipids. *Cold Spring Harbor Perspectives in Medicine*, *4*(10), 1–22. https://doi.org/10.1101/cshperspect.a021105

Jain, P., Hsu, T., Arai, M., Biermann, K., Thaler, D. S., Nguyen, A., & González, P. A. (2014). Specialized Transduction Designed for Precise High-Throughput Unmarked Deletions in Mycobacterium tuberculosis. *Methods in Molecular Biology (Clifton, N.J.)*, *5*(3), e01245-14. https://doi.org/10.1128/mBio.01245-14.Editor

Johansen, M. D., Herrmann, J. L., & Kremer, L. (2020). Non-tuberculous mycobacteria and the rise of Mycobacterium abscessus. In *Nature Reviews Microbiology* (Vol. 18, Issue 7, pp. 392–407). Nature Publishing Group. https://doi.org/10.1038/s41579-020-0331-1

Johnson, B. K., Colvin, C. J., Needle, D. B., Mba Medie, F., Champion, P. A. D. D., & Abramovitch, R. B. (2015). The Carbonic Anhydrase Inhibitor Ethoxzolamide Inhibits the Mycobacterium tuberculosis PhoPR Regulon and Esx-1 Secretion and Attenuates Virulence. *Antimicrobial Agents and Chemotherapy*, *59*(8), 4436–4445. https://doi.org/10.1128/AAC.00719-15

Jung, K., Fried, L., Behr, S., & Heermann, R. (2012). Histidine kinases and response regulators in networks. *Current Opinion in Microbiology*, *15*(2), 118–124. https://doi.org/10.1016/j.mib.2011.11.009

Kalscheuer, R., Palacios, A., Anso, I., Cifuente, J., Anguita, J., Jacobs, W. R., Guerin, M. E., & Prados-Rosales, R. (2019). The Mycobacterium tuberculosis capsule: A cell structure with key implications in pathogenesis. In *Biochemical Journal* (Vol. 476, Issue 14, pp. 1995–2016). NIH Public Access. https://doi.org/10.1042/BCJ20190324

Karbalaei Zadeh Babaki, M., Soleimanpour, S., & Rezaee, S. A. (2017). Antigen 85 complex as a powerful Mycobacterium tuberculosis immunogene: Biology, immune-pathogenicity, applications in diagnosis, and vaccine design. In *Microbial*

Pathogenesis (Vol. 112, pp. 20–29). Microb Pathog. https://doi.org/10.1016/j.micpath.2017.08.040

Kaufmann, S. H. E. (2021). Vaccine Development Against Tuberculosis Over the Last 140 Years: Failure as Part of Success. In *Frontiers in Microbiology* (Vol. 12, p. 750124). Frontiers Media S.A. https://doi.org/10.3389/fmicb.2021.750124

Kendall, B. A., & Winthrop, K. L. (2013). Update on the epidemiology of pulmonary nontuberculous mycobacterial infections. *Seminars in Respiratory and Critical Care Medicine*, *34*(1), 87–94. https://doi.org/10.1055/S-0033-1333567

Khawbung, J. L., Nath, D., & Chakraborty, S. (2021). Drug resistant Tuberculosis: A review. In *Comparative Immunology, Microbiology and Infectious Diseases* (Vol. 74, p. 101574). Pergamon. https://doi.org/10.1016/j.cimid.2020.101574

Kirschner, D. E., Young, D., & Flynn, J. A. L. (2010). Tuberculosis: Global approaches to a global disease. *Current Opinion in Biotechnology*, *21*(4), 524–531. https://doi.org/10.1016/j.copbio.2010.06.002

Koh, W. J., Stout, J. E., & Yew, W. W. (2014). Advances in the management of pulmonary disease due to Mycobacterium abscessus complex. *International Journal of Tuberculosis and Lung Disease*, *18*(10), 1141–1148. https://doi.org/10.5588/IJTLD.14.0134

Kremer, L., Baulard, A., Estaquier, J., Poulain-Godefroy, O., & Locht, C. (1995). Green fluorescent protein as a new expression marker in mycobacteria. *Molecular Microbiology*, *17*(5), 913–922. https://doi.org/10.1111/J.1365-2958.1995.MMI_17050913.X

Kulyté, A., Nekhotiaeva, N., Awasthi, S. K., & Good, L. (2005). Inhibition of Mycobacterium smegmatis gene expression and growth using antisense peptide nucleic acids. *Journal of Molecular Microbiology and Biotechnology*, *9*(2), 101–109. https://doi.org/10.1159/000088840

Kumar, S., Rulhania, S., Jaswal, S., & Monga, V. (2021). Recent advances in the medicinal chemistry of carbonic anhydrase inhibitors. In *European Journal of Medicinal Chemistry* (Vol. 209, p. 112923). Elsevier Masson. https://doi.org/10.1016/j.ejmech.2020.112923

Lamrabet, O., & Drancourt, M. (2012). Genetic engineering of Mycobacterium tuberculosis: A review. *Tuberculosis*, *92*(5), 365–376. https://doi.org/10.1016/j.tube.2012.06.002

Lange, C., Aaby, P., Behr, M. A., Donald, P. R., Kaufmann, S. H. E., Netea, M. G., & Mandalakas, A. M. (2022). 100 years of Mycobacterium bovis bacille Calmette-Guérin. *The Lancet Infectious Diseases*, *22*(1), e2–e12. https://doi.org/10.1016/S1473-3099(21)00403-5

Lee, J. S., Krause, R., Schreiber, J., Mollenkopf, H. J., Kowall, J., Stein, R., Jeon, B. Y., Kwak, J. Y., Song, M. K., Patron, J. P., Jorg, S., Roh, K., Cho, S. N., & Kaufmann, S. H. E. (2008). Mutation in the Transcriptional Regulator PhoP Contributes to Avirulence of Mycobacterium tuberculosis H37Ra Strain. *Cell Host and Microbe*, *3*(2), 97–103. https://doi.org/10.1016/j.chom.2008.01.002

Lee, J.-H., Yoo, J.-S., Kim, Y., Kim, J.-S., Lee, E.-J., & Roe, J.-H. (2020). The WblC/WhiB7 Transcription Factor Controls Intrinsic Resistance to Translation-Targeting Antibiotics by Altering Ribosome Composition. *MBio*, *11*(2). https://doi.org/10.1128/mBio.00625-20

Lewis, K. N., Liao, R., Guinn, K. M., Hickey, M. J., Smith, S., Behr, M. A., & Sherman, D. R. (2003). Deletion of RD1 from Mycobacterium tuberculosis Mimics Bacille Calmette-Guérin Attenuation. *The Journal of Infectious Diseases*, *187*(1), 117–123. https://doi.org/10.1086/345862

Lim, A. Y. H., Chotirmall, S. H., Fok, E. T. K., Verma, A., De, P. P., Goh, S. K., Puah, S. H., Goh, D. E. L., & Abisheganaden, J. A. (2018). Profiling non-tuberculous mycobacteria in an Asian setting: characteristics and clinical outcomes of hospitalized patients in Singapore. *BMC Pulmonary Medicine*, *18*(1). https://doi.org/10.1186/S12890-018-0637-1

Lin, L., Tan, B., & Pantapalangkoor, P. (2012). Inhibition of LpxC Protects Mice from Resistant Acinetobacter. *MBio*, *3*(5), 23–29. https://doi.org/10.1128/mBio.00312-12.Editor

Luetkemeyer, A. F., Getahun, H., Chamie, G., Lienhardt, C., & Havlir, D. v. (2011). Tuberculosis drug development: Ensuring people living with HIV are not left behind. In *American Journal of Respiratory and Critical Care Medicine* (Vol. 184, Issue 10, pp. 1107–1113). American Thoracic Society. https://doi.org/10.1164/rccm.201106-0995PP

Lyu, J., Jang, H. J., Song, J. W., Choi, C. M., Oh, Y. M., Lee, S. do, Kim, W. S., Kim, D. S., & Shim, T. S. (2011). Outcomes in patients with Mycobacterium abscessus pulmonary disease treated with long-term injectable drugs. *Respiratory Medicine*, *105*(5), 781–787. https://doi.org/10.1016/j.rmed.2010.12.012

Ma, Z., Lienhardt, C., McIlleron, H., Nunn, A. J., & Wang, X. (2010). Global tuberculosis drug development pipeline: the need and the reality. In *The Lancet* (Vol. 375, Issue 9731, pp. 2100–2109). Lancet. https://doi.org/10.1016/S0140-6736(10)60359-9

Madacki, J., Orgeur, M., Fiol, G. M., Frigui, W., Ma, L., & Brosch, R. (2021). Esx-1-independent horizontal gene transfer by mycobacterium tuberculosis complex strains. *MBio*, *12*(3). https://doi.org/10.1128/mBio.00965-21

Madsen, C. T., Jakobsen, L., Buriánková, K., Doucet-Populaire, F., Pernodet, J. L., & Douthwaite, S. (2005). Methyltransferase Erm(37) slips on rRNA to confer atypical resistance in Mycobacterium tuberculosis. *Journal of Biological Chemistry*, *280*(47), 38942–38947. https://doi.org/10.1074/jbc.M505727200

Mahajan, R. (2013). Bedaquiline: First FDA-approved tuberculosis drug in 40 years. *International Journal of Applied and Basic Medical Research*, *3*(1), 1. https://doi.org/10.4103/2229-516x.112228

Marín-Menéndez, A., Montis, C., Díaz-Calvo, T., Carta, D., Hatzixanthis, K., Morris, C. J., McArthur, M., & Berti, D. (2017). Antimicrobial Nanoplexes meet Model Bacterial Membranes: The key role of Cardiolipin. *Scientific Reports*, *7*(November 2016), 1–13. https://doi.org/10.1038/srep41242

Martin, C., Aguilo, N., & Gonzalo-Asensio, J. (2018). Vaccination against tuberculosis. *Enfermedades Infecciosas y Microbiologia Clinica*, *36*(10), 648–656. https://doi.org/10.1016/j.eimc.2018.02.006

Martín, C., Marinova, D., Aguiló, N., & Gonzalo-Asensio, J. (2021). MTBVAC, a live TB vaccine poised to initiate efficacy trials 100 years after BCG. *Vaccine*, *39*(50), 7277–7285. https://doi.org/10.1016/j.vaccine.2021.06.049

Mata, E., Tarancon, R., Guerrero, C., Moreo, E., Moreau, F., Uranga, S., Gomez, A. B., Marinova, D., Domenech, M., Gonzalez-Camacho, F., Monzon, M., Badiola, J., Dominguez-Andres, J., Yuste, J., Anel, A., Peixoto, A., Martin, C., & Aguilo, N. (2021). Pulmonary BCG induces lung-resident macrophage activation and confers long-term protection against tuberculosis. *Science Immunology*, *6*(63), 1–13. https://doi.org/10.1126/sciimmunol.abc2934

Medjahed, H., & Reyrat, J. M. (2009). Construction of mycobacterium abscessus defined glycopeptidolipid mutants: Comparison of genetic tools. *Applied and Environmental Microbiology*, *75*(5), 1331–1338. https://doi.org/10.1128/AEM.01914-08

Miller, B. K., Zulauf, K. E., & Braunstein, M. (2017). The Sec Pathways and Exportomes of Mycobacterium tuberculosis. *Microbiology Spectrum*, *5*(2). https://doi.org/10.1128/MICROBIOLSPEC.TBTB2-0013-2016

Mougari, F., Guglielmetti, L., Raskine, L., Sermet-Gaudelus, I., Veziris, N., & Cambau, E. (2016). Infections caused by Mycobacterium abscessus: epidemiology, diagnostic tools and treatment. In *Expert Review of Anti-Infective Therapy* (Vol. 14, Issue 12, pp. 1139–1154). Taylor & Francis. https://doi.org/10.1080/14787210.2016.1238304

Nahid, P., Dorman, S. E., Alipanah, N., Barry, P. M., Brozek, J. L., Cattamanchi, A., Chaisson, L. H., Chaisson, R. E., Daley, C. L., Grzemska, M., Higashi, J. M., Ho, C. S., Hopewell, P. C., Keshavjee, S. A., Lienhardt, C., Menzies, R., Merrifield, C., Narita, M., O'Brien, R., … Vernon, A. (2016). Executive Summary: Official American Thoracic Society/Centers for Disease Control and Prevention/Infectious Diseases Society of America Clinical Practice Guidelines: Treatment of Drug-Susceptible Tuberculosis. *Clinical Infectious Diseases*, *63*(7), 853–867. https://doi.org/10.1093/CID/CIW566

Nessar, R., Cambau, E., Reyrat, J. M., Murray, A., & Gicquel, B. (2012). Mycobacterium abscessus: A new antibiotic nightmare. *Journal of Antimicrobial Chemotherapy*, *67*(4), 810–818. https://doi.org/10.1093/jac/dkr578

Olivença, F., Ferreira, C., Nunes, A., Silveiro, C., Pimentel, M., & Gomes, J. P. (2022). Identification of drivers of mycobacterial resistance to peptidoglycan synthesis inhibitors. *Frontiers in Microbiology*, *September*. https://doi.org/10.3389/fmicb.2022.985871

Orme, I. M. (2010). The Achilles heel of BCG. *Tuberculosis*, *90*(6), 329–332. https://doi.org/10.1016/j.tube.2010.06.002

Parish, T. (2014). Two-Component Regulatory Systems of Mycobacteria. *Microbiology Spectrum*, *2*(1). https://doi.org/10.1128/MICROBIOLSPEC.MGM2-0010-2013/ASSET/D70A413B-FB85-4527-87C3-1B2A9DD93569/ASSETS/GRAPHIC/MGM2-0010-2013-FIG1.GIF

Passemar, C., Arbués, A., Malaga, W., Mercier, I., Moreau, F., Lepourry, L., Neyrolles, O., Guilhot, C., & Astarie-Dequeker, C. (2014). Multiple deletions in the polyketide synthase gene repertoire of mycobacterium tuberculosis reveal functional overlap of cell envelope lipids in host-pathogen interactions. *Cellular Microbiology*, *16*(2), 195–213. https://doi.org/10.1111/CMI.12214/SUPPINFO

Paulson, T. (2013). A mortal foe. *Nature*, *502*(7470), S2. https://doi.org/10.1038/502S2a

Pérez, E., Samper, S., Bordas, Y., Guilhot, C., Gicquel, B., & Martín, C. (2001). An essential role for phoP in Mycobacterium tuberculosis virelence. *Molecular Microbiology*, *41*(1), 179–187. https://doi.org/10.1046/j.1365-2958.2001.02500.x

Pérez, I., Campos-Pardos, E., Díaz, C., Uranga, S., Sayes, F., Vicente, F., Aguiló, N., Brosch, R., Martín, C., & Gonzalo-Asensio, J. (2022). The Mycobacterium tuberculosis PhoPR virulence system regulates expression of the universal second messenger c-di-AMP and impacts vaccine safety and efficacy. *Molecular Therapy - Nucleic Acids*, *27*, 1235–1248. https://doi.org/10.1016/j.omtn.2022.02.011

Pérez, I., Uranga, S., Sayes, F., Frigui, W., Samper, S., Arbués, A., Aguiló, N., Brosch, R., Martín, C., & Gonzalo-Asensio, J. (2020). Live attenuated TB vaccines representing the three modern Mycobacterium tuberculosis lineages reveal that the Euro–American genetic background confers optimal vaccine potential. *EBioMedicine*, *55*, 1–10. https://doi.org/10.1016/j.ebiom.2020.102761

Pethe, K., Alonso, S., Biet, F., Delogu, G., Brennan, M. J., Locht, C., & Menozzi, F. D. (2001). The heparin-binding haemagglutinin of M. tuberculosis is required for extrapulmonary dissemination. *Nature*, *412*(6843), 190–194. https://doi.org/10.1038/35084083

Pezzella, A. T. (2019). History of Pulmonary Tuberculosis. *Thoracic Surgery Clinics*, *29*(1), 1–17. https://doi.org/10.1016/j.thorsurg.2018.09.002

Philley, J. v., Wallace, R. J., Benwill, J. L., Taskar, V., Brown-Elliott, B. A., Thakkar, F., Aksamit, T. R., & Griffith, D. E. (2015). Preliminary Results of Bedaquiline as Salvage Therapy for Patients With Nontuberculous Mycobacterial Lung Disease. *Chest*, *148*(2), 499–506. https://doi.org/10.1378/CHEST.14-2764

Preiss, L., Langer, J. D., Yildiz, Ö., Eckhardt-Strelau, L., Guillemont, J. E. G., Koul, A., & Meier, T. (2015). Structure of the mycobacterial ATP synthase Fo rotor ring in complex with the anti-TB drug bedaquiline. *Science Advances*, *1*(4). https://doi.org/10.1126/sciadv.1500106

Prevots, D. R., & Marras, T. K. (2015). Epidemiology of human pulmonary infection with nontuberculous mycobacteria a review. In *Clinics in Chest Medicine* (Vol. 36, Issue 1, pp. 13–34). NIH Public Access. https://doi.org/10.1016/j.ccm.2014.10.002

Pym, A. S., Brodin, P., Brosch, R., Huerre, M., & Cole, S. T. (2002). Loss of RD1 contributed to the attenuation of the live tuberculosis vaccines Mycobacterium bovis BCG and Mycobacterium microti. *Molecular Microbiology*, *46*(3), 709–717. https://doi.org/10.1046/j.1365-2958.2002.03237.x

Quang, N. T., & Jang, J. (2021). Current Molecular Therapeutic Agents and Drug Candidates for Mycobacterium abscessus. *Frontiers in Pharmacology*, *12*(August). https://doi.org/10.3389/fphar.2021.724725

Queval, C. J., Song, O. R., Carralot, J. P., Saliou, J. M., Bongiovanni, A., Deloison, G., Deboosère, N., Jouny, S., Iantomasi, R., Delorme, V., Debrie, A. S., Park, S. J., Gouveia, J. C., Tomavo, S., Brosch, R., Yoshimura, A., Yeramian, E., & Brodin, P. (2017). Mycobacterium tuberculosis Controls Phagosomal Acidification by Targeting CISH-Mediated Signaling. *Cell Reports*, *20*(13), 3188–3198. https://doi.org/10.1016/j.celrep.2017.08.101

Rahlwes Kathryn, C., Dias Beatriz, R. S., Campos Priscila, C., Alvarez-Arguedas, S., & Shiloh Michael, U. (2022). Pathogenicity and virulence of Mycobacterium tuberculosis. *Virulence*, *13*(1), 1752–1771. https://doi.org/10.1080/21505594.2022.2150449

Ratnatunga, C. N., Lutzky, V. P., Kupz, A., Doolan, D. L., Reid, D. W., Field, M., Bell, S. C., Thomson, R. M., & Miles, J. J. (2020). The Rise of Non-Tuberculosis Mycobacterial Lung Disease. In *Frontiers in Immunology* (Vol. 11, p. 303). Frontiers Media S.A. https://doi.org/10.3389/fimmu.2020.00303

Rezzoagli, C., Archetti, M., Mignot, I., Baumgartner, M., & Kümmerli, R. (2020). Combining antibiotics with antivirulence compounds can have synergistic effects and reverse selection for antibiotic resistance in Pseudomonas aeruginosa. *PLoS Biology*, *18*(8), 861799. https://doi.org/10.1371/JOURNAL.PBIO.3000805

Riojas, M. A., McGough, K. J., Rider-Riojas, C. J., Rastogi, N., & Hazbón, M. H. (2018). Phylogenomic analysis of the species of the Mycobacterium tuberculosis complex demonstrates that Mycobacterium africanum, Mycobacterium bovis, Mycobacterium caprae, Mycobacterium microti and Mycobacterium pinnipedii are

later heterotypic synonyms of Mycob. *International Journal of Systematic and Evolutionary Microbiology*, *68*(1), 324–332. https://doi.org/10.1099/ijsem.0.002507

Ripoll, F., Pasek, S., Schenowitz, C., Dossat, C., Barbe, V., Rottman, M., Macheras, E., Heym, B., Hermann, J. L., Daffé, M., Brosch, R., Risler, J. L., & Gaillard, J. L. (2009). Non mycobacterial virulence genes in the genome of the emerging pathogen Mycobacterium abscessus. *PLoS ONE*, *4*(6). https://doi.org/10.1371/journal.pone.0005660

Rominski, A., Selchow, P., Becker, K., Brülle, J. K., Dal Molin, M., & Sander, P. (2017). Elucidation of Mycobacterium abscessus aminoglycoside and capreomycin resistance by targeted deletion of three putative resistance genes. *Journal of Antimicrobial Chemotherapy*, *72*(8), 2191–2200. https://doi.org/10.1093/jac/dkx125

Ruhl, C. R., Pasko, B. L., Khan, H. S., Kindt, L. M., Stamm, C. E., Franco, L. H., Hsia, C. C., Zhou, M., Davis, C. R., Qin, T., Gautron, L., Burton, M. D., Mejia, G. L., Naik, D. K., Dussor, G., Price, T. J., & Shiloh, M. U. (2020). Mycobacterium tuberculosis Sulfolipid-1 Activates Nociceptive Neurons and Induces Cough. *Cell*, *181*(2), 293. https://doi.org/10.1016/J.CELL.2020.02.026

Ryan, N. J., & Lo, J. H. (2014). Delamanid: first global approval. *Drugs*, *74*(9), 1041–1045. https://doi.org/10.1007/S40265-014-0241-5

Rybniker, J., Chen, J. M., Sala, C., Hartkoorn, R. C., Vocat, A., Benjak, A., Boy-Röttger, S., Zhang, M., Székely, R., Greff, Z., Orfi, L., Szabadkai, I., Pató, J., Kéri, G., & Cole, S. T. (2014). Anticytolytic screen identifies inhibitors of mycobacterial virulence protein secretion. *Cell Host and Microbe*, *16*(4), 538–548. https://doi.org/10.1016/j.chom.2014.09.008

Sakula, A. (1979). Robert Koch (1843-1910): Founder of the science of bacteriology and discoverer of the tubercle bacillus. A study of his life and work. *British Journal of Diseases of the Chest*, *73*(C), 389–394. https://doi.org/10.1016/0007-0971(79)90078-0

Samoilova, A., Skornykova, S., Tudor, E., Variava, E., Yablonskiy, P., Everitt, D., Wills, G. H., Sun, E., Olugbosi, M., Egizi, E., Li, M., Holsta, A., Timm, J., Bateson, A., Crook, A. M., Fabiane, S. M., Hunt, R., Mchugh, T. D., Tweed, C. D., … Trial, Z. (2022). *Bedaquiline–Pretomanid–Linezolid Regimens for Drug-Resistant Tuberculosis*. 810–823. https://doi.org/10.1056/NEJMoa2119430

Samper, S., & Martín, C. (2007). Spread of extensively drug-resistant tuberculosis. *Emerging Infectious Diseases*, *13*(4), 647–648. https://doi.org/10.3201/eid1304.061329

Schreuder, L. J., Carroll, P., Muwanguzi-Karugaba, J., Kokoczka, R., Brown, A. C., & Parish, T. (2015). Mycobacterium tuberculosis H37Rv has a single nucleotide polymorphism in PHoR which affects cell wall hydrophobicity and gene expression. *Microbiology (United Kingdom)*, *161*(4), 765–773. https://doi.org/10.1099/mic.0.000036

Segala, E., Sougakoff, W., Nevejans-Chauffour, A., Jarlier, V., & Petrella, S. (2012). New mutations in the mycobacterial ATP synthase: New insights into the binding of the diarylquinoline TMC207 to the ATP synthase C-Ring structure. *Antimicrobial Agents and Chemotherapy*, *56*(5), 2326–2334. https://doi.org/10.1128/AAC.06154-11

Shallom, S. J., Moura, N. S., Olivier, K. N., Sampaio, E. P., Holland, S. M., & Zelazny, A. M. (2015). New real-time PCR assays for detection of inducible and acquired clarithromycin resistance in the mycobacterium abscessus group. *Journal of Clinical Microbiology*, *53*(11), 3430–3437. https://doi.org/10.1128/JCM.01714-15

Shelby J, D., Rajni, G., Benjamin K, J., & Robert B, A. (2022). *Carbon dioxide regulates Mycobacterium tuberculosis PhoPR signaling and virulence*. https://doi.org/10.1101/2022.04.12.488064

Silva Miranda, M., Breiman, A., Allain, S., Deknuydt, F., & Altare, F. (2012). The tuberculous granuloma: An unsuccessful host defence mechanism providing a safety shelter for the bacteria? In *Clinical and Developmental Immunology* (Vol. 2012). Clin Dev Immunol. https://doi.org/10.1155/2012/139127

Silva, P. E. A., Bigi, F., Santagelo, M. de la P., Romano, M. I., Martin, C., Cataldi, A., & Ainsa, J. A. (2001). Characterization of P55, a Multidrug Efflux Pump in Mycobacterium bovis and Mycobacterium tuberculosis. *Antimicrobial Agents and Chemotherapy*, *45*. https://doi.org/10.1128/AAC.45.3.800

Simeone, R., Sayes, F., Song, O., Gröschel, M. I., Brodin, P., Brosch, R., & Majlessi, L. (2015). Cytosolic Access of Mycobacterium tuberculosis: Critical Impact of Phagosomal Acidification Control and Demonstration of Occurrence In Vivo. *PLoS Pathogens*, *11*(2). https://doi.org/10.1371/journal.ppat.1004650

Sinha, A., Gupta, S., Bhutani, S., Pathak, A., & Sarkar, D. (2008). PhoP-PhoP interaction at adjacent PhoP binding sites is influenced by protein phosphorylation. *Journal of Bacteriology*, *190*(4), 1317–1328. https://doi.org/10.1128/JB.01074-07

Solans, L., Gonzalo-Asensio, J., Sala, C., Benjak, A., Uplekar, S., Rougemont, J., Guilhot, C., Malaga, W., Martín, C., & Cole, S. T. (2014). The PhoP-Dependent ncRNA Mcr7 Modulates the TAT Secretion System in Mycobacterium tuberculosis. *PLoS Pathogens*, *10*(5). https://doi.org/10.1371/journal.ppat.1004183

Song, H., & Niederweis, M. (2007). Functional expression of the Flp recombinase in Mycobacterium bovis BCG. *Gene*, *399*(2), 112–119. https://doi.org/10.1016/j.gene.2007.05.005

Soto, C. Y., Menéndez, M. C., Pérez, E., Samper, S., Gómez, A. B., García, M. J., & Martín, C. (2004). IS6110 Mediates Increased Transcription of the phoP Virulence Gene in a Multidrug-Resistant Clinical Isolate Responsible for Tuberculosis Outbreaks. *Journal of Clinical Microbiology*, *42*(1), 212–219. https://doi.org/10.1128/JCM.42.1.212-219.2004

Spertini, F., Audran, R., Chakour, R., Karoui, O., Steiner-Monard, V., Thierry, A. C., Mayor, C. E., Rettby, N., Jaton, K., Vallotton, L., Lazor-Blanchet, C., Doce, J., Puentes, E., Marinova, D., Aguilo, N., & Martin, C. (2015). Safety of human immunisation with a live-attenuated Mycobacterium tuberculosis vaccine: A randomised, double-blind, controlled phase I trial. *The Lancet Respiratory Medicine*, *3*(12), 953–962. https://doi.org/10.1016/S2213-2600(15)00435-X

Stackebrandt, E., Rainey, F. A., & Ward-Rainey, N. L. (1997). Proposal for a new hierarchic classification system, Actinobacteria classis nov. *International Journal of Systematic Bacteriology*, *47*(2), 479–491. https://doi.org/10.1099/00207713-47-2-479/CITE/REFWORKS

Starkey, M., Lepine, F., Maura, D., Bandyopadhaya, A., Lesic, B., He, J., Kitao, T., Righi, V., Milot, S., Tzika, A., & Rahme, L. (2014). Identification of Anti-virulence Compounds That Disrupt Quorum-Sensing Regulated Acute and Persistent Pathogenicity. *PLoS Pathogens*, *10*(8). https://doi.org/10.1371/journal.ppat.1004321

Stock, A. M., Robinson, V. L., & Goudreau, P. N. (2000). Two-component signal transduction. *Annual Review of Biochemistry*, *69*, 183–215. https://doi.org/10.1146/annurev.biochem.69.1.183

Stout, J. E., Koh, W. J., & Yew, W. W. (2016). Update on pulmonary disease due to non-tuberculous mycobacteria. In *International Journal of Infectious Diseases* (Vol. 45, pp. 123–134). Elsevier. https://doi.org/10.1016/j.ijid.2016.03.006

Stover, C. K. K., de La Cruz, V. F., Fuerst, T. R., Burlein, J. E., Benson, L. A., Bennett, L. T., Bansal, G. P., Young, J. F., Lee, M. H., Hatfull, G. F., Snapper, S. B., Barletta, R. G., Jacobs, W. R., & Bloom, B. R. (1991). New use of BCG for recombinant vaccines. *Nature*, *354*(6326), 456–460. https://doi.org/10.1038/351456a0

Tameris, M., Mearns, H., Penn-Nicholson, A., Gregg, Y., Bilek, N., Mabwe, S., Geldenhuys, H., Shenje, J., Luabeya, A. K. K., Murillo, I., Doce, J., Aguilo, N., Marinova, D., Puentes, E., Rodríguez, E., Gonzalo-Asensio, J., Fritzell, B., Thole, J., Martin, C., … Veldsman, A. (2019). Live-attenuated Mycobacterium tuberculosis vaccine MTBVAC versus BCG in adults and neonates: a randomised controlled, double-blind dose-escalation trial. *The Lancet Respiratory Medicine*, *7*(9), 757–770. https://doi.org/10.1016/S2213-2600(19)30251-6

Tan, Y., Su, B., Shu, W., Cai, X., Kuang, S., Kuang, H., Liu, J., & Pang, Y. (2018). Epidemiology of pulmonary disease due to nontuberculous mycobacteria in Southern China, 2013-2016. *BMC Pulmonary Medicine*, *18*(1). https://doi.org/10.1186/S12890-018-0728-Z

Thabit, A. K., Eljaaly, K., Zawawi, A., Ibrahim, T. S., Eissa, A. G., Elbaramawi, S. S., Hegazy, W. A. H., & Elfaky, M. A. (2022). Silencing of Salmonella typhimurium Pathogenesis: Atenolol Acquires Efficient Anti-Virulence Activities. *Microorganisms*, *10*(10), 1–16. https://doi.org/10.3390/microorganisms10101976

Theron, G., Peter, J., van Zyl-Smit, R., Mishra, H., Streicher, E., Murray, S., Dawson, R., Whitelaw, A., Hoelscher, M., Sharma, S., Pai, M., Warren, R., & Dheda, K. (2011). Evaluation of the Xpert MTB/RIF assay for the diagnosis of pulmonary tuberculosis in a high HIV prevalence setting. *American Journal of Respiratory and Critical Care Medicine*, *184*(1), 132–140. https://doi.org/10.1164/rccm.201101-0056OC

Theuretzbacher, U., Outterson, K., Engel, A., & Karlén, A. (2020). The global preclinical antibacterial pipeline. *Nature Reviews Microbiology*, *18*(5), 275–285. https://doi.org/10.1038/s41579-019-0288-0

Tiberi, S., du Plessis, N., Walzl, G., Vjecha, M. J., Rao, M., Ntoumi, F., Mfinanga, S., Kapata, N., Mwaba, P., McHugh, T. D., Ippolito, G., Migliori, G. B., Maeurer, M. J., & Zumla, A. (2018). Tuberculosis: progress and advances in development of new

drugs, treatment regimens, and host-directed therapies. In *The Lancet Infectious Diseases* (Vol. 18, Issue 7, pp. e183–e198). Lancet Infect Dis. https://doi.org/10.1016/S1473-3099(18)30110-5

Tiemersma, E. W., van der Werf, M. J., Borgdorff, M. W., Williams, B. G., & Nagelkerke, N. J. D. (2011). Natural history of tuberculosis: Duration and fatality of untreated pulmonary tuberculosis in HIV negative patients: A systematic review. In *PLoS ONE* (Vol. 6, Issue 4). PLoS One. https://doi.org/10.1371/journal.pone.0017601

To, K., Cao, R., Yegiazaryan, A., Owens, J., & Venketaraman, V. (2020). General overview of nontuberculous mycobacteria opportunistic pathogens: Mycobacterium avium and mycobacterium abscessus. In *Journal of Clinical Medicine* (Vol. 9, Issue 8, pp. 1–24). Multidisciplinary Digital Publishing Institute (MDPI). https://doi.org/10.3390/jcm9082541

Tortoli, E., Brown-Elliott, B. A., Chalmers, J. D., Cirillo, D. M., Daley, C. L., Emler, S., Andres Floto, R., Garcia, M. J., Hoefsloot, W., Koh, W. J., Lange, C., Loebinger, M., Maurer, F. P., Morimoto, K., Niemann, S., Richter, E., Turenne, C. Y., Vasireddy, R., Vasireddy, S., … van Ingen, J. (2019). Same meat, different gravy: Ignore the new names of mycobacteria. *European Respiratory Journal*, *54*(1). https://doi.org/10.1183/13993003.00795-2019

Totsika, M. (2016). Benefits and Challenges of Antivirulence Antimicrobials at the Dawn of the Post-Antibiotic Era. *Drug Delivery Letters*, *6*(1), 30–37. https://doi.org/10.2174/2210303106666160506120057

Uddin, T. M., Chakraborty, A. J., Khusro, A., Zidan, B. R. M., Mitra, S., Emran, T. bin, Dhama, K., Ripon, M. K. H., Gajdács, M., Sahibzada, M. U. K., Hossain, M. J., & Koirala, N. (2021). Antibiotic resistance in microbes: History, mechanisms, therapeutic strategies and future prospects. *Journal of Infection and Public Health*, *14*(12), 1750–1766. https://doi.org/10.1016/j.jiph.2021.10.020

van der Wel, N., Hava, D., Houben, D., Fluitsma, D., van Zon, M., Pierson, J., Brenner, M., & Peters, P. J. (2007). M. tuberculosis and M. leprae translocate from the phagolysosome to the cytosol in myeloid cells. *Cell*, *129*(7), 1287–1298. https://doi.org/10.1016/J.CELL.2007.05.059

van Kessel, J. C., & Hatfull, G. F. (2007). Recombineering in Mycobacterium tuberculosis. *Nature Methods*, *4*(2), 147–152. https://doi.org/10.1038/nmeth996

van Kessel, J. C., & Hatfull, G. F. (2008). Efficient point mutagenesis in mycobacteria using single-stranded DNA recombineering: Characterization of antimycobacterial drug targets. *Molecular Microbiology*, *67*(5), 1094–1107. https://doi.org/10.1111/j.1365-2958.2008.06109.x

Victoria, L., Gupta, A., Gómez, J. L., & Robledo, J. (2021). Mycobacterium abscessus complex: A Review of Recent Developments in an Emerging Pathogen. In *Frontiers in Cellular and Infection Microbiology* (Vol. 11, p. 338). Frontiers Media S.A. https://doi.org/10.3389/fcimb.2021.659997

Viljoen, A., Gutiérrez, A. V., Dupont, C., Ghigo, E., & Kremer, L. (2018). A simple and rapid gene disruption strategy in Mycobacterium abscessus: On the design and application of glycopeptidolipid mutants. *Frontiers in Cellular and Infection Microbiology*, *8*(MAR). https://doi.org/10.3389/fcimb.2018.00069

Walker, K. B., Brennan, M. J., Ho, M. M., Eskola, J., Thiry, G., Sadoff, J., Dobbelaer, R., Grode, L., Liu, M. A., Fruth, U., & Lambert, P. H. (2010). The second Geneva Consensus: Recommendations for novel live TB vaccines. *Vaccine*, *28*(11), 2259–2270. https://doi.org/10.1016/j.vaccine.2009.12.083

Walters, S. B., Dubnau, E., Kolesnikova, I., Laval, F., Daffe, M., & Smith, I. (2006). The Mycobacterium tuberculosis PhoPR two-component system regulates genes essential for virulence and complex lipid biosynthesis. *Molecular Microbiology*, *60*(2), 312–330. https://doi.org/10.1111/j.1365-2958.2006.05102.x

Wang, L., Xu, M., Southall, N., Zheng, W., & Wang, S. (2016). A High-Throughput Assay for Developing Inhibitors of PhoP, a Virulence Factor of Mycobacterium tuberculosis. *Combinatorial Chemistry & High Throughput Screening*, *19*(10), 855. https://doi.org/10.2174/1386207319666161010163249

WHO. (2018). WHO Preferred Product Characteristics for New Tuberculosis Vaccines. *Geneva: World Health Organization; 2018*, *Licence: C*. https://www.who.int/publications/i/item/WHO-IVB-18.06

WHO. (1993). WHO Calls Tuberculosis a Global Emergency - Los Angeles Times. *Los Angeles Times*. https://www.latimes.com/archives/la-xpm-1993-04-24-mn-26683-story.html

WHO. (1994). *TB : a global emergency, WHO report on the TB epidemic*. 32. https://apps.who.int/iris/handle/10665/58749

Wiker, H. G., & Harboe, M. (1992). The antigen 85 complex: a major secretion product of Mycobacterium tuberculosis. *Microbiological Reviews*, *56*(4), 648–661. https://doi.org/10.1128/mr.56.4.648-661.1992

Winthrop, K. L., Ku, J. H., Marras, T. K., Griffith, D. E., Daley, C. L., Olivier, K. N., Aksamit, T. R., Varley, C. D., Mackey, K., & Prevots, D. R. (2015). The tolerability of linezolid in the treatment of nontuberculous mycobacterial disease. *European Respiratory Journal*, *45*(4), 1177–1179. https://doi.org/10.1183/09031936.00169114

WHO. (2020a). *Global Tuberculosis Report 2020*. http://apps.who.int/bookorders.

WHO. (2020b). Meeting report of the WHO expert consultation on the definition of extensively drug-resistant tuberculosis. In *Wold Health Organization* (Issue October). https://www.who.int/publications/i/item/meeting-report-of-the-who-expert-consultation-on-the-definition-of-extensively-drug-resistant-tuberculosis

WHO. (2020c). *WHO consolidated guidelines on tuberculosis. Module 4: treatment - drug-resistant tuberculosis treatment. Online annexes.*

WHO. (2022a). Global tuberculosis report 2022. In *Wold Health Organization* (Vol. 4, Issue 1). https://www.who.int/teams/global-tuberculosis-programme/tb-reports/global-tuberculosis-report-2022

WHO. (2022b). *WHO consolidated guidelines on tuberculosis. Module 4: Treatment Drug-susceptible tuberculosis treatment*. World Health Organization. moz-extension://cb76e549-da11-4601-8c3f-808486f8eb45/enhanced-reader.html?openApp&pdf=https%3A%2F%2Fapps.who.int%2Firis%2Frest%2Fbitstreams%2F1421257%2Fretrieve

Xu, W., DeJesus, M. A., Rücker, N., Engelhart, C. A., Wright, M. G., Healy, C., Lin, K., Wang, R., Park, S. W., Ioerger, T. R., Schnappinger, D., & Ehrt, S. (2017). Chemical genetic interaction profiling reveals determinants of intrinsic antibiotic resistance in Mycobacterium tuberculosis. *Antimicrobial Agents and Chemotherapy*, *61*(12). https://doi.org/10.1128/AAC.01334-17

Zhang, J. H., Chung, T. D. Y., & Oldenburg, K. R. (1999). A simple statistical parameter for use in evaluation and validation of high throughput screening assays. *Journal of Biomolecular Screening*, *4*(2), 67–73. https://doi.org/10.1177/108705719900400206

Zhu, L., Lee, A. W. T., Wu, K. K. L., Gao, P., Tam, K. K. G., Rajwani, R., Chaburte, G. C., Ng, T. T. L., Chan, C. T. M., Lao, H. Y., Yam, W. C., Kao, R. Y. T., & Siu, G. K. H. (2022). Screening Repurposed Antiviral Small Molecules as Antimycobacterial Compounds by a Lux-Based phoP Promoter-Reporter Platform. *Antibiotics*, *11*(3). https://doi.org/10.3390/antibiotics11030369